BERICHTE
aus dem Fachbereich Geowissenschaften
der Universität Bremen

No. 281

Bohrmann, G., E. Akasu, A. Bahr, M. Bergenthal, K. Dehning, V. Diekamp, B. Domeyer, C. dos Santos Ferreira, R. Düßmann, T. Freudenthal, M. Haeckel, K. Hatsukano, O. Herschelmann, H.-J. Hohnberg, D. Hüttich, K. Kaszemeik, T. Klein, G. Komakhidze, E. Kopiske, J.-H. Körber, U. Lomnitz, T. Malakhova, G. Meinecke, D. Meyerdierks, D. Nadezhkin, S. Oelfke, A. Özmaral, T. Pape, E. Piñero, V. Rădulescu, A. Raeke, A. Reitz, J. Renken, M. Reuter, M. Römer, U. Rosiak, H. Sahling, M. Schmager, A. Stachowski, M. Tomczyk, D. Wangner, J. Wei, P. Wintersteller, T. Wu

REPORT AND PRELIMINARY RESULTS OF RV METEOR CRUISE 84/2, ISTANBUL – ISTANBUL, 26 FEBRUARY – 02 APRIL, 2011.
Origin and Distribution of Methane and Methane Hydrates in the Black Sea.

Berichte, Fachbereich Geowissenschaften, Universität Bremen, No. 281, 164 pages, Bremen 2011

ISSN 0931-0800

The "Berichte aus dem Fachbereich Geowissenschaften" are produced at irregular intervals by the Department of Geosciences, Bremen University.

They serve for the publication of experimental works, Ph.D.-theses and scientific contributions made by members of the department.

Reports can be ordered from:

Monika Bachur

DFG-Forschungszentrum MARUM

Universität Bremen

Postfach 330 440

D 28334 BREMEN

Phone: (49) 421 218-65516

Fax: (49) 421 218-65515

e-mail: MBachur@uni-bremen.de

Citation:
Bohrmann, G. and cruise participants
Report and preliminary results of RV METEOR Cruise M84/2, Istanbul – Istanbul, 26 February – 02 April, 2011. Origin and Distribution of Methane and Methane Hydrates in the Black Sea.
Berichte, Fachbereich Geowissenschaften, Universität Bremen, No. 281, 164 pages. Bremen, 2011.

ISSN 0931-0800

R/V METEOR
Cruise Report M84/2

Origin and Distribution of Methane and Methane Hydrates in the Black Sea

M84, Leg 2
Istanbul – Istanbul
26 February – 02 April, 2011

Cruise sponsored by: Deutsche Forschungsgemeinschaft (DFG)
Bundesministerium für Bildung und Forschung (BMBF)

Edited by
Gerhard Bohrmann and Greta Ohling
With contributions of cruise participants

The cruise was performed by
MARUM Center for Marine Environmental Sciences

Universität Bremen

marum

R/V METEOR Cruise Report M84/2

Table of Contents

PREFACE

Investigations of natural gas emission sites and gas hydrates within sediment deposits were the scientific mission. This expedition was based on former results of earlier cruises and on the experiences of our cooperating partners in Russia and Ukraine. Methane emission sites from the seabed are well known from sediments in the Black Sea, and we intended to define the emission rates of the methane using different methods. Methane emissions in the water column are connected to the presence of near-surface gas hydrate deposits. The quantification and the dynamics of gas hydrates are very important for geoscientists because methane as a greenhouse gas reaching the atmosphere can also be relevant for climate change. From sediments of the Black Sea the first gas hydrates ever had been recovered.

Fig. 1: Research areas in Turkey, Ukraine and Georgia of the Black Sea visited during R/V METEOR Cruise M84/2 from Istanbul to Istanbul.

The cruise and the research program were planned, coordinated, and carried out by the Earth Science Department and MARUM of the University of Bremen. We thank all participants and persons who contributed to this cruise. We thank the “Leitstelle” in Hamburg for all support in advance, during and after the cruise. The shipping operator (Reederei F. Laeisz GmbH) provided technical support on the vessel. We thank the captain Michael Schneider and his crew for the outstanding support. The German embassies in Tbilisi, Ankara and Kiev and the Ministry of Foreign Affairs in Berlin helped in obtaining the permission necessary to work in Ukrainian, Turkish and Georgian waters.

Fig. 2: Research vessel METEOR on mission in the Black Sea (left). Launching of the mobile drilling system from R/V METEOR during M84/2 (right).

Fig. 3: View inside the control container during drilling a MeBo drill site (left). The Dynamic Autoclave Piston Corer during the deployment onboard R/V METEOR (right).

Personnel aboard R/V METEOR M84/2

Table 1: Scientific crew

Name	Working group	Affiliation	Participation
Gerhard Bohrmann	Chief Scientist	GeoB, Bremen	Leg 2a & b
Emine Akasu	Observer	MTA, Ankara	Leg 2b
André Bahr	Sedimentology	IFG, Frankfurt	Leg 2a & b
Markus Bergenthal	MeBo	MARUM, Bremen	Leg 2a
Klaus Dehning	DAPC, Corers	MARUM, Bremen	Leg 2b
Volker Diekamp	Sediments	MARUM, Bremen	Leg 2a & b
Bettina Domeyer	Pore water	IFM-GEOMAR, Kiel	Leg 2a
Christian d. Santos Ferreira	Mapping	MARUM, Bremen	Leg 2b
Ralf Düßmann	MeBo	MARUM, Bremen	Leg 2a
Tim Freudenthal	MeBo	MARUM, Bremen	Leg 2a
Matthias Haeckel	Pore water	IFM-GEOMAR, Kiel	Leg 2a & b
Kenji Hatsukano	Sedimentology	IFG, Frankfurt	Leg 2b
Oliver Herschelmann	MeBo	MARUM, Bremen	Leg 2a
Hans-Jürgen Hohnberg	Autoclave tools	GeoB, Bremen	Leg 2a & b
Daniel Hüttich	DAPC	MARUM, Bremen	Leg 2b
Kai Kaszemeik	MeBo	MARUM, Bremen	Leg 2a
Thorsten Klein	MeBo	MARUM, Bremen	Leg 2a
George Komakhidze	Observer	BSMC, Batumi	Leg 2a
Eberhard Kopiske	AUV	MARUM, Bremen	Leg 2a
Jan-Hendrik Körber	Parasound	MARUM, Bremen	Leg 2a
Ulrike Lomnitz	Pore water	IFM-GEOMAR, Kiel	Leg 2b
Tatiana Malakhova	Observer	IBSS, Sevastopol	Leg 2b
Gerrit Meinecke	AUV	MARUM, Bremen	Leg 2a
Doris Meyerdierks	Media	HWK, Bremen	Leg 2b
Dimitry Nadezhkin	Sedimentology	MSU, Moscow	Leg 2b
Stefanie Oelfke	Multibeam	GeoB, Bremen	Leg 2b
Asli Özmaral	Parasound	ITU, Istanbul	Leg 2a
Thomas Pape	Gas analyses	GeoB, Bremen	Leg 2a & b
Elena Piñero	Pore water	IFM-GEOMAR, Kiel	Leg 2a
Vlad Rădulescu	Multibeam	MAREXIN, Bucharest	Leg 2a

Andreas Raeke	Meterology	DWD, Hamburg	Leg 2a & b
Anja Reitz	Pore water	IFM-GEOMAR, Kiel	Leg 2b
Jens Renken	AUV	MARUM, Bremen	Leg 2a
Michael Reuter	MeBo	MARUM, Bremen	Leg 2a
Miriam Römer	Flare mapping	GeoB, Bremen	Leg 2a & b
Uwe Rosiak	MeBo	MARUM, Bremen	Leg 2a
Heiko Sahling	Mapping/interpretation	GeoB, Bremen	Leg 2a
Marten Schmager	Multibeam	GeoB, Bremen	Leg 2b
Adrian Stachowski	MeBo	MARUM, Bremen	Leg 2a & b
Michal Tomczyk	Parasound	MARUM, Bremen	Leg 2b
David Wangner	Gas analyses	GeoB, Bremen	Leg 2b
Jiangong Wei	Sedimentology	GeoB, Bremen	Leg 2a & b
Paul Wintersteller	Maps	MARUM, Bremen	Leg 2a & b
Tingting Wu	Parasound	GeoB, Bremen	Leg 2b

Participating Institutions

BSMC	National Environmental Agency, Black Sea Monitoring Center, 51 Rustaveli Str., 6010, Batumi, **Georgia**
DWD	Deutscher Wetterdienst, Seeschifffahrt, Bernhard-Nocht-Str. 76, 20359 Hamburg, **Germany**
GeoB	Fachbereich Geowissenschaften, University of Bremen, Klagenfurter Str., 28334 Bremen, **Germany**
HWK	Hanse-Wissenschaftskolleg, Lehmkuhlenbusch 4, 27753 Delmenhorst, **Germany**
IBSS	A. O. Kovalevsky Institute of Biology of the Southern Seas, Ukrainian Academy of Sciences, 2 Nakhimov Av., 99011 Sevastopol, **Ukraine**
IFG	Institut für Geowissenschaften, Goethe-Universität, Altenhöferallee 1, 60438 Frankfurt, **Germany**
IFM-GEOMAR	Leibniz-Institut für Meereswissenschaften an der Universität Kiel, Wischhofstr. 1-3, 24148 Kiel, **Germany**
ITU	Istanbul Technical University, Department of Geophysical Engineering; Ayazaga Kampusu, Maden Fakultesi, 34469 Maslak Sariyer/Istanbul**, Turkey**
MAREXIN	Marine Resources Exploration International, 301-311 Barbu Vacarescu Blvd., 020276, District 2, Bucharest, **Romania**
MARUM	MARUM Zentrum für marine Umweltwissenschaften, University of Bremen, Leobener Str., 28334 Bremen, **Germany**
MSU	Geology and geochemistry of fuel minerals, Geological faculty Moscow State University, Leninskie Gory, 119992 Moscow, **Russia**
MTA	General Directorate of Mineral Research & Exploration (MTA); Üniversiteler Mahallesi Dumlupinar Bulvari No.139, 06800 Çankaya, Ankara, **Turkey**

Fig. 4: Groups of scientists and technicians sailed during Legs M84/2a (left) and M84 /2b (right).

Table 2: Crew members onboard

Name	Work onboard	Name	Work onboard
Michael Schneider	Master	Kai Rabenhorst	Seaman
Heike Dugge	Chief officer	Erdmann Wegner	Seaman
Helge Volland	Officer	Alexander Wolf	Seaman
Moritz Langhinrichs	Officer	Evg. Drakopoulos	Seaman
Volker Hartig	Chief engineer	Hans-Joachim Behlke	Seaman
Paul Dölling	Engineer	Manfred Gudera	Seaman
Ralf Heitzer	Engineer	Rainer Götze	Chief steward
Frederic Tardeck	System manager	Hans-Jürgen Gaude	Steward
Michael Reiber	SET	Torsten Dibenau	Steward
Olaf Willms	Chief electronics	Klaus Hermann	Cook
Eduard Fabrizius	Electronics	Mike Fröhlich	Cooks mate
Sebastian Frank	Locksmith	Gou Min Zhand	Laundry
Manfred Schröder	Motorman	Christian Otto Meyer	Trainee
Nils Clasen	Motorman	Allan Seemann	Naut. trainee
Klaus Kudrass	Motorman	Jan Erik Wilhelm	Trainee
Peter Hadamek	Bosun	Johann Anger	Trainee
Rainer Schaller	Seaman	Klaus Rathnow	Doctor

Shipping Operator

Reederei F. Laeisz GmbH “Haus der Schiffahrt”, Lange Str. 1a, D-18055 Rostock, **Germany**

1. Introduction and Geological Background

(G. Bohrmann)

1.1 Objectives

Recent drilling campaigns and quantification approaches of natural methane hydrate in marine sediments showed that we generally have to count with an inhomogeneous distribution of gas hydrates. This is relevant for both, the question of quantitative estimation of global methane hydrate concentration, and for the dynamics of formation and decomposition of methane hydrates, and processes in this connection (seepage, cementation of marine sediments, etc.). While the lowermost depth level of gas hydrate deposits is indicated by the presence of a BSR (Bottom Simulating Seismic Reflector), the uppermost depth level is hardly known although this would be of high relevance for the estimation of the total volume.

By means of the seafloor drilling device MeBo developed at the MARUM in Bremen, drill holes were planned to be used in order to understand the downhole distribution of methane hydrates in gas hydrate areas of the Black Sea. The use of newly developed autoclave technology for quantification of even small methane hydrate quantities was planned in addition. These analyses will deliver robust data which will generally contribute to a better understanding of the methane origin, the structure of gas hydrate and the fluid flow between sediment and water column. Emphasis of the analyses is the distribution and dynamics of gas hydrate deposits below the seafloor, in the upper 50 metres of the sedimentary column, from where methane can reach very fast the seafloor and also the sea water column and possibly the atmosphere. We are interested in understanding the methane flux and the gas hydrate distribution for the global carbon cycle. The anoxic Black Sea is highly suitable for those investigations because it is a marginal sea with the highest dissolved methane concentrations which are fed by several hundreds to thousands of methane seeps. With the drilling device MeBo and the autoclaves deployed on different positions of the drill string (similar to the ODP pressure core sampler) we will be able to sample the upper 50 metres in order to quantify the gas hydrate distribution.

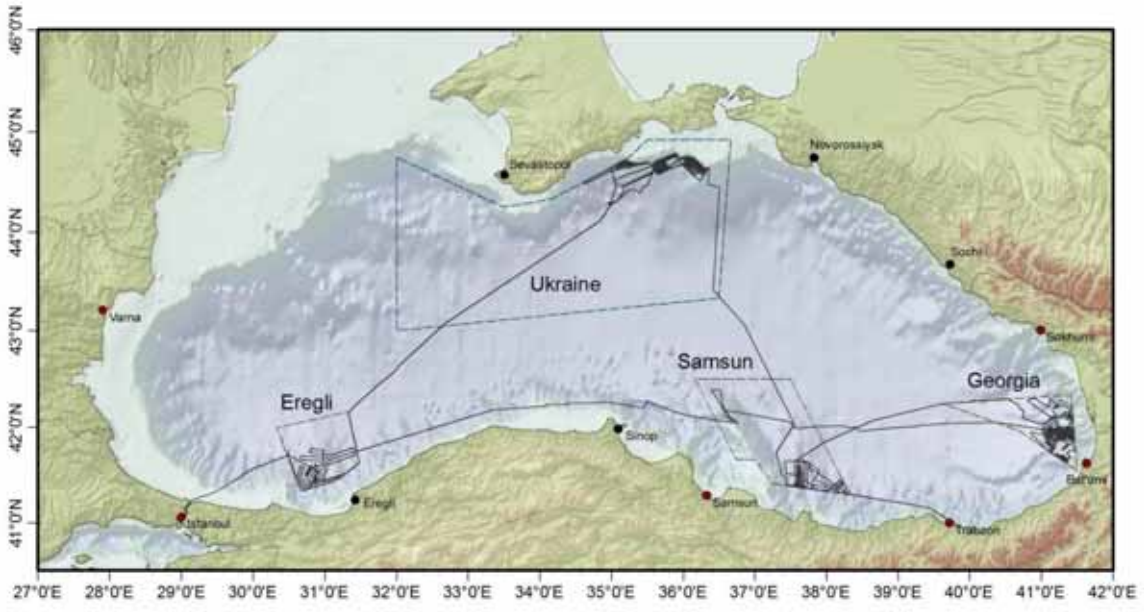

Fig. 5: Cruise track of R/V METEOR M84/2 within the Black Sea. Research areas in Turkey, Georgia, and Ukraine.

In detail we addressed the following questions:
- How much gas hydrate can be detected near the surface in and outside the seep areas, and how much gas hydrate appears in deeper areas?
- Which textures, which fabrics and which gas hydrate structures (sI, sII, sH) can be found from gas hydrates, which relations in the depth distribution occur? Are there any rock veins or cemented tracks, or is the gas hydrate dispersed or enriched in layers?
- In which depth generally upper level of gas hydrate deposits are to be found, which mainly should be governed by dissolution processes?
- Can the pore water gradients give answers regarding the establishment or the dynamics of this upper level?
- Can we prove a fast gas rise with a formation of gas hydrate and salt concentration in the seep areas? Which fluid flows occur? Transport of a free gas phase versus dissolved gas in the fluid?
- Which hydrocarbons are to be found in gas hydrates? How is the interaction with the gas hydrate phase? What are the differences between seep and non-seep locations?

The main program were the gas hydrate drill sites with MeBo which were planned to be accomplished down to a depth of 50 resp. 70 metres in the sediments of the Black Sea. Preliminary investigations had been accomplished during the past 10 years in the Black Sea during several expeditions and contained multichannel-seismic and Parasound records, sidescan sonar profiles, partly AUV micro-bathymetric maps, data from ROV dives and sediment sampling from upper layers. MeBo drill sites allowed now deeper insight in sediments and gas hydrates down to tens of meters. The pore water was analysed in several ways (nutrients, inorganic species and stable isotope measurements) both, on board and at home labs of the working group IFM-GEOMAR. Gases and other hydrocarbons and their isotope relations were analysed, as well as the sediments and carbonate precipitates.

Gas hydrate samples were preserved in liquid nitrogen and will be examined by CT-analyses regarding their structure, as well as mineralogical, petrological, geochemical work (cryo-XRD, gas chromatography, cryo-SEM, synchrotron measuring, etc.). Supplementary to the MeBo drill sites, also gravity cores, DAPCs, and AUV micro-bathymetrical mapping (AUV SEAL) were accomplished. Flare imaging and sediment-stratigraphic analyses with the ship's own Parasound device have been quite succesfull. The cruise leaded through the territory of three countries (Fig. 5) to the areas of Eregli at the western and Samsun at the eastern Turkish margin (Turkey), to the Caucasian Continental Rise (Georgia) and the Sorokin Trough (Ukraine). For exchange of observers we had a stopover in Trabzon (Turkey).

1.2 Black Sea Overview

The Black Sea is located north of Turkey and south of Ukraine and Russia. To the West it is bordered by Romania and Bulgaria and to the East by Georgia. It is a marginal ocean with a water depth of 2-2.2 km. The Black Sea is surrounded by Cenozoic mountain belts like the Great Caucasus, the Pontides, and the Balkanides (Fig. 6; Robinson, 1997). Two deep basins, the western and eastern Black Sea basins, are underlain by oceanic or thinned continental crust with a sediment cover of 10-19 km thickness (Tugolesov et al., 1985).

The area changed to a compressional regime during the Eocene, and the tectonic evolution

of the basin is characterized by a subsidence history that resulted in the separation of the two basins (Nikishin et al., 2003). Modern stress field observations from structural data, earthquake foci, stress field measurements onshore in the Crimean and Caucasus regions, and GPS data show that the Black Sea region is still in a dominantly compressional environment (Reilinger et al., 1997; Nikishin et al., 2003). The general source of compression is the collision between the Arabian, Anatolian, and the Eurasian plates (Fig. 6).

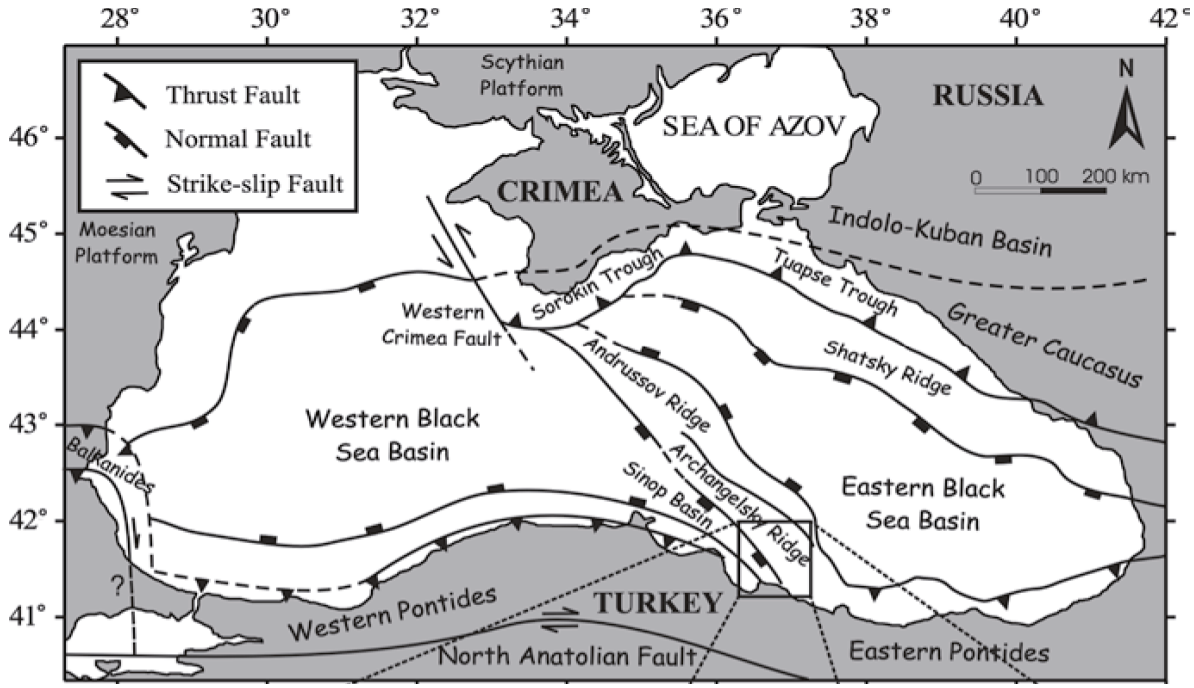

Fig. 6: Simplified tectonic map showing the major tectonic elements of the Black Sea (from Çifçi et al., 2003).

The basins are separated by the Andrusov Ridge which is formed from continental crust and overlain by only 5-6 km of sediment. The origin of the Black Sea is interpreted as a back-arc basin evolved during late cretaceous times (Nikishin et al., 2003). The Sorokin Trough is a foredeep basin of the Crimean Mountains belonging to the eastern basin of the Black Sea. It forms a large depression, which is 150 km in length and 50 km in width, southeast of the Crimean Peninsula (Tugolesov et al., 1985). A large number of its mud volcanoes evolved from diapiric zones in a compressional regime between the Cretaceous to Eocene blocks of the Tetyaev Rise and the Shatsky Ridge (Tugolesov et al., 1985). The sediments extruded in the mud volcanoes are clay-rich deposits from the Maikopian Formation that forms an Oligocene-Lower Miocene sequence of 4-5 km in thickness. The Maikopian Formation is overlain by at least 2-3 km thick Pliocene to Quaternary sediments. A second foredeep basin specially filled with thick Maikopian sediments forms the Tuapse Trough which strikes parallel to the northeast coast of the Black Sea. Similar to the Sorokin Trough, the basin was compressed between the Shatsky Ridge and the Greater Caucasus (Nikishin et al., 2003). Sediments from the Caucasus fold belt are overthrusting deposits of the Tuapse basin to the west.

2. Cruise Narrative

(G. Bohrmann)

On Saturday 26 February, 2011 R/V METEOR left at 1 p.m. local time her place situated on Ahirkapi roads, south from the Golden Horn of Istanbul and reached the Black Sea after crossing the Bosphorus. Before sailing the R/V METEOR had a demurrage of only 4 days in the port of Istanbul while scientists and scientific devices for the legs 1 and 2 were exchanged. New devices on board are the seafloor drill rig MeBo and the autonomous underwater vehicle AUV SEAL 5000. In total 10 containers were loaded which had been sent from Germany to Istanbul with our scientific working materials. The scientists from Germany, China, Austria, Spain, Georgia, Romania and Turkey embarked between 22-24 February, and used the time for the necessary work on deck together with the ship's crew, and also to set up the labs.

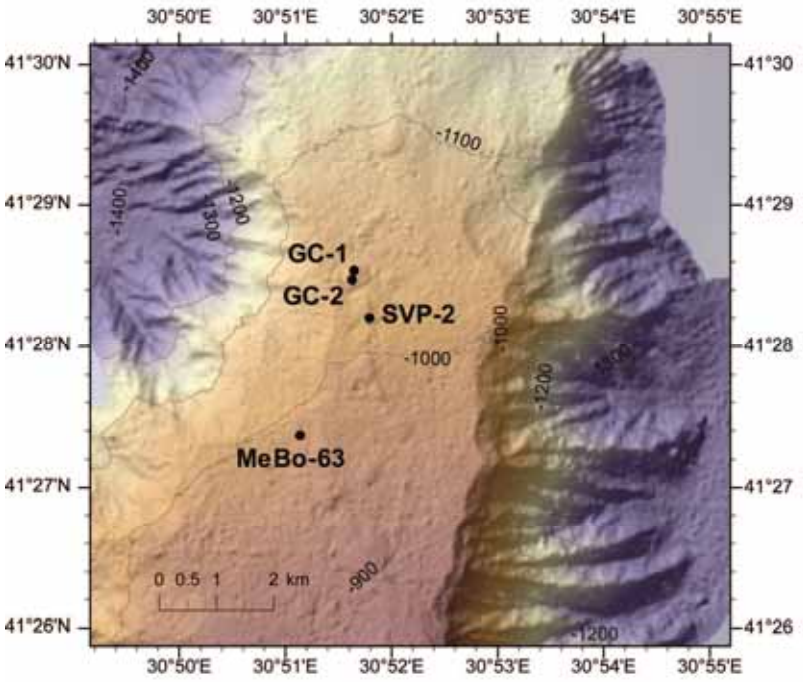

Fig. 7: Location map from area Eregli at the western continental margin from Turkey.

Entering the Black Sea we first of all were surprised by the heavy swell and the strong wind. But according to the forecast the wind turned down in the second half of the night, and at breakfast time everyone seemed to be quite healthy again. During the night we also reached the first working area at Eregli, and we started to record the data from the multi-beam EM122 and the PARASOUND systems. Due to scientific information from former cruises we could find acoustic anomalies in the water column very fast with the PARASOUND, which showed us strong emissions of free gas into the water column.

During the second week of our cruise first of all we investigated methane emissions in the western working area of the Turkish sector (Fig. 7). If free methane escapes from the seafloor deeper than 750 m water depth the emission of gas is always associated with methane hydrate occurrence in the sediments. The 750 m water depth at 9° C marks the upper stability boundary for methane hydrate of structure I within the Black Sea. For different reasons we wanted to examine more in detail those methane hydrate occurrences during our 5-weeks expedition in the Black Sea. Earlier samplings could prove methane hydrates down in the sediment to about 3-4 m

below seafloor, and with the portable drilling system MeBo we can penetrate the sediments even deeper, to understand also there the methane hydrate spreading.

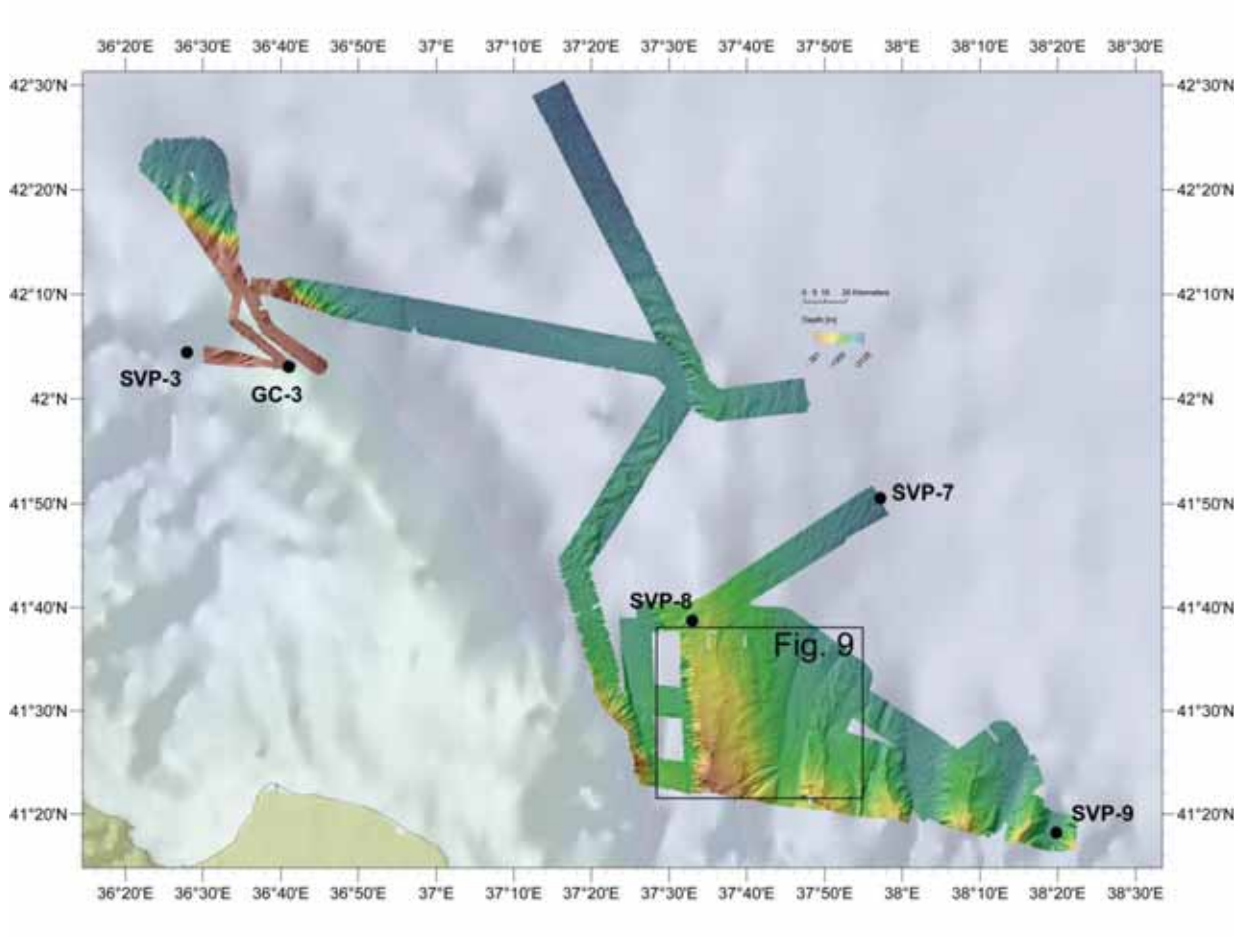

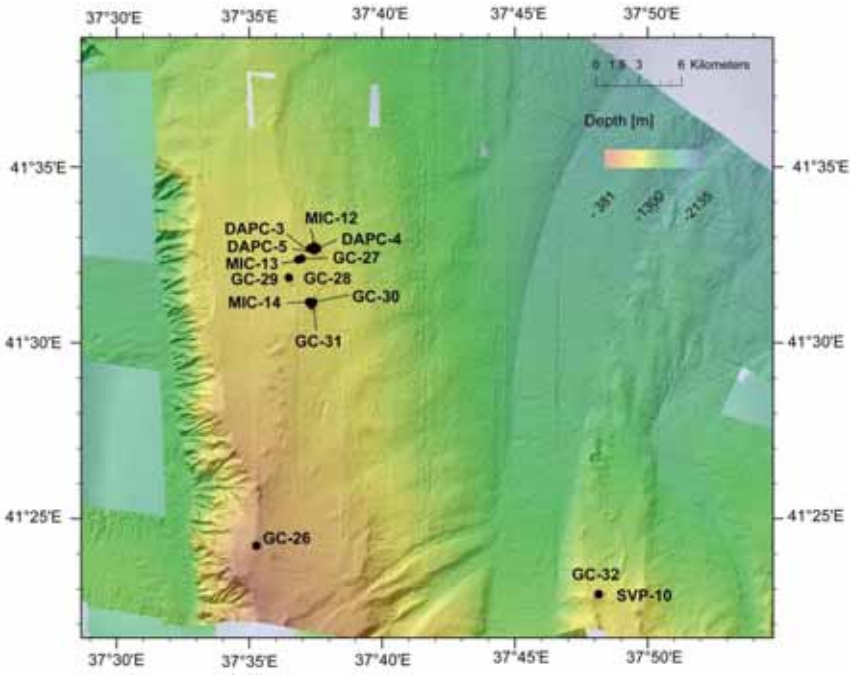

Fig. 8: Overview map of the Samsun area (above). Box is showing the location of Ordu Ridge (see details in Fig. 9).

Fig. 9: Sampling locations on Ordu Ridge, which was newly named after the city Ordu at the coast of Turkey.

There is the imagination that a relatively high quantity of methane hydrate occurrences exists in the oceans - thus there are only few quantitative measurements available which could give a

solid estimation on this. With our drillings we want to give a contribution regarding the distribution and quantification of methane hydrates in the Black Sea. For this we took advantage of any preliminary investigation, and we plan drilling profiles with the Bremen seafloor drill rig in two areas of Turkey (Eregli and Samsun), in Georgia and towards the end of the cruise also in Ukraine.

The acoustic systems of R/V METEOR, the multibeam echosounders EM122 and EM710 and the PARASOUND system were the most important tools we applied during our search for methane hydrate occurrences. For instance we intensively applied these echo sounders in the western Turkish work area of Eregli in water depths around 1000 m on a plateau-like ridge, framed by two canyon systems. We had in hands a sidescan sonar map from a former cruise of R/V POSEIDON showing round structures on the seafloor of about 350 m in diameter and giving a hint on gas and gas hydrate. These round gas ascent zones in the sediments could be traced in the backscatter signals of the new EM122 mapping whereas we found more than twice as many of those structures. The result was really amazing, and we could say that the EM122 system installed last year on RV METEOR enables a highly expanded application compared with the former EM120 system. Further for the first time also gas emissions in the water column could systematically be detected, which up to now could only be visualised directly under the ship with PARASOUND. Drilling with MeBo at Eregli (Fig. 7) showed only a drilling result of a few meters, at least it sampled young sediments of the classic Black Sea sequence which we could not have sampled with the gravity corer in this area with considerably higher sedimentation rates. Further drillings in this area we saved for our way back to Istanbul.

The further course of the expedition followed the Turkish Black Sea coast to the East into the next working area near the city of Samsun. Also there, in the later process of the cruise, drillings shall be accomplished at Archangelsky Ridge (Figs. 8 and 9). The side trip was only short, and our course led us to the Georgian continental margin - our main work area (Fig. 10). We arrived there on Thursday, 3 March, and also here we started with the acoustic systems to map known seep structures whose activity is documented for several years already, in order to understand the dynamic of a methane hydrate area over a longer period. For instance we have an area at Batumi seep of half a square kilometre size whose gas hydrate presence in the upper 2.5 m of sediments was quantified to represent 5,000-10,000 tons of methane. Alone the gas flow of free methane in the water column is in the range of 55 x 106 mol per year and seems considerably increased during our actual mission. The weekend brought us fantastic weather which did not only give good conditions for the deployment of our devices but also a spectacular view on the surrounding snow-covered mountains in the southeastern-most corner of the Black Sea. About 50 m from the coast, in the South, we could see the mountain chain of the Eastern Pontides in Turkey, whereas the eastside gave a free view on the as well deeply snow-covered mountain chain of the Caucasus. In between we saw the more than 5,600 m high twin peak of the Elbrus Mountains.

The third working week was entirely dedicated to the investigation of gas hydrates off Georgia, and we wanted to investigate in the depth the earlier well pre-investigated seepage areas of Batumi seep and the Pechori Mound by MeBo drillings. Yet on Saturday evening we started the drilling at Pechori Mound. The Pechori Mound is an active, relatively high in seafloor morphology seep structure overtopping the seafloor by several tens of meters. We could core a sediment sequence of about 20 m providing in the majority massive gas hydrates. Above all the

thickness of the gas hydrate layers were surprisingly high. The gas hydrates were associated with natural oil so that the originally white gas hydrates were stained in yellowish brown. Big pieces of gas hydrate were frozen in liquid nitrogen for further analyses in our lab. Altogether this drilling was highly important to understand the formation of the Pechori Mound. This is one of a few structures in the Black Sea releasing constantly oil drops up to the water surface which can be observed for years already as thin oil slicks in satellite imaging analyses. We used those satellite imaging analyses to even find the seepage areas like Pechori Mound.

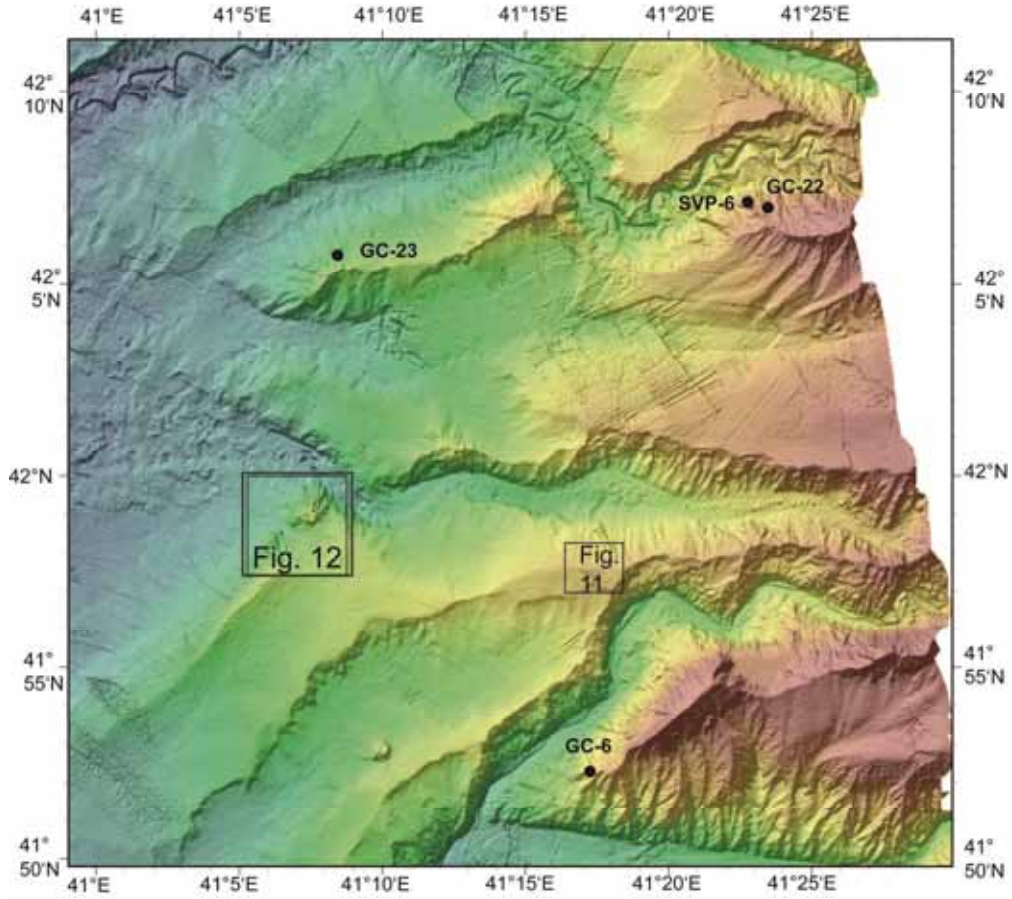

Fig.10: Overview map from the Georgian sector with sample locations on Kobuleti Ridge (two boxes shown in detail in Figures 11 and 12), Adjara and Kulevi Ridges.

During the following nights we mainly performed profiles with the ship's own acoustic systems where we measured repeatedly the already known gas seeps in order to understand the time variability of the gas emissions. Monday night we investigated a so far unknown area at Kulevi Ridge (Fig. 10), and also there we detected massive gas flares in the water column whose emissions almost reached the water surface. At this occasion we learned to combine the single beams of the echo sounder EM122, which often show due to the narrow overlapping of the water column, and to compose them in a 3-D-illustration to a very realistic image of the single gas plumes in the water column. Much to our surprise we now could see that the upper ends of the gas plumes are clearly influenced by the flow conditions in the water. This might explain why in the 2-D-profiles view normally the gas plumes are cut to the upper end. It is an important conclusion that this is not true, but that the gas definitely migrates towards the water surface.

On Thursday March 3 we started the MeBo drillings at Batumi Seep (Fig. 11), our most important seep area. During a 20-hours deployment we could proceed only very slowly as the

soft sediments of the Black Sea lead to a heavy sinking of MeBo, and therefore the motors of the drill rig constantly had to be cooled before continuing the drilling. Up to a drill depth of 10 m we could drill plenty of gas hydrates which are very valuable for our scientific examination in Bremen. Unfortunately, due to damage at the drill rig we had to cease our drilling activities for this cruise. Also the second hydraulic pump was broken during the drilling procedure so that we did not have further replacement parts in order to repair the drill rig by ship's means. Probably the heavy load of the engine caused to a repeated breakdown of the pumps. This means that despite of the high efforts of the MeBo drill team we could not further deploy our very important tool for this expedition. During an emergency meeting in the afternoon we discussed the consequences for our scientific program. After an intensive discussion we decided that it will be possible to successfully continue the last part of our expedition also by means of the remaining devices. We therefore decided to disembark the MeBo team and the drill rig on the occasion of our port stay in Trabzon at the forthcoming Thursday/Friday in order to continue the M84/2 expedition without drilling activities for the last 1.5 weeks. First of all this is a good opportunity to use more intensively than originally planned the echo sounder and PARASOUND systems in order to study gas and gas hydrate occurrences. Since Friday we accomplish an intensive core sampling program in Georgia.

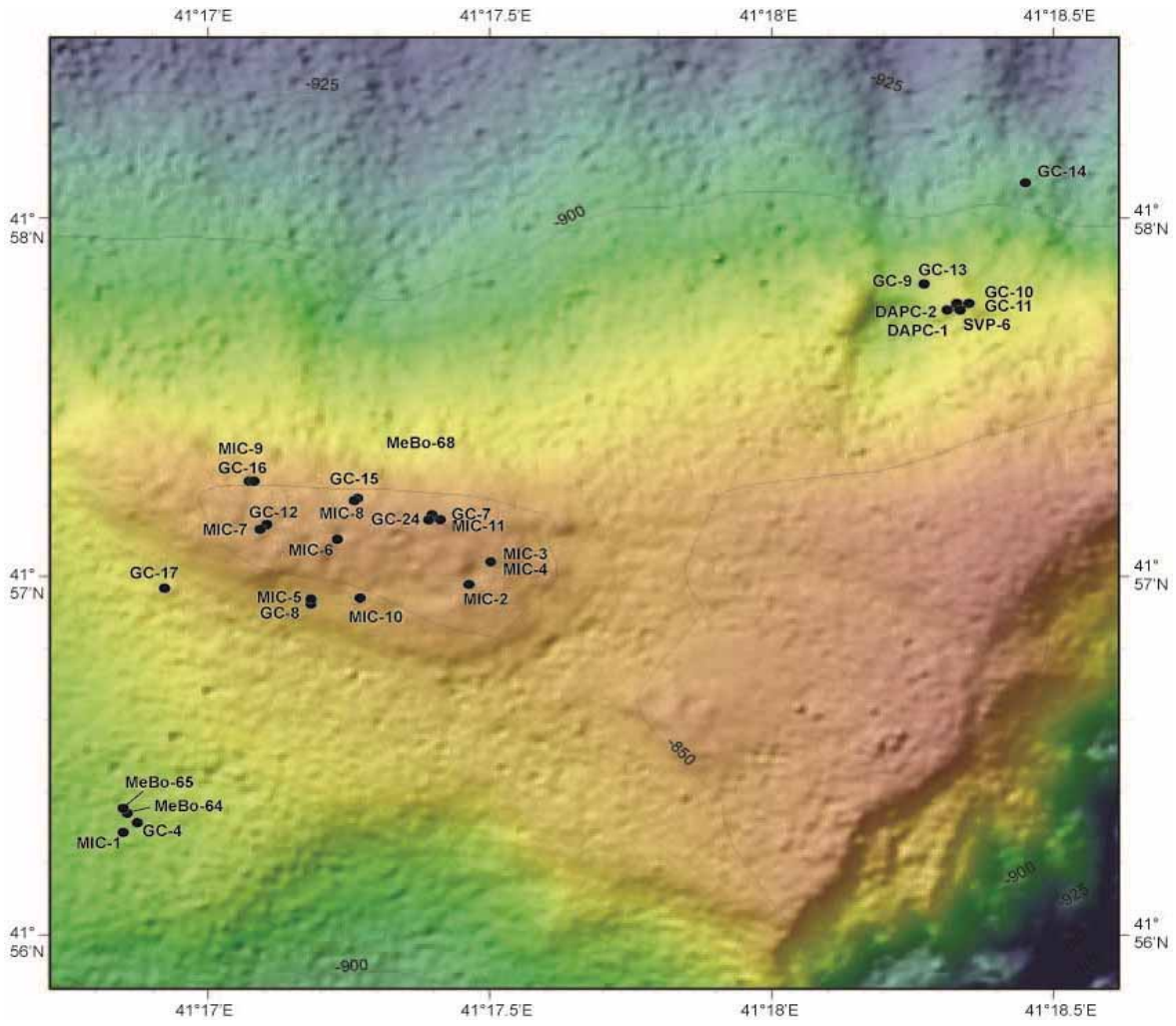

Fig. 11: Map showing the Batumi and Poti seep areas on Kobuleti Ridge and sites sampled during M84/2 (for location see Fig. 10).

At the beginning the fourth week of the cruise was related to an intensive sampling program at the different seep locations in Georgia. On this occasion for the first time during this cruise the dynamic autoclave piston corer (DAPC) could be deployed for sampling the upper 250 cm of the sediments. Besides the sediments also gases and gas hydrates were sampled under in-situ pressure of the seafloor in the pressure-tight autoclave. While during the normal sampling using the gravity corer the gas fractions get lost in high quantity and the gas hydrates decompose because of the pressure reduction during heaving, the gases and gas hydrates in the autoclave survive and allow a quantitative determination. The DAPC deployment at Poti Seep (Fig. 11) was successful, more than 230 litres of gas could be determined corresponding to 15-25 % of an average gas hydrate concentration. This average concentration which was confirmed in further measurements can be well integrated by an estimation of the area based on our backscatter map, so that we can develop a pretty precise estimation on the gas hydrate content in the entire seep area. In the further course we could recover gas hydrates from all the seeps we know in the working area in Georgia and also at three completely new locations, and will analyse them in our labs onshore for their composition and structure. These new seeps we had discovered by their oil slicks are shown in satellite imaging (Fig. 12). The hydro-acoustic measurements of these oil seeps showed that they are connected to gas emissions, and the sampling proved that near the seafloor gas hydrates can be encountered. The gas-chromatographic analyses we made on board with regard to the gas composition showed that we already now have quite different sources, whereas the deep thermogenic gas sources can clearly be distinguished from the biogenic generated methane sources. According to the different gases also different gas hydrate structures should exist which we will only be able to examine at home.

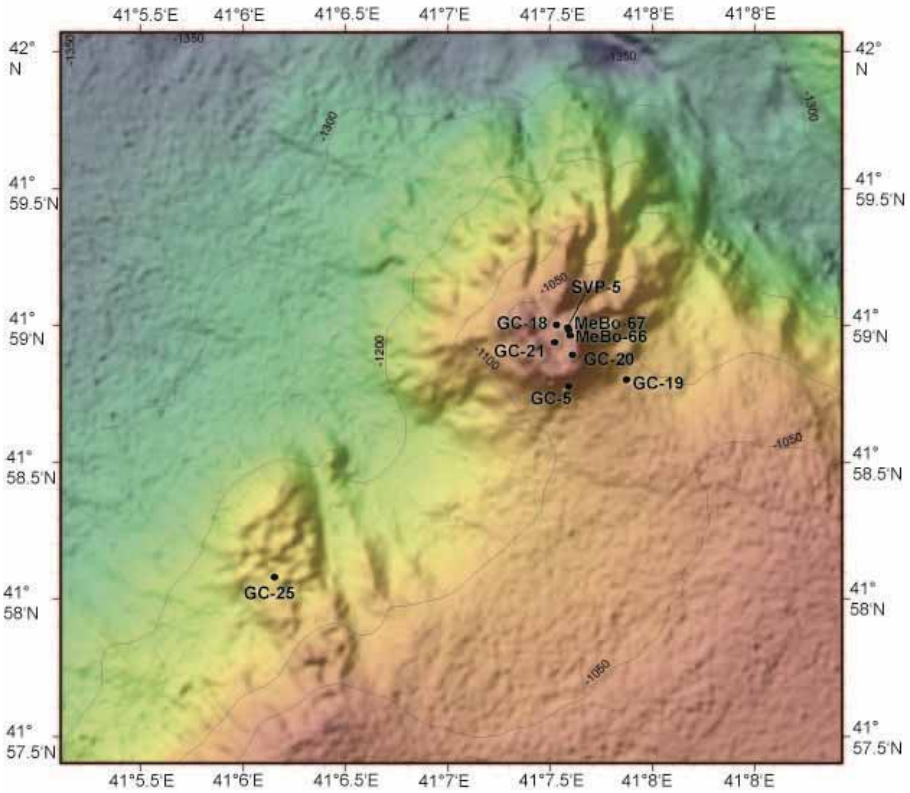

Fig. 12: Location map including the seep areas of Colkheti Seep and Pechori Mound on the nortwestern flank of Kobuleti Ridge (for location see Fig. 10).

After this intensive deployment of our devices we left the working area in Georgia on Tuesday and arrived at the Samsun working area in Turkey after a 7-hour transit. Also here several areas with a higher backscatter signal on the seafloor in 1,200-1,400 m water depth were known from former expeditions, and we had the suspicion that also these were gas emissions on the seafloor. Here again we used the EM122 and tried to compare the backscatter pattern measured with the deep-towed Sidescan Sonar with the backscatter images of the EM122 mapping. We were surprised to find identical figures of structures in the areas of the overlapping measurements, which made us map the entire ridge during the first night. We found that we could trace 22 areas with higher backscatter signals along the approx. 25 km ridge, half of the patches showing active gas emissions to the water column. A sampling program with the gravity corer on five of these patches with higher backscatter proved that everywhere gas hydrate was abundant so that we could clearly document the rise of gas from the underground. The gas emissions seem to follow a tectonic line. As the ridge up to now was unnamed, and we intend to publish our investigations, we named this ridge in accordance with our Turkish colleagues on board Ordu Ridge (Fig. 9). The ridge can be morphologically clearly separated and is situated in a South/North prolongation of the provincial town Ordu, so that we think to have found a suitable name for our subject matter of investigation.

On Thursday, March 17 R/V METEOR entered the port of Trabzon in order to embark part of the scientific crew and also the expedition equipment on Thursday and Friday. On Saturday we moved back to the Samsun working area where we accomplished our final investigations. After that we planned to accomplish further scientific work in the Ukraine.

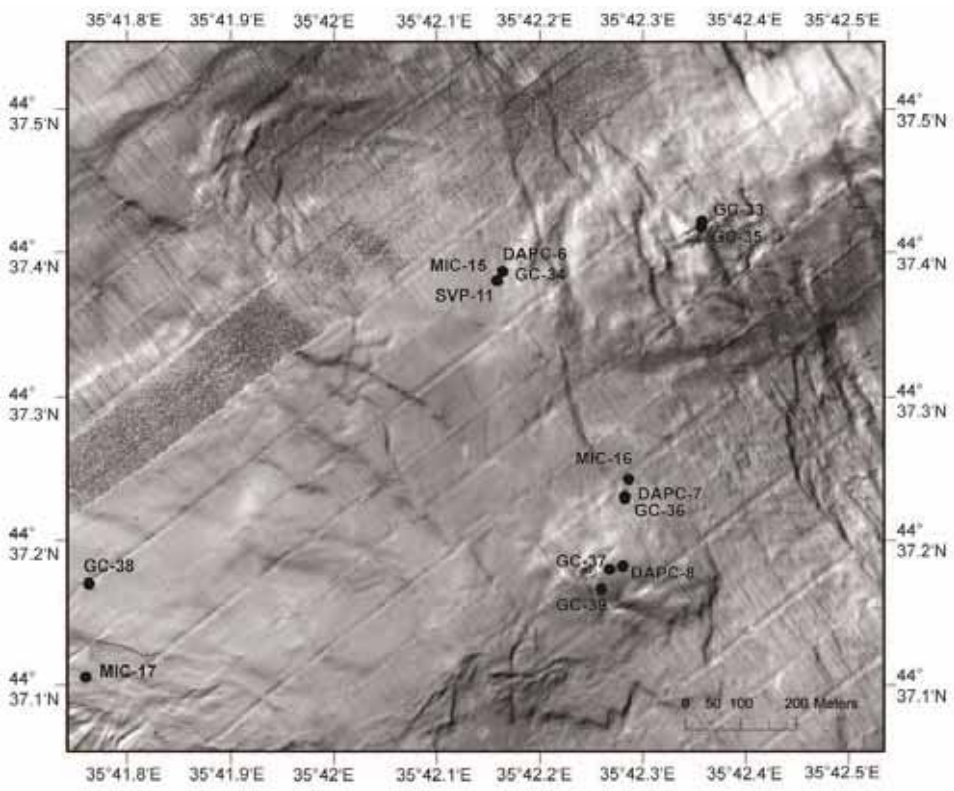

Fig. 13: Micro topography of Kerch Flare area measured during AUV deployment 35 (MSM 15/2) with locations of samples taken during M84/2.

During week 5 of our cruise we completed the work in the Turkish working area Samsun. This work was first limited to the Ordu Ridge but could be expanded to two parallel running ridges by using multi beam echo sounder and PARASOUND mappings. Furthermore, by registration of very clear backscatter signals, active gas seeps at the hilltops and plateau-like ridges could be mapped. A large part of the seep areas showed both, active gas emissions in the water column and gas hydrate occurrence in the sediments. After a final measurement up to the edge of the Turkish area we started the transit to Ukraine. The transit to that working area was very exhausting as under strong wind around 8 Beaufort the METEOR could proceed only very slowly. With just 4-5 knots METEOR fought through the waves of up to 4 m, and this was especially for the scientists who had embarked in Trabzon a first practical test at sea. After passing the Ukrainian border we switched on again the acoustic systems on board the METEOR in order to obtain sufficient geophysical data during our trip to the Kerch deep sea fan. Unfortunately the quality of data also suffered due to the strong swell so that we had to be a bit patient with our mapping until the sea calmed down. But this is easy in the Black Sea because of its limited water volume and if the wind ceases a bit.

In Ukraine our first destination was a strong gas emission site in a water depth of 900 m which is well-known by the name Kerch Flare. South of Kerch Strait, in the exit of the Sea of Azov, in the prolongation of the Kerch Peninsula the Kerch deep sea fan is developed, which is an area of considerable high sediment accumulation with a high potential of methane production. This situation is similar to the Danube and Dnieper deep sea fan. At water depth shallower than 700 m above the gas hydrate stability zone hundreds of gas emissions were found whereas below this zone gas flares in the form of acoustic anomalies in the water column occur only infrequently. Nevertheless these gas emissions are of a certain importance - a good portion of gas is bound in gas hydrates - but the emission of free gas also means that there is a spill-over of gas that cannot be bound in hydrates any more. Kerch Fan is such a highly active system, and we had been able to quantify the gas emissions during several ROV dives during MSM15/2 expedition by means of optical methods. We did not succeed with a gas hydrate sampling then, although gas quantities had been quantified from two autoclave piston corer samplings which clearly gave hint of the presence of hydrates (Fig. 13). This time at once the sampling of a sediment core rich in gas hydrate succeeded as we could locate the emissions more exactly. An extensive sampling program was executed until Thursday evening. The night as well as the entire Friday we used for mapping on the continental slopes of Kerch deep sea fan, development of the mountains as well as the Crimean Peninsula. These showed how dependant on the landward side the continental ridge shows completely different morphologies. For instance we found very much and closely lying canyon systems below the Crimean mountains which considerably furrowed the slope by downward transport of rocky material. On the slope of the delta, however, we can see single sliding bodies, especially in the high resolution bathymetry of EM710 multibeam echo sounder, which give a completely different structure to the continental slope.

A further peak waited for us at the weekend when we visited a bit more in the West at Sorokin Trough the closely related mud volcanoes Dvurechenskii and Helgoland. Both were fed with mud from the underground by the same diapir structure whereas Dvurechenskii is filled up to the edge with mud, and Helgoland shows a caldera-like depression whose mud filling is just in the beginning. During our last year's expedition both were active and showed strong gas emissions whereas this time only Helgoland mud volcano showed activity. Also here we could

sample gas hydrates for the first time in the closer edge of Helgoland whereas the direct emission point is too warm for the hydrate generation according to our temperature measurements in the sediment. The gas hydrate pieces we recovered showed a pervasive structure which during closer examination turned out a typical bubble structure.

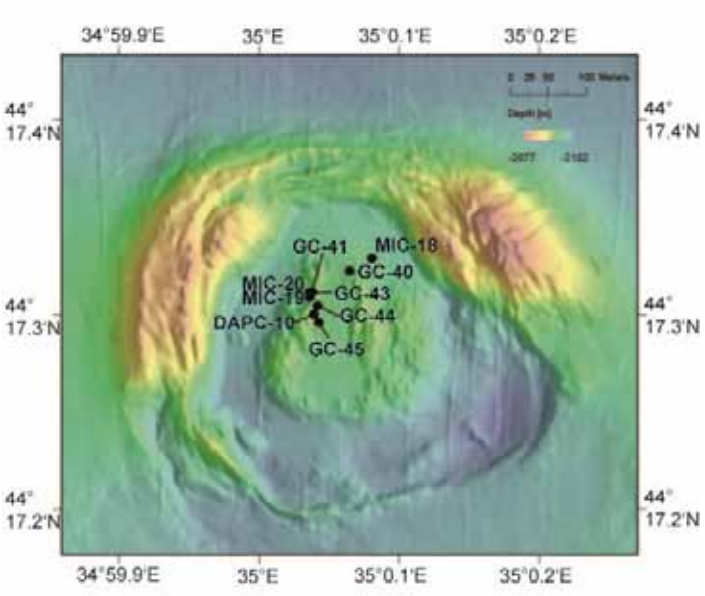

Fig. 14: Sample locations in the centre of Helgoland mud volcano.

On Sunday we had already visited the two mud volcanoes Dvurechenskii MV and Helgoland MV and had recorded gas activity by acoustic analyses as well as we had sampled sediments of the mud volcanoes. With this we wanted to continue next day. But meanwhile our little post-processing group on board had completely processed the multibeam echo sounder data measured so far along the Ukrainian continental slope, and we looked amazed at the brilliant maps. Though there were unfortunately several blanks in the data due to the lack of time which we would rather have liked to fill in by reproduced measurements.

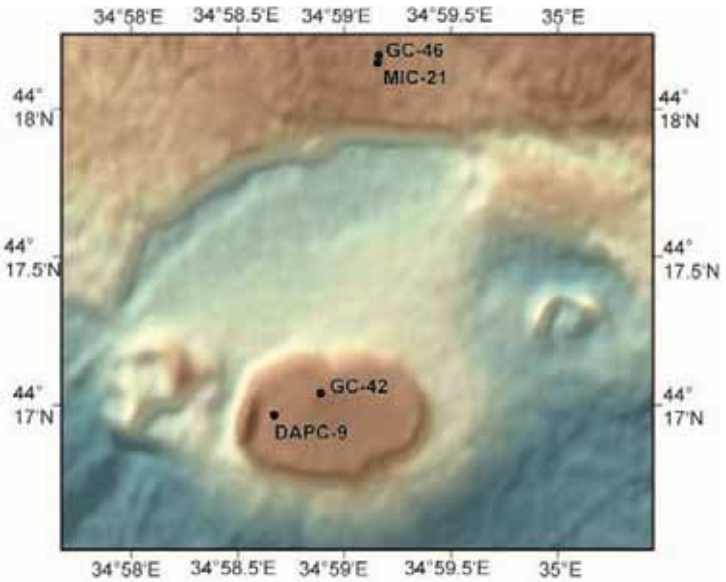

Fig. 15: Sample locations on Dvurechenskii mud volcano and background stations. Locations on Helgoland mud volcano are shown in Figure 14.

Furthermore we found a couple of gaps in the backscatter intensity maps which we liked to fill by further measurements. We therefore quickly decided to plan a further measuring day in the area of Kerch Fan in order to substantiate the pressing questions with further data. So far we had left behind an area in the North on the Ukrainian Shelf, which had been restricted for us because of military exercises for several days from 7:30 a.m. until 11:30 p.m. We had hoped now to have another chance to measure those parts of the shelf by this new measurement. But on Monday morning the vessel received another message which restrained us from doing so. We had to give way once again. But in the end we could fill in the gaps during the measurements on the upper continental slope, and so we could achieve a complete detailed image from this highly interesting slope morphology giving us an important insight into the geological processes. We were astonished about the highly detailed structures which are characterized by the down-slope transport. The overlaying areas with high backscatter intensity turned out as areas with stronger gas emissions which strengthens our work hypothesis of quantifying these emissions.

On our way back to the West to the two mud volcanoes we crossed numerous mud volcanoes among which the Tbilisi MV, the Odessa MV, Vodianitskii MV as well as the NIOZ mud volcano clearly showed activities in the form of flares. Also the Dvurechenskii mud volcano now showed a definite gas flare in its centre. The mud volcanoes of the Sorokin Trough in general are related to the zone of diapirs formed by the Maikop Formation in the underground. In the cap area of the mud diapirs, due to the higher gas pressure, often appears break-through of relatively liquid and gas bearing mud channelling upwards along discontinuities and developing cone-like structures on arrival at the seafloor which we consider the virtual mud volcanoes. The Sorokin Trough itself is characterized by crustal compression supporting the diapir-like uplifting of the mud formation and which had been shaped in the course of the Caucasus mountain's development. Back to the two mud volcanoes, the Dvurechenskii and the Helgoland MV, both turned out active whereas two days ago the Dvurechenskii seemed to be in a calm phase. A precise analysis of echo sounder data taken two days ago thus showed that the Dvurechenskii MV had already been active, however, we could not see this in the proximate profile below the vessel. An 18-hours long sampling program followed up mainly at Helgoland mud volcano, and we could take highly interesting sediment cores (Fig. 15). One gravity core was very near to the conduit of the mud volcano where we measured temperatures of about 20° C and we could directly sample fluids rising from very deep. The extremely high ammonium concentrations of the pore waters give a hint on special diagenesis conditions occurring in greater depth. Ten meters beneath we could sample gas hydrates with a gravity corer, i. e. there the temperature is already lower than 16° C. A bit deeper in the area of the edge of the inner volcano structure we had already 9° C corresponding to the normal bottom water temperature in the deep Black Sea. After further measurements at Ukraine and in Turkey we finished our station and profile work of this cruise on Friday, 1 April at 10:37 a.m.

The cruise finished on Saturday April 2, when RV METEOR finished the passage through the Bosphorus and reached the berth of Haydarpasa (berth 13) at 19:12. This was around one day later than planned, because of the intensive fog in the channel which strictly limited the passage and as many other ships RV METEOR was forced to wait at the entrance of the channel.

3. Sound Velocity Profiles (SVP)

(P. Wintersteller, M. Roemer, J. Körber, H. Sahling)

Investigations on the oceanography of the Black Sea over the last 30 years show complex coastal to open water-body interactions, based on major and minor eddy-like structures linked to meandering rim currents (e.g. Tolmazin, 1985; Oguz et al., 1996).

The related seasonal and local variability of the sea surface temperatures of the Black Sea (Oguz et al.1993, Ginzburg et al., 2004) is affecting the sound velocity of this water masses remarkably. Since a proper sound velocity is essential for accurate acoustic underwater distance measurements 14 sound velocity profiles (SVP's) have been taken during this cruise. SVP8 failed due to problems with the power supply cable. Two profiles, one off Turkey, near Eregli (SVP1) and one off Georgia (SVP3) are complete profiles through the water column. These profiles show just minor change of <0.5m/s in sound velocity below 300-400m water depth. The highest variability in sound velocity can be observed in the uppermost 200 m of the water column (Fig. 16; Cruise Report MSM15/2, Bohrmann et al. 2011).

A shipside SvPlus 3453 probe was used to acquire the SVP's. The probe is rated to a maximum of 2000 m water depth. It is measuring sound velocity directly and additionally records pressure and temperature. SVP1, 2 and 14 were taken off Eregli. One can clearly see an exchange of water masses and temperature within this month, comparing the three curves.

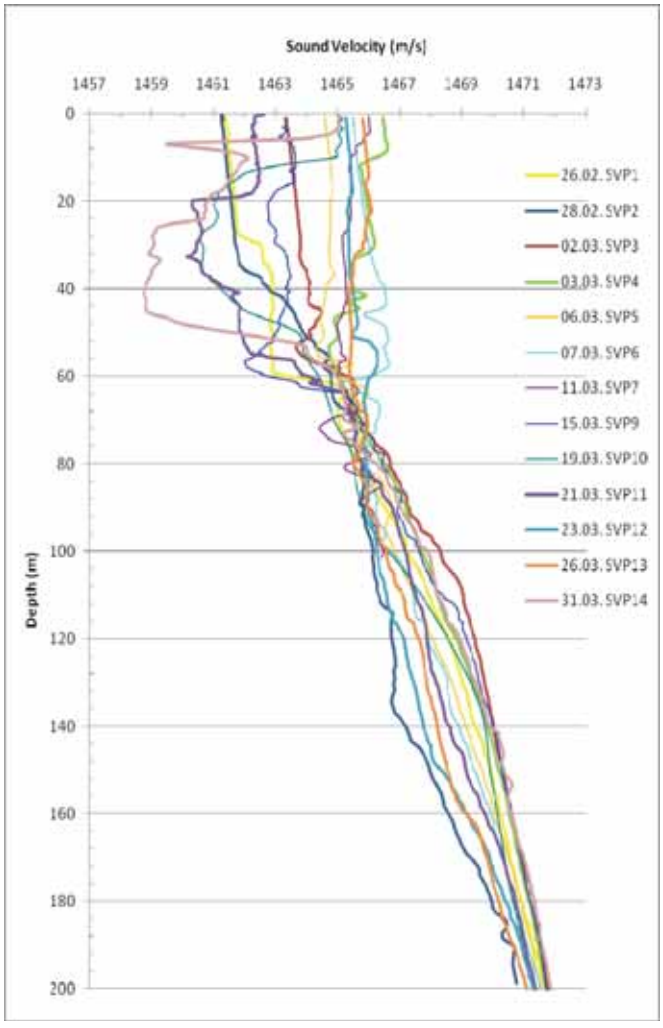

Fig. 16: Sound velocities of the uppermost 200 m water column.

After every SVP acquisition the profile has been applied to the Kongsberg's acquisition software SIS in order to collect corrected multibeam echosounder (MBES) data. Beside the MBES, the sound velocities have been used for ultra short base line (USBL) IXSEA POSIDONIA and the ATLAS PARASOUND sub bottom profiler. The later has just two values to be given, a mean SV and the SV at transducer. To be as accurate as possible the MBES are supplied with real time SV from a shipside mounted SV-Probe. This probe is located within the ships salt water supply station, next to the thermosalinograph. It turned out, that the temperature of the water pumped into vessel is about 0.5-1° C above the temperature at the transducers. Also, the water measured in the vessel comes from 2-3 m below sea surface where else the MBES-transducers are at a depth of about 5.8 m. The measured SV in the vessel shows an offset of 2-3 m/s to the expected SV at transducer. We decided to use the SV at transducer from the SVP's taken during this cruise. This setting can be done in the acquisition software SIS.

4. Underwater Navigation

(H. Sahling, P. Wintersteller)

The POSIDONIA ultra short baseline system (USBL) is available at METEOR for sub-positioning of underwater tools (GC, MIC, DAPC, LDP). It consists of a permanently mounted antenna on the ship's hull, the ships powering and processing unit and three underwater transponders that can be mounted on the tools. These are the minitransponders with the serial numbers 069 and 070 and a releaser combined with a transponder (serial number 413). During the Cruise M84/2a two of the transponders (070, 413) were deployed several times but did not work. The only transponder that worked well was mounted on MeBo but became available for mounting on other tools after the MeBo operations stopped (069). Those stations where POSIDONIA positions are available are marked with (P) in the station list. In this case, the POSIDONIA position is given in the station list. This position was estimated by reading out the POSIDONIA positions from the DSHIP database and averaging over some positions. To ensure that the transponder positions are recorded in the DSHIP database POSIDONIAS acquisition software ABYSS must give a transponder ID between 1 and 3 to the used transponder. The ID can be changed by the order of the configuration files given for each transponder.

For the MeBo deployments, the POSIDONIA transponder (069) was used and worked very well. During the deployment phase POSIDONIA is useful to land the drill rig on or close to the given position. Before recovery the underwater navigation system in addition with the DP-system is used to guide the ship A-frame directly above the drill to maintain minimum torsion and tension on the cable and drill rig.

In general, the quality of the sub-positioning depends on the quality of the ship position. The later was reduced during the leg M84/2a as d-GPS was often not available due to technical problems. It is difficult to estimate, however, how much the imprecise ship's position contributed to the uncertainty of the underwater positioning. In addition, it is not clear how well POSIDONIA itself is calibrated. The last calibration was conducted in June 2010. Actual sound velocity profiles were used during the Cruise M84/2. Technically the accuracy of POSIDONIA is limited to about 1-3 % of the slant range.

Due to the fact that POSIDONIA transponder had technical problems, some stations (GC, MIC, DAPC, LDP) were deployed without POSIDONIA. In addition, several gravitycorer (and DAPC) stations were conducted without POSIDONIA as we made the experience when heavy tools are directly under the ship it is possible to accurately position them horizontally without POSIDONIA. However, for this procedure it needs to account for the offset between the ships reference point, when using SEAPATH as GPS, or the antenna position (mainly the main antenna mast), when using e.g. CNAV-GPS and the point where the tool is lowered to the water (below the block of the movable side crane "Schiebebalken"). This is illustrated in Figure 17. From the ship's reference point the tools location is about 15 m towards the aft and 10 m to starboard. The mates on the bridge were positioning this point to the desired target position, which worked very well for the heavy tools. They are regularly less than 5 m away from the target position. This procedure did not work, however, for not so heavy tools MIC and LDP, which were shifted probably due to currents, as seen in Figure 17.

Due to the fact that the gravitycorer could be precisely positioned at the target position we deployed it several times without POSIDONIA as this allows faster access to the samples, which is relevant when recovering gas hydrates. As the target position described better the actual position

of the ship (at the reference point) this target position is given in the station list marked with (T). In case POSIDONIA was not available for the other tools, such as MIC and LDP, this position is also given.

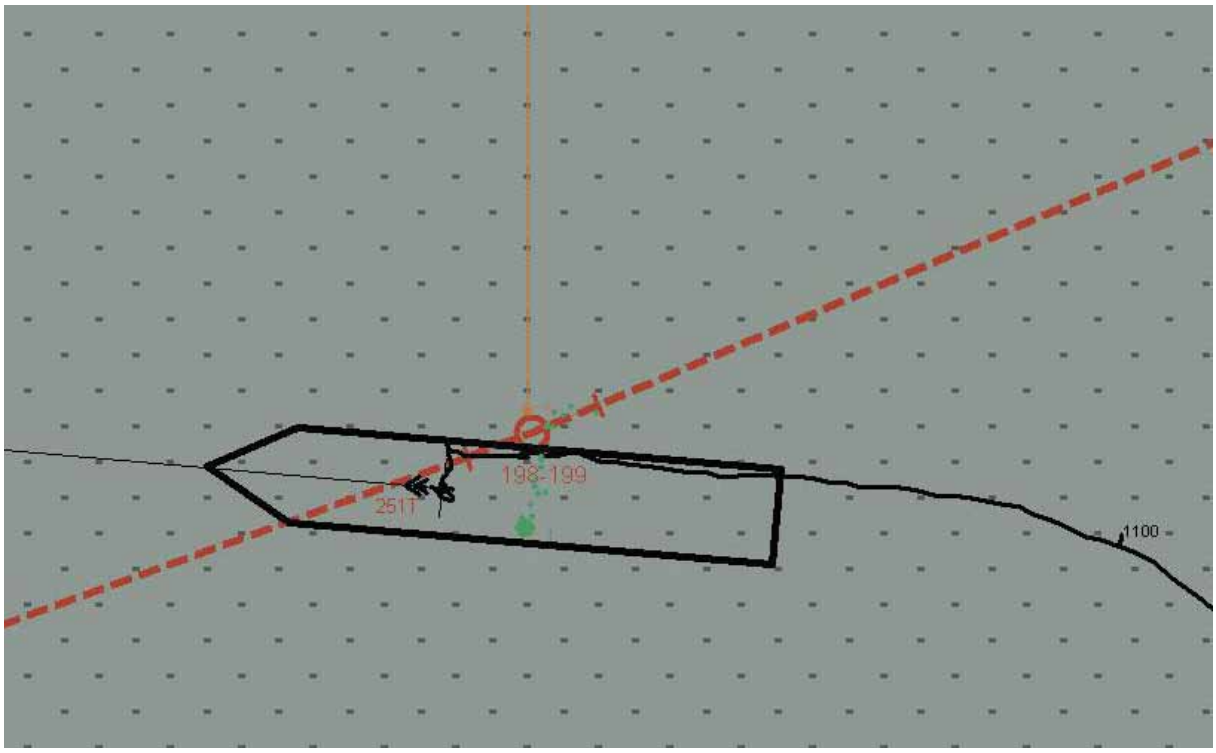

Fig. 17: Screenshot of the ECDIS navigation monitor on the bridge. The ship is seen at actual scale. The tool lowered at the side frame (Schiebebalken) is located about 15 m backward and 10 m to starboard side. This location is subsequently positioned over the target position (shown as red circle on the barbed line). In green the position of POSIDONIA mounted on the MIC is shown.

5. Multibeam Mapping

(P. Wintersteller, C. S. Ferreira, H. Sahling, A. Özmaral, M. Schmager, S. Oelfke, V. Radulescu, E. Akarsu, M. Römer, J. Körber)

During Cruise M84/2 multibeam surveys were made using the vessel mounted echosounders. Since one aim of this cruise was related to hydroacoustic water column investigations, the equipment and settings of the echo sounders used for surveying are described in detail in chapter 6: Subbottom Profiling. A few statements according to problems during the acquisition are pointed out here.

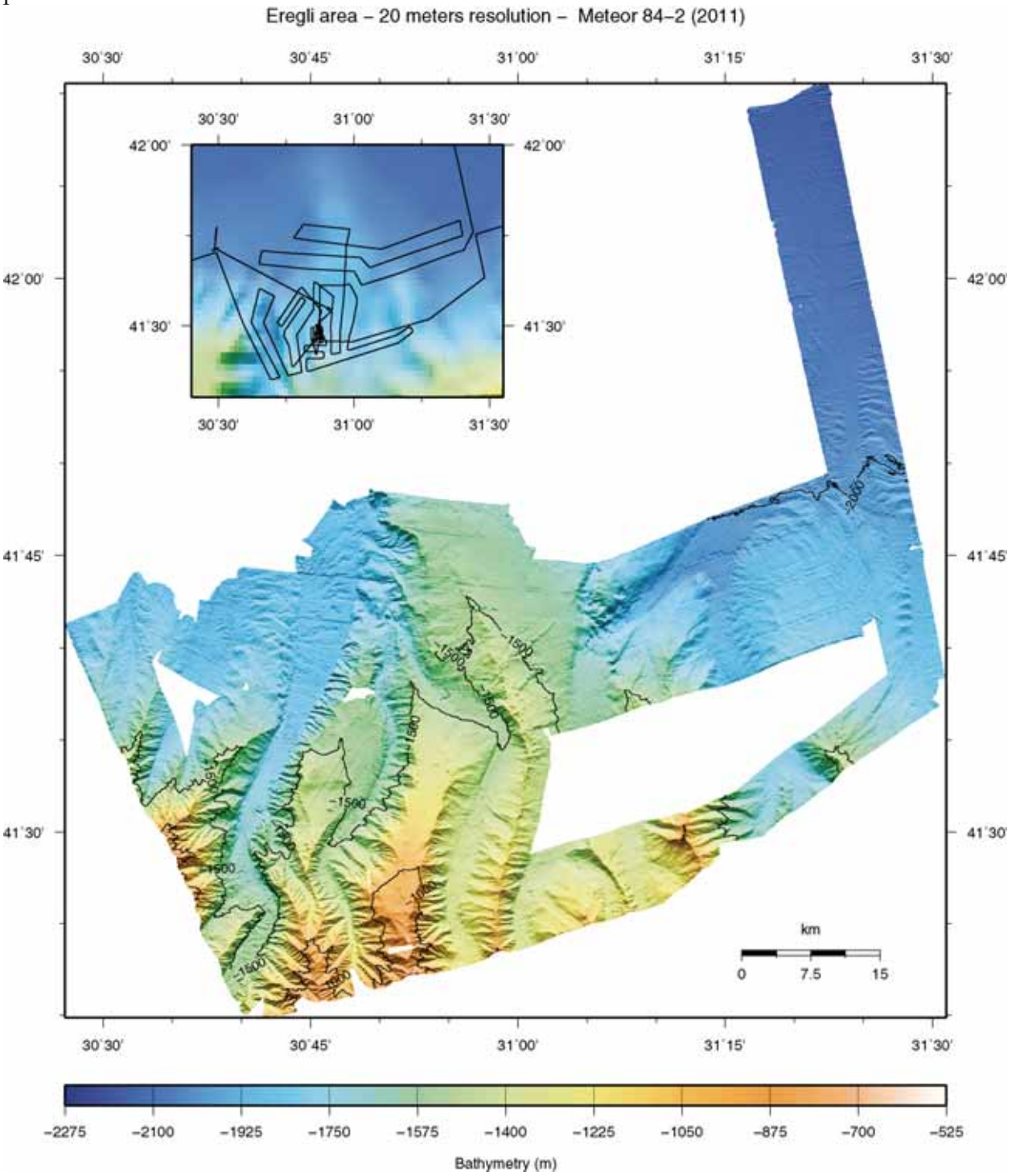

Fig. 18: Multibeam mapping in the area off Eregli (western part of the Turkish margin).

5.1 Methods

The deep sea KONGSBERG EM122 echosounder was used at all surveys during the whole cruise, meaning either designated bathymetry surveys or flare imaging-surveys. Meanwhile, the shallow to medium water echosounder EM710 was switched on only at shallower areas, with depths up to max. 1200 m. The swath coverage during bathymetric surveys was kept around 110-130° at both echosounders to avoid loss of data (due to system malfunctions) and data artifacts (like spikes and wobbling). As mentioned above the settings of both systems are shown in Table 3 and Table 4 in Chapter 6. Both systems run in dual swath mode.

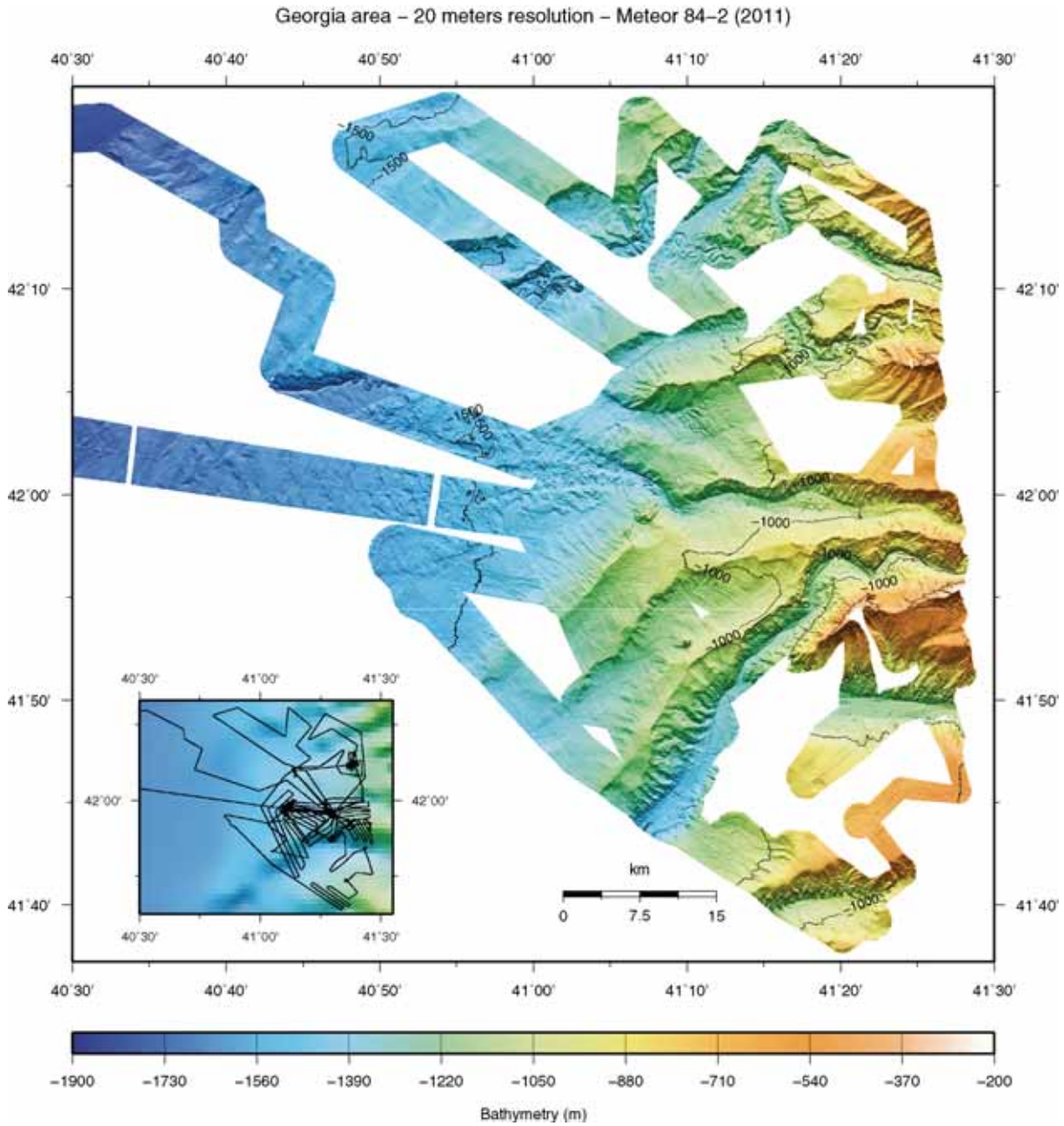

Fig. 19: Lines of multibeam mapping off Georgia.

During the cruise, maps were produced from the main working areas mainly using the data from the EM122 echosounder. This choice was based on the fact that this echosounder was the only one able to cover the full range at all areas surveyed. Nevertheless, the bathymetric maps

done with EM710 evidenced much more fine/smaller geological structures and the dataset from the Kerch area turned to be a remarkable achievement of this cruise.

The processing of the data has been done with the open source package *MB System* (Caress and Chayes, 2001) and/or CARIS 7.0 HIPS&SIPS. In comparison to the named software *IVS Fledermaus* has been used for backscatter and sidescan data as well. Currently the water column data of both echosounders can only be processed in *Fledermaus*.

5.2 Acquisition and Related Challenges

As described in chapter 3, 14 SVP's were taken and applied to the *KONGSBERG SIS*, the software for acquisition, right after recording to avoid acoustic ray tracing problems during beam forming. Nevertheless problems occurred during Leg 2a doing proper bottom detection on EM122. The inner swath-segment formed a u-shape profile on a flat bottom, port and starboard side of the nadir. It looks like a typical tube-form profile that appears usually on the whole swath when having sound velocity problems. But this time only the inner approx. 60 beams were bordered. Many beams had to be erased and left big gaps in an otherwise good and high resolution grid. Overcoming this problem the Leg 2a surveys where done mainly with >120% overlap. After investigations from both sides, scientists and KONGSBERG technicians, we decided to reinstall the PU-software of EM122 during the port time at Trabzon.

Wobbling is another problem bordering both systems EM122 and EM710. Due to the commonly used SEAPATH/MRU5 motion sensor, which still has difficulties producing accurate output at high sample rates and probably too large lever arms for the accuracy needed, there is a strong wobbling at the outer beams visible. The problem is described and sent to IFM Hamburg, the shipping company and KONGSBERG in detail and is ongoing to find a solution. The workaround meanwhile is to narrow the swath-width to max. 120-130°.

5.3 Results

The high resolution of the data allows 20-5 m grids and accurately highlights even small morphologic features. Commonly an N-NE illumination and a 4-8 times exaggeration is used to hillshade the grids for a more interpretative view. The following maps show the compiled data from the Black Sea (with working areas, and trackline for M84/2 cruise). The morphology surveyed in this areas show various structures and types of sedimentation from shelf to continental rise. Figure 18 shows huge mass transportation and refill of a canyon in the western part, cutting sharply the pervious formed side-canyons. The main working area off Eregli is situated on an exposed oblique, table-mountain-like platform that clearly shows the only slightly elevated patches of autigenous carbonates.

The northern area off Georgia (Fig. 19) is dominated by recently developed, meandering submarine rivers and canyons where else steeper canyons with clearly high energy deposits are formed in the centre of the mapped region. Towards the west, at depths of about 1500 m an oblique abyssal plain affiliates the deep-sea fan. The working area of Batumi is situated similar to the Eregli working area where else the areas of Colkheti Seep and Pechori Mound are outstanding morphologic features at the north western rim of Kobuleti Ridge, shown in the centre of the mapped region.

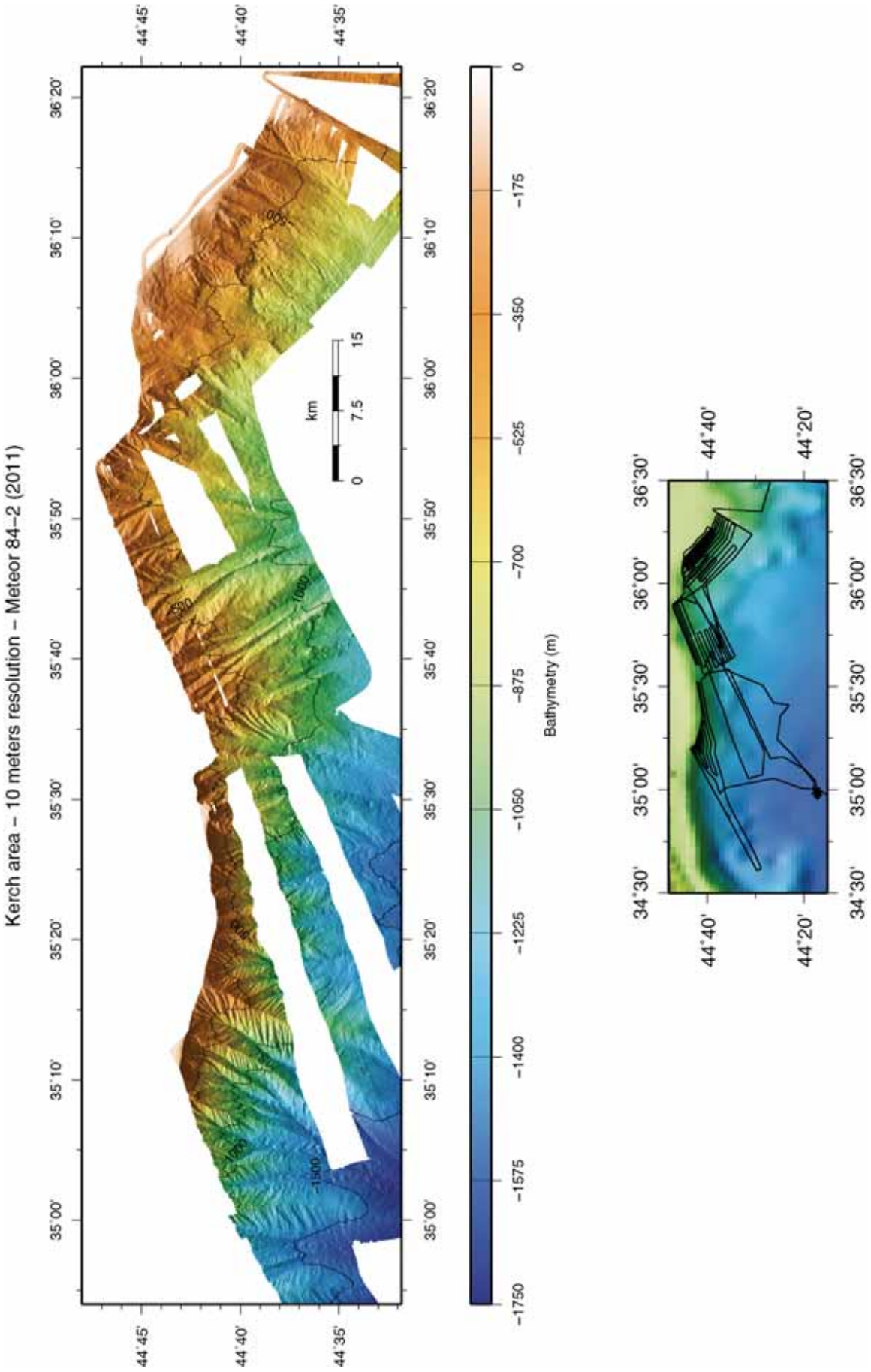

Fig. 20: Data from Kerch area and Sorokin Trough.

The continental slopes off Kerch and north of the Sorokin Trough are shown in Figure 20. The western part is dominated by sharply contoured canyons with steep incline that fits to the southern Crimean range as hinterland. Towards the east, off the Strait of Kerch, the continental slope flattens and a large shelf is developed. Slumps and slides, mud and debris flows can be seen clearly, as well as partly undercutting of slope by contour currents which accounts for soft and semiconsolidated slope sediments.

Likewise Eregli and Batumi, the centre part off Samsun, shown in Figure 21, is an oblique platform. Here only bordered with a steep western slope it is dipping softly towards NE. Patches of very low elevation but with high backscatter, similar to Eregli and Batumi were found all over in the area but outstanding in contrast to the soft sediments on the platform.

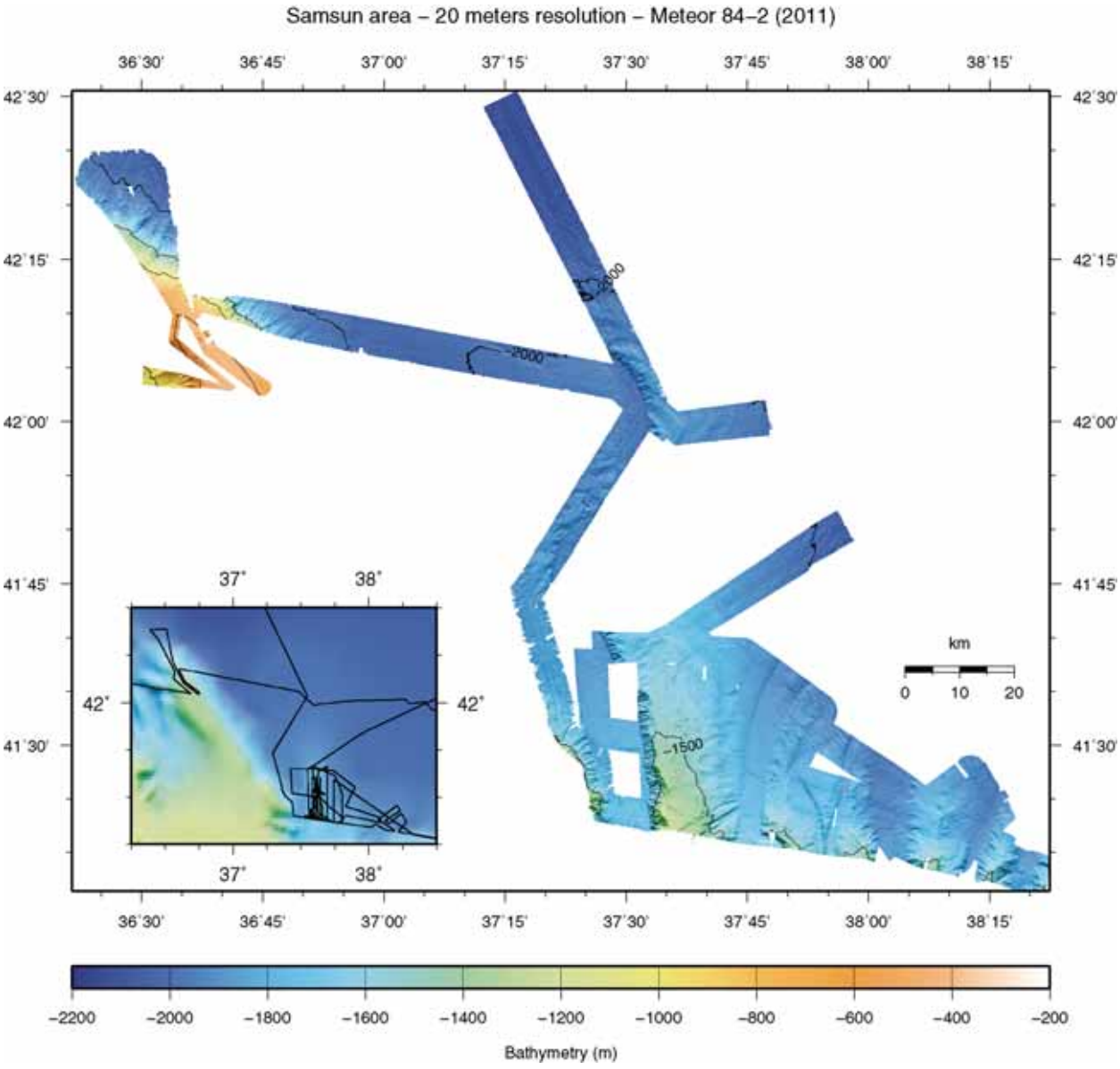

Fig. 21: Multibeam mapping in the Samsun & Ordu area (eastern part of the Turkish margin).

6. Subbottom Profiling and Plume Imaging

(H. Sahling, M. Römer, J.-H. Körber, P. Wintersteller, C. dos Santos Ferreira, M. Tomczyk, T. Wu, V. Radulescu, A. Özmaral, M. Schmager, S. Oelfke, E. Akarsu)

RV METEOR is equipped with a suit of excellent hydroacoustic techniques including the KONGSBERG multibeam echosounder EM 710 and EM122 as well as PARASOUND sediment echosounder. These techniques provide images of the sub-seafloor, the seafloor, and the water column above the seafloor giving detailed insight into processes related to fluid seepage. The multibeam systems are routinely used to obtain bathymetry of the seafloor. Seafloor properties such as seabed roughness, sediment density, or seafloor inclination may be obtained using the backscatter information of the beams or sidescan-sonar like images of the seafloor. Gas hydrate, gas, or authigenic carbonates at shallow sediment depths may be identified in backscatter maps due to the fact that these fluid seepage related features alter the physical properties of the seafloor. This has been especially well documented with data from deep-towed sidescan sonar, where gas hydrates and carbonates are clearly visible due to increased backscatter (Klaucke et al., 2006).

In addition, the multibeam systems allow to record acoustic signals from the water column, which can be used to map gas bubble emissions (Nikolovska et al., 2008). Gas bubbles have very different acoustic impedance due to the large differences in sound velocity between water and gas and, therefore, bubbles strongly reflect and scatter sound waves. As bubbles rise upward in the water column, their appearance in echosounder records resembles a flare that is why these features are commonly termed as such. Flares can be identified in the water column record of the multibeam systems. Flares can also been identified in the 18 kHz signal of PARASOUND sediment echosounder but at lower resolution compared to the multibeam system (Nikolovska et al., 2008). PARASOUND has the advantage of providing a composite view of the water column (19 kHz signal) as well as the sub-surface (4 kHz signal). The 4 kHz images provide evidence for seep-related features such as gas in sediments leading to signal absorption (blanking) or enhanced reflections due to deposition of gas hydrates and/or carbonates (Nikolovska et al., 2008).

The main intention of using the hydroacoustic systems during M84/2 was to obtain bathymetry and to map cold seep-related features in the working areas, such as gas and gas hydrates in the sediments as well as gas emissions from the sediments into the water column. A summary of all hydroacoustic surveys is given in Appendix 3.

6.1 Methods

The **EM 122 KONGSBERG multibeam echosounder** operates at 12 kHz. The transducers have a nominal opening of 1° in along track direction, which corresponds to ~1.7% of the water depth (e.g. 14 m at 800 m water depth). The opening in across track direction is 2°. Despite this physical limitation, the multibeam echosounder is capable to record up to 432 individual beams across track within a swath of up to 150°. However, due to insufficient data quality in the outer beams, the maximum swath width used during this cruise was 110°. The multibeam system settings were optimized for the different purposes of bathymetric mapping and flare imaging. These settings are given, together with annotations, in Table 3. Actual sound velocity profiles

were recorded with the ships sound velocity probe and inserted as basis for optimized performance (see Chapter 3). For the purpose of flare imaging, the swath width was regularly reduced to 70° while for bathymetry/backscatter mapping a swath of 110° was chosen. Data of the water column and the seafloor were recorded in one *.all file.

Table 3: Settings (runtime parameters) of the EM 122 for water column flare imaging. Highlighted settings need to be adjusted according to the depth and actual sounder performance.

Tab	Parameter	Setting	Comment
Sounder Main	Sector coverage	35° / 35°	55°-65° for bathymetry mapping
	Max Coverage	5000 / 5000	7k / 7k in deep water for bathy. map.
	Angular Mode	Auto	
	Beam Spacing	HDENS EQDIST	
	Force Depth	Real Depth	
	Min	6	
	Max	2500	
	Dual Swath Mode	Dynamic	
	Ping Mode	shallow	At speed > 6kn “auto”, depends on weather & water depths
	FM enable	Not checked	
	Pitch Stab	checked	
	Along Div	0	
	Yaw Stab	Rel Mean Heading	
	Heading filter	Medium	
	External Trigger	Not checked	
Filters & Gains	Spike filter strength	Medium	
	Range Gate	Large	Helps to decrease noise in nadir
	Phase ramp	Normal	
	Penetration filter strength	Medium	
	Slope	Checked	
	Aeration	No / Checked	Maybe checked in rough sea
	Tx power level	max	
	Angle from nadir	15	
Data cleaning	Rule Set	Standard	

The **EM 710 KONGSBERG multibeam echosounder** operates at 70 to 100 kHz. The opening angle of the transducer array is 1° by 1°. The swath is composed of up to 400 beams. Maximum swath width for bathymetric mapping was 90° due to insufficient data quality of the outer beams at wider opening angles. The swath was regularly reduced to 70° for water column flare mapping. The actual sound velocity profile obtained by the ships sound-velocity-probe (SVP) was used. Settings of the runtime parameter are summarized in Table 4. Data of the water column and the seafloor were recorded in one *.all file.

Table 4: Settings (runtime parameters) of the EM 710. Highlighted settings need to be adjusted according to the depth and actual sounder performance.

Tab	Parameter	Setting	Comment
Sounder Main	Sector coverage	35° / 35°	45°-60° for bathymetry mapping
	Max Coverage	2000 / 2000	
	Angular Mode	Auto	
	Beam Spacing	HDENS EQDIST	
	Force Depth	Real depth	
	Min	Real depth -100 m	
	Max	Real depth +100 m	
	Dual Swath Mode	Dynamic	

	Ping Mode	shallow	Auto to greater depths and/or bad weather cond.
	FM enable	Checked	
	Pitch Stab	checked	
	Along Div	0	
	Yaw Stab	Rel Mean Heading	
	Heading filter	Medium	
	Max Ping Frequency	20	
	External Trigger	Not checked	
Filters & Gains	Spike filter strength	Medium	
	Range Gate	Large	Helps to decrease noise in nadir
	Phase ramp	Normal	
	Penetration filter strength	Medium	
	Slope	Checked	
	Aeration	No / Checked	Maybe checked in rough sea
	Interference	Checked	
	Tx power level	max	
	Angle from nadir	10	
Data cleaning	Rule Set	Standard	

PARASOUND echosounder uses two high frequencies (primary high frequency PHF and secondary high frequency (SHF) of ~19 and ~42 kHz, which can be recorded and used for imaging of gas bubbles in the water column. Non-linear interference of the high frequencies produces a secondary low frequency (SLF) of about 4 kHz. This SLF is used for sub-seafloor imaging. Opening angle of the transducer is ~4°, which corresponds to a footprint size of about 7 % of the water depth.

In order to image gas emissions those settings given in Table 5 were chosen in PARASOUND Hydrocontrol. The program PARASTORE is used for storing and displaying echographs. The settings applied in PARASTORE for PHF and SLF displaying are variable and dependent on the actual performance influenced by, e.g., water depth, water and weather conditions. Generally the filtering in the PHF window has been used to image gas emissions in the water column: Low pass: on, Iteration: 2, High cut: 1. The amplitude scale is also important for this purpose: Clip: between 1000 and 1500 mV, no Threshold, negative Flanks Suppression or Gain. For SLF subbottom imaging no filtering has been used. Amplitude scale with a Clip between 5000 and 10000 mV, no Threshold and Negative Flanks Suppression, but sometimes a Gain: Bottom TVC of 0.1 to 0.25 was chosen to get a deeper bottom penetration.

Three file formats are recorded during PARASOUND operations: *.asd files, which can be replayed in PARASOUND contain data of the entire water column as well as the sub-seafloor. PARASTORE also produces *.ps3 and *.sgy-files recorded along with the auxiliary data. The depth range of the *.ps3 files was set identical to those of the online display window. While *.sgy-files are not used by us, *.ps3-files were plotted in the program SENT for interpretation. *.ps3 and *.sgy-files can also be produced by replaying the *.asd files in PARASTORE.

There have been error messages when for the storage of the PHF a window scale over 1000 m was chosen, so the window scale has been set always to 1000 m and not for the entire water column have been stored in the case the water depth was deeper than 1000 m. For storage mode the option “with phase and carrier” has been selected.

Table 5: Settings in PARASOUND Hydrocontrol optimized for flare imaging.

Tab	Parameter	Setting
Basic settings:		
Transmission sequence:	Single Pulse	
Transmission Source level: Manual	Max TX Voltage: 145.00 V	
Pulse characteristics:	Pulse length: manual	
	Manual Pulse length: 0.500 ms	
	No. of periods: 2	
	Pulse Type: Continuous wave	
	Pulse Shape: Rectangular	
Frequencies:	Desired PHF: 20 kHz	
	Desired SLF or PLF: 4.00 kHz	
Advanced settings:		
Transmission Beam Width:	standard (8*16 Elements)	
Reception shading (for PHF+SHF and SLF+PLF):	Mode: Shading Table:	No Shading
Receiver Band Width:	PHF+SHF:	Mode: manual
	PHF: output sample rate:12.2 kHz	Band width: 33%
	SHF: output sample rate: 6.1 kHz	Band width: 66%
	SLF+PLF: Output sample rate: 6.1 kHz	Mode: manual Band width: 66%
Receiver Amplification:	PHF:	Mode: Automatic Gain shift: 30.00 dB
	SLF:	Automatic
Sonar Target Settings:	Correlation: yes	
	Targets in the water column: no	
	S/N Ratio:	20.00 dB for 1 m below Transducer
	Automatic Transmission Termination:	OFF
	Stave Data Recordings:	no
Sounder Environment:	System Depth Source:	Controlled by PHF, manual if needed
	Blanking Output:	no
	C-Mean:	Source: Manual Manual: 1485 m/s
	C-keel:	Source: Manual Manual: 1467 m/s
	Desired Bottom Penetration:	150 m
	Mode: Variable Min/Max Depth limit	(Min. Depth: 200 m, Max. Depth: 2500 m)
Operation:		
	Trigger: autonomous Operation	
	Data recording: all: Full Profile	

Two legs later, during Cruise M84/4 it turned out, that the settings for the lever-arm X-value in Parastore on RV METEOR were wrong. The effect can mainly be seen in shallow water, less than 400 m depth. To change and replay the data one needs to enter hidden "Advanced Parameters" in the "Echogram Window". To display this parameters setting in the registry of the program must change:

1. *Open the registry with "regedit"*
2. *Go to "hkey_local_machine → software/atlashydrographic/parastore"*
3. *Add a "string" of the type "REG_SZ", name it "HiddenFunctions" and give it the value "1"*
4. *Open the Echogram Window and put an X-value of "-36" at the "Motion Sensor Location"*

During **post processing of multibeam data**, water column data of EM 710 and EM 122 were imported in the program Fledermaus, which has a special sub-program the FM Midwater for replaying and analyses of water column data. With this program, flares can be visualized in three dimensions (Fig. 22). The program does not allow, however, to quickly pick the positions from flares, which is therefore a task that will be conducted after the cruise.

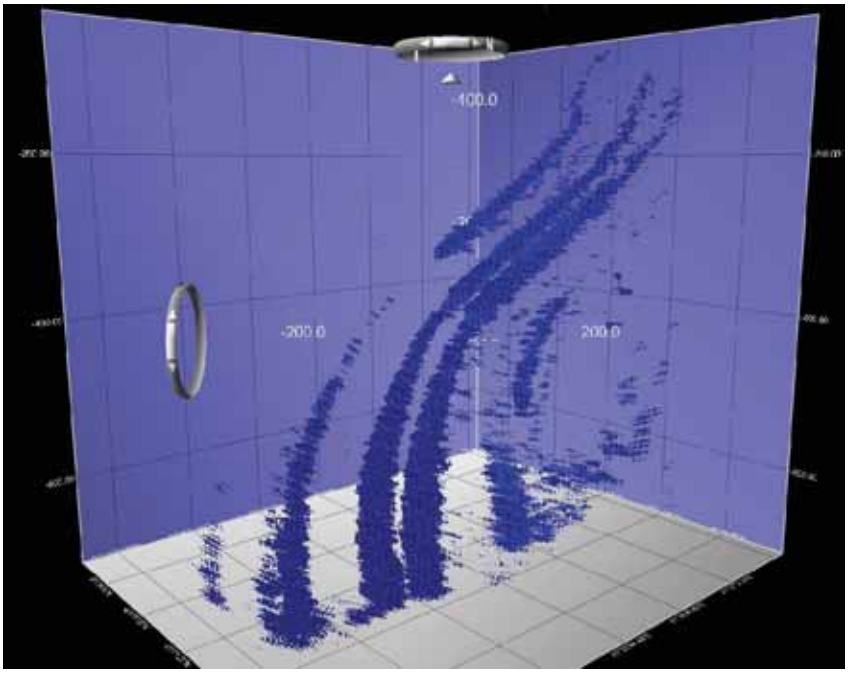

Fig. 22: Three-dimensional visualization of flares recorded by EM 122 using the FM Midwater and Fledermaus. The flares rise from water depth of ~500 m to depth of about 100 m. Currents lead to deflection of the bubble streams in the water column.

PARASOUND, EM 122 and EM 710 were used for flare mapping during cruise. The opening angle of PARASOUND is about 4° (corresponding to ~7% of the water depth). Thus, gas emissions can be recorded as flares when they are within this sound coil. In contrast, the multibeam systems can detect gas emissions across the entire swath regularly set to 70° with an along-track resolution of 1° (corresponding to ~1.7 % of the water depth). Therefore, the EM multibeam systems have, compared to PARASOUND, a higher spatial resolution and, at the same time, a larger coverage.

The different frequencies of the KONGSBERG multibeam systems result in significant differences in imaging gas emissions. We found that EM 122 is much more sensitive and shows many more water column signals that can be attributed to gas bubbles in the water column. EM 122 showed always more flares than EM 710. We hardly ever observed a flare in EM 710 that was not seen in EM 122. The higher sensitivity of EM 122 is accompanied by more noise that is caused by gas bubbles in the water column as illustrated in Figure 23. The prominent flare in EM 122 is seen at the same time in EM 710 but appears more intensive and larger in EM 122 compared to EM 710. However, around the main flare in EM 122 are additional anomalies in the water column that have the same shape as the main flare but are less intensive and smaller in size. We interpret these as artefacts. There might be, however, a second flare in EM 122 that is not seen in EM 710. Careful interpretation of the EM 122 water column image is needed when using this multibeam system for mapping of gas emissions.

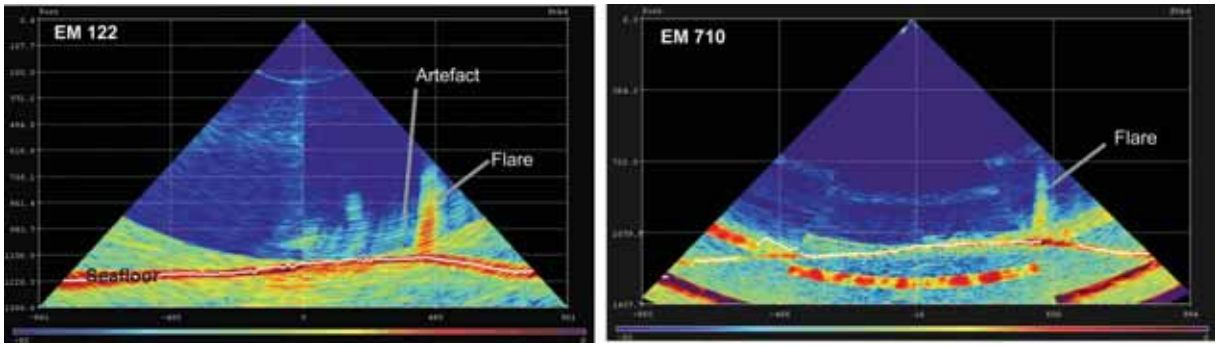

Fig. 23: Comparison of EM 122 (left) and EM 710 (right) online water column data taken at the same time showing the seafloor and flares.

We explain the higher sensitivity of the EM 122 as a result of the operation frequency around 12 kHz. This frequency is exactly the resonance frequency of typical 2.5 mm radius gas bubbles (e.g. Sahling et al., 2009) in 900 m water depth, which can be calculated according to the equation (Ulrick, 1975): fr = 3.25 * (1 + 0.1 * d) 0.5 * r-1 with water depth (d) in meter and bubble radius (r) in mm. Due to the resonance of the bubbles, the sound scattering is significantly increased at 12 kHz (EM 122) compared to the scattering at frequencies of 75-100 kHz (EM 710) well above the resonance frequency. This fact can explain the sensitivity of EM 122.

6.2 Georgia

The working area offshore Georgia has been studied during several proceeding cruises before, namely P317/4 (Sahling et al., 2004), M72/3 (Bohrmann et al., 2007), TTR-15 (Akhmetzhanov et al., 2007), and MSM 15/2. Swath bathymetry, deep-towed sidescan sonar data, and seismic data are available (Klaucke et al., 2005; Klaucke et al., 2006; Wagner-Friedrichs, 2007). Gas hydrates as well as authigenic carbonates have been sampled and the geochemical signature of gas and gas hydrates have been intensively studied (Bahr et al., 2010; Klapp et al., 2010; Pape et al., 2010).

The working area offshore Georgia was the focus of the first leg during M84/2 cruise in order to complement earlier studies. Due to the excellent performance of the hydroacoustic systems the area was extensively mapped in order to obtain additional information on the bathymetry, backscatter, and the occurrence of gas emissions. Many MBPS surveys were conducted with different objectives. A summary of all hydroacoustic surveys is given in Appendix 3.

One objective of the cruise was to search for flares in areas where oil slicks occur. In an ongoing PhD project, oil on the sea surface has been mapped using SAR satellite images, which show higher reflectivity due to the smoothing of the surface by oil. Systematic mapping of oil on the sea surface allows to pin-point the location of the oil source at the seafloor. This point is named oil slick origin (OSO) in the maps shown here but in reality, it is a calculated location taking into account several oil slick observations at different times. The oil slick origins have been surprisingly accurate in guiding us to locations with gas emissions. Following the finding by Solomon et al. (2009) and De Beukelaer et al. (2003), oil is mainly transported from the seafloor to the sea surface by oil-coated bubbles. The oil-coating prevents methane from

diffusing out of the bubble into the water column. As a consequence, methane might reach the atmosphere. Therefore, we were interested to, firstly, confirm the presence of gas emissions at the locations with oil slicks and, secondly, investigate how high bubble streams rise in the water column. The latter question can be answered by thorough analyses of the EM 122 water column data, which will be conducted after the cruise. At first glance, it seems as if bubbles rise very high in the water column, rising at least above the permanent pycnocline at ~160 m depth (Fig. 22).

In summary, we found several new flare locations during M84/2, some by chance but most based on dedicated surveys in areas with known oil slick origins as summarized in Figure 24. The map shows all flare locations that we have preliminary identified. However, many more individual flare locations have been recorded by EM 122 and EM 710 but this information has not been extracted from the data yet. Furthermore, the locations of most flares mapped by the multibeam systems are not exact and need further refinement. Flares that have been found based on known oil slick origins are: Adjara Ridge with the three flare clusters A1, A2, A3 and flares at the locations G1 and G2 at the western and eastern Kulevi Ridge, respectively. The dedicated flare surveys in these areas are shown in detail in the maps Figures 25-27. In general, we found that the oil slick origin from satellite data is a very reliable way of predicting gas bubble emission sites. The location of the oil slick origin was found to coincide strongly with the observed gas emissions, which suggests that oil is either transported with the gas bubbles or raised from the same locations as the bubble emissions from the seafloor. A further observation is that flares occur usually in cluster. Due to the large coverage of the multibeam systems, we were able to observe many flares in those areas that we studied in detail. From the summary Figure 24 it is evident that most flares are found at ridges, either at the crest of the main ridges or at the secondary smaller ridges.

Detailed flare surveys have been conducted at Pechori Mound and Colkheti Seep, as these are the structures at which the most significant oil slicks were observed. The exact location of almost all gas emission sites were extracted from the EM 122 data and are plotted in Figure 25 showing that most flares occur close to the central part of the features. Several dozens of individual flares have been picked illustrating the high activity with respect to gas emission. In addition, we observed oil at the sea surface while being on sites. The oil slicks were large, covering hundreds of meters on the sea surface. Sometime, the air on the ship had a faint smell of gasoline illustrating that significant amounts of oil are released and rise to the surface. In order to study the temporal variability of flares, a dedicated MBPS survey was conducted. We crossed Colkheti Seep about seven times always along the same track in order to estimate how continuous the emission sites are. These data will be analysed after the cruise. A compilation of all flare sites is given in Figure 27.

Further focuses for mapping were the seep structures Batumi, Kobuleti, and Poti Seep located at Kobuleti Ridge. Based on the preliminary documentation of flares, it appears as if gas emissions are not limited to areas of high backscatter but also occur outside. This finding is certainly a result of the great sensitivity of the EM 122 system. The sensitivity may also have disadvantages that require further investigation after the cruise. It may well be that a few bubbles in the water column cause a similar acoustic anomaly in EM122 as vigorous bubble streams due to the fact that the EM 122 operates at frequencies that lead to bubble resonance. It should be one task after the cruise to carefully compare EM 710 data with EM 122 data in order to distinguish

between major and minor flares. Seafloor observations of significant bubble streams have been recorded with EM 710 data before, thus providing independent information on the amount of bubbles required to cause flares (Nikolovska et al., 2008).

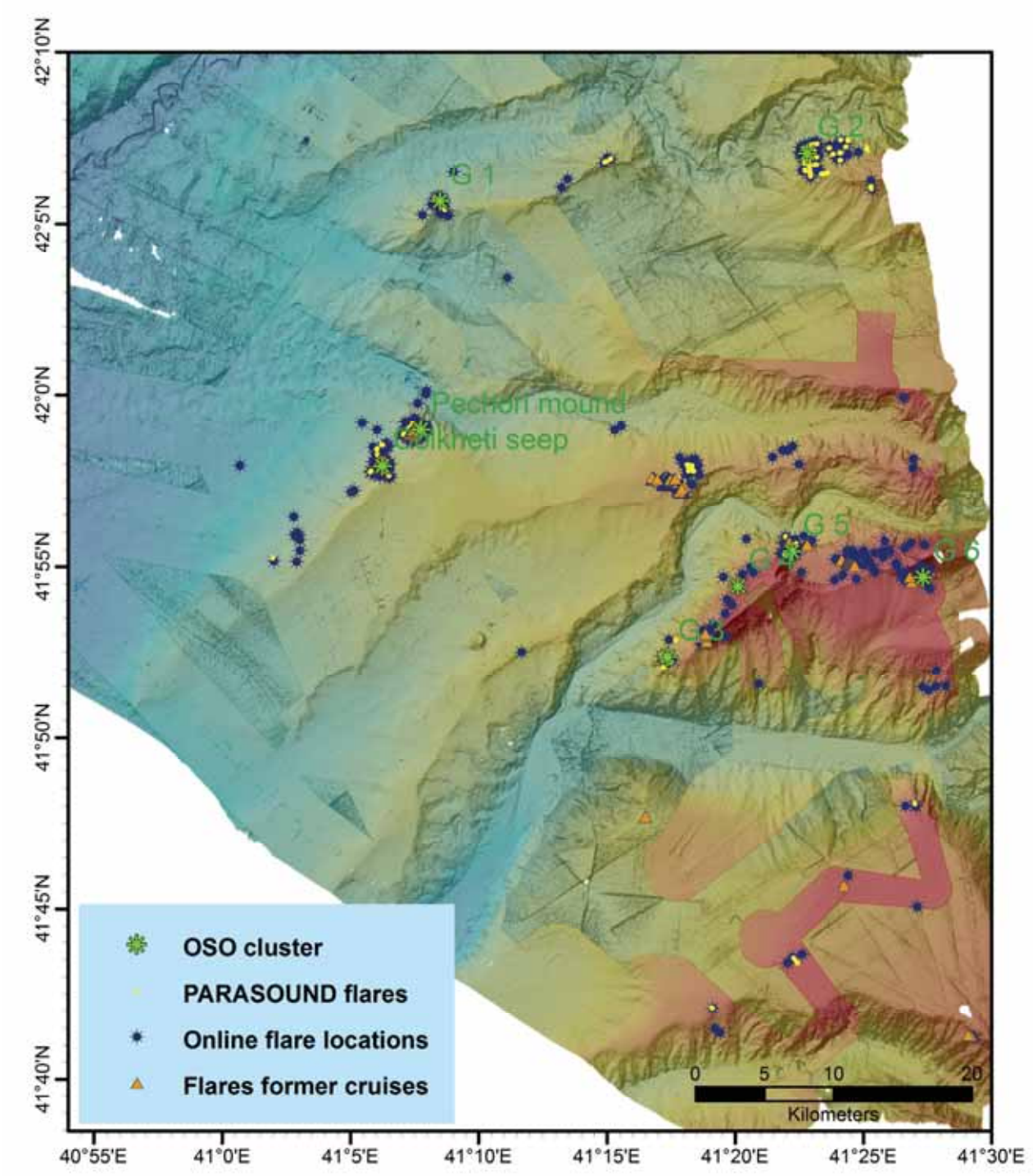

Fig. 24: Flare positions in the working area offshore Georgia plotted on top of the bathymetry. Several flare sites have been recorded during previous cruises. Flares by the multibeam systems are only roughly positioned. Many more flares exist but have not been analysed in the EM 710 and EM 122 data.

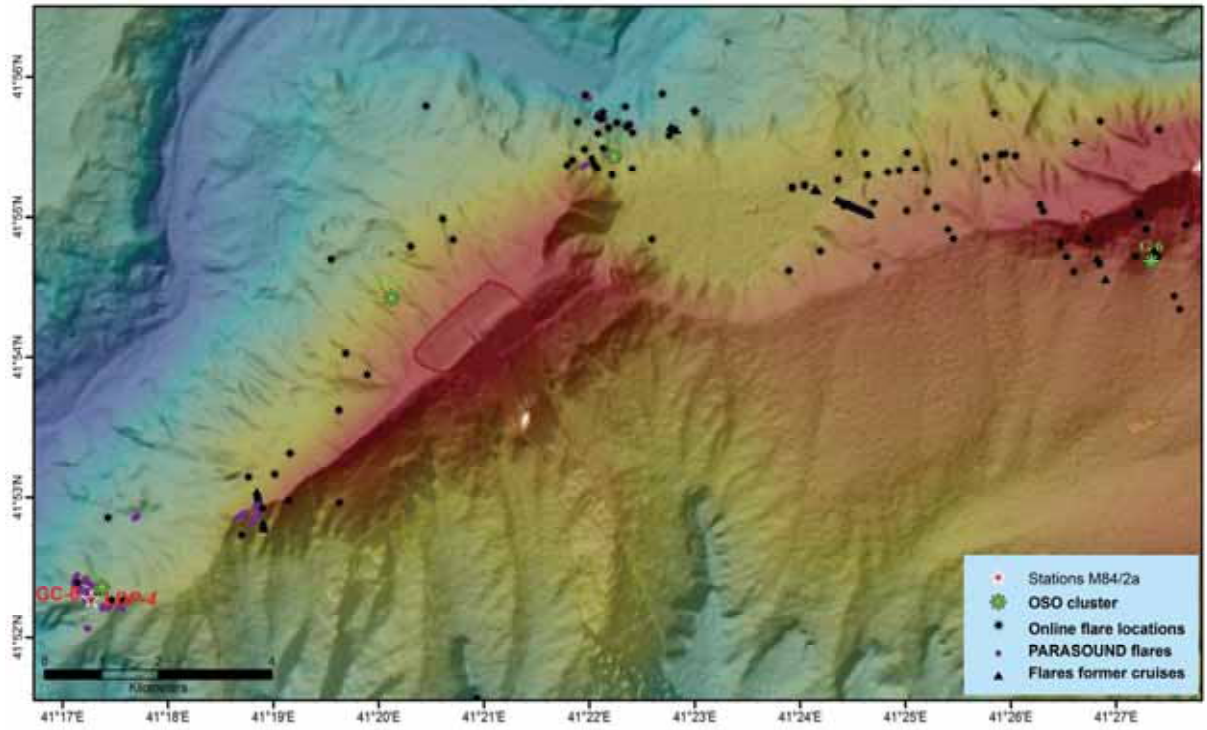

Fig. 25: Flare positions at Adjara Ridge.

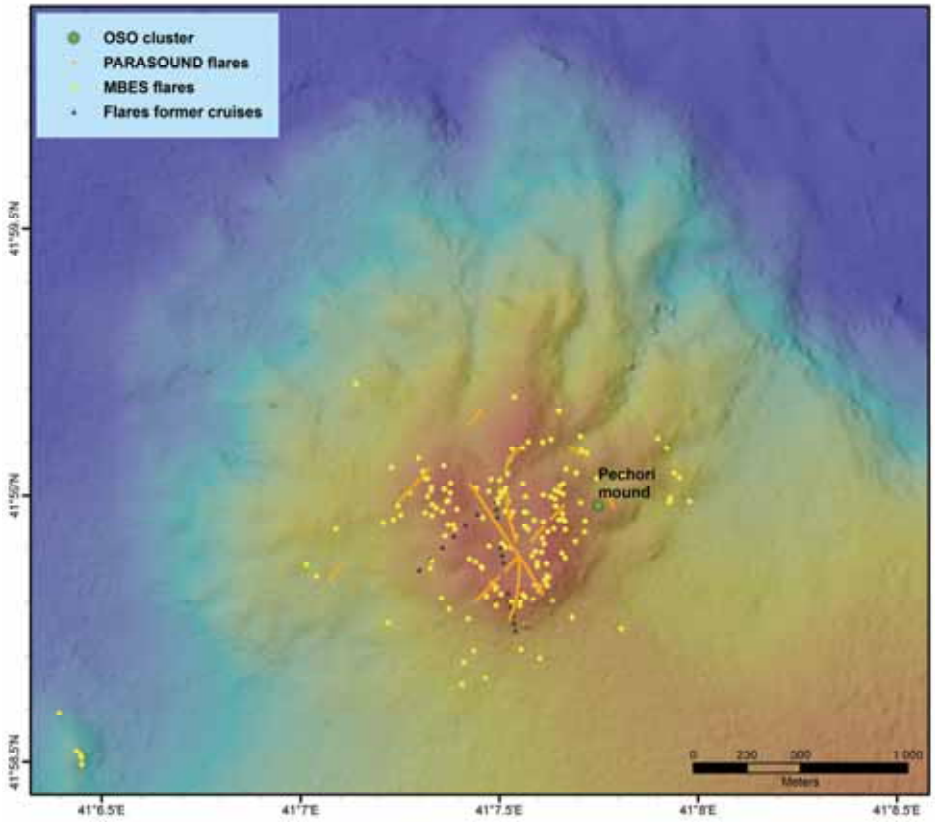

Fig. 26: Flare positions of various systems located in the area of Pechori Mound.

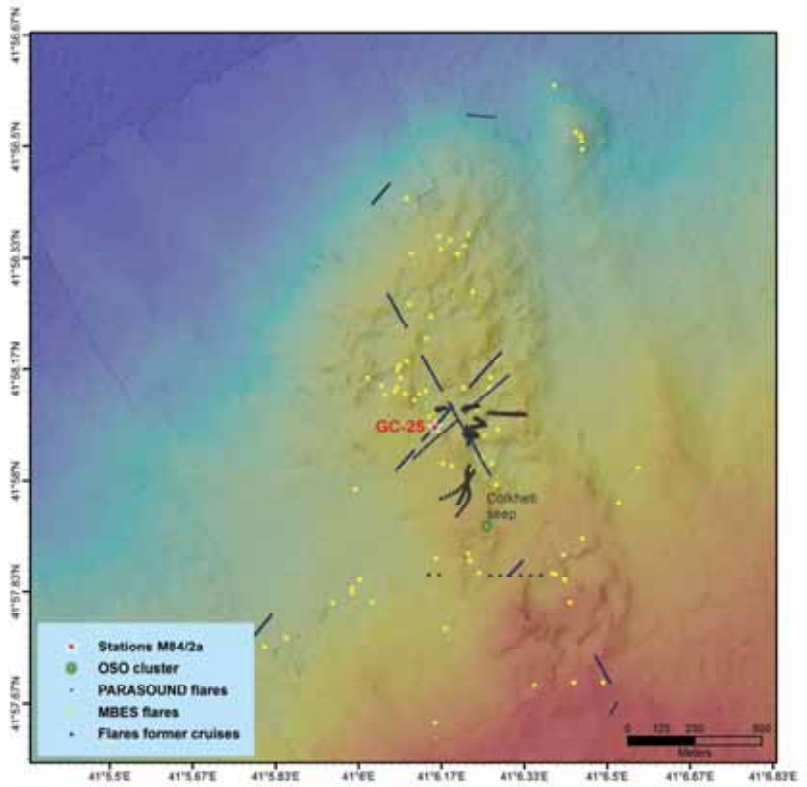

Fig. 27: Flare positions in the area of Colkheti Seep measured by the different systems onboard RV METEOR.

6.3 Samsun

Two regions have been studied within the working area Samsun: the Archangelsky Ridge and the much smaller ridge, named during this cruise Ordu Ridge, running parallel to it. Seismic and hydroacoustic evidence for methane seepage at shallow water depth at Archangelsky was published earlier (Çifçi et al., 2003). In addition, long-range Okean sidescan sonar, deep-towed sidescan sonar using the MAK system and coring has been conducted in the deep part of the area during the Cruise TTR-15 with R/V LOGACHEV (Akhmetzhanov et al., 2007).

Gas emissions and pockmarks were observed at Archangelski Ridge at water depth of ~430 m as shown in Figure 28. The pockmarks are ~10 m deep. Similar to the finding by (Çifçi et al., 2003), the pockmarks were found to be circular or elongated in outline. The circular pockmarks are 250 m and more in diameter; the elongated are less than 100 m wide and ~800 m long. The central part of the circular pockmark is characterized by higher backscatter compared to the surrounding, which suggests a change in sediment properties such as gas or authigenic carbonate precipitation. Acoustic turbidity was observed below the pockmarks. In addition, active gas bubble emission was observed by PARASOUND as well as EM 122 showing that the gas is emitted through the pockmarks.

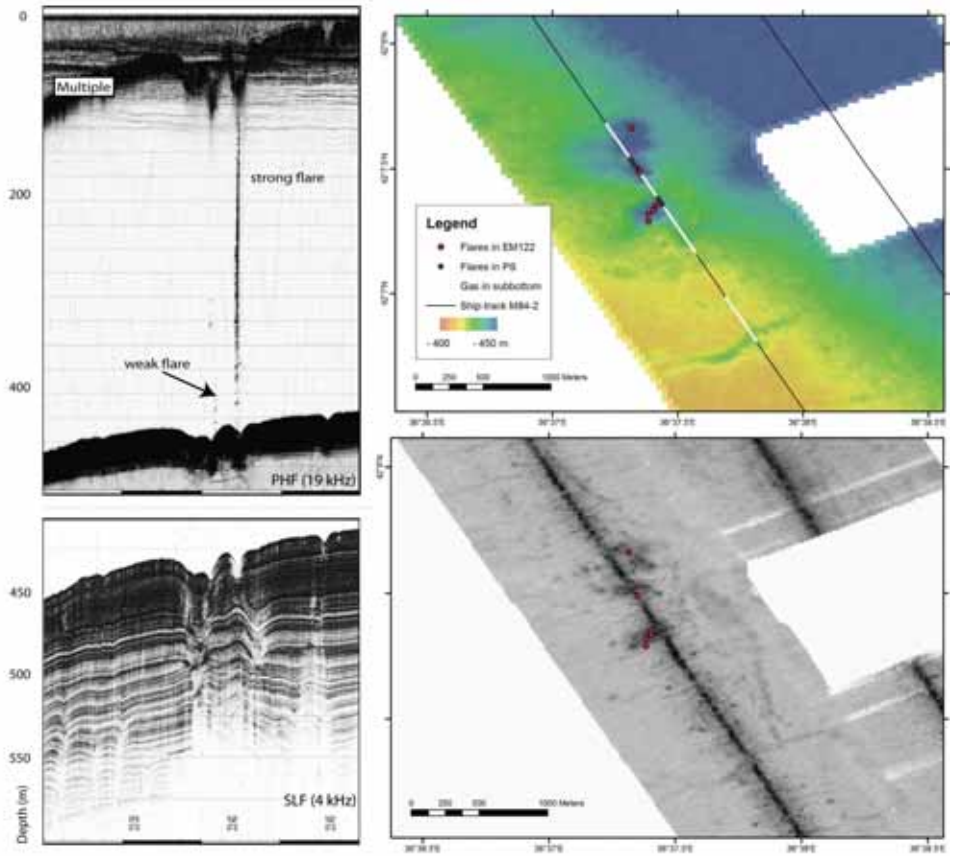

Fig. 28: Pockmarks and gas emissions at Archangelski Ridge imaged by 19 kHz PARASOUND (upper left), 4 kHz PARASOUND subbottom profiler (lower left), bathymetry (upper right) and EM 122 backscatter (lower right).

Several gas emissions have been recorded also at the Ordu Ridge, which in contrast to the emissions along the Archangelski Ridge are located in deeper water depth over 1000 m and instead of a relation to negative morphological features as pockmarks they are connected to slightly mounded structures (Fig. 29 left). These positive elevations could be detected as well by higher backscatter values and the amplitude map of the area shows clearly distinguished dark patches (Fig. 29 right).

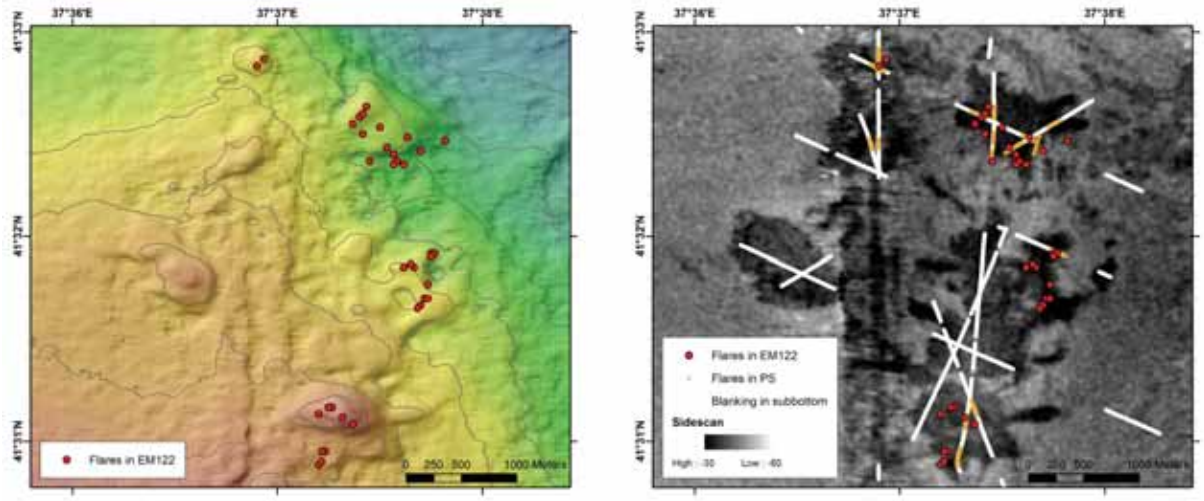

Fig. 29: Mounded structures on top of the Ordu Ridge (left), which are characterized by high backscatter (right). The PARASOUND subbottom signal recorded blanking zones (white lines). Some of the structures are actively degassing into the water column.

PARASOUND observations by crossing the patches show acoustic columnar blanking zones below the patches in the subbottom (Fig. 30 left) and some of the patches also emit gas into the water column as clearly indicated by gas flares on top or at the rim recorded with the PHF signal (Fig. 30 right). The gas bubbles sometimes rise about 500 m up from the seafloor into the water column.

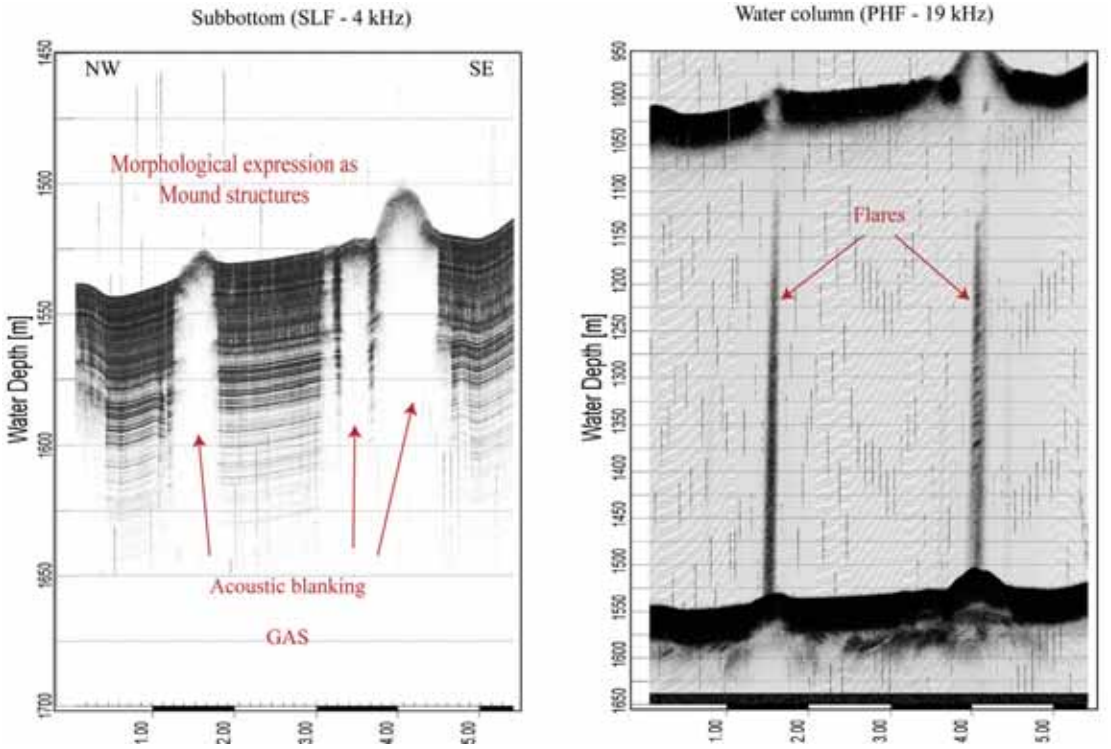

Fig. 30: PARASOUND echograms for SLF (left) and PHF (right) recorded by crossing the high reflectivity patches. They show clear columnar blanking in the sediments indicating high gas contents. Some have gas flares emanating on top or at the rim of the elevated structures.

During several surveys the Ordu Ridge as well as the four following smaller ridges to the east had been mapped. It becomes obvious that high reflectivity patches and gas emissions are generally located above the flat platforms on top of the different ridges running from south to the deep basin northwards (Fig. 31). Additional surveys have been conducted to observe the activity of the numerous patches, what resulted that only a small part has been active during our observation time. By using the water column information of the EM122, gas emissions had been detected at 15 of the in total about 60 high reflectivity patches (Figs. 31 and 32). In the south-eastern edge of the working area a circular structure with a flare emanating from its center was found (Fig. 31). Together with acoustic turbidity in the subbottom recorded by PARASOUND (4 kHz) the observations suggest that the structure is a mud volcano.

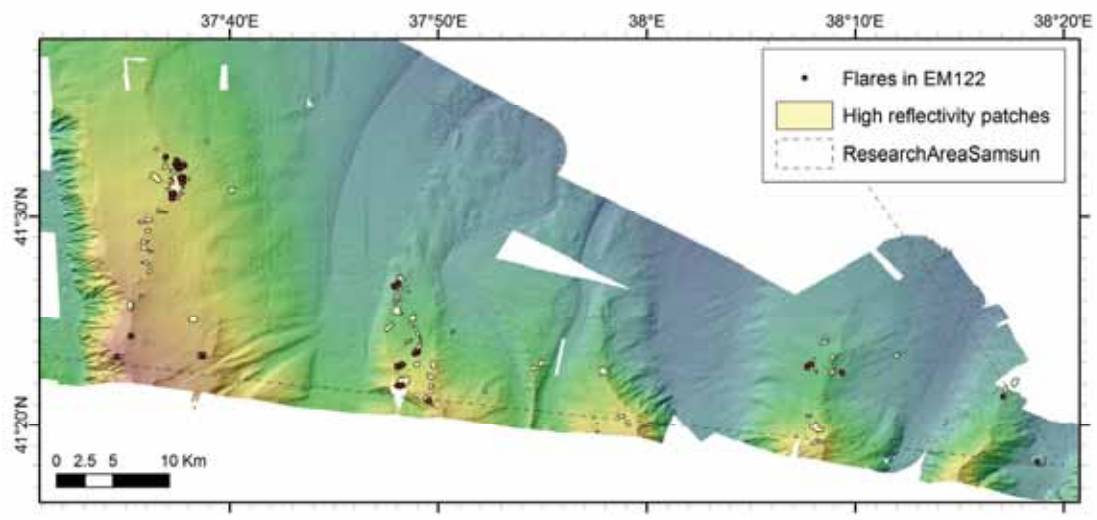

Fig. 31: Several surveys covered Ordu Ridge on the western side and four smaller ridges eastwards. Patches of high backscatter have been found on top of each ridge. In total about 60 patches have been mapped of which 15 are recently active degassing.

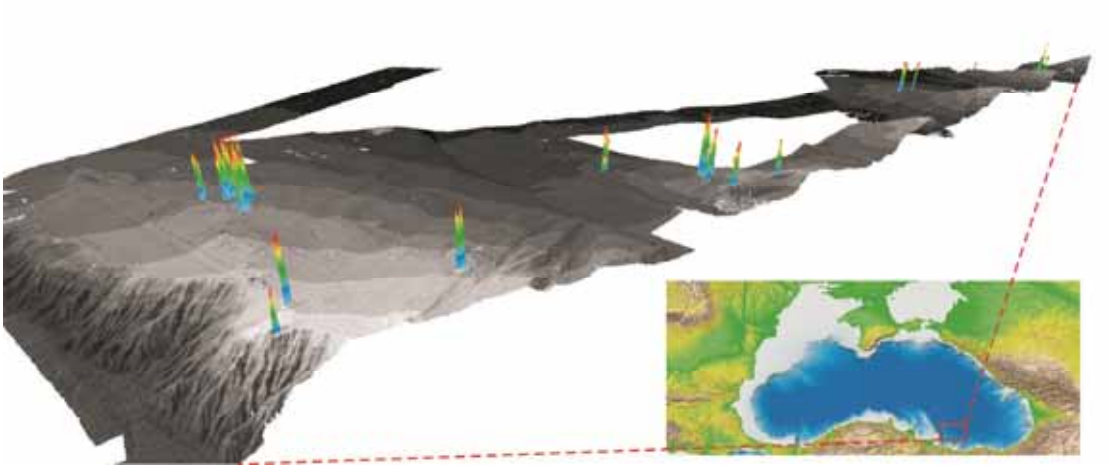

Fig. 32: 3-D image of the surveyed area showing the flare emanating from the seafloor.

6.4 Eregli

Work in the area offshore the Turkish town Eregli (Kozlu High) was based on bathymetry and backscatter maps from deep-towed sidescan sonar DTS 1 that had been obtained during POSEIDON Cruise 317/4 in 2004 (Sahling et al., 2004). During that proceeding cruise, seep-related backscatter anomalies were found at the seafloor and flares were recorded by sidescan sonar in the water column as described in Klaucke et al. (2005).

During Cruise M84/2 the bathymetry could be significantly extended (Fig. 33). We found several new flare locations in the area using PARASOUND. In addition, EM122 recorded flares of which some are shown in Figure 33. For a complete inventory of all flares the EM122 data need to be replayed and analysed, which we were not able to do during the cruise. Therefore, it is likely that more flares exist in the area than shown in Figure 33. The data quality of the novel EM 122 multibeam echosounder is very high resulting in good bathymetric resolution but also in very useful backscatter information. As shown in Figure 34, major morphological structures such as erosive features or sediment hosted plains can be seen in the backscatter. In addition, backscatter anomalies related to fluid seepage can be detected. To illustrate the great scientific

potential of the EM 122 echosounder especially with regard to cold seep studies, several data sets obtained at Eregli Ridge are shown in Figure 35.

Eregli Ridge is characterized by a plateau-like top bordered by flanks that are subject to erosion, which leads to the typical fish-bone like pattern caused by gullies and channels. These are seen in deep-towed sidescan (Fig. 35A), bathymetry (Fig. 35B, D), and EM 122 backscatter (Fig. 35C). The deep-towed sidescan shows that the plateau-like top of the ridge is generally characterized by low backscatter indicative for soft sediments. In certain areas, however, circular patches of high backscatter exist as highlighted by the arrows in Figure 35A, which are seep-related features (Sahling et al., 2004). In contrast to the deep-towed sidescan backscatter images, the backscatter obtained by EM 122 show additional circular backscatter anomalies on top of Eregli Ridge (Fig. 35C). We attribute these remarkable differences in the two backscatter images to the different frequencies of the systems. The sound waves of the DTS sidescan sonar operating at 75 kHz do not penetrate as deeply into the sediments as those emitted by the EM 122 using 12 kHz. (Please note that the lowermost deep-towed sidescan survey line in Figure 35A has to be shifted a few hundred meters to the SW for being at the correct position). In general, we interpret the high backscatter patches as sediments being influenced by fluid seepage, i.e. the presence of gas hydrates, gas bubbles, or authigenic carbonates. The observation that some backscatter anomalies are only seen in EM 122 and not in deep-towed sidescan may indicate that the gas hydrates, gas, or carbonates occur deeper in the sediments. However, whatever the cause of the high backscatter is, it also influences the seafloor morphology as shown in the high resolution bathymetry of EM 122 in Figure 35B. We were surprised to see that the high backscatter patches are associated with a smoother seafloor surface as well as slight elevations (Fig. 35B). We interpret this as a result of gas hydrate deposits in the sediments leading to a more distinct upper surface reflection as well as up-doming of the sediments.

Along the track, we mapped the occurrence of gas in the sediments (blanking) as well as gas bubble emissions with PARASOUND (Fig. 35D). The map shows that all of the areas of high backscatter in EM 122 are characterized by gas in the sediments. Gas emissions were mapped using two different methods: with PARASOUND we were able to detect gas emissions below the ship (along the ship track) as seen in Figure 35D. With EM 122 we were able to map the distribution of gas emissions in greater detail in a larger area. For example, while PARASOUND shows that gas emissions are somehow related to the high backscatter patches, EM 122 reveals that at some patches, the gas emissions occur within the high backscatter whereas in others the gas mainly escapes around at the fringes of the high backscatter (Fig. 35C). This further illustrates the high scientific potential of the EM 122 swath echosounder for cold seep studies.

After analysing the distribution of gas emissions by PARASOUND and EM 122, it is worth discussing the differences between the backscatter of the deep-towed sidescan sonar and EM 122. It seems as if deep-towed sidescan sonar images better those sites that are actively emitting gas bubbles compared to EM 122 showing more sites of high backscatter that appear to be presently inactive. For example, three of the five backscatter anomalies in sidescan sonar are presently active while EM 122 shows more areas of high backscatter but none of them is active with respect to gas emission at present.

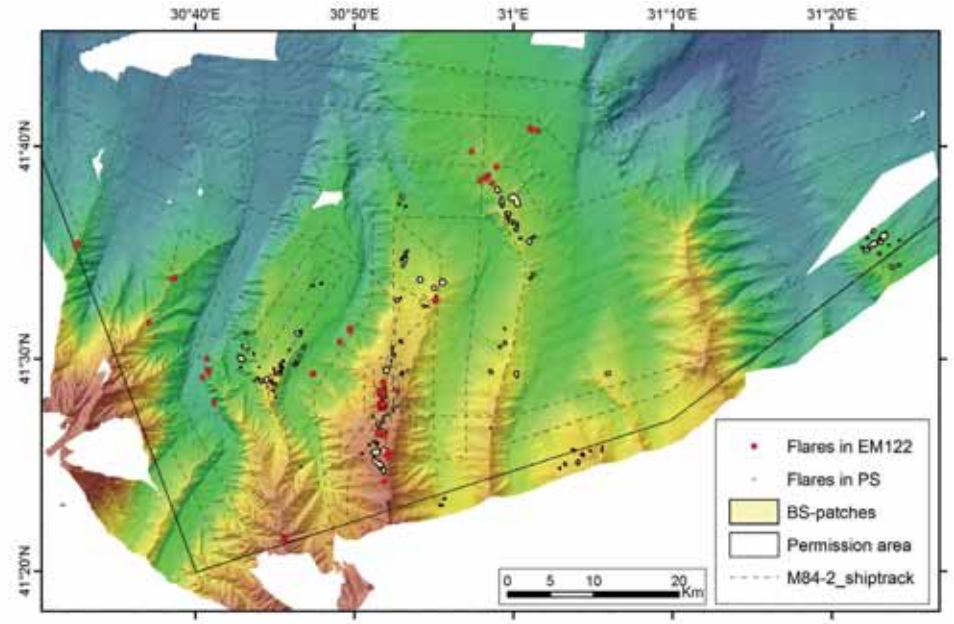

Fig. 33: Cruise track of M84/2 along which swath bathymetry obtained by EM 122 echosounder. The map shows also the location of gas bubble emissions recorded as flares in the echosounder systems EM 122 and PARASOUND during this cruise.

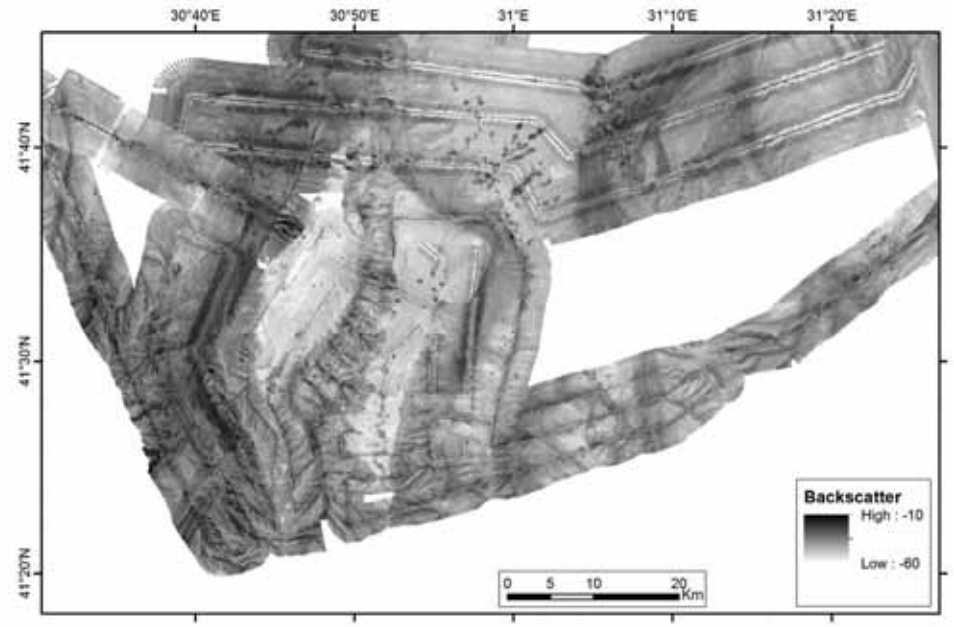

Fig. 34: EM 122 backscatter map obtained during Cruise M84/2. The map shows the same area as the bathymetric chart in Figure 33. Major morphological features can be seen along with backscatter anomalies caused by fluid seepage.

The distribution of backscatter patches and gas emissions is mainly above the flat platform-like tops of the ridges (Fig. 35). Nevertheless, there are two areas with high activity at the foot of the ridges to the incised valley (Fig. 33). The abrupt contact indicates that the valley evolved along a fault zone, that probably also could lean to a pathway for fluid migration to the seafloor.

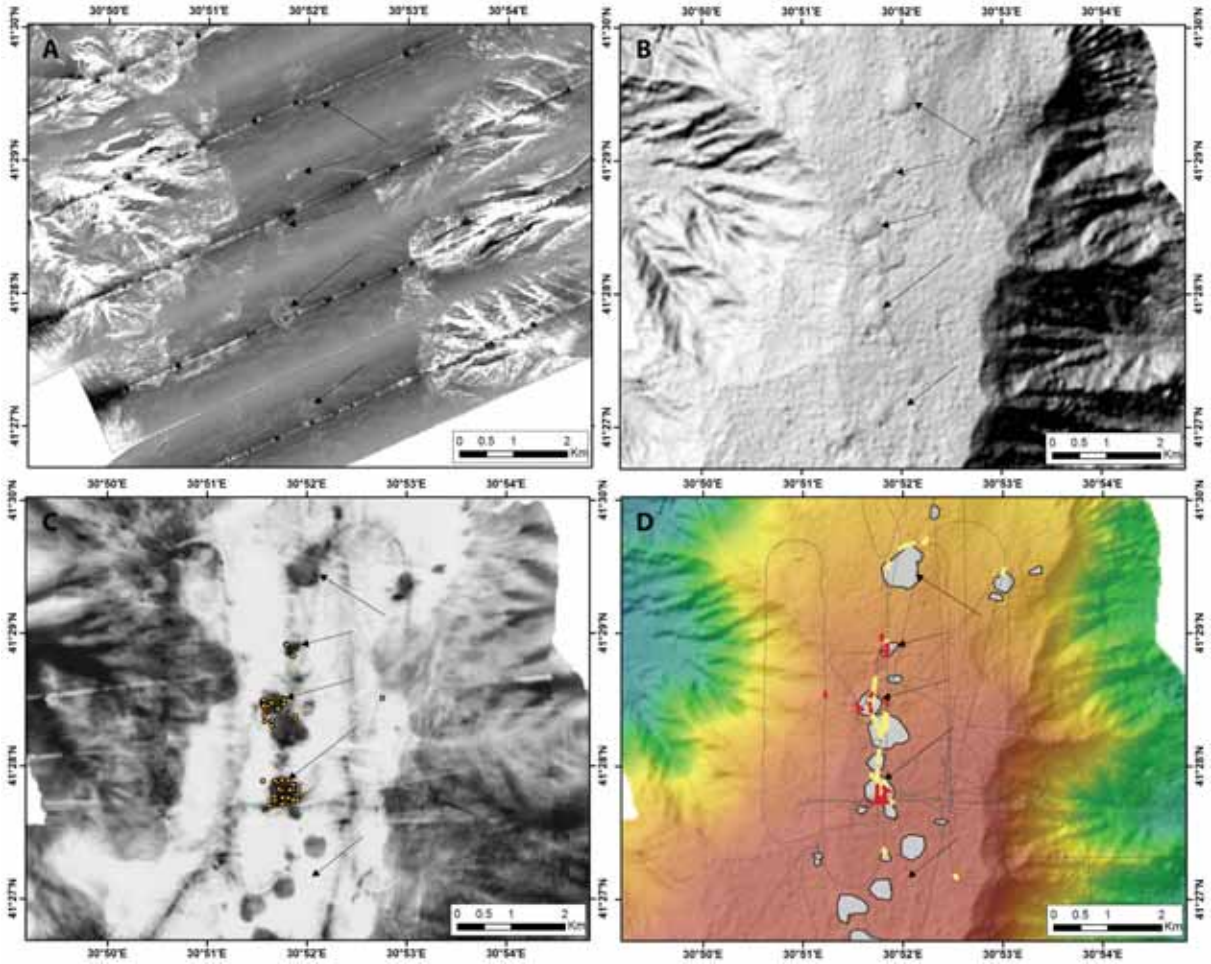

Fig. 35: Eregli Ridge. (A) DTS sidescan sonar. (B) EM 122 shaded bathymetry. (C) EM 122 backscatter and flares picked from EM 122 water column data. (D) EM 122 bathymetry (colour coded and shaded), outline of EM 122 high backscatter, blanking in the sediments (yellow) and flares (red) from PARASOUND.

6.5 Kerch

A large part of the Kerch fan has been covered for bathymetry and backscatter mapping as well as flare imaging using multibeam EM122, EM710 and PARASOUND. Three areas of the margin may be distinguished showing very different morphological characteristics, as the distance to the Kerch strait increase to the west. The westernmost area is a very steep margin, continuing the mountain belt of the Crimean peninsula. Erosional processes lean to deeply incised valleys and the fishbone-like ridges. In contrast to this part, the easternmost area is a smooth margin segment characterized by intensive sliding processes. The fan of the Kerch strait has a shallow shelf with water depths of 80 to 120 m and shows a flat sea bottom surface. Along the shelf edge scarps indicate the uppermost surface expressions of numerous sliding events. There are no deep incised canyons in this area as in both other surveyed regions. The area in between shows several deeply incised canyons but the ridges are not affected by erosional processes as intensively as has been observed in the western area.

In all three areas numerous flares have been recorded by EM122, EM710 and PARASOUND. The entire margin shows a strong activity in gas emission. The huge dataset of the multibeam systems needs to be analysed later on land, but the recorded flares by PARASOUND have been picked onboard and plotted (Fig. 36). In total, about 1400 flares have been counted in all three

areas. Remarkably is, that in the western area only few flares have been found in contrast to the very high amounts in the other two areas in the eastern part, that is related to the Kerch fan.

Already during surveying, it became obvious, that most flares are located along the crests of the ridges. To give a better impression of the intensities of the gas emissions and their distributions, all flares have been classified into weak and strong flares and plotted in different colours. Weak flares are generally a lot more abundant than strong flares. And at least in the central area, the shallow part is covered only by weak flares whereas strong flares only appear in the deeper part.

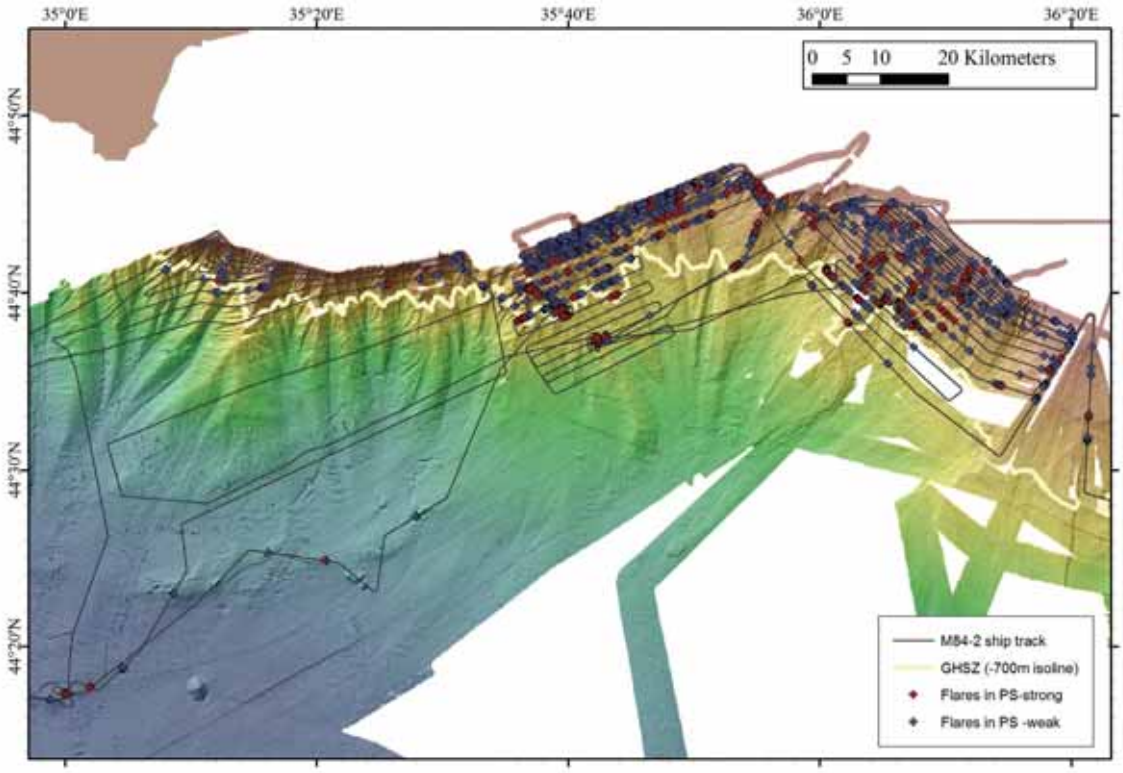

Fig. 36: Flares detected by PARASOUND (19 kHz) along three surveys margin areas at the Kerch fan. With only few outliers, flares are located above the GHSZ, which has been calculated to begin in about 700 m water depth. In contrast to the middle and eastern part of the margin, the western area shows a lot weaker gas emission activity.

The abundance of flares is also related to the gas hydrate stability zone, which upper limit has been calculated for this area to be at ~700-710 m water depth. Only a very few flares have been found below this water depth. One example is Kerch Flare, which is located in about 890 m water depth and a very intense seep area. It is known from former cruises and was always observed to be highly active. During MERIAN cruise MSM15/2 this site has been investigated in detail with hydroacoustics as well as by coring. Three ROV dives have been conducted additionally which have proven the seep areas also visually and allowed further sampling and measuring at the bubble sites found at the seafloor. Two AUV dives over the area resulted in a high-resolution bathymetry map that first showed circular and subcircular elevated patches (Fig. 38) and flare activity seems to be connected to these patches as flares and also blanking zones plot together with these areas.

During this cruise the activity and intensity have been investigated during a detailed survey crossing all known flare areas detected in former cruises (Fig. 37). Although Kerch Flare is still

highly active, the gas emissions are recently concentrated in less areas and the location of the most intense gas emissions changed as well. In 2010 during MSM15/2 the most intense area was located north of the smaller southern patch whereas during this cruise in that area only weak activity has been observed and the strongest flares are located at the western rim of the bigger northern patch (Fig. 37).

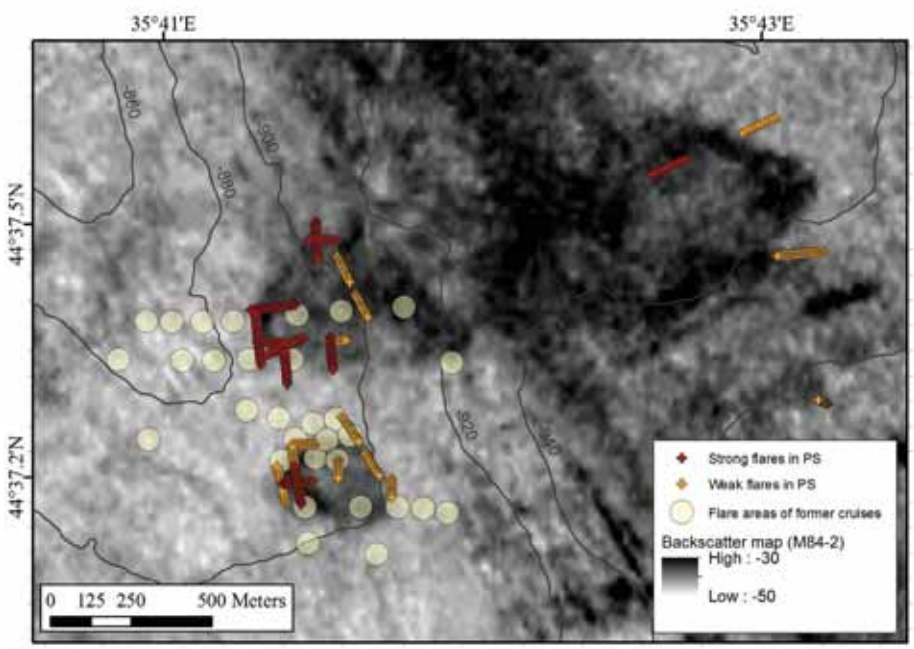

Fig. 37: The location of Kerch Flare is clearly indicated by high backscatter areas. Areas where flares have been recorded in former cruises scatter around the smaller southern patch and west of the bigger northern patch. PARASOUND observations of this cruise show also flares in that areas but the strongest gas emissions are located at the rim of the northern patch.

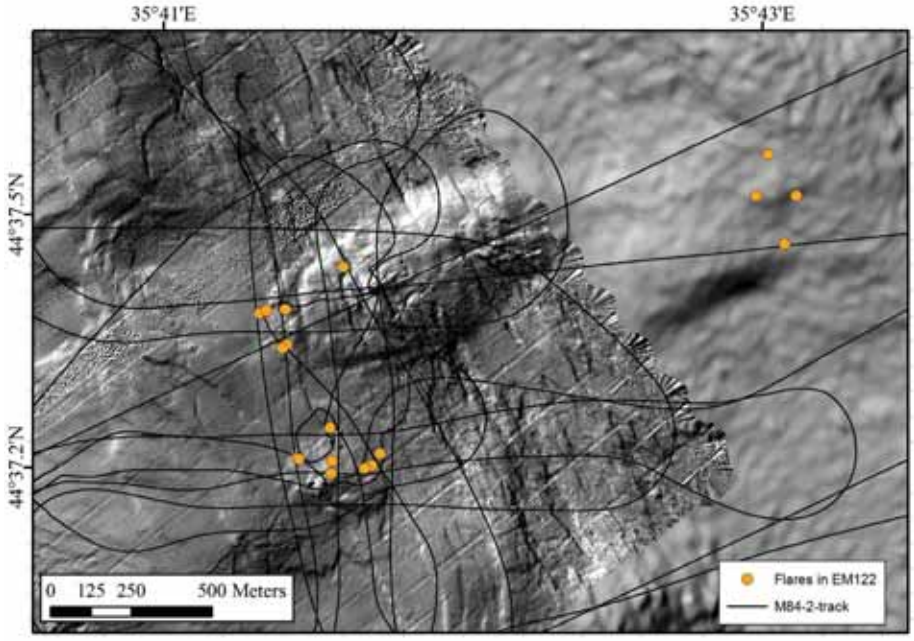

Fig. 38: The high resolution bathymetry map from an AUV-dive performed during MSM15/2 shows the elevated areas that are also characterized by elevated backscatter visible in Figure 37. The picked center points of EM122 flares also plot at these structures. This flare positions are more accurate than flares estimated by PARASOUND recordings.

North of Kerch Flare a very pronounced backscatter patch has been found, that has been crossed another time in two directions to prove whether it is related to stronger gas emissions or an inactive site. It is located in almost 700 m water depth and therefore almost at the boundary to the GHSZ. Above the structure a high activity has been found and several flares have been recorded in the water column (Figs. 39 and 40). In the subbottom record from the PARASOUND are also several blankings documented that indicate high gas content in the sediments below the structure.

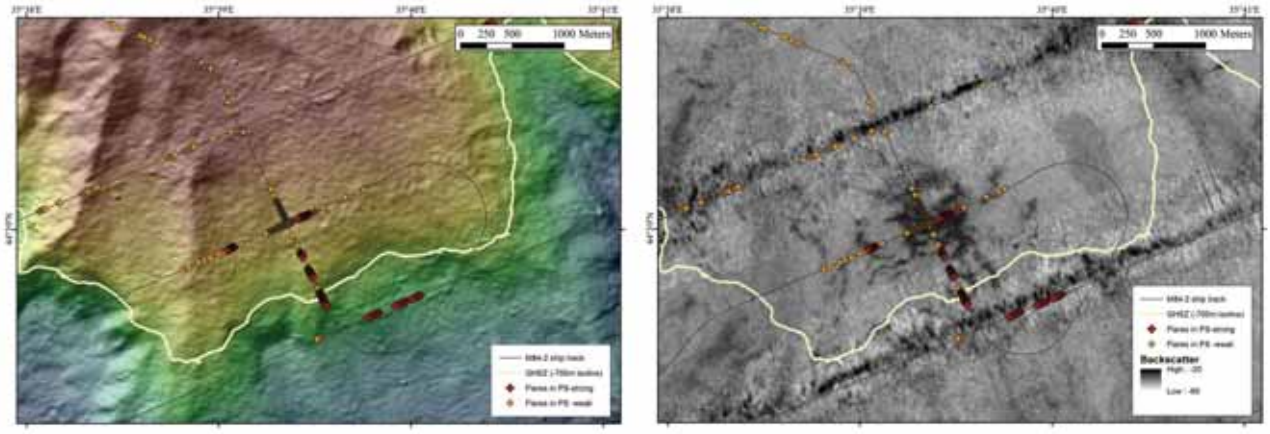

Fig. 39: Backscatter anomaly found north of Kerch-Flare that is related to intense flares observed with PARASOUND. The location is just above the boundary of the GHSZ. In that case the bathymetric map does not show a morphologic expression of the seep site.

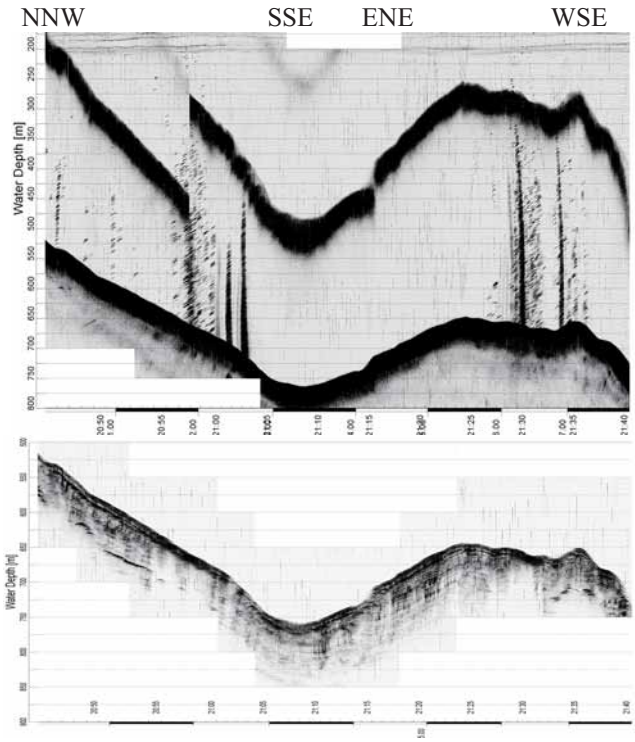

Fig. 40: PARASOUND echograms of PHF (above) and SLF (below) recordings by crossing the BS-anomaly.

6.6 Sorokin Trough

Gas emission in the Sorokin Trough is related to mud volcanism. Numerous mud volcanoes are known in this area in water depths of around 2000 m (Tab.6). During M84/2 a survey crossing most of the mud volcanoes in the northern part of the Sorokin Trough has been conducted in order to proof if they are recently active and to compare the results with former observations. The cruise track and flare observations are shown in Figure 36. In this figure, the Sorokin Trough is located in the south-western part. Table 6 summarizes the flare observations.

Table 6: Flare observations related to seafloor structures within the Sorokin Trough during M84/2 and for comparison also during MSM15/2.

Mud volcano/structure	Flare observation	Intensity	Activity in 2010 (MSM15/2)
Dvurechenskii MV	yes	weak	yes
Helgoland MV	yes	strong	yes
Vodianitskii MV	yes	strong	yes
Nioz MV	yes	weak	yes
Odessa MV	yes	weak	yes
Tblisi	yes	weak	yes
NFS	yes	strong	yes
Istanbul MV	no		no
M12	no		yes
M16	yes	weak	Not passed

At Helgoland Mud Volcano (HMV) and Dvurechenskii MV additional detailed surveys have been conducted for best localisation of each flare center. The flares observed with EM122 have been mapped and the distribution is shown in Figure 41. Both gas emission areas are in the central parts of the mud volcano structures. Flares have been recorded with the PARASOUND system as well and confirm the position located by using the EM122 data. The flare at Dvurechenskii MV is a lot weaker in comparison to the one recorded at Helgoland MV.

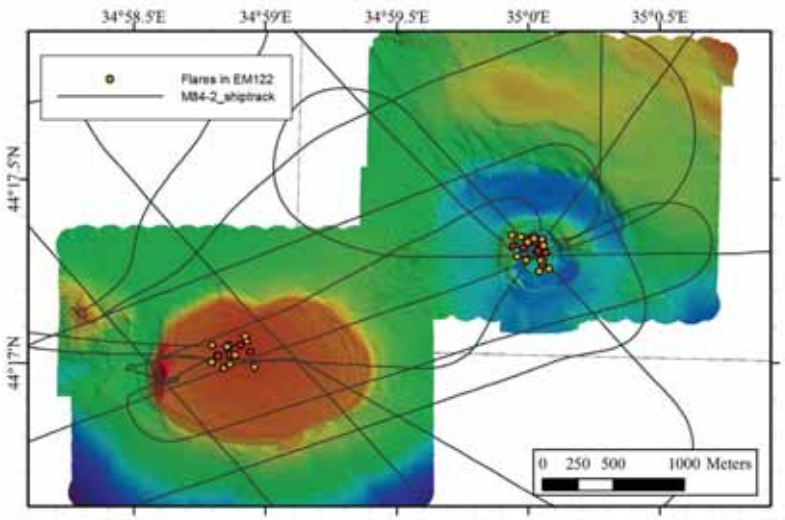

Fig. 41: Dvurechenskii MV and Helgoland MV were both active degassing during M84/2. The red points show the center points of each recorded flare with EM122, whereas the yellow points mark the outer boundary of each flare observation.

7. Station Work With the Autonomous Underwater Vehicle (AUV) SEAL 5000

(G. Meinecke, E. Kopiske, J. Renken)

7.1 Introduction

In the year 2006 the MARUM ordered a deep diving autonomous underwater vehicle (AUV), designed as a modular sensor carrier platform for autonomous underwater applications. The AUV was built in Canada by the company International Submarine Engineering (I.S.E.). In June 2007 the AUV "SEAL" was delivered to MARUM and tested afterwards on the French vessel N/O SUROIT (June 2007) and the German R/V POSEIDON (November 2007) in the Mediterranean Sea as extended Factory Acceptance test. Since then, the AUV was prepared to be set step by step in operational mode, which is in fact much more complicated due to missing technical maturity of autonomous systems in general.

7.2 SEAL Vehicle: Basics

The AUV Seal is No. 5 of the Explorer-AUV series from the company I.S.E. Two other very similar AUVs are operated by IFREMER (La Seine sur Mer), one by University New Foundland and one by Memorial University Mississippi. Recently, the Canadian Government also bought two 5000 vehicles, being the largest ones together with the SEAL vehicle.

The AUV is nearly 5.75 m long, with 0.73 m diameter and a weight of 1.35 tons. The AUV consists of a modular atmospheric pressure hull, designed from 2 hull segments and a front and aft dome. Inside the pressure hull, the vehicle control computer (VCC), the payload control computer (PCC), 8 lithium batteries and spare room for additional "dry" payload electronics are located. Actually, the inertial navigation system PHINS and the RESON multibeam-processor are located as dry payload here. The tail and the front section, build on GRP-material, are flooded wet bays. In the tail section the motor, beacons for USBL, RF-radio, flash light, IRIDIUM antenna, DGPS antenna and the pressure-sensor are located. In the front section the Seabird SBE 49 CTD, the Sercel MATS 200 acoustic modem, the DVL (300kHz), KONGSBERG Pencil beam (675kHz), the RESON MBES 7125B (400kHz) and the BENTHOS dual frequency (100/400kHz) side scan sonar are located. The SEAL AUV has a capacity of approx. 15 kWh main energy and additional capabilities for 4.0 – 6.0 kWh more main energy without design change.

For security aspects, several hard- and software mechanisms are installed on the AUV to minimize the risk for malfunction, damage and total loss. More basic features are dealing with fault response tables, up to an emergency drop weight, either released by user or completely independent by AUV itself.

MARUM put special emphasis on open architecture in hard- and software design in order to be as much as possible modular and flexible with the vehicle after delivery. Therefore the VCC is based to large extend on industrial electronic components and compact PCI industrial boards and only very rare proprietary hardware boards. The software is completely built QNX 4.25 – a licensed UNIX derivate, to large extend open for user modifications. The payload PC is built on comparable hardware components, but running with Windows and/or Linux on demand.

On the support vessel, the counterpart to the VCC is located on the surface control computer (SCC). It is designed as an Intel based standard PC, also running with same QNX and a Graphic

User Interface (GUI) to control and command the SEAL AUV. Direct communication with the AUV is established by Ethernet-LAN, either by hardwired 100 mb LAN cable plugged to AUV on deck, or by Ethernet-RF-LAN modem once vehicle is on water. The typical range of RF-communication is around 1 – 2 km distance to vehicle. Within this range the user has all options to operate the AUV in Pilot-Mode, e.g. to manoeuvre the AUV on water or change settings. Once the AUV is under water, all communication links were shut down automatically and the AUV has to be in Mission-Mode, means it is working based on specific user-defined mission.

Despite being in mission-mode it is necessary to communicate with the AUV when it is under water, for instance asking for actual position, depth and status. To achieve this, onboard the support vessel an acoustic underwater modem with dunking transducer has to be installed (Sercel MATS modem) communicating with the counterpart on the AUV, on request. Due to limited acoustic bandwidth only rare data sets are available.

7.3 Mission Mode

The AUV as dedicated autonomous vehicle has to be pre-defined operated under water. As mentioned, only at sea surface a manoeuvring by the pilot is possible - once it dives, it will loose communication and therefore must be in a mission-mode. Initialized correctly, fault prevention mechanisms should prevent the AUV for damage/loss in that case.

Simplified, an AUV mission is a set of targets, clearly defined by its longitude, latitude, and a given depth/altitude the vehicle should reach/keep by a given speed of AUV in a distinct time. The AUV needs to be in a definite 3-dimensional underwater space to know exactly its own position over mission time in order to actively navigate on this. To achieve this basic scenario, the AUV is working at sea surface with best position update possible, e.g. DGPS position. Once it dives, it takes the actual position as starting point of navigation, looks for its own heading and the actual speed and calculating its ongoing position change based on the last actual position, e.g. method known as dead reckoning. To achieve highest precision in navigation, a combination of motion reference unit (MRU) and Inertial Navigation System (INS) is installed on the SEAL AUV – the PHINS inertial unit from IXSEA Company. Briefly, the MRU is “feeling” the acceleration of the vehicle in all 3 axis (x,y,z). The INS is built on 3 fibre-optic gyro’s (x,y,z) and gives a very precise/stable heading, pitch and roll information, based on rotation-changes compared to the axis. Even on long duration missions, the position calculating by the AUV should be very accurate based on that technique.

7.4 Mission Planning

In principle and very briefly, it would be accepted by the vehicles VCC to receive a simple list of waypoints as targets for the actual mission, in a specific syntax. In order to arrange it more efficient and convenient a graphical planning tool is used for this mission planning. The MIMOSA mission planning tool is a software package, developed by IFREMER, specially designed to operate underwater vehicles (AUVs, ROVs). The main goal of this software is to plan the current mission, observe to AUV once it is underwater and to visualize gathered data from several data sources and vehicles.

MIMOSA is mainly built on 2 software sources, e.g. an ArcView 9.1 based Graphical Information System (GIS) and a professional Navigation Charting Software offered by Chersoft UK.

In order to plan a mission the user has to work on geo-referenced charts with a given projection (MERCATOR), either GIS-maps, raster-charts or S-57 commercial electronic navigational charts (ENCs). These basic charts set could easily be enlarged with user specified GIS projects, enhanced with already gathered data, e.g. multibeam data, points of interest. Once installed in MIMOSA, one can create AUV missions by drawing the specific mission by mouse or using implemented set of tools (MIMOSA planning mode). Missions created in that way are completely editable, movable to other geographical locations and exportable to other formats. In order to be interpretable by the SEAL AUV, the created mission will be translated in the I.S.E. specific syntax; a set of targets, waypoints, depth informations and timer will be created and written into an export path. From here the mission file can be uploaded via the SCC (support vessel) into the VCC (AUVs control PC); the AUV has its mission and is capable to dive based on mission plan.

7.5 Mission Observing/Tracking

The MIMOSA planning tool is also used to monitor the vehicle at sea surface, more interesting under water (MIMOSA observation mode). The MIMOSA software is client based, means one dedicated server is used for planning, while the others are in slave/client mode, picking up actual missions. Therefore, position data strings from the AUV are being sent to local network and fed into the MIMOSA software to display actual vehicle position, e.g. DGPS signal once it is on sea surface. During dive the AUV can be tracked automatically via ultra short baseline systems (USBL), e.g. IXSEA GAPS or POSIDONIA, using the on-board AUV installed USBL transponder beacon (deliver position where the vehicle “actually” is).

In addition to this independent position source vehicles own position (deliver where the vehicle “thinks” it is) can be displayed also. This position is based on transmitted data strings from MATS underwater acoustic modem, only coming from AUV on user request.

To summarize, usually you have displayed in tracking mode:

- position of support vessel
- either DGPS of AUV during surface track, or
- USBL position (GAPS or POSIDONIA)
- and MATS position (underwater acoustic on request)

7.6 Operational Aspects

The SEAL AUV was used at least 6 times on field cruises so far (2 times for technical trials). Thus, several different vessels have been in operation and on each vessel the handling of the AUV is quite a bit different. In principle, the A-frame seems to be the best position to launch and recovery the AUV, because the tendency to hit ships wall is minimized compared to sideward operation, based on experiences.

On R/V METEOR the launch and recovery was planned with the recently installed crane No.1 at starboard side of vessel, because the gear boom was used not appropriate for AUV operations and the A-frame was blocked by MeBo operations.

In principle the AUV can be operated out of the lab, based on simple PC-console racks. On METEOR M84/2a cruise, the AUV operations were run out of a 20" operation/workshop van, located on the main deck. The consoles, file-server and printer are installed in the container, workbench, tools and spares also.

Prior to launch of AUV, the PHINS on-board the AUV needs to be calibrated. Therefore, the PHINS needs to be reset and the vessel has to be still standing for at least 5 minutes. After that initial phase (coarse align), the vessel needs to run a rectangular course of 5 minutes times 3 knots each line (fine align). At the end of that time span and course, the PHINS is in so called "normal mode", means it has it highest position quality.

7.7 Station Work on M84/2a Cruise

During installation of AUV on-board METEOR in Istanbul harbour it was obvious that the vehicle was damaged during transportation. The nose of the vehicle showed a crack in the GFR wet-bay, resulting from a hard hit against the inside container wall during shipping/loading of container.

Prior to cruise, the AUV was neutrally trimmed in Bremen test tank at approx. 4 ‰ salinity. Thus, it was necessary to adjust the AUV to ambient salinity conditions at Black Sea. Therefore, the first operation was a trim or balancing test with the AUV at station. Due to specific salinity situation at Black Sea, the uppermost 130-150 m of water column are at only 18 ‰ salinity, while the deeper part of water column are at approx. 21 ‰ salinity. The trim has to be the balance between a just floating, deep lying heavy vehicle (negative trim) at sea surface and more light vehicle at depth (positive trim), in more dense water columns. The more light the vehicle is on sea surface the more the vehicle has to fight against the more uplifting force in denser deep water.

The first test was performed during more rough sea state conditions in around 5-6 bft. During first test at Dive 39, it was obvious, that the vehicle was too heavy, it was deep lying in the waves. Lot of wash over at the stern plane took place and strongly influenced the remote RF communication with vehicle. During operation in rough sea state plane no. 5 stopped working with a fault, therefore the vehicle had to be recovered, anyway. Finally, we decided to remove some ballast weights from the AUV. The plane could be fixed in repair of mechanics.

On dive no. 40 the vehicle was trimmed lighter and behaved a bit better in waves. Nevertheless, RF communication restrictions have been recognized several times during test. First initial test (so called Label 20, dive down to 30 m, circle 5 minutes on depth) failed with a present indication of a ground fault on 48V main power bus of vehicle, detected by the very sensitive groundfault detection system (GF), which is installed on AUV in order to ensure the vehicle is in optimal electronic condition – all sensors in the flooded sections are connected to several channels of the GF system. For security reasons, it is not possible to set the AUV in mission mode if the GF system indicates a fault – except really hard-coded overriding of the GF response in the Fault Response Table (FRT), which inhabits the potential to ignore a complex fault of the system at depth, occasionally resulting in a total loss of vehicle.

Once on deck, the vehicle hull was opened, in order to check whether the hit during container transport damaged some parts of main electronics inside. Opening of hull under sea conditions is not really appropriate, because the vehicle hull is evacuated and therefore very humid and even salt ballasted air is venting the inner hull and electronics during opening procedure. No visible damages have been recognized during visible inspection. Afterwards, several potential fault

sources have been checked afterwards on deck, in order to solve the problem. Finally, we changed the main thruster unit as most potential fault source.

On dive no. 41 the GF on 48V channel was persistent, without no chance of diving. The vehicle had to be recovered again. Finally, we had to open the main hull of the vehicle again, in order to change the main bulkhead on thruster connection. In addition, the main switch was removed and the bulkhead was changed, as well.

On dive no. 42 the GF on 48V channel was not active, means we solved the problem. During label 20 test, a next GF appears on depth. Now, the GF system recognized a GF on different GF channels – mainly related to the steering planes, but also related to the main vehicle control computer VCC, the Paroscientific depth sensor and the GPS system. The consequence was the same – no chance e to dive with the AUV.

In the following days it was tried to isolate the very wide-ranged potential fault source. The several tests have been done, with the planes, lost of connectors, replacements of different sensors. None of these maintenance actions solved the problem. During the next dives 43 and 44 the vehicle performed well on sea surface, without no indication on GF problems, even the test labels run all smooth. Once the vehicle was set to mission mode and the vehicle started to descend to target depth, on different depth levels in around 100 - 120 m waterdepth the vehicle stopped working with a fault response. Each time, the fault response was related to persisting GF on the cumulative GF channels 1, 3 and 4, triggering the planes, VCC , Paro and the GPS.

Finally, we decided to cancel the AUV work, because further investigation especially on planes and main electronics are extremely necessary to solve the strange vehicle behaviour on depth. Due to humid and rainy weather conditions, we have been unable to open the hull again, in order to run electronic tests on deck.

7.8 Results

Despite the lack on scientific results on AUV operations during the cruise, several operational aspects could be proven during the AUV operations on M84/2a cruise. Launch and recovery worked very well and smooth. Operations with the new crane no. 1 have been absolutely fine. For recovery, the first time the lock-latch was used to connect the floating AUV to ships crane. The system runs very reliable and simplified the critical zodiac operation near ships hull to great extent.

As result for AUV team itself, a long list on electronic modifications has been written during cruise in order to be better prepared for complex faults, active during the M84/2a cruise.

8. Coring with the Sea Floor Drill Rig MeBo

(T. Freudenthal, M. Bergenthal, R. Düßmann, O. Herschelmann, K. Kaszemeik, T. Klein, M. Reuter, U. Rosiak, W. Schmidt, A. Stachowski)

8.1. Introduction

During R/V METEOR Cruise M84/2, the seafloor drilling rig MeBo was used for getting long sediment cores (Fig. 42). This device is a robotic drill that is deployed on the sea bed and remotely controlled from the vessel (Fig. 42). The complete MeBo system, including drill, winch, launch and recovery system, control unit, as well as workshop and spare drill tools is shipped within six 20' containers. A steel armored umbilical with a diameter of 32 mm is used to lower the 10-tons heavy device to the sea bed where four legs are being armed out in order to increase the stability of the rig. Copper wires and fiber optic cables within the umbilical are used for energy supply from the vessel and for communication between the MeBo and the control unit on the deck of the vessel. The maximum deployment depth in the current configuration is 2000 m.

Fig. 42: The sea floor drill rig MeBo during the first deployment of expedition M84/2 (picture.

The mast with the feeding system forms the central part of the drill rig (Fig. 43). The drill head provides the required torque and rotary speed for rock drilling and is mounted on a guide carriage that moves up and down the mast with a maximum push force of 4 tons. A water pump provides sea water for flushing the drill string for cooling of the drill bit and for removing the drill cuttings. Core barrels and rods are stored on two magazines on the drill rig. We used wire-line core barrels (HQ) and hard metal drill bit with 55 mm core diameter (push coring). The stroke length was 2.35 m each. With complete loading of the magazines a maximum drilling depth of about 70 m can be reached. Station time can reach more than 24 hrs per deployment.

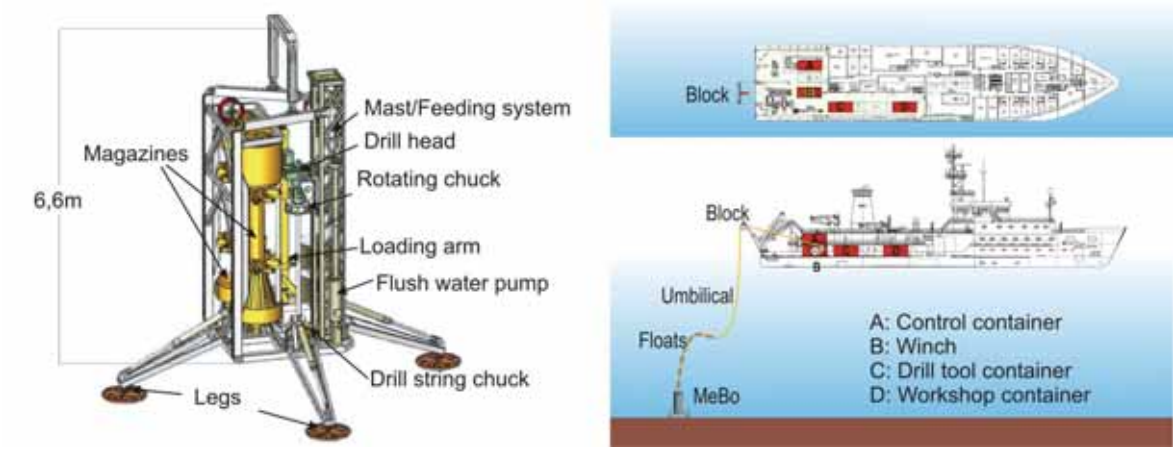

Fig. 43: Schematic overview on the MeBo drill rig (left) and its deployment from a research vessel (right).

The MeBo was deployed 6 times. In total the MeBo was operated nearly 76 hrs. The main goal of the deployments was the investigation of the occurrence of gas hydrates in the Black Sea sediments. Altogether 52.15 m were drilled and about 40 m core was recovered. Muddy sediments as well as gas hydrate bearing sediments and massif hydrates were drilled. Detailed information on deployment of MeBo and recovery of sediments is summarized in the station list (Table 7). Optimal recovery rates for the massif hydrates were achieved by rotary drilling technique while push coring technique was better suited for the soft sediments.

The extremely soft upper sediments at the sea floor were a major challenge for the deployment of MeBo at all sites besides of GeoB15227-3. Since the electro-hydraulic drive of the drill rig is mounted at the bottom of the drill rig it was covered by mud immediately after landing the system on the sea floor. This resulted in an inefficient cooling of the electric motors and the pumps. The drive had to be switched off after short periods of drilling operations in order to prevent the system from overheating. We supposed that the repeated switches of the drive in combination with the inefficient cooling of the pumps resulted in the failure of the hydraulic pumps during the first and last deployment. An efficient cooling of the electro-hydraulic drive is mandatory for future deployments of the drill rig on these kinds of extremely soft sediments.

Table 7: Station list for MeBo deployments.

Station GeoB No.	Deployment duration [hrs:min]	Latitude [N]	Longitude [E]	Water depth [m]	Drill depth [cm]	Recovery [cm/]	Remarks
15208-1	13:49	41°27.412	30°51.138	975	800	598/75%	Stopped due to failure of hydraulic pump
15220-3	3:42	41°57.159	41°16.842	878	0		Failure of Can-Bus
15220-5	17:15	41°57.156	41°16.842	878	1415	1090/77%	
15226-2	6:28	41°58.938	41°07.587	1025	505	376/74%	
15227-3	14:01	41°59.000	41°07.540	1027	1910	1317/69%	
15236-2	20:38	41°57.590	41°17.350	838	985	596/61%	Stopped due to failure of hydraulic pump

8.2 Prototype Tests of MDP-Pressure Core Barrel
(H.-J. Hohnberg)

Within the joint BMBF/BMWI project SUGAR I, a novel pressure core barrel, the MeBo-Druckkern-Probennehmer (MDP), was developed for the use with the sea floor drill rig MeBo to recover deep hydrate-bearing sediments under in situ pressure. The MDP is to be used similar to a conventional MeBo wire-line inner core barrel, but additionally allows for quantitative sampling of gas within the sediments. The MDP consists of (a) a cutting shoe or drill bit for cutting the sediment core with the required core diameter, (b) an upper piston using hydrostatic pressure to force the penetration of the core into the core barrel, (c) a pressure housing and a lower valve that is closed subsequent to the coring process in order to keep the in-situ pressure within the core barrel, (d) a core catcher that prevents loss of sediment before the valve is closed, and (e) a latching device that ensures correct positioning of the MDP within the MeBo drill string and that activates the closing of the valve when the MDP is hooked up by wire inside the drill string.

During M84/2 the main goal of the MDP prototype experiments was to test the patent pending piston system, which is based on the pressure gradient between the pressure enclosed in the core barrel housing and the in-situ pressure. This system controls the movement of a piston that forces the sediment core into the core barrel while the core barrel is pushed into the sediment. The piston is locked mechanically until a touch sensor hits the sediment at the bottom of the drilled hole during the start of the coring process.

During M84/2 the MDPs could unfortunately not be tested as a functional part of MeBo, since the hydraulic-pump of MeBo failed few days after the first MeBo deployment. Therefore, the tests were conducted with a modified MDP-prototype (‘Lotvariante’-MDP, the LDP) that was deployed on the ship’s wire similar to a conventional piston corer (Fig. 44). The LDP is a complete MDP additionally equipped with pilot-plates. The LDP was lowered towards the sea bed with a speed of 1.0 m/s until contact with the sea floor activated the sampling. After a few seconds of holding time, the LDP was lifted off the sediment and recovered on the ship’s deck.

Fig. 44: Deployment of the LDP from board the R/V METEOR during M84/2.

Aspects investigated during the LDP/MDP tests were:

Is there an influence of the sea motion and of the descending speed on the locking of the piston?

Is the sensitivity of the touch sensor sufficient during contact with the sediment?

How fast is the piston activated during contact with the sediment?

Has the dynamic of the piston to be damped after releasing?

How much nozzles and which nozzle diameter are necessary for damping the piston at different water depths and sediment types?

How reliable is the function of the handmade breaker plates (carbon-fiber-reinforced plastic) at different pressure levels and their 'snapping through' -behavior during the activation of the piston?

Does the tool need for penetration kinetic energy depending on freefall-distance and its own mass?

How much force is required to overcome the friction between liner-retraction system and O-rings?

How deep does the tool penetrate into the sediment?

Does the core length correspond to the penetration depth?

Is there any obvious core disturbance attributable to the sampling procedure?

How reliable is the core catcher?

Is the stability of the different materials used sufficient at different pressure gradients and at maximum deployment depth?

What are the dynamic loads during the unlocking of the piston?

Is it important to have a piston retaining system that shall impede a backward movement of the piston after the coring?

Does the piston retaining system work properly?

Does the sealing-flap work properly?

Table 8: Station list for LDP deployments. Note: Because the LDP is not equipped with an active core cutting mechanism, the flap could not be closed properly at the seabed and, thus, the in situ pressure was always lost.

GeoB No.	Ship station No.	Date 2011	Deployment start UTC [hrs:min]	Latitude [°N]	Longitude [°E]	Water depth [m]	Recovery [cm]
15211	145	01.03.	9:40	41°28.075	30°52.392	996	140
15220-2	155	04.03	05:23	41°57.145	41°16.851	878	140
15227-4	169	07.03.	08:59	38°10.43	41°58.981	1026	140
15235-2	180	09.03.	05:54	41°52.278	41°17.237	878	140
15503-2	238	20.03.	12:40	41°32.440	37°36.890	1521	100
15512-3	255	24.03.	12:10	44°37.419	35°42.357	895	140
15529	274	29.03.	04:48	44°16.950	34°58.670	2054	000
15533-3	283	29.03.	23:30	44°18.166	34°59.162	2054	000

During M84/2 the LDP prototype was deployed for the first time and at eight stations (Table 8). Down to 1500 m water depth the entire system worked properly, although the flap could not be closed because of the lack of an active core cutting mechanism below the core-catcher which

is an integral part of the MeBo system. The last two deep-sea deployments at 2000 m water depth failed because the friction force between the liner retraction system and the O-rings was too strong. As a result the breaker plates did not break as intended, the piston did not release, and the liner retraction system could not be pulled.

Results obtained during LDP deployments were:

The motion of the sea did not influence the locking of the piston.

The touch sensor worked properly and the piston is activated during contact with the sea floor on impulse.

The breaker plates worked reliably down to a water depth of about 1500 m.

Not much kinetic energy is required for penetration of the LDP.

The penetration depth and the relation between core length and penetration depth could be evaluated during M84/2.

The vertical movement of the piston is very fast if not damped. Damping of the piston-speed is achieved by water fillings in combination with the introduction of water flow-jets in the liner.

The core catcher with blade strength of 0.2 mm was suitable for keeping the sediment inside the core barrel. The dynamic load during the activation of the piston caused no damage of the blades during damped deployments.

The evaluation of the core structure will be based on the results of geochemical investigations (typical porewater profiles).

In conclusion the MDP/LDP system is working according to the expectations. Modifications that have to be realized after the cruise and should improve the functionality are according to the test results:

The maximum speed of the piston can be controlled and adjusted to the coring speed by controlling the size of the water pathways.

The piston retaining system requires a slight technical modification.

Some O-ring-sealings have to be changed to sliding ring sealings.

A core cutter has to be designed and added to the system.

The core catcher in combination with the lower liner-end requires a technical modification.

In order to avoid contamination of the flap mechanism by sediment the upper liner release mechanism has to be modified to install a pressure equilibration system.

8.3 Results of MeBo Cores

(A. Bahr, J. Wei, D. Nadezhkin)

8.3.1 MeBo-63, Eregli Patch 1

This site targets a high-backscatter patch found in the Eregli Area which is related to gas seep activity. With a total drilling depth of 800 cm a total of 598 cm of sediment have been recovered belonging to Unit 1, 2, 3. Unit 1 and 2 reach down to ca. 6.30 drill depth, the Holocene sedimentation rate at this site is therefore much higher than in comparable cores from the NW Black Sea but similar to that of the adjacent cores MD04-2760/2788 and GeoB 7622-2 located off the Sarkarya River mouth (Lamy et al., 2006; Kwiecien et al., 2008). As described from GeoB 7622-2 numerous homogeneous clay layers of up to 1 cm thickness are intercalated

between the darker laminae in Unit 2 and light laminae (coccolith)/dark laminae of Unit 1. These clay layers have been interpreted to represent riverine transported suspended matter related to high-discharge events rather. Notably, the surface salinity at the GeoB 15298-1 site is 17.5 PSU (shipboard sensor) which is lower than the common 18.5 in Black Sea surface waters, indicating freshwater influence. While moderately strong H_2S smell was observed, some parts of sediment have been affected by degassing but no indication of gas hydrate presence is evident.

Table 9: Overview of drilling depth and core recovery of MeBo station GeoB 15208-1.

Core Nr.	Start of drilling (cmbsf)	End of drilling (cmbsf)	Sections	Recovery (cm)	Whole round samples (cm)	Samples
1P	0	270	1	137	127-137	Porewater
			CC	15		
2P	270	505	1	97	87-97	Porewater
			CC	15		
3P	505	740	1	118	108-118	Porewater
			2	91	81-91	Porewater
			CC	13		
4P	740	800	1	96	86-96	Porewater
			CC	16		
	Total recovery (cm)			**598**		

8.3.2 MeBo-64 and 65, Batumi Reference Site

These drill locations were intended to drill a representative profile of the background sedimentation in the Batumi area. While MeBo Station 64 (GeoB 15220-3) has been abandoned due to technical problems, MeBo-65 (GeoB 15220-5) reached a total drilling depth of 1415 cm and a total of 1090 cm of sediment have been recovered. The upper 1.16 m comprise the marine Units 1 and 2 while Unit 3 is characterized below 5.8 m by a regular succession of dark, slightly sandy layers (likely turbidites) alternating with lighter, clayey intervals. Red layer intervals known from the western part of the Black Sea have not been found. Based on the shipboard data reliable information on the maximum age of the recovered sediments could not be obtained, however, the regular intercalation of turbiditic material suggests high glacial sedimentation rates. Moderate H_2S smell was noticed from the core and some parts of sediment have been affected by degassing but indications for the presence of gas hydrates were not recognized.

Additional information regarding the recovery and core quality can in this case be obtained by the comparison of the reflectance data from the MeBo drill site and the parallel gravity core GeoB 15220-1. Figure 46 shows the proposed correlation between both sites, indicating that, first, the MeBo did not lose much sediment at top, and, second, the MeBo core seems to be compressed during drilling and core retrieval relative to the gravity corer. Furthermore, the data seems to suggest that voids between incompletely recovered segments are relatively minor.

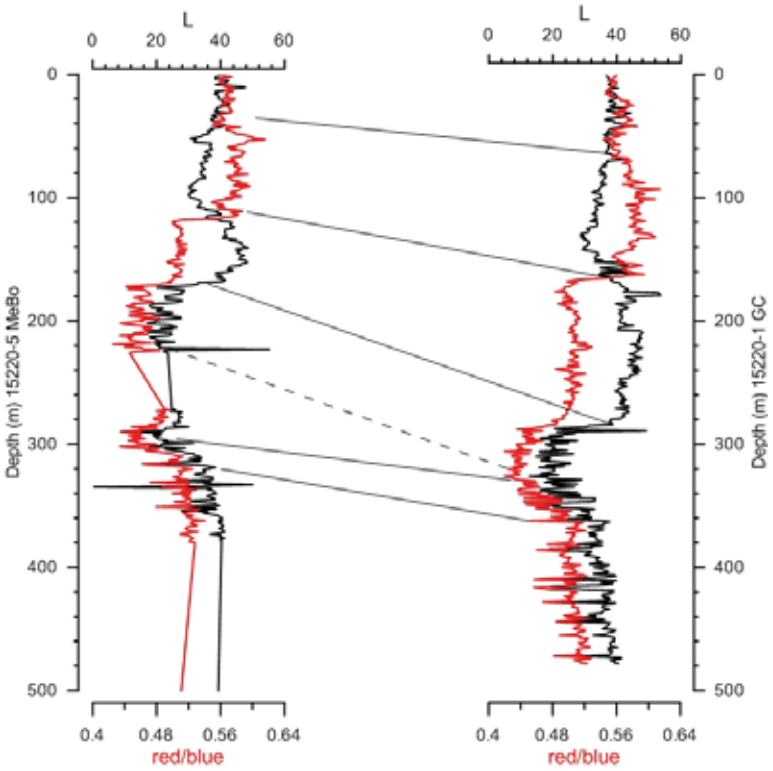

Fig. 46: Correlation of MeBo Site GeoB 15220-5 and parallel gravity core GeoB 15220-1. Lightness is shown as black line, red/blue ratio as red line with respective correlations.

Table 10: Overview of drilling depth and core recovery of MeBo-65 (GeoB 15220-5).

Core Nr.	Start of drilling (cmbsf)	End of drilling (cmbsf)	Sections	Recovery (cm)
1P	0	270	1	121
			2	89
			CC	17
2P	270	505	1	95
			CC	18
3P	505	740	1	121
			2	90
			CC	16
4P	740	975	1	96
			CC	13
5P	975	1210	1	120.5
			2	94
			CC	14.5
6P	1210	1415	1	120
			2	50
			CC	15
	Total recovery (cm)			**1090**

8.3.3 MeBo-66 and 67, Pechori Mound

In Pechori Mound an attempt was made to drill oil-stained, hydrate-rich sediments. MeBo-66 (GeoB 15227-1) was drilled down in the push-core technique to 505 cmbsf, when drilling operation was stopped due to the encounter of a hard substrate. The core recovered mostly oil-stained clay with gas hydrates. In the uppermost section 1P-1 relatively stiff clay with dark lamination and light coccolith-layers has been cored, while below the sediment is generally characterized by moussy to soupy consistency. Only in some parts that were less affected by gas hydrate decomposition, degassing and oil staining, distinguishable coccolith-bearing layer were found. It might therefore be assumed that the sediment is a mixture of extruded clayey sediment and more or less homogenized hemipelagic sediment belonging to Unit 1. Except section 1P-1, all sections contained gas hydrates in abundance with sizes exceeding 1 cm in thickness. Notable, authigenic carbonates have not been found. Due to the highly disturbed sediments no color scanning has been performed.

Fig. 47: Gas hydrates in oil-stained sediments (GeoB 15227-1, section 1P-2A).

Table 11: Overview of drilling depth and core recovery of MeBo (GeoB 15227-1).

Core Nr.	Start of drilling (mbsf)	End of drilling (mbsf)	Sections	Recovery (cm)
1P	0	270	1	42
			2	94
			CC	0
2P	270	500	1	121
			2	119
			CC	0
3P	500	505		
			Total recovery (cm)	**376**

This drill site is a parallel core to GeoB15227-2, which was abandoned due to hard hydrate layers accounted. With rotary drilling, a total drill depth of 19.10 m was reached. No hemipelagic sediments were accounted, the entire core consists of expelled mud from the mound. The sediment is characterized by thoroughly oil-stained brownish silty clay with fine sand components that are constituted of indurated clay (fine grained "mud breccia"). Otherwise, the core contains abundant, massive oily hydrates. Some sections (in particular 5R-2, 4R-1, 8R-1, 9R-1) were entirely filled with hydrates, leaving only water, oil and very few sediment particles after decomposition. When comparing recovery and the drill log it seems that the recovered intervals represent hydrate-rich layers while hydrate-poor or barren sediments where lost during drilling.

Table 12: Overview of drilling depth and core recovery of MeBo-67 (GeoB 15227-3).

Core Nr.	Start of drilling (mbsf)	End of drilling (mbsf)	Sections	Recovery (cm)	Remarks
1P	0	245	1	120	
			2	126	
			CC	15	gas hydrate, length estimated
2R	245	270	--		
3R	270	505	1	100	
4R	505	740	1	120	
			2	118	
			CC	15	gas hydrate, length estimated
5R	740	975	1	65	
			2	65	
			CC	15	gas hydrate, length estimated
6R	975	1210	1	50	
7R	1210	1445	1	61	
			CC	15	gas hydrate, length estimated
8R	1445	1680	1	120	
			2	125	
			CC	15	gas hydrate, length estimated
9R	1680	1910	1	120	
			2	37	
			CC	15	gas hydrate, length estimated
		Total recovery (cm)		**1317**	

8.3.4 MeBo-68, Batumi Seep

This MeBo site (GeoB 15236-2) targeted gas hydrate-bearing sediments but in contrast to Pechori Mound without association to oil. The top of the recovered sediments belong to Unit 2, thus, missing the overlying coccolith ooze. Unit 2 shows no influence of hydrates, the underlying Unit 3 in section 1P-1 displays some degassing structures, however, finely dispersed hydrates appear in section 1P-2 and below. In contrast to earlier gravity cores which retrieved disperse clathrates, massive gas hydrate layers of at least 10 cm thickness have been encountered in sections 2P-1 and 3P-1 below a drill depth of 2.70 m (Fig. 48). Unit 3 in the gas hydrate bearing parts has also a slight sandy component which seems to derive from indurated clay particles of uncertain origin.

Fig. 48: Gas hydrate from GeoB 15236-2, from the top of section 3P-1.

Table 13: Overview of drilling depth and core recovery of MeBo-68 (GeoB 15236-2).

Core Nr.	Start of drilling (cmbsf)	End of drilling (cmbsf)	Sections	Recovery (cm)	Remarks
1P	0	270	1	137	
			2	126	
			CC	-	
2P	270	565	1	72	discarded (massive gas hydrate, stored in liquid nitrogen)
			CC	10	gas hydrate, stored in liqu. N_2
3P	565	740	1	120	
			2	126	
			CC	5	gas hydrate, stored in liqu. N_2
4R	740	975	-	-	No recovery
			CC	-	
5P	975	985	-	-	No recovery
			CC	-	
			Total recovery (cm)	**596**	

9. Sediment Sampling

(A. Bahr, H. Sahling, M. Haeckel, T. Pape, J. Wei, D. Nadezhkin, K. Hatsukano)

Near-surface sediments have been sampled (Appendix 1) with a gravity corer (GC), a minicorer (MIC), the Dynamic Autoclave Piston Corer-I (DAPC I), and the Lotvariante Druckkern Probennehmer (LDP). The GC was deployed in order to (1) sample gas hydrates, (2) obtain geochemical and geothermal gradients, and (3) sample sediments for sedimentological studies. The MIC was deployed in order to sample surface sediments for porewater and gas investigations. A list of all GC and MIC deployments with station specifics is given in the Appendix 2.

The working principle of the autoclave tools, the Dynamic Autoclave Piston Corer-I (DAPC–I) and the LDP, which were built to recover, preserve, and analyze sediment cores under in situ hydrostatic pressure are explained in detail in Chapters 8.2 and 9.2. During incremental degassing of the cores, subsamples of the released gas were taken for analyses of their molecular composition (Chapter 12).

9.1 Gravity Corer (GC) and Mini Corer (MIC)

The gravity corer (GC) from MARUM was regularly deployed with a 6 m steel barrel. The total weight was about 1250 kg (28 slices of 40 kg weight each plus ~130 kg frame and barrel). Two types of core catcher, a classical one with steel lamella (core catcher – lamella) and another type with robust steel lids (core catcher – lids; Fig. 49, left), were used. Deployment of the GC was done by the ship's crane and winch W11 on the starboard side (Fig. 49, right). Due to the onboard handling procedure, the maximum length of the barrel was limited to 6 m. At selected stations, autonomous temperature loggers (T-logger) were mounted as outriggers on the steel barrel (Chapter 10). Usually, lowering and hoisting the tool were done with rope speeds of 1 m/s. Maximum rope speeds were restricted to 1.2 m/s due to technical problems with the winch becoming intolerably loud at higher rope speeds. Typical rope speed for lowering the tool into the sediment was 0.5 to 1.2 m/s. Gravity cores were either collected with plastic foil or solid plastic (PVC) liner.

After recovery, gravity cores in PVC liners were cut into 1-m-segments and capped. Subsequently, core segments were cut lengthwise yielding a 'work half' and 'archive half'. Archived cores were stored in D-Tubes at 4° C. Gas hydrates extracted from gravity cores in plastic foil were either preserved in liquid nitrogen (ca. –196° C) or subject to preparation of hydrate-bound gas (Chapter 12).

Fig. 49: The core catcher with lids and the lowermost T-Logger (left). Deployment of the gravity corer equipped with a 6 m long steel barrel and T-loggers (right).

The MIC from MARUM allows to sample up to four 60 cm long cores of 62 mm in diameter. It was lowered with the winch W2, which is commonly used for CTD deployments, over the starboard frame. Typical rope speeds for lowering the tool into the sediments were 0.4 to 0.6 m/s.

Sediment samples were taken for porewater extraction (Chapter 11) and methane concentration analyses (Chapter 12). Near-surface sediments obtained by MIC were stored for analysis of lipid biomarkers. After sampling, sediments were described, and photographs were taken of cores that were archived afterwards. In some cases smear slides were prepared, to e.g. check for the presence of coccoliths.

For suited cores (i.e. those with sufficient core recovery and undisturbed surface), the light reflectance was measured with a GretagMacbethTM Spectrolino hand-held spectrophotometer. For this, the sediment surface was smoothed and covered with a purpose-made foil avoiding the formation of air bubbles on the foil-sediment interface. The spectral reflectance was measured over a wavelength spectrum ranging from 380 to 730 nm in 10 nm intervals. Routine measurements were made at 1 cm-intervals and automatically recorded using the KeyWizard software. Calibration of the instrument was done before measuring each segment. L, a, and b CIELAB colors are automatically calculated by the software. Processing of the raw color scanning data included the correction for outliers and sections where the instrument had poor surface contact due to voids or very coarse sediment. The resulting lightness (L) and red/blue ratios (= 700 nm / (700 nm + 450 nm)) were correlated with lithological core descriptions.

9.2. DAPC-Autoclave Sampling

(H.-J. Hohnberg, T. Pape, K. Dehning, D. Hüttich)

The Dynamic Autoclave Piston Corer I (DAPC-I) was developed and built in the frame of the BMBF-funded joint project OMEGA (2000 – 2003) with the aim of recovering, preserving and analyzing hydrate bearing sediment cores from the deep sea under in-situ hydrostatic pressure (Abegg et al., 2008). It was designed to cut sediment cores from the shallow sediments to a maximum length of 2.65 m and preserve them at in situ pressure corresponding to water depths of up to 1500 m. It can be released from variable heights (1–5 m) and enters the seafloor in free fall. The cutting pipe, which is relatively short (2.7 m), hits the seafloor with a very strong impact. Therefore, it is especially suitable for sampling gas-hydrate bearing sediment. The pressure chamber is 2.6 m long and weighs about 180 kg. The DAPC-I total length is 7.2 m and its total weight ca. 500 kg. The DAPC pressure chamber is made of stainless steel (1.4571), aluminum bronze (CuAl10Ni) and a glass-fiber reinforced plastic (GRP) pipe. The pressure barrel consists of GRP, aluminum alloys, seawater resistant steel and aluminum bronze. The balls of the ball valves are made of stainless steel (1.4404). The cutting system, consisting of a cutting-shoe and an outer cutting-pipe, is made of steel (St52). Further materials used are ball-bearing-steel, stainless steel 1.4301 and PVC. All parts of the pressure chamber exposed to sea water are suitable for long-term storage of cores under pressure for several weeks. The DAPC-I is to be deployed from a research vessel on the deep sea cable. The pressure chamber was checked and approved by the Berlin TÜV (Technischer Überwachungsverein, technical inspection authority of Germany).

The DAPC-I was deployed during several studies in recent years (Heeschen et al., 2007; Pape et al., 2010a, 2010b; Pape et al. 2011) and is in routine use nowadays.

DAPC deployment

The deployment of DAPC-I from board the R/V METEOR was similar to that of conventional piston corers, pushed by a weight and released by a release mechanism connected to a trigger weight (see Abegg et al., 2008). Prior to seafloor deployment, the pressure inside the DAPC-I accumulator was always adjusted to a value surpassing the hydrostatic pressure at the sampling depths. The deployment-speed was 0.5 m/s.

During M84/2 the DAPC-I was deployed at ten stations (Table 14).

Table 14: Details of DAPC-I deployments during M84/2.

Deployment No.	GeoB No.	Site	Date	Position at seafloor contact (N; E)	Water depth (m)
DAPC-01	15244-4	Poti seep	13.03.11	41°57.871; 41°18.312	870
DAPC-02	15244-5	Poti seep	14.03.11	41°57.874; 41°18.331	868
DAPC-03	15268-1	Ordu Ridge patch 02	16.03.11	41°32.661; 37°37.449	1,534
DAPC-04	15268-4	Ordu Ridge patch 02	20.03.11	41°32.678; 37°37.440	1,536
DAPC-05	15268-5	Ordu Ridge patch 02	21.03.11	41°32.670; 37°37.460	1,536
DAPC-06	15513-2	Kerch flare	23.03.11	44°37.386; 35°42.164	878
DAPC-07	15516-2	Kerch flare	24.03.11	44°37.230; 35°42.282	889
DAPC-08	15518-2	Kerch flare	25.03.11	44°37.180; 35°42.270	885
DAPC-09	15526-1	Dvurechenskii MV	27.03.11	44°16.970; 34°58.670	2,054
DAPC-10	15530	Helgoland MV	29.03.11	44°17.300; 35°0.040	2,080

Stations conducted with the DAPC

DAPC-1: The first deployment of the DAPC on M84/2 was successful with a recovery pressure of 98 bar maintained in the pressure chamber. The gas content in the core was determined by quantitative degassing and the degassed core of about 262 cm in length was used for porewater analyses and sedimentological descriptions.

DAPC-2: The second DAPC core lost pressure entirely during recovery because of leakage of the ball valve. By means of hydroacoustic imaging a strong degassing during hauling through the water column could be followed. During removal from the pressure chamber some part of the core was lost from the core liner. The remaining core material was subject to core descriptions.

DAPC-3: The third deployment of the DAPC was successful with a retrieval pressure of 145 bar and a core length of 145 cm. Upon recovery, the core was degassed quantitatively and used for subsequent analyses (Chapter 12).

DAPC-4: Due to technical problems with the ball valve adjustment no core was torn into the pressure chamber at the seafloor.

DAPC-5: Leakage of the system occurred during recovery and no pressure was left in the pressure chamber. The core was about 110 cm in length and subject to core descriptions.

DAPC-6: This station was successful with the recovery pressure being 82 bar. The core of about 199 cm in length was degassed, removed from the pressure chamber and subject to porewater sampling and sedimentological descriptions.

DAPC-7: A small leakage of the system caused a pressure loss down to about 27 bar. The core was 247 cm in length and used for quantitative degassing, porewater and sedimentological analysis.

DAPC-8: This station was successful with the recovery pressure being 57 bar and about 200 cm of sediment recovered with this core. The core was degassed, sampled for porewater analysis and used for sedimentological descriptions.

DAPC-9: During this DAPC station about 260 cm of sediment were recovered and the pressure inside the pressure chamber was about 118 bar. The core was degassed quantitatively and used for subsequent analyses.

DAPC-10: The last DAPC deployment during M84/2 was successful as well. The recovery pressure was about 115 bar and the core length was about 257 cm. This core revealed the highest gas volume ever obtained with the DAPC. The core was degassed, sampled for porewater analysis and used for sedimentological descriptions.

Development and design of the DAPC-I	H.-J. Hohnberg
Degassing and scientific program	T. Pape
Preparation and deployment during Leg 1	H.-J. Hohnberg
Preparation and deployment during Leg 2	K. Dehning, D. Hüttich

9.3 Core Descriptions

Sediments retrieved during the METEOR 84/2a cruise mostly reflect the common sedimentation in the Black Sea basin, overprinted to different degrees by diagenetic processes related to hydrocarbon seepage. Exceptions are deposits from sites where deep-rooted sediments are expelled due to diapiric activity and/or fluid seepage. A complete overview over the lithologies of cores retrieved with GC, MIC, and DAPC is given in the Appendix.

Typical Black Sea sediments from a non-seep area have been recovered in GeoB 15220-1 from a location close to the Batumi seep area (Fig. 50). These sediments comprise from top to bottom: a finely laminated coccolith ooze (Unit 1 according to the scheme proposed by Ross and Degens, 1974), followed by a finely laminated sapropel (Unit 2) with distinct light laminations rich in needle-shaped authigenic aragonite towards the base. Both, Unit 1 and 2, represent the marine stage of the Black Sea. The underlying grayish mud is of lacustrine origin and represents the lake stage of the Black Sea during the last glacial. During this time, the global sea level fell below the sill depth of the Bosphorus, leading to disconnection of the Black Sea from the Sea of Marmara and Mediterranean Sea. The reconnection of the Black Sea with the Sea of Marmara occurred at around 9.4 kyrs (Major et al., 2006). The inflow of saline marine water caused the formation of the present stratification of the Black Sea water column and the manifestation of

anoxic conditions below ca. 160 m water depth. These anoxic conditions lead to the accumulation of the organic-rich sediments of Units 1 and 2. The base of the sapropel (Unit 2) has been dated to 7.5 kyrs by Jones and Gagnon (1994), an age that has later been refined to 8.0 kyrs (Lamy et al., 2006). The first prolonged invasion of coccolithophorides occurred at 2.7 kyrs (Jones and Gagnon, 1994) marking the base of Unit 1.

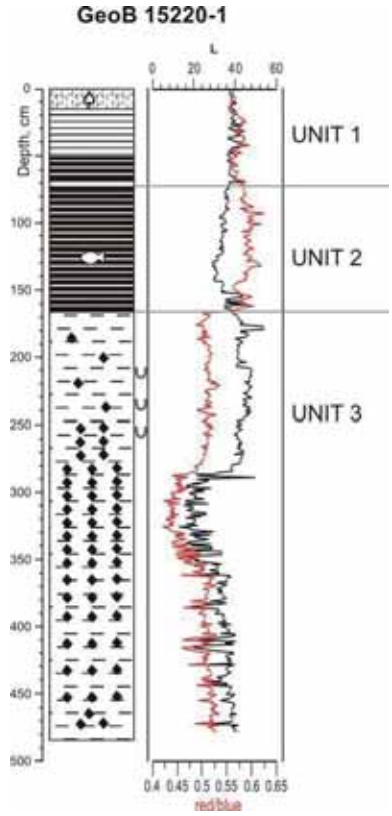

Fig. 50: Core description of Batumi reference site GeoB 15220-1 (GC-4) with typical Black Sea sediments. Indicated are the Units 1-3 after Ross and Degens (1974) as well as lightness (black) and red/blue ratio (red) from the reflectance data. For legend see Appendix 6.

An often recurring feature of Unit 3 is a distinct black interval (in 280-360 cm core depth in GeoB 15220-1) rich in amorphous Fe-sulfides (Neretin et al., 2004), termed „hydrotroilite“ in the Russian literature (Limonov et al., 1994). These black horizons are related to the migration of a sulfidization front. The black color is lost within a few hours if the core is opened, since these Fe-sulfides are instable and oxidize rapidly. Seep-influenced cores often show disturbed bedding due to degassing (particularly during core retrieval), making exact assignment of unit boundaries difficult. Additionally, these sediments often contain carbonate-cemented intervals (Bahr et al., 2010). These seep-carbonates are common at seep sites and relate to the increase of alkalinity caused by the microbial activity during the anaerobic oxidation of methane.

The dissociation of gas hydrates leaves characteristic sediment textures termed „soupy“ (sediment with very high water content) and „moussy“, referring to heavily degassing sediment, rich in small gas bubbles, stiffer than soupy sediments. In both cases the primary structure of the sediment is almost completely destroyed. Especially in sediments with soupy sediment textures the exact determinations of stratigraphic boundaries is difficult and might have an uncertainty of at least ±5 cm.

In the following a more detailed description of the sediments found at the various research areas will be given.

Working Area Eregli

Areas of high backscatter were found in the working area Eregli offshore Turkey. Sediments were sampled by GC GeoB 15203 and GeoB 15204 in order to check for the causes of such backscatter anomalies. Samples were taken at a high backscatter patch termed Eregli 1 that is identifiable in DTS sidescan sonar images as well as in the backscatter map of EM122.

Cores from Eregli (including the MeBo drillsite GeoB 15208) are characterized by unusual high sedimentation rates for the Holocene Units 1 and 2, as both gravity cores exclusively comprise Unit 1 sediments (Fig. 51). Similar high sedimentation rates have been described from other cores from this area (Lamy et al., 2006, Kwiecien et al., 2008), which is due to the influence of terrigenous material delivered by the Sakarya River to this area. Typical for the sediments in this area is the regular intercalation of homogenous clay layers presumably derived from suspension load brought in by the river.

The recovered 2.5 and 3.1 m sediments, respectively, have been gas-rich but did not contain visible pieces of hydrate or seep-related authigenic carbonates. It may be concluded that gas hydrates occur either disseminated or deeper in the sediments, and that these cause the backscatter anomalies.

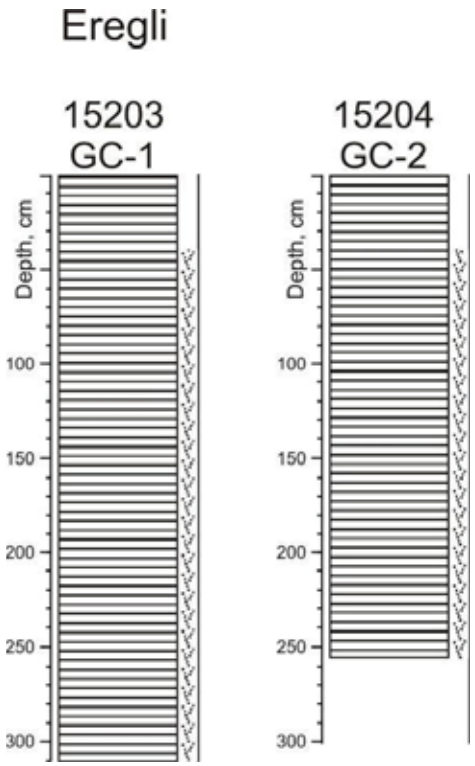

Fig. 51: Gravity core taken at the Eregli working area. For legend see Appendix 6.

Working Area Samsun

Initially it was planned to drill with the drilling device MeBo on top of the Archangelski Ridge in the working area Samsun offshore Turkey. In order to sample the sediments prior to the drilling, GC GeoB 15216 was taken and 5.76 m sediments were recovered. The core has only ~20 cm of Unit 2 recovered and consists otherwise of Unit 3 sediments (Fig. 52). A preliminary stratigraphic constraint might be the occurrence of slightly reddish sediments between 370-430 cm core depths (increased red/blue ratio). If this interval corresponds to the “red layer” interval found in the north-western Black Sea this might indicate an age of approx. 14.5 to 16 ka.

However, this preliminary age assignment needs confirmation by radiocarbon dating. If this holds true, this site did not show unusual low sedimentation rate as contrarily was observed at a deeper site on Archangelsky Ridge (~1200 m) which reached down to the Eemian sapropel (unpub. data by Helge Arz, IOW).

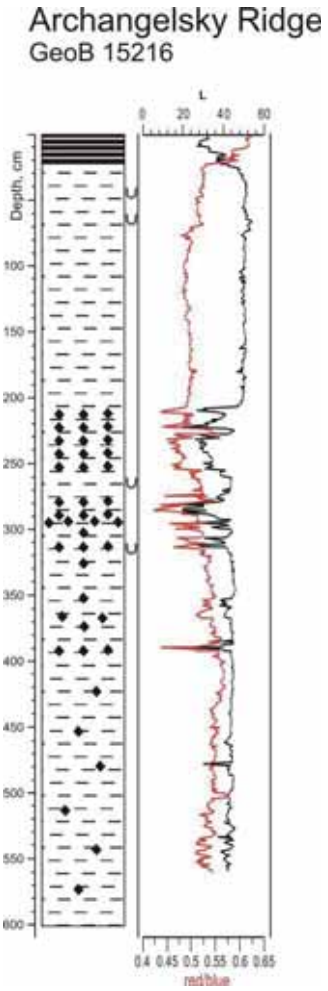

Fig. 52: Core descriptions of gravity core GeoB 15216 (GC-3) from Archangelski Ridge. Color reflectance results are displayed on the right with the lightness L in black and the red/blue ratio in red.

Working Area Georgia

Several GCs and MICs were taken in the area offshore Georgia with different intentions (Appendix 2: gravity corer and mini corer deployments).

At the Batumi seep area, a set of samples was taken to accompany the drilling by MeBo (Chapter 8): At a reference site 600 m southwest of the Batumi seep area at a water depth of 850 m, GC-4 (GeoB 15220-1) and MIC-1 (GeoB 15220-4) complement MeBo-65 (GeoB 15220-5). GC-7 (GeoB 15236-1) complemented MeBo-68 (GeoB 15236-2) at the Batumi seep area. Additionally, a series of GC and MIC were sampled in order to model geochemical processes. For this purpose, GCs and MICs were deployed in areas characterized by different backscatter as imaged by DTS deep towed sidescan sonar (Fig. 53).

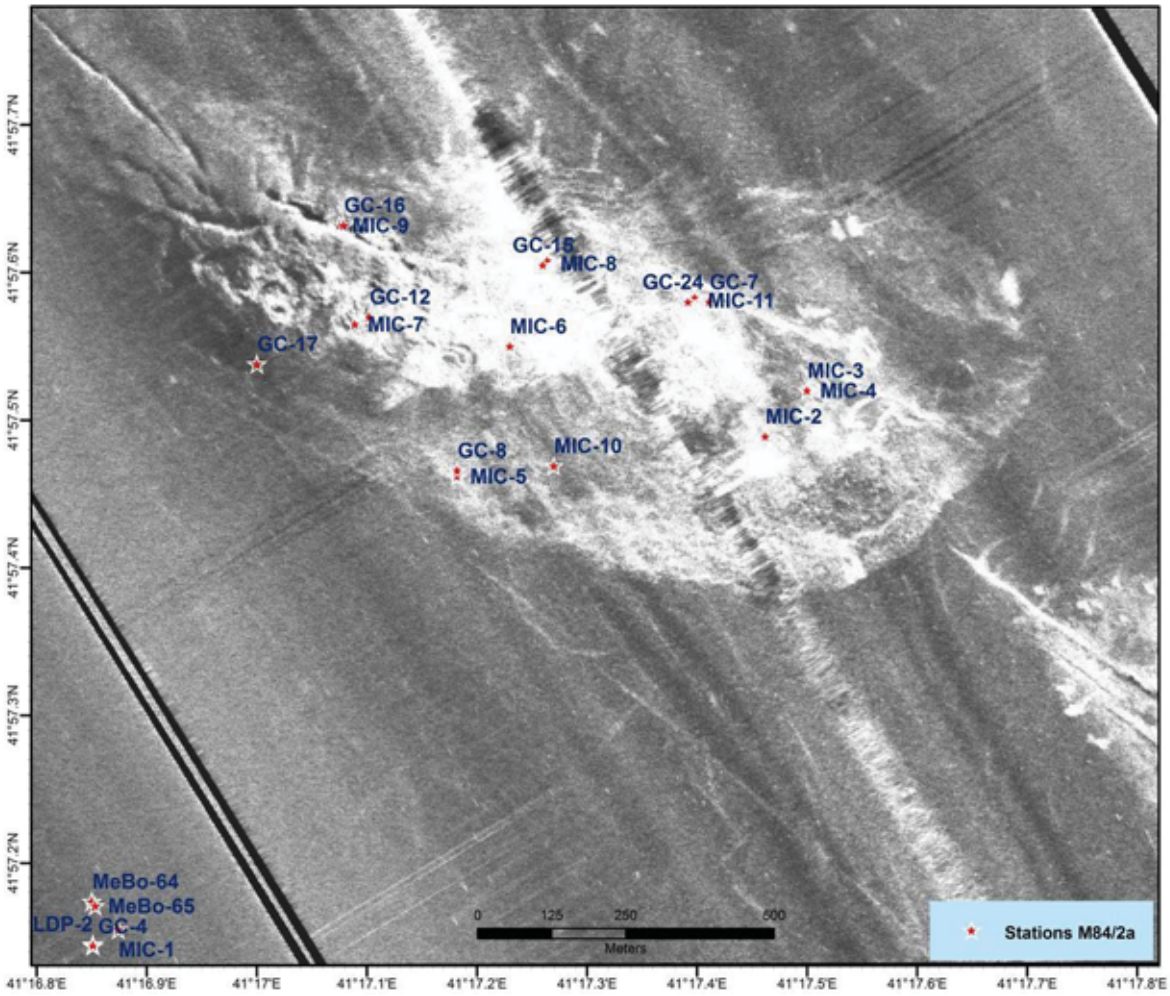

Fig. 53: Location of GC and MIC stations taken in the Batumi seep area. The stations are plotted on a sidescan sonar image obtained by DTS sidescan sonar (75 kHz) published in Klaucke et al. (2006).

Sediments from the Batumi seep area basically show the common sedimentary sequence of the deep Black Sea (Fig. 54). Seep-influence is manifested in the presence of platy carbonates, commonly as cemented Unit 1 layers, less frequently also cemented Unit 2. Unit 1 and 2 were missing in GeoB 15251-1. Similar to observations during previous cruises (Pape et al., 2010; Pape et al., 2011) gas hydrates were found below the sapropel of Unit 2 either at the base of Unit 2 or slightly deeper below 150 cm in the limnic sediments of Unit 3. Peculiar features were observed in core GeoB 15249-1 (GC-15) which showed a highly disturbed sequence below ~90 cm with sapropel clasts interbedded in the Unit 3 pointing at reworking processes active at this location. GeoB 15251-1 (GC-16) directly located on the main fault running through the Batumi seep area did not recover hydrates but showed a soupy to moussy texture below 100 cm, indicative of the former presence of finely dispersed hydrates.

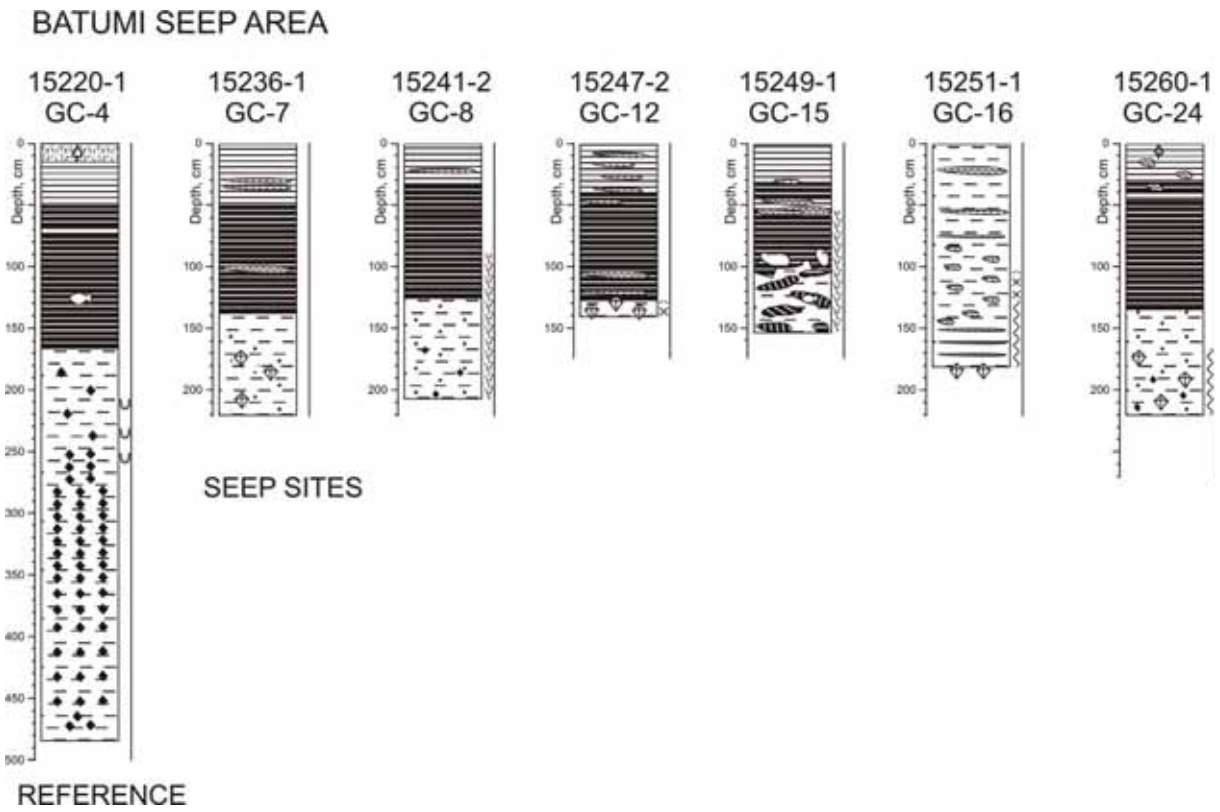

Fig. 54: Core descriptions of gravity cores taken from the Batumi seep area divided into the reference site GeoB 15220-1 and the seep-locations (other cores).

Poti Seep is located half a nautical mile northeast of Batumi seep area on Kobuleti Ridge. Similar to the Batumi seep area, Poti Seep is characterized by high backscatter in the deep-towed sidescan sonar (as well as in the EM 122 backscatter) and gas emissions. In contrast to the Batumi seep area, the backscatter is very intensive but smaller in size. Sampling with GC revealed the presence of gas hydrates at depth of ~150 cm (Table 15 and Appendix 2). At one location (GC-11, GeoB 15244-2), the hydrate formed a massive layer up to ~10 cm in thickness with some sediments in between while at the other (GC-9; GeoB 15243) very small hydrates were restricted to the core catcher (Fig. 55). Two pressure core stations (DAPC-1 and -2) were deployed at the positions of GeoB 15244-4 and GeoB 15244-5. All cores taken showed the Unit 1 and 2 succession as observed in the Batumi Seep area. A reference core for sedimentological studies was taken close to Poti Seep and archived (GC-14; GeoB 15248).

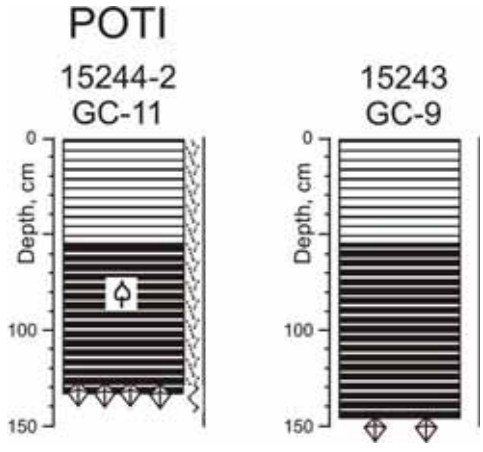

Fig. 55: Core descriptions of gravity cores taken from the Poti seep site at locations of high backscatter.

At Pechori Mound (Fig. 56), two MeBo deployments took place: MeBo-66 (GeoB 15227-1) and MeBo-67 (GeoB 15227-3) with the positions being close to each other. There was no GC taken before the MeBo deployment during this cruise because cores taken during M72/3 and TTR-15 already revealed the presence of gas hydrates in oily sediments. Later, GC-18 (GeoB 15227-5) was deployed to complement the MeBo-67 drilling. In contrast to the hydrate-rich MeBo cores, the shallow sediments recovered by GC-18 did not contain any hydrates but were, similar to MeBo-67 sediments and gravity cores recovered during earlier cruises, heavily oil impregnated. GC-19 (GeoB 15254) outside the rim recovered the regularly found near-surface Black Sea sediment sequences, whereas GC-20 (GeoB 15255) at the rim and GC-21 (GeoB 15256) in the center have been oil-rich with gas hydrates at the base of the cores. The gas hydrates were white, in contrast to those drilled by MeBo at Pechori Mound, which were yellowish-brownish. This may indicate different hydrate structures at different sediment depths. In addition, the hydrates at site GC-21 have been unique with respect to their porous appearance and behavior (Chapter 9.4). They were composed of individual aggregates of about half a centimeter in size. They made sounds similar to ice breaking apart or "popcorn". When breaking apart, fragments flew away.

Sediments from the inner part of the mound consisted of extruded brownish mud, different from the common hemipelagic sedimentation. Interestingly, core GeoB 15226 (GC-5) from the rim of the structure showed a ca. 30 cm thick interval of brownish mud within the limnic sediments. From this mud layer oil-stained fractures originated (Fig. 57) which suggests that the brownish mud contained some oil migrating upward along the fractures after deposition.

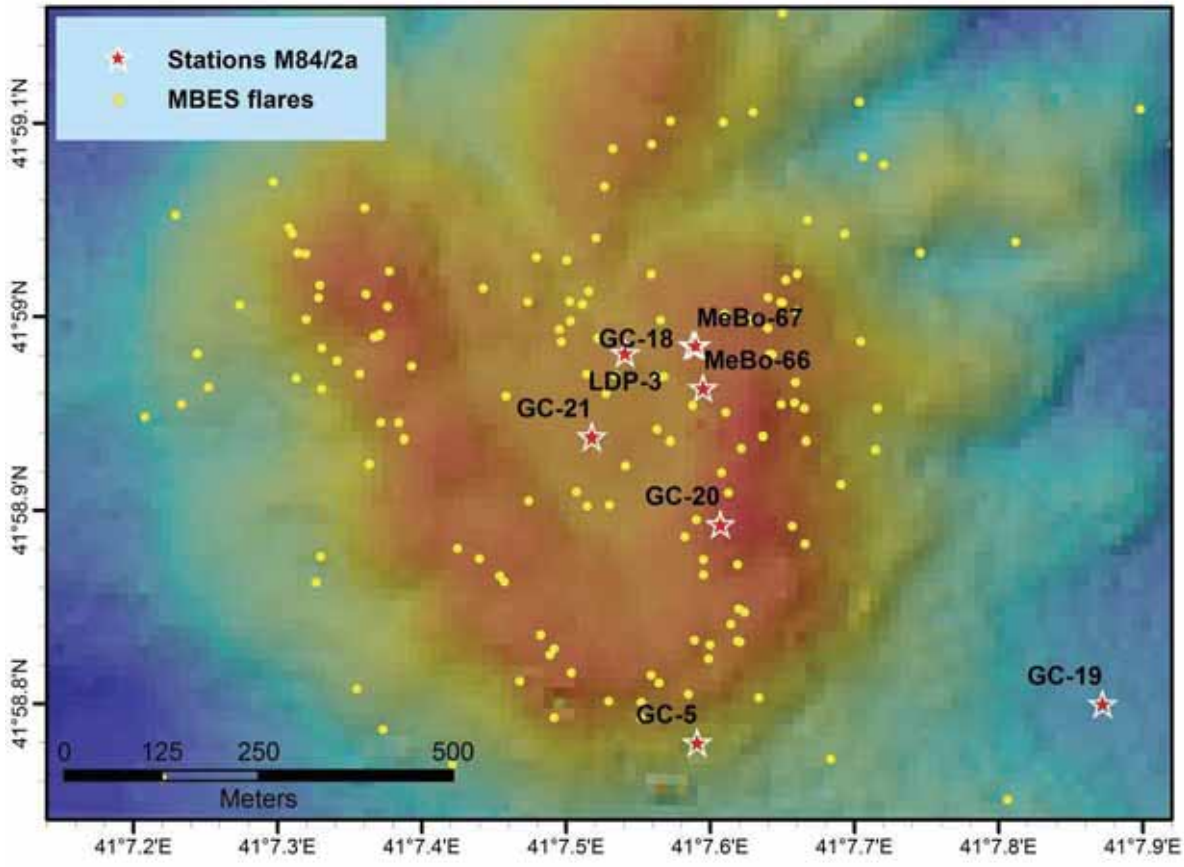

Fig. 56: Locations of GC- and MeBo-stations at Pechori Mound.

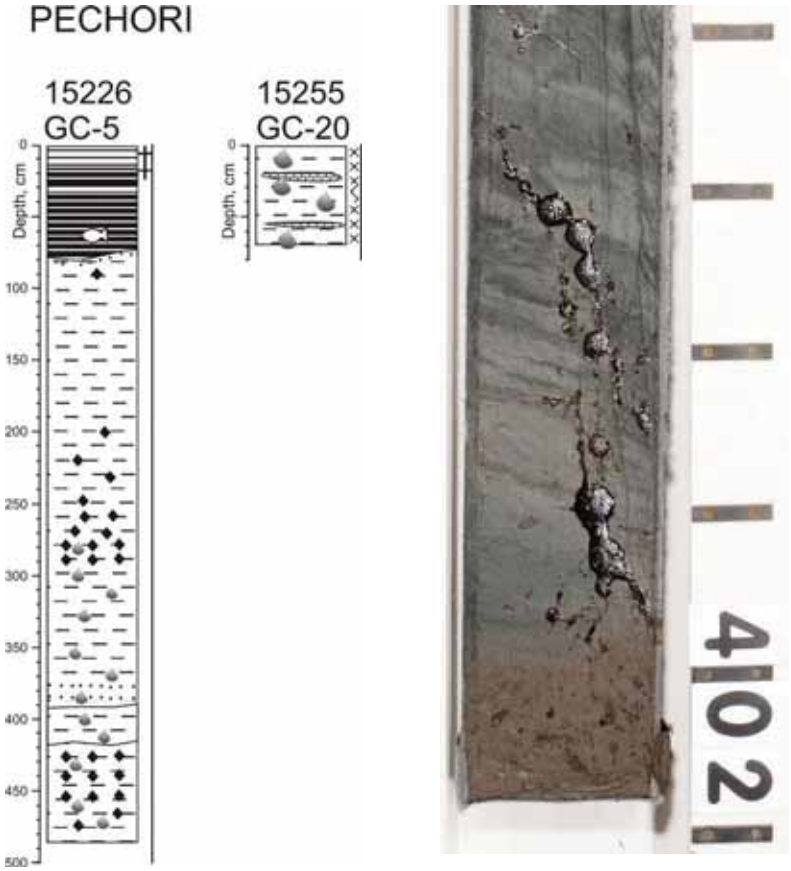

Fig. 57: Left: Lithological description of selected gravity cores from Pechori Mound (without reference station). Right: Photograph of core section from GeoB 15226 (GC-5) from the rim of Pechori Mound showing brownish mud within the limnic sediments. Oil is seeping out of the core along cracks and faults above this interval which presumably represents mud expelled from the mound.

Several GCs were taken in addition to those from Pechori Mound at sites where SAR satellite images showed oil slicks on the sea surface. During this cruise we could confirm the emission of gas that may accompany oil seepage at all of these sites. At all of the station oil impregnated sediments were found (Fig. 58). These include the Flare Cluster 3 at Adjara Ridge (GC-6; GeoB 15235-1), which showed some oil stained sediment in Unit 3. The oil slick sites G2 at Kulevi Ridge-East (GC-22; GeoB 15258) and G1 at Kulevi Ridge-West (GC-23; GeoB 15259) were quite different in terms of their sedimentology. At site G2 a fine-grained mud breccia has been recovered with bigger-sized mud clasts, thus, active expulsion of mud seems to take place here. In contrast, at the G1 flare (GeoB 15259) hemipelagic sediments heavily affected by presumably slump-related deformation have been found. Below just one meter of Unit 3 sediments another finely laminated and deformed sapropel is preserved, underlain by non-deformed calcareous sand which is interrupted by fine layers of bituminous clay with slight oil-staining. These deposits might tentatively be related to the Eemian sapropel deposition. Notably, both, the sapropel as well as the calcareous sand, are rich in coccoliths, pointing at a marine origin.

Moreover, Colkheti Seep was sampled at a position where gas bubble emissions were detected with EM122. At that site, no gas hydrates were found but the sediments have been rich in oil and carbonates (GC-25; GeoB 15261).

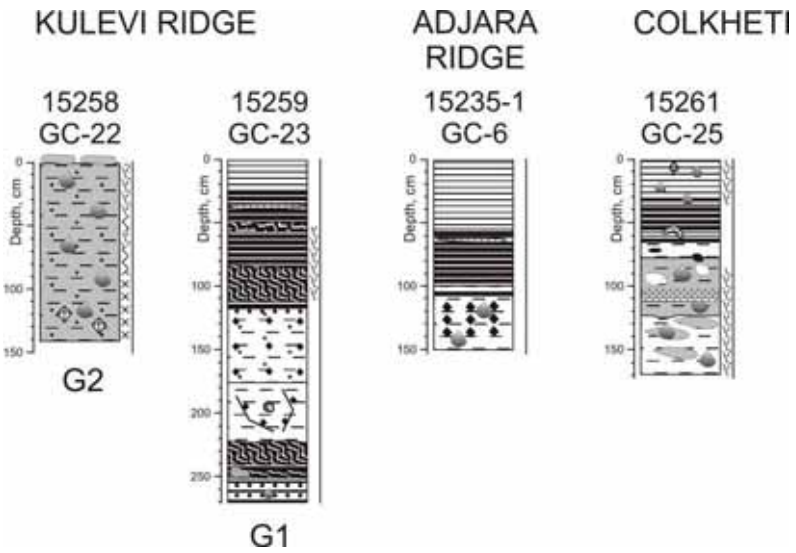

Fig. 58: Core descriptions of selected cores from Kulevi Ridge, Adjara Ridge and Colkheti.

Working Area Turkey

Towards the end of the M84/2 Leg A and at the beginning of Leg B a reconnaissance study of newly discovered flare sites has been performed on Ordu Ridge in the Samsun Area (Fig. 59). While GC-26 (GeoB 15267; patch 18) showed some bubbling in the water column during retrieval, no hydrates were observed in the core. A further flare site (patch 02) was investigated with GC-27 (GeoB 15268-2) and DAPC-3 and 5 (GeoB15268-1, -4, -5). In case of GeoB 15268-2 massive hydrates have been found in a certain depth interval assigned to Unit 3 (Figs. 60 and 61). Gas hydrate occurrence terminates at a depth of ca. 250 cm, where stiff sediments containing clasts of sapropel-like material are present (Fig. 62). This basal layer seemed to be derived from extruding mud that transported underlying strata to the surface. The entire sediment in this core is thoroughly deformed, which might be related to the intrusion of the mud. Interestingly, a similar lithology was found in DAPC-3 (GeoB15268-1) and MIC-12 (GeoB15268-3) but not in DAPC-5 (GeoB15268-5) from the same location, evidence of spatially highly variable geology. The other cores from the Ordu Ridge (GC-27 to 31, i.e. GeoB 15268-2, 15503-1, 15504, 15505-1, 15507, 15508) showed a similar pattern with a mud breccias-like inclusion of sapropelic fragments. Cores GeoB 15504, 15205-1 from Patches 5 and 7 contained light sandy material such as found at the base of GeoB 15259 at Kulevi Ridge. However, distinctly lacking are clasts of deeper routed strata such as those belonging to the Maikopian formation. This might point to a shallower origin (i.e. at maximum a few hundreds of meters) of the diapirically extruded sediment.

Different from the hydrate-bearing sites on Ordu Ridge, the flare site investigated at “New Ridge” (not shown in Fig. 59) lacked mud breccia and gas hydrates, although the sediment showed distinct signs of degassing. As hydrates usually occur at the base of Unit 2 and below, hydrates might occur deeper in the sediments beyond the sampled interval.

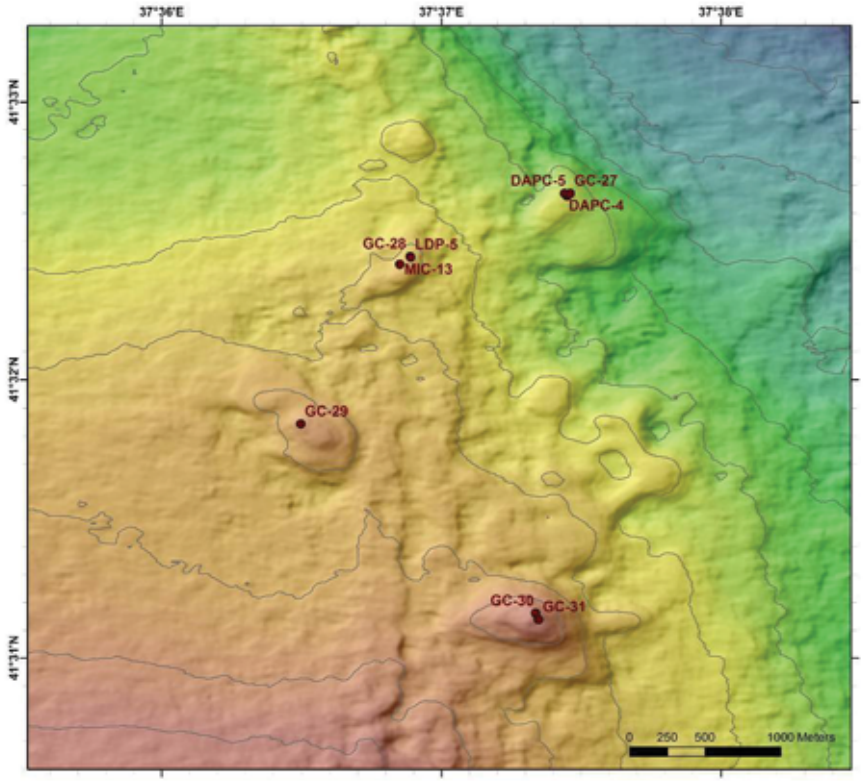

Fig. 59: Bathymetric map indicating positions of cores taken on Ordu Ridge.

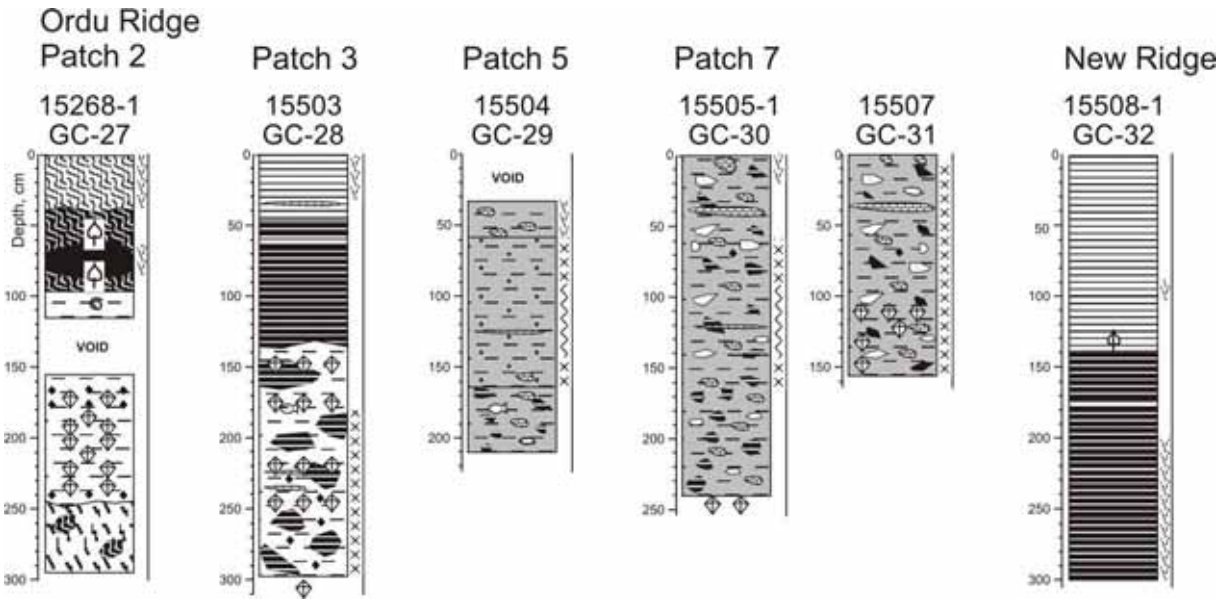

Fig. 60: Lithological descriptions of cores from the Samsun Research Area (Ordu Ridge and New Ridge).

Working Area Ukraine

Fig. 61: Thick gas hydrate layers in core GC-27 (GeoB 15268-2).

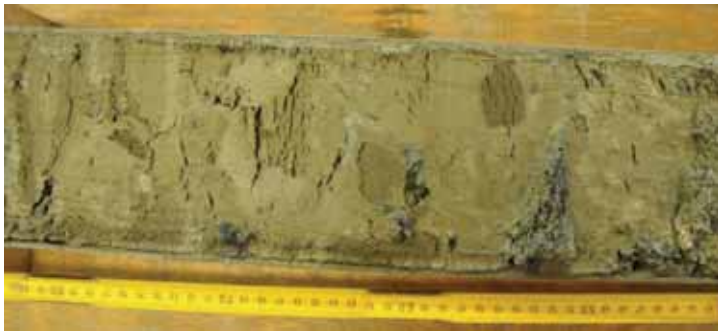

Fig. 62: Mud with clasts of pre-Holocene sapropel below the hydrate-bearing lacustrine clay in GC-28 (GeoB 15268-2).

Based on results (flare mapping and gravity coring) from previous cruises several GCs and MICs have been taken in the research area south of the Kerch Strait (Fig. 63). As shown in Figure 64 mainly two different types of targets can be discerned: 1) those on top of small mound structures and 2) those retrieved at the margin of these sites.

Fig. 63: Bathymetric map of the working area south of the Kerch Strait.

Cores from the summits of the mounds (GC-33, -35, -39; i.e. GeoB 15512-1, -2; 15520) have been relatively short in length (max. 170 cm), retrieved gas-rich sediment but no hydrates. Unit 1 and 2 were mostly present, but all sites showed clear evidence for reworking and the presence of carbonate precipitates. Since these locations are not situated at the flank of a mound, slumping is unlikely to have caused the hiatuses and discontinuities. Alternatively, diapiric activity may have led to the tilted hemipelagic layers followed by subsequent erosion. The cores obtained from the marginal sites (GC-34, -36, -37; i.e. GeoB 15513-1, 15516-1, 15518-1) were much longer and contained hydrates in high abundances, especially in GeoB 15513-1 and 15516-1. As for the parallel DAPC-6 to 8, the retrieved lithology consists of Unit 1-3 sediments, strongly affected by degassing. These hydrates occurred parallel to the bedding, particularly in the hydrotroilite intervals, but in GeoB 15516-1 also in vain-fillings. Carbonate cementation, potentially a limiting factor for penetration and, thus, hydrate retrieval at the summit of the mounds, has not been observed at the marginal sites.

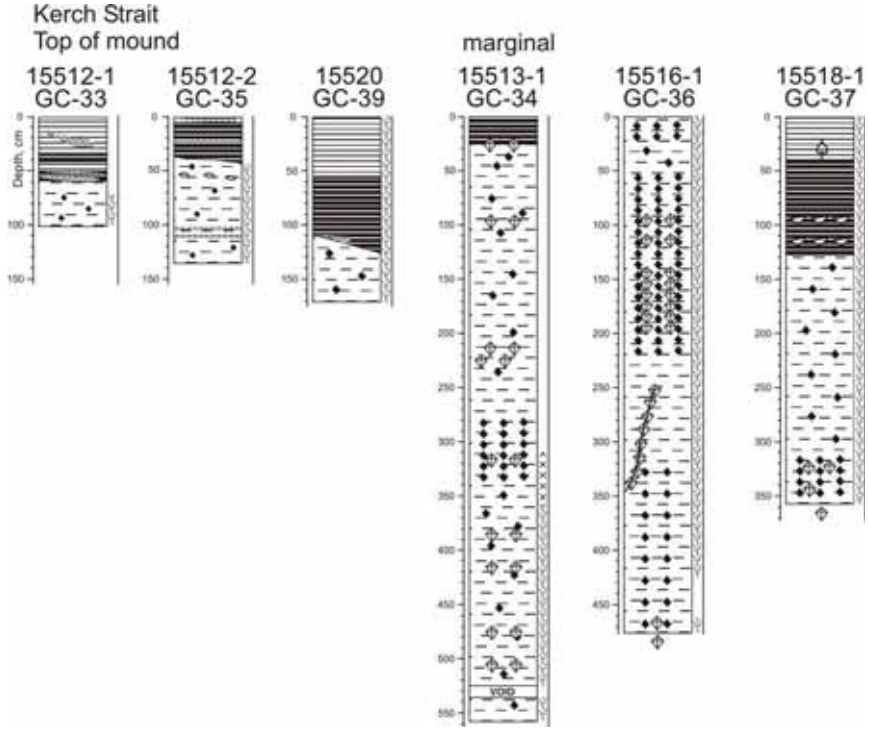

Fig. 64: Lithological descriptions of representative gravity cores retrieved from the flare sites south of the Kerch Strait**.**

In the Sorokin Trough south of the Kerch Strait working areas, the neighboring Dvurechenskii and Helgoland mud volcanoes (MVs) have been sampled (Figs. 65 and 66). Both are part of a chain of MVs and mound structures situated at water depths between about 1,700 and 2,100 mbsl. In contrast to the cores obtained on the continental slopes off Georgia, Turkey and the Ukraine, the background sedimentation in the Sorokin Trough, slightly over 200 m deep, is characterized by turbidite deposition, particularly during the lake stage of the Black Sea. This dominance of reworked, allochthonous material is evident at the reference site GeoB 15533-1 (GC-46) which is dominated by frequent layers of sand and shell hash layers, particularly below 200 cm core depth. Especially massive shell debris horizons were observed (Fig. 67). In this interval between 420-430 cm pockets of shell debris are intercalated with clay patches and folded sand layers giving the impression of a slump-related transport rather than in-situ deposition by turbidity currents. Notable is the general increase in grain size and shell content in

the limnic sediments compared to the marine Units 1 and 2. This might be related to the low sea level stand during the last glacial enabling direct transport of sediments into the deep Black Sea basin without being trapped on the shelf.

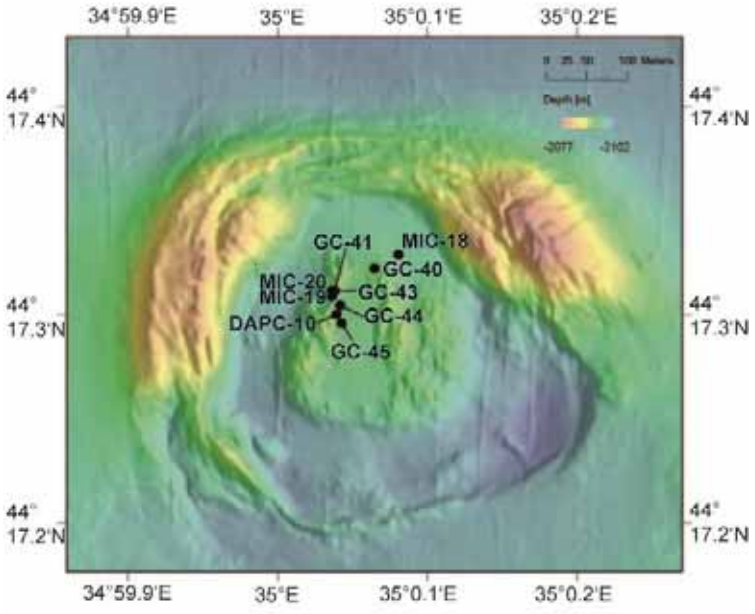

Fig. 65: Bathymetric map of Helgoland MV indicating location of cores retrieved during M84/2.

Coring activity in this region concentrated mainly on the Helgoland MV which has been surveyed before in particular during MSM15/2, but has not been sampled as extensively as for instance the Dvurechenskii MV. Although situated close to each other, both MVs are very different in terms of their morphological expression and their sedimentological characteristics. Material extruded from the Dvurechenskii MV typically consists of mud breccia, which is rich in sand to gravel-sized rock fragments derived from the deep subsurface, as e.g. the Maikopian Formation (GC-42, GeoB 15527; DAPC-9, GeoB 15526-1). While the crater of this MV has a mud pie-like surface expression, the Helgoland MV displays a complex circular structure (Fig. 65). The sediments retrieved lack the mud breccia characteristics of the Dvurechenskii MV but consist of a clayey to sandy material with tiny shell fragments such as found at the common background sediments. Based on that observation it might be inferred that the Helgoland MV is not as deeply rooted as the Dvurechenskii MV but is recycling liquefied Pleistocene sediments. Particular attention has been paid to sample mud pools observed during ROV dives on cruise MSM15/2. Two deployments of gravity cores (GC-41 and 44; i.e. GeoB 15525-1, 15531) equipped with T-loggers aimed to retrieve a deep temperature profile similar to experiments performed during MSM15/2. However, during both attempts we did not succeed in penetrating several tens of meters into the sediment, potentially because massive hydrates blocked the descent of the GC (cf. the hydrate-rich core GeoB 15525-1). A relatively deep penetration has been achieved with GC-45 (GeoB 15532), probably down to ~35 mbsf. This core retrieved warm (ca. 21° C in the lowermost segment directly after retrieval) gaseous, shell bearing sandy mud. Hydrate-bearing sandy mud without shell fragments has been found in DAPC-10 (GeoB 15530). Remarkably, shallow hydrates have also been found in MIC-19 (GeoB 15525-2) while MIC-20 (GeoB 15525-4) targeted for the same position did not retrieve hydrates but an intact surface with coccolith ooze above a layer of shell-bearing sandy clay. Hence, small scale variability is characterizing the central region of the Helgoland MV.

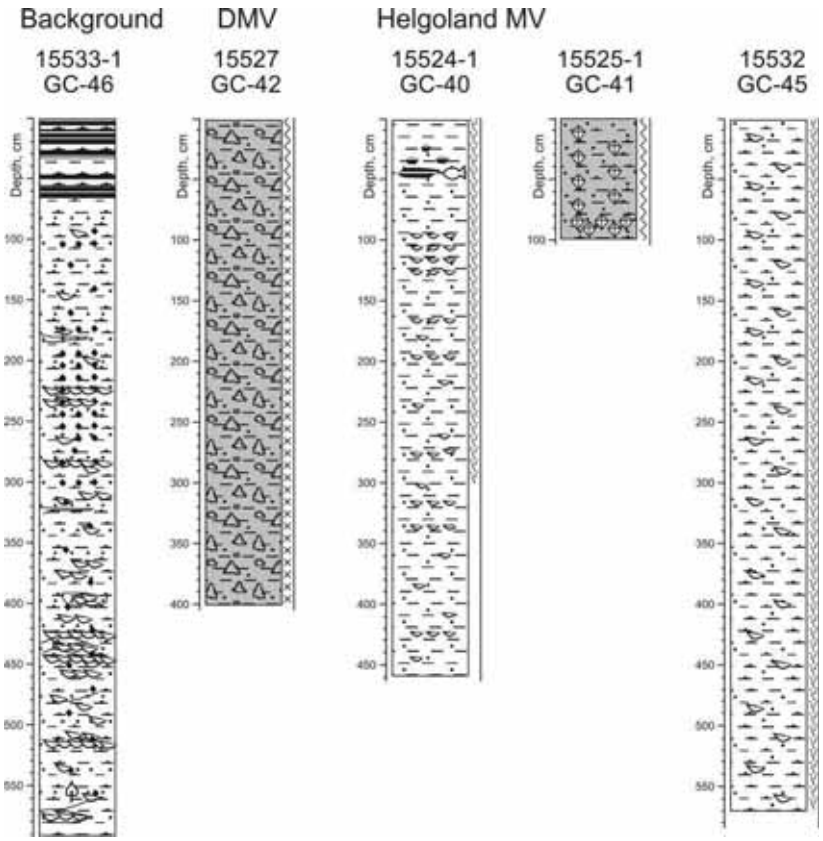

Fig. 66: Lithological descriptions of cores obtained in the Sorokin Trough on a background station, on the Dvurechenskii MV (DMV) and on the Helgoland MV.

Fig. 67: Photograph of the interval with massive layers of shell debris in GeoB 15532 (420-454 cm core depth).

9.4 Gas Hydrate Sampling

(T. Pape, H. Sahling, J. Wei, D. Wangner, A. Bahr, K. Hatsukano, G. Bohrmann)

During M84/2 intact gas hydrates have been sampled by use of a gravity corer and the seafloor drill rig MeBo. Hydrate samples were either prepared for onboard analysis of hydrate-bound gases (Chapter 12) or stored in liquid nitrogen (ca. –196° C) immediately upon recovery for onshore analysis (Table 15, Appendix 4). These samples will be analyzed for their texture, crystallographic structure, microstructure, and the molecular and isotopic composition of hydrate-bound gases.

Table 15: List of gas hydrate samples taken during Cruise M84/2 and stored in liquid nitrogen for onshore analysis.

Tool	Sample code	Area	MeBo core barrel
MeBo-67	GeoB 15227-3	Pechori Mound	1P
MeBo-67	GeoB 15227-3	Pechori Mound	3R
MeBo-67	GeoB 15227-3	Pechori Mound	4R
MeBo-67	GeoB 15227-3	Pechori Mound	5R
MeBo-67	GeoB 15227-3	Pechori Mound	7R
MeBo-67	GeoB 15227-3	Pechori Mound	8R
MeBo-67	GeoB 15227-3	Pechori Mound	9R
MeBo-68	GeoB 15236-2	Batumi Seep	2P
MeBo-68	GeoB 15236-2	Batumi Seep	3P
GC-7	GeoB 15236-1	Batumi Seep	
GC-24	GeoB 15260-1	Batumi Seep	
GC-12	GeoB 15244-2	Poti Seep	
GC-13	GeoB 15244-3	Poti Seep	
GC-27	GeoB15268-1	Ordu Ridge, patch #02	
GC-28	GeoB15503-1	Ordu Ridge, patch #03	
GC-29	GeoB15505-3	Ordu Ridge, patch #05	
GC-31	GeoB15507	Ordu Ridge, patch #07	
GC-34	GeoB15513-1	Kerch flare	
GC-36	GeoB15516-1	Kerch flare	
GC-37	GeoB15518-1	Kerch flare	
GC-41	GeoB15525-1	Helgoland MV	
GC-43	GeoB15525-3	Helgoland MV	

Selected photographs of gas hydrates from different sampling areas are shown in Figures 68 - 82.

Working area off Georgia

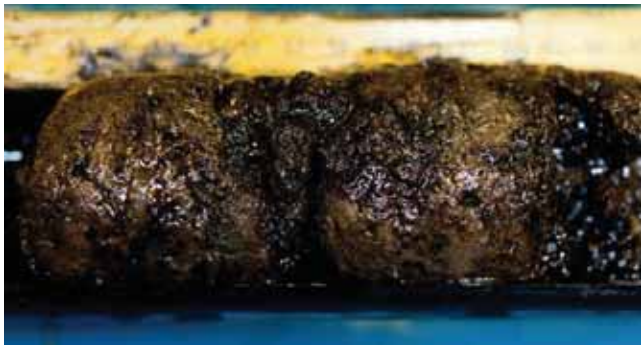

Fig. 68: Oil stained massive gas hydrate from Pechori Mound drilled by MeBo (MeBo-67; GeoB 15227-3 9R-1A; photo: _VD14074). Core diameter 55 mm.

Fig. 69: Massive gas hydrate from Pechori Mound drilled by MeBo (MeBo-67; GeoB 15227-3 8R-2A 96-106cm; photo: _VD14033). Core diameter 55 mm.

Fig. 70: Internal structure of gas hydrate from Pechori Mound drilled by MeBo (MeBo-67; GeoB 15227-3 8R-2A 96-106cm; photo: _VD14055).

Fig. 71: Porous gas hydrate from Pechori Mound recovered with GC-21 (Geo B15256; photo _DSC2268).

Fig. 72: Gas hydrate from the Batumi seep area drilled by MeBo (MeBo-68; GeoB 15236-2 3P-1A; photo: _VD14360). Core diameter 55 mm. Oil impregnations do not occur at this site.

Fig. 73: Gas hydrate drilled by MeBo at the Batumi seep area (MeBo-68; GeoB 15236-2 2P-1A; photo: _VD14355). Core diameter 55 mm.

Fig. 74: Finely laminated hydrates in core GC-16 from the Batumi seep area (GeoB 15251-1; photo: _VD14763).

Fig. 75: Dispersed hydrates in core GC-17 taken at the Batumi seep area (GeoB 15252; photo _DSC2206).

Fig. 76: Massive 10 cm-thick gas hydrate at the base of GC-11 (~130-140 cm) taken at Poti Seep (GeoB 15244-2; photo: _VD14412).

Fig. 77: Massive gas hydrates recovered with GC-11 from Poti seep (GeoB 15244-2; photo: _VD14416).

Working area off Turkey

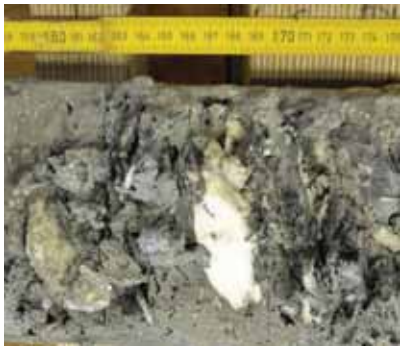

Fig. 78: Massive ~2cm thick layer of pure white gas hydrate at depth (~168-170 cm) at backscatter patch 02 Ordu Ridge (GC-27; GeoB15268-2 photo: _DSC2396) stored in liquid nitrogen.

Fig. 79: Dispersed hydrates recovered with GC-28 from Ordu Ridge patch 03 (GeoB15503-1; photo: _VD15382).

Working area off Ukraine

Fig. 80: Plates of hydrate recovered from Kerch Flare at station GC-34 (GeoB15513-1) (photo 0-74 GH (12)).

Fig. 81: White gas hydrate plates in black sediments at Kerch flare (GC-36; GeoB15516-1; photo: 74-104 GH 7).

Fig. 82: Very porous, white gas hydrate with sediment of Helgoland MV (GC-41; GeoB15525-1; photo: SL_GeoB_15525_1_VD15910.JPG). Length of aggregate about 3 cm.

10. In Situ Temperature Measurements

(H. Sahling, J. Wei)

The seepage of fluids (liquids and gas) often leads to elevated temperatures in the sediments. While the regular geothermal gradient is around 26° C/km in the Batumi area offshore Georgia (derived from BSR depth, Minshull and Keddie, 2010), it may be elevated in areas influenced by fluid seepage. Elevated temperature gradients may be expected in gas driven seep systems. However, even stronger temperature gradients may be expected at sites with clear evidence for pore water advection or mud volcanisms, such as the Dvurechenskii Mud Volcano (Feseker et al., 2009). At Dvurechenskii Mud Volcano, not only elevated temperatures were measured but a gravity corer penetrated more than 50 m into the feature during a former cruise (Feseker et al., 2009). The intention during the present cruise was to study gas and fluid seepage dominated systems in the different areas. Furthermore, temperature profiles from gravity corer that deeply penetrate into Dvurechenskii and Helgoland Mud Volcanoes were longed for in order to compare the temporal evolution of these systems.

Autonomous temperature loggers, so-called miniturized temperature data loggers (MTL) from Antares Datensystem GmbH were mounted as outriggers on the steel barrel of the gravity corer in order to measure temperature gradients in the sediments. The T-loggers were programmed to record one temperature reading every second. The resolution of the sensors is 0.6 mK allows highly accurate relative temperature measurements. However, the absolute precision is low as the loggers were not calibrated.

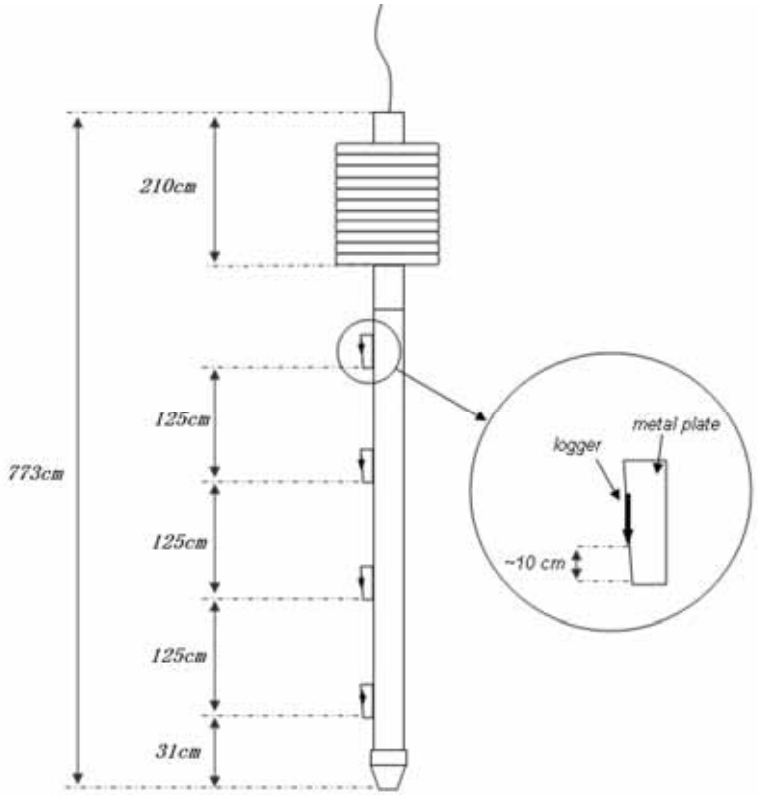

Fig. 83: Schematic drawing of the Antares T-loggers deployed as outriggers on the gravity corer. This set-up was used from GC-18 until the end of the cruise.

T-loggers were mounted either 60 cm or 125 cm apart from each other, depending on the expected GC penetration depth. The distances of the lowermost T-logger to the lower sides of

the gravity corer were: 42 cm to core catcher with lids, 31 cm to classical core catcher, 25 cm to end of steel barrel. Numbering of the loggers started with 1 for the lowermost one and ends with 4 or 5 for those closer to the weight. In order to allow the T-loggers to equilibrate with the surrounding sediments, the gravity corer was left in the sediments for about 10 minutes after penetration.

The preliminary data analyses included plotting of temperature versus time for all loggers. The temperature difference (delta-T) between the loggers shortly before penetrating the sediments and at the end of the measurement period (shortly before the gravitycorers were taken out of the sediments) were calculated. Delta-T was plotted versus the relative depth of the loggers to each other. The absolute depth of the loggers was then shifted such that the profiles (when linear) would theoretically intercept with the interception of the graph (delta-T=0; depth=0). This shift is given in the table as uppermost logger depth, which is the depth of the uppermost logger in the sediments.

Eregli

In the area of Eregli, two gravitycorers with T-loggers were deployed. Due to the facts that logger number 2 did not register and that the penetration depth was small (<3m) only the deepest logger measured the sediment temperature. As only one data point is available, it is impossible to estimate the penetration depth based on the temperature gradient. Judged from the amount of sediments in the core barrel and the sediments attached to the outside of the barrel, temperatures of 70 to 100 °C/km may be estimated, which are rather high.

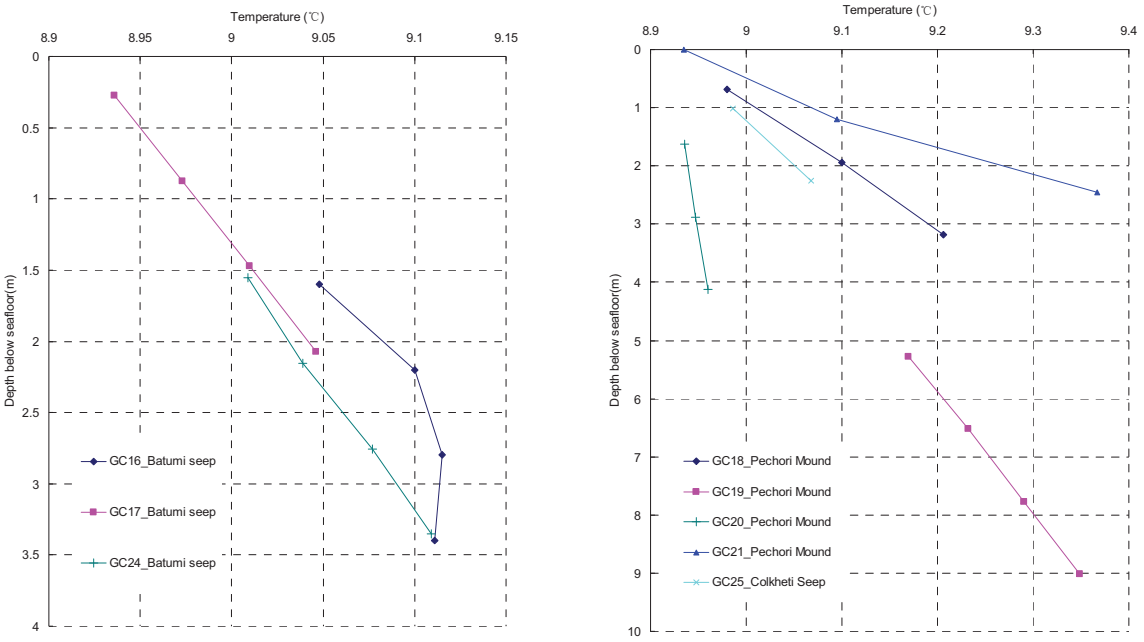

Fig. 84: Temperature profiles (Georgia area).

Georgia

Batumi Seep is a gas driven seep system at which gas hydrates occur in the sediments. Due to the fact that we recovered several times only ~2 m of sediments at Batumi, a T-logger spacing of 60 cm was chosen. After analysing the data, however, it became apparent that all loggers of the gravity corer penetrated the sediments and that depth corrections had to be applied. This is an interesting observation as it has influence on our understanding of how deep gas hydrates occur

in the sediments. Two of the Batumi Seep temperature profiles are linear (Fig. 84, left) and have a similar gradient of about 60° C/km, which is twice that of the regular background value (Minshull and Keddie, 2010).

Pechori Mound and Colkheti Seep are deeply rooted seep systems, as indicated by seismic studies and geochemical data. At these structures, oil impregnated sediments occur along with gas hydrates. For these reasons, fluid advection may be expected. The obtained temperature gradients are linear (Fig. 84, right), indicating that fluid advection is too slow at the measurement sites to cause the typical concave-upward profiles. Four profiles were obtained at Pechori Mound, in order to study the distribution of hydrates and temperature gradients. In general, a trend is seen that the central crater is characterized by the highest temperature gradient with about 170° C/km (GC-21) that decreases to 90° C/km at the rim (GC-18) and 57° C/km (GC-19) outside of the rim. At one station (GC-20), however, the temperature gradient is extremely low with 10° C/km. The fact that only 70 cm of sediments were recovered may suggest that the gravity corer did not penetrate vertically into the sediments. It may hit a hydrate layer as there were hydrates in the core catcher and then felt to the side, which could explain the low temperature gradients and the short core recovery.

At Colkheti Seep an elevated temperature gradient of 66° C/km was recorded, which fits to the view that this is a deep-rooted system with elevated heatflow. On the other hand, the corer did not contain any gas hydrates, that may indicate that the measurement sites has not been strongly influenced by fluid seepage.

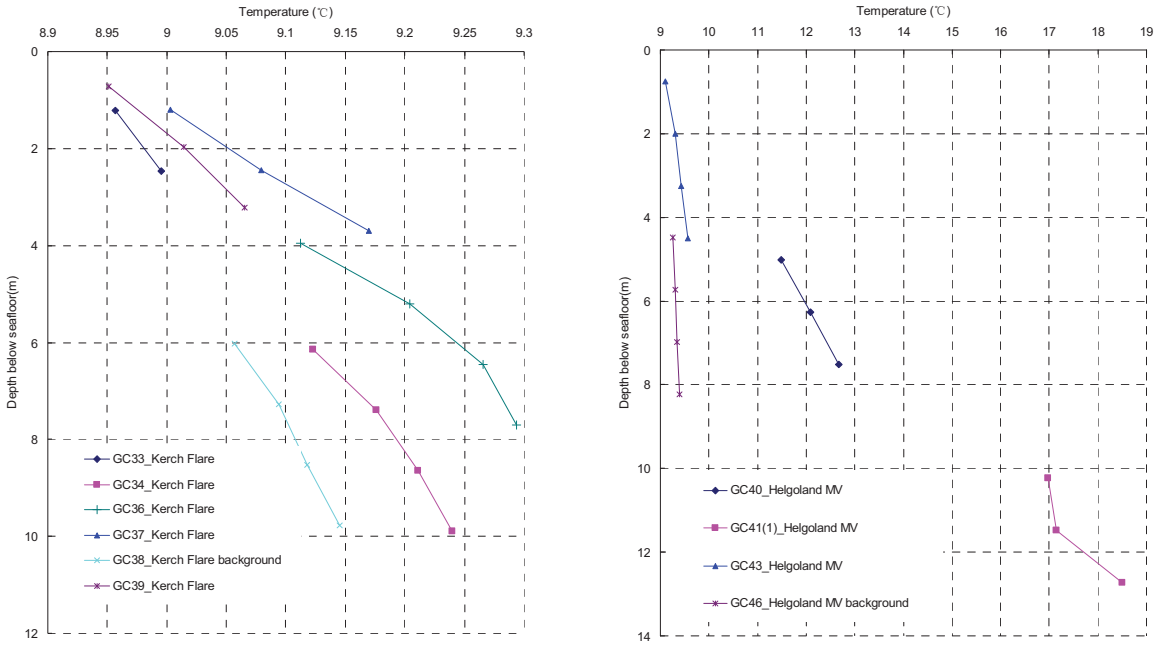

Fig. 85: Temperature profiles (Kerch Flare area and Helgoland MV).

Kerch Flare

Six temperature profiles were measured at Kerch Flare. GC38 was deployed to calculate the background temperature gradient in the Kerch Flare area which is 0.02° C/m. The penetration depth at the background site was very high; the uppermost logger penetrated about 6 m below the surface. The other five stations were deployed at or very close to the gas emissions at Kerch

Flare and show higher temperature gradients that range from 0.026° C/m to 0.067° C/m indicating elevated heatflow caused by fluid advection.

Helgoland Mud Volcano and Dvurechenskii Mud Volcano

Seven deployments of gravity corer were performed at Helgoland Mud Volcano (HMV) to measure the in-situ temperature in order to better understand the thermal structure of this mud volcano. The stations and the corresponding results of the measurement are listed in Table 16, while the temperature profiles are shown in Figure 85.

GC40 was deployed with a speed of 0.3 m/s into the sediment. 25 seconds after the lower most T-logger touched the seafloor, the temperature became stable for 2.5 minutes in all the three loggers with an extraordinary high geothermal gradient of 0.477°C/m. After a phase of stabiltiy, a sharp increase of temperature indicates that the gravity corer farther sunk into the sediments for about 60 seconds.

GC41 was conducted in order to deeply penetrate into the mud volcano, which had been done at the same position about one year ago intending to study the evolution of the geothermal structure over time in HMV. Unfortunately, the sharp decrease of the rope tension showed that the gravitiycorer did not penetrate deeply. However, the non-linear profile and a geothermal gradient as high as 0.61°C/m indicate the unusual temperature structure at this position. A second attempt was carried out by heaving the core to 1980 meters and moving the ship 20 meters SW. Again, this attempt failed. We speculate that the gravity corer lied on the seafloor based on the low temperature in all three T-loggers. The unstable temperature might have some relationship with massive gas hydrate which was recovered from the bottom of the gravity corer after it was on deck. GC43 and GC44 were also deployed in order to deeply penetrate into HMV, but neither was successful. The four failures in penetrating deep into the mud volcano illustrate the high spatial heterogeneity.

After four attempts that failed, GC45 was a real success of deep penetration, the lower most sensor reached as deep as about 45 m estimated from the rope tension and the rope length. The gravity corer penetrated with a speed of 1.2 m/s, and the final rope length was 2115 m (Fig. 90). Then it was left in the sediment with this rope length to allow the T-logger to equilibrate with the sediments. The gravity corer was then pulled up with a constant speed of 0.1m/s (Fig. 90). The profile (Fig. 86) shows a sharp increase from the bottom water temperature which is about 9°C to 27°C in the first 10 mbsf, followed by a relatively slow increase from about 27°C to 33°C in the other 35 m. Based on the previous geochemical data, Aloisi et al. (2004) concluded that the temperature at the source of the DMV is around 100°C, corresponding to a depth of about 2.5-3 km at regular geothermal gradients around 30°C/km. The seismic data shows the mud flow of DMV and HMV rooted in the same source (Krastel et al. 2003). If the speculation is right, then the high temperature might be caused by hot upflow mud fluid and nearly 65% of its initial heat has lost when it reaches the depth of 40 meters below seafloor. The high geothermal gradient indicates the mud flow of HMV is extraordinary robust and was cooled down sharply by the cold sea water when in contact with the bottom water near the sea floor.

GC46 is deployed for measuring the temperature gradient outside of the fluid seepage influenced area. The geothermal profile shows a perfect liner shape and 0.034°C/m, which indicates a quite normal geothermal gradient regularly found in the Black Sea.

In DMV (Dvurechenskii MV), only one deep penetration was performed to compare the temperature data that were obtained last year in order to better understand the evolution of the geothermal structure at DMV. Based on the rope length and the rope tension (Figs. 88 and 89), about 78 m is estimated as the maximum depth of the lowermost sensor. The gravity corer was heaved every ten minutes for 5 or 10 meters with a speed of 0.2 m/s, until the gravity corer left the seafloor. The temperature profile (Fig. 87) was almost constant at 16.7°C below about 32 mbsf. Feseker et al. (2009) discussed this as a result of a "gas hydrate thermostat". In sediments within the GHSZ at the DMV, an increase in fluid seepage will cause the dissociation of gas hydrates, which may compensate changes in heat flow. The dynamic system will keep the temperature stable at 16.7°C which is the maximum temperature needed for the existence of gas hydrate in this area.

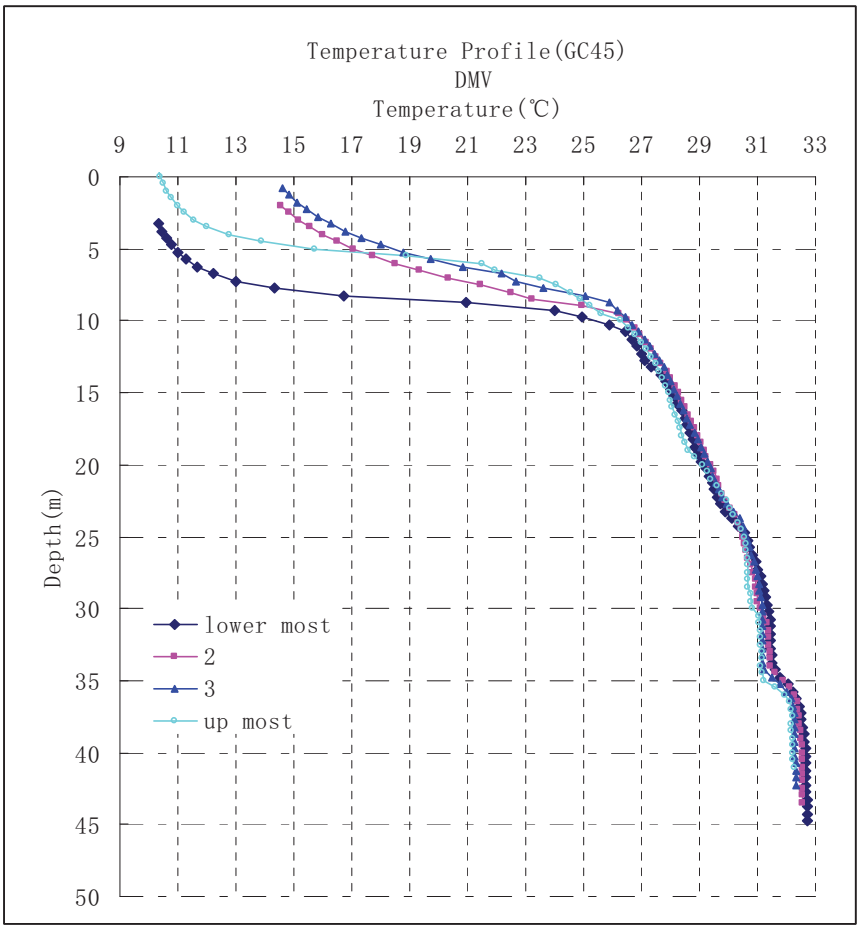

Fig. 86: Temperature-depth profiles at Helgoland MV.

The temperature shows a sharp increase from about 32 to 23 mbsf, followed by a zigzagging between 20.3° and 22° from about 23 mbsf to 8 mbsf. This pattern was discussed by Feseker et al. (2009) as a result of frictional heat, which may develop at these sites without gas hydrate deposits.

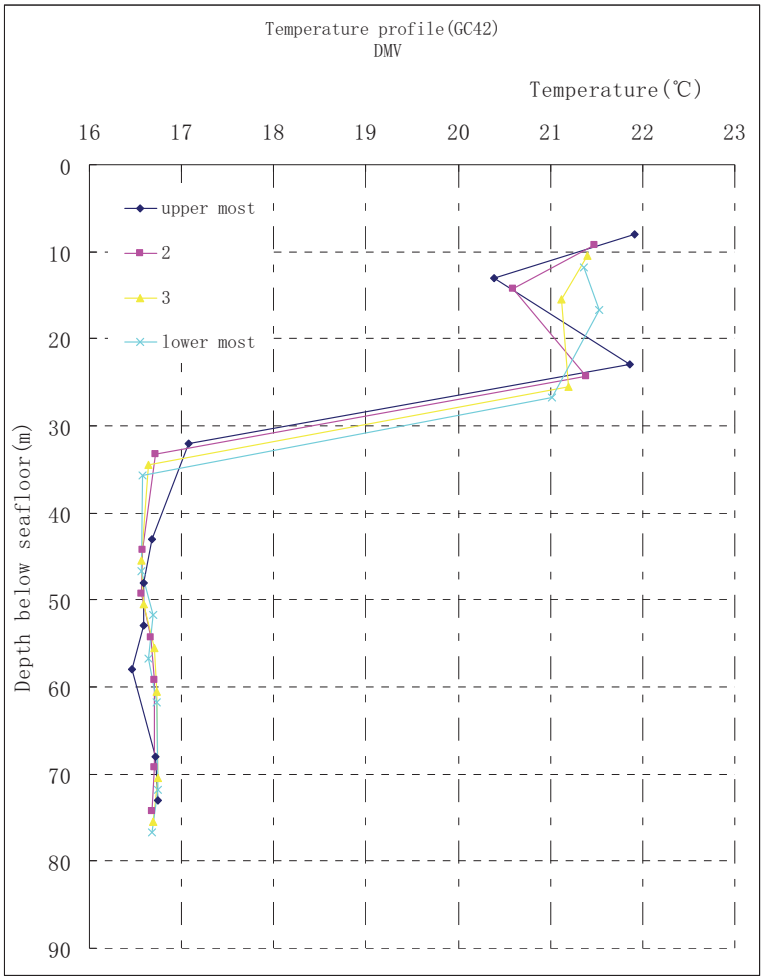

Fig. 87: Temperature-depth profiles at DMV.

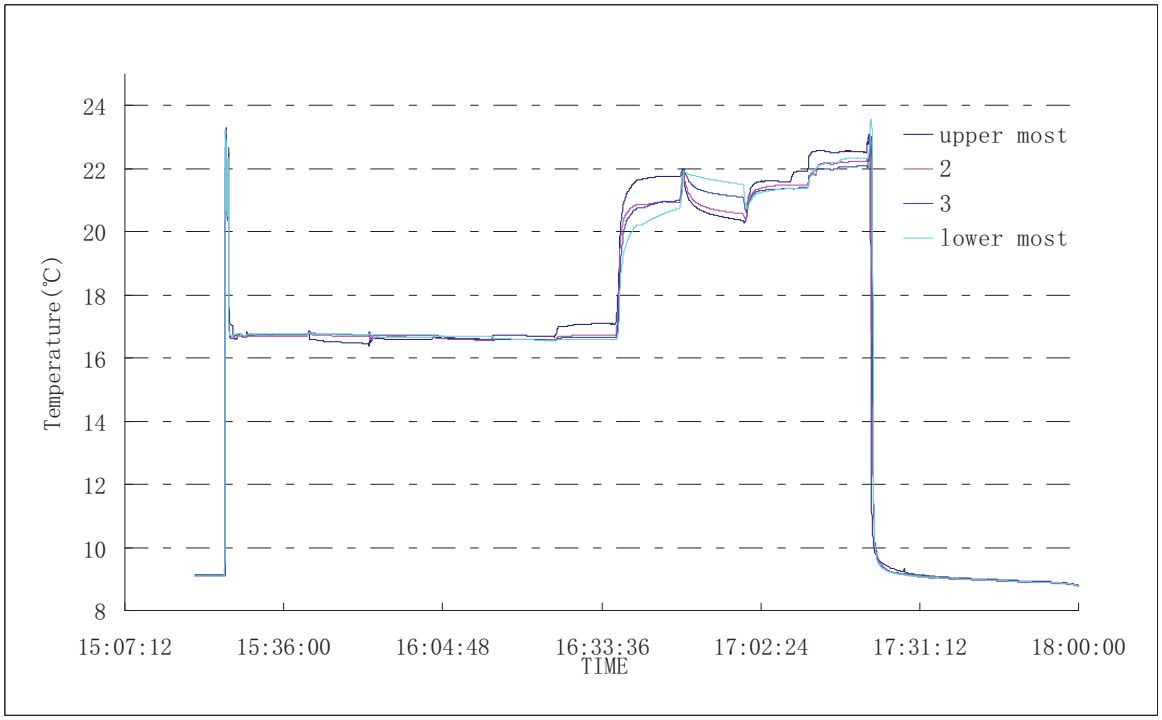

Fig. 88: Temperature versus time at DMV (GC-42).

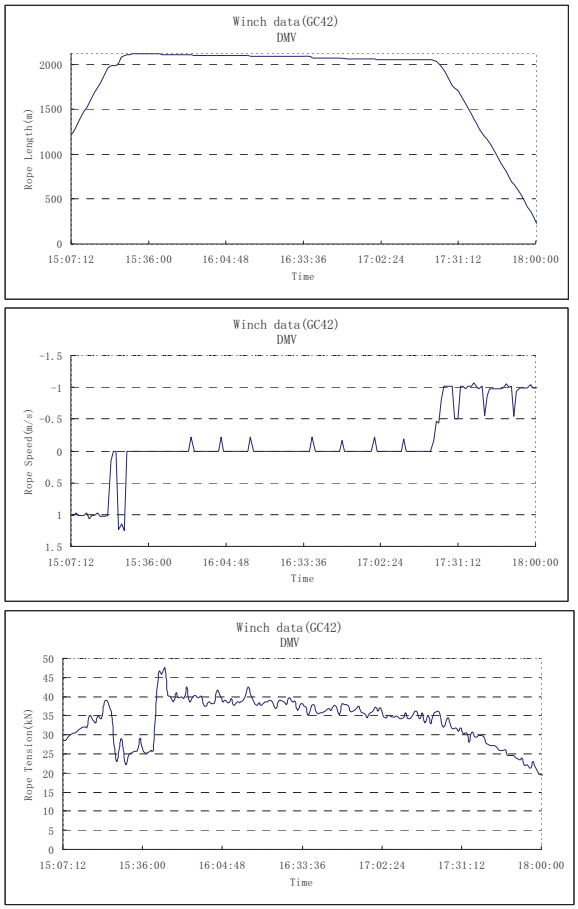

Fig. 89: Rope characteristics (rope length, rope speed and rope tension) versus time during GC 42 deployment at DMV.

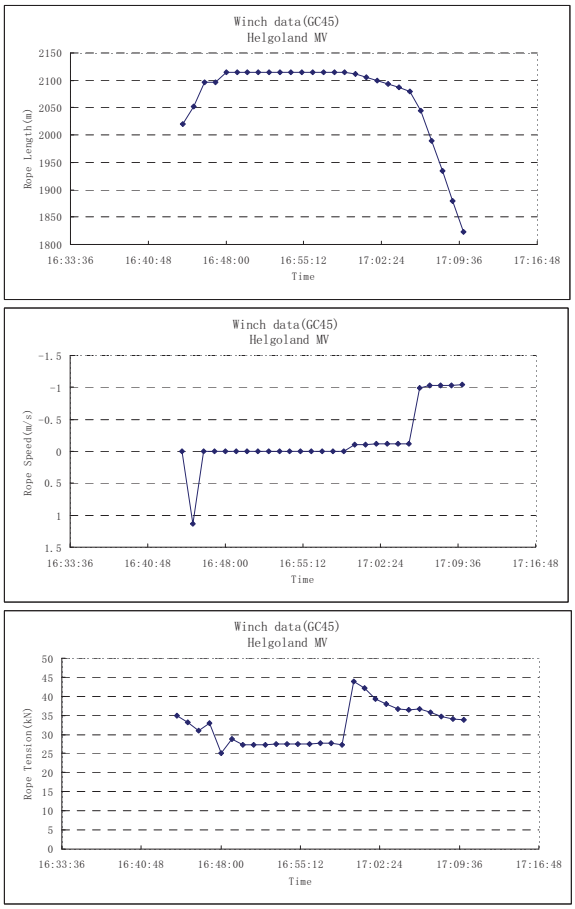

Fig. 90: Rope characteristics (rope length, rope speed and rope tension) versus time during GC 45 deployment at HMV.

Table 16: In situ temperature measurements during gravity corer deployments during Cruise M84/2.

Station Number	Area	T-logger	Technical description	Results	Gradient °C/m
GC - 1 Stat. 137 GeoB 15203	Eregli 1 Turkey	Logger 1-5 (SN 1854330, 1854333, 1854335, 1854336, 1854339)	Spacing: 125 cm T- Logger SN 1854333 no recording, logger SN 1854339 lost.	Only one logger penetrated into the sediment. Exact depth of penetration difficult to estimate, probably somewhere around 3 m.	~ 0.068
GC - 2 Stat. 138 GeoB 15204	Eregli 1 Turkey	Logger 1-5 (SN 1854330, 1854333, 1854335, 1854336)	Spacing: 125 cm T-logger SN 1854336 nearly lost	Only one logger penetrated into the sediment. Exact depth of penetration difficult to estimate, probably somewhere around 2.5 m.	~ 0.1
GC-16 Stat. 207 GeoB15251-1	Batumi Seep	T-ogger 1-4 (SN1854330, 1854335, 1854404, 1854407)	Spacing: 60 cm	All four loggers show increased temperature, non-linear profile, when taking the uppermost logger steep temperature gradient, uppermost logger depth 1.6 m.	0.087
GC-17 Stat. 209 GeoB15252	Batumi Seep	T-logger 1-4 (SN1854330, 1854335, 1854404, 1854407)	Spacing: 60 cm	All four logger in sediment, linear profile, depth correction: uppermost logger depth 27 cm.	0.061
GC-18 Sta. 211 GeoB15227-5	Pechori Mound	T-logger 1-4 (SN1854330, 1854335, 1854404, 1854407)	Spacing: 125 cm	Three loggers in sediments, linear profile, uppermost logger depth 0.69 cm.	0.090
GC-19 Stat. 212 GeoB15254	Pechori Mound – outside rim	T-logger 1-4 (SN1854330, 1854335, 1854404, 1854407)	Spacing: 125 cm	All four loggers in sediment, linear profile, uppermost logger depth 5.3 m!	0.047

Station Number	Area	T-logger	Technical description	Results	Gradient °C/m
GC-20 Stat. 213 GeoB15255	Pechori Mound –rim	T-logger 1-4 (SN1854330, 1854335, 1854404, 1854407)	Spacing: 125 cm	All four loggers with slight temperature increase, no linear profile, probably GC fallen aside.	0.010
GC-21 Stat. 214 GeoB15256	Pechori Mound – center	T-logger 1-4 (SN1854330, 1854335, 1854404, 1854407)	Spacing: 125 cm	Only 5 min in sediments, tip of logger 1 (SN1854330) broken, no data of that logger, linear profile, sediment depth of logger 2 about 1.2 m.	0.173
GC-24 Stat. 218 GeoB15260-1	Batumi Seep	T-logger 1-4 (SN1854334, 1854335, 1854406, 1854407)	Spacing: 60 cm	All four loggers in sediment, linear profile, uppermost logger depth 1.55 m	0.058
GC-25 Stat. 220 GeoB15261	Colkheti Seep	T-logger 1-4 (SN1854334, 1854335, 1854406, 1854407)	Spacing: 125 cm	Only two loggers in sediment, uppermost logger depth 1 m.	0.066
GC-33 Stat.248 GeoB15512	Kerch Flare	T-logger 1-4 (SN1854335, 1854406, 1854334, 1854407)	Spacing: 125 cm	Two t-loggers are in sediment, the penetration is about 2.5 m, uppermost logger depth -1.3 m.	0.03
GC-34 Stat.249 GeoB15513-1	Kerch Flare	T-logger 1-4 (SN1854335, 1854406, 1854334, 1854407)	Spacing: 125 cm	All four loggers in sediment, nearly linear profile, uppermost logger depth 6 m!	0.026
GC-36 Stat.256 GeoB15516-1	Kerch Flare	T-logger 1-4 (SN1854334, 1854335, 1854406, 1854407)	Spacing: 125 cm	All four loggers in sediment, nearly linear profile, uppermost logger depth 4 m!	0.036
GC-37 Stat.260 GeoB15518	Kerch Flare	T-logger 1-4 (SN1854334, 1854335, 1854406, 1854407)	Spacing: 125 cm	Only three loggers in sediment, nearly linear profile, uppermost logger depth 0 m.	0.067
GC-38 Stat.261 GeoB15519-1	Kerch Flare (back ground)	T-logger 1-4 (SN1854334, 1854335, 1854406, 1854407)	Spacing: 125 cm	All four loggers in sediment, nearly linear profile, uppermost logger depth 6 m!	0.020
GC-39 Stat.262 GeoB15520	Kerch Flare	T-logger 1-4 (SN1854334, 1854335, 1854406, 1854407)	Spacing: 125 cm	Only three loggers in sediment, nearly linear profile, uppermost logger depth -0.5 m.	0.046
GC-40 Stat.268 GeoB15524-1	Helgoland MV	T-logger 1-4 (SN1854334, 1854335, 1854406, 1854407)	Spacing: 125 cm	The upper two loggers were almost lost, no data logger 1854407, linear profile, uppermost logger depth 3.7 m.	0.477
GC-41(1) Stat.270 GeoB15525	Helgoland MV	T-logger 1-4 (SN1854334, 1854335, 1854406, 1854407)	Spacing: 125 cm	No data logger 1854407, curved profile, uppermost logger depth 9 m.	0.6-1
GC-41(2) Stat.270 GeoB15525	Helgoland MV	T-logger 1-4 (SN1854334, 1854335, 1854406, 1854407)	Spacing: 125 cm	No data logger 1854407, the temperature is varied, massive GH occurred in the bottom of the core.	
GC-42 Stat.272 GeoB15526-2	Dvurechenskii MV	T-logger 1-4 (SN1854332, 1854334, 1854335, 1854406,)	Spacing: 125 cm	Deep penetration up to about 70 m.	
GC-43 Stat.276 GeoB15525-3	Helgoland MV	T-logger 1-4 (SN1854332, 1854334, 1854335, 1854406,)	Spacing: 125 cm	Nearly linear profile, uppermost logger depth 0.7 m.	0.1
GC-44 Stat.279 GeoB15530	Helgoland MV	T-logger 1-4 (SN1854332, 1854334, 1854335, 1854406,)	Spacing: 125 cm	The change of the temperature indicate that the corer lied on the seafloor.	
GC-45 Stat.280 GeoB15531	Helgoland MV	T-logger 1-4 (SN1854332, 1854334, 1854335, 1854406,)	Spacing: 125 cm	Deep penetration, upper most t-logger 40 m.	
GC-46 Stat.281 GeoB15532-1	Background	T-logger 1-4 (SN1854332, 1854334, 1854335, 1854406,)	Spacing: 125 cm	Linear profile, uppermost logger depth 4.5 m.	0.034

11. Porewater Geochemistry

(M. Haeckel, A. Reitz, B. Domeyer, E. Pinero, U. Lomnitz)

11.1 Introduction

The geochemical analyses of the porewaters and sediments of seepage sites in the Black Sea, offshore Georgia, Turkey, and Ukraine, aim to quantify methane fluxes and turnover rates of associated biogeochemical processes as well as the investigation of gas and fluid sources emanating in these areas.

Therefore, a comprehensive geochemical dataset has been collected on this cruise.

Onboard, the collected samples were analysed for their content of NH_4^+, PO_4^{3-}, SiO_4^{4-}, H_2S, Cl^-, and alkalinity. In addition, sub-samples were taken for further shore-based analyses: DIC content and its $\delta^{13}C$ isotope ratio, dissolved metal cations, SO_4^{2-}, Br^-, Cl^-, and I^- concentrations, isotopic ratios of Sr, Cl, Li, H, and O in the porewater, porosity and carbonate, POC, PON, and sulfur content of the solid phase (Appendix 7).

In total, 782 samples from 57 cores were collected. The sampling locations were primarily chosen based on backscatter information and gas flare observations from this and previous cruises (e.g., POS317, TTR-15, M72/3, and MSM15/2) that suggested potential fluid and gas seepage.

11.2 Materials and Methods

Sediment and porewater sampling

Surface and subsurface sediment samples were retrieved using a mini-corer (MIC), a gravity corer (GC), a dynamic autoclave piston corer (DAPC), and mobile seafloor drilling device (MeBo). The sediments were extruded out of the MIC plastic liners with a piston and cut into 1-3 cm thick slices, whereas GC, DAPC and MeBo cores were cut in half and 3-5 cm thick slices were taken in approximately 20-40 cm (for MeBo up to 100 cm) intervals. Subsequently, the porewater was extracted in the ship's cold room (4 °C) using a low pressure-squeezer (argon at 3-5 bar, sometimes up to 7 bar). While squeezing, the porewater was filtered through 0.2 µm cellulose acetate Whatman filters and collected in recipient vessels. Alternatively, from DAPC cores (except for DAPC 9 and 10, which were squeezed) the porewater was extracted via Rhizon technique (Seeberg-Elverfeldt et al., 2005), i.e., porewater was sucked into an evacuated 20-ml syringe through a porous (0.2 µm pore diameter) hydrophilic polymer tube. Several Rhizons were placed directly into the sediment in the core liner in 20-40 cm spacing.

About 5 ml of wet sediment of each sediment slice was collected for porosity, carbonate and CNS element analyses at home. Aliquots of the extracted porewater were sub-sampled for various onboard and further shore-based analyses (Appendix 7). Subsamples for ICP-AES analysis were acidified with 30 µl of conc. suprapure HNO_3 per 3 ml of porewater sample (i.e, pH<1) and subsamples (~1.9 ml each) for $\delta^{13}C$ and DIC were treated with 10 µl of $HgCl_2$ to inhibit further microbial degradation. All samples for home-based analyses were stored refrigerated.

Porewater analyses

Analyses for the nutrients NH_4^+, PO_4^{3-}, SiO_4^{4-} as well as H_2S were completed onboard using a Hitachi UV/VIS spectrophotometer. The respective chemical analytics follow standard

procedures (Grasshoff et al., 1999), i.e. ammonium was measured as indophenol blue, phosphate and silicate as molybdenum blue, and sulfide as methylene blue. Since high sulfide contents (> 1 mM) interfere with the reactions of NH_4^+, PO_4^{3-}, and SiO_4^{4-}, these sub-samples were acidified with 30% suprapure HCl (10 µl per 1 ml of sample) and bubbled with argon to strip any H_2S prior to the analysis.

The total alkalinity of the porewater was determined by titration with 0.02 N HCl using a mixture of methyl red and methylene blue as indicator. The titration vessel was bubbled with argon to strip any CO_2 and H_2S produced during the titration. The IAPSO seawater standard was used for the calibration of the method. The porewater content of chloride was determined by ion chromatography. Again, the IAPSO seawater standard was used for calibration.

The analytical precision and accuracy of each method are given in Table 17.

Table 17: Analytical methods of onboard geochemical analyses.

Parameter	Method	Detection limit	Analytical precision/accuracy
H_2S	Photometer	3 µmol/l	3 %
NH_4^+	Photometer	5 µmol/l	5 %
PO_4^{3-}	Photometer	1 µmol/l	5 %
SiO_4^{4-}	Photometer	5 µmol/l	2 %
Cl^-	Ion chromatography	<1 mmol/l	5 %
Alkalinity	Titration	0.1 meq/l	2 %

11.3 Results

In all research areas (see maps with coring locations in Chapter 2) porewater was collected from sediment cores and analyzed, however, the primary areas of interest of our group were the seeps in the Samsun area (Ordu Ridge), offshore Georgia (Batumi, Poti, Pechori), in the Kerch fan area, and the Helgoland mud volcano in the Sorokin Trough. Surface sediments collected with the MIC will allow to calculate methane fluxes and AOM rates (anaerobic oxidation of methane) at seep sites, whereas longer cores (GC and MeBo drillings) provide information on fluid and gas sources of these environments.

General Black Sea Sediment Geochemistry

In all of these areas, background sediments were sampled that are not influenced by methane gas and oil seepage or mud expulsion and fluid flow. Since those sediments are overlain by completely anoxic bottom water – in the Black Sea oxygen and nitrate are typically consumed within the upper 100-150 m of the water column – sulfate reduction and methanogenesis dominate early diagenetic processes. In fact, the upward diffusing methane completely consumes the dissolved sulphate that is diffusing into the sediment within the upper 300-350 cm of the sediment. This anaerobic oxidation of methane (AOM) leads to an increase in total alkalinity and hydrogen sulphide. The produced hydrogen sulphide then reacts with dissolved iron in the porewater forming FeS that is readily recognized as black spots and layers in the sediment and often builds up a continuous zone of several decimeters to a meter in thickness (Chapter 9.3). Similarly, dissolved phosphate is consumed by mineral formation with e.g., dissolved iron, roughly 1-1.5 m below the depth of H_2S depletion. Dissolved ammonium and phosphate are

released during the microbially mediated degradation of organic material in the sediment, primarily via sulphate reduction and methanogenesis. In contrast to phosphate, ammonium, however, is not involved in any mineral formation or other reactions and hence continuously accumulates in the porewater leading to concentrations of a few milli-moles. Likewise, concentrations of methane, one of the final products of organic carbon degradation, are also increasing with sediment depth. This can be witnessed on deck by a downcore increasing intensity of degassing of the sediment, since methane solubility drops drastically due to pressure reduction during core retrieval.

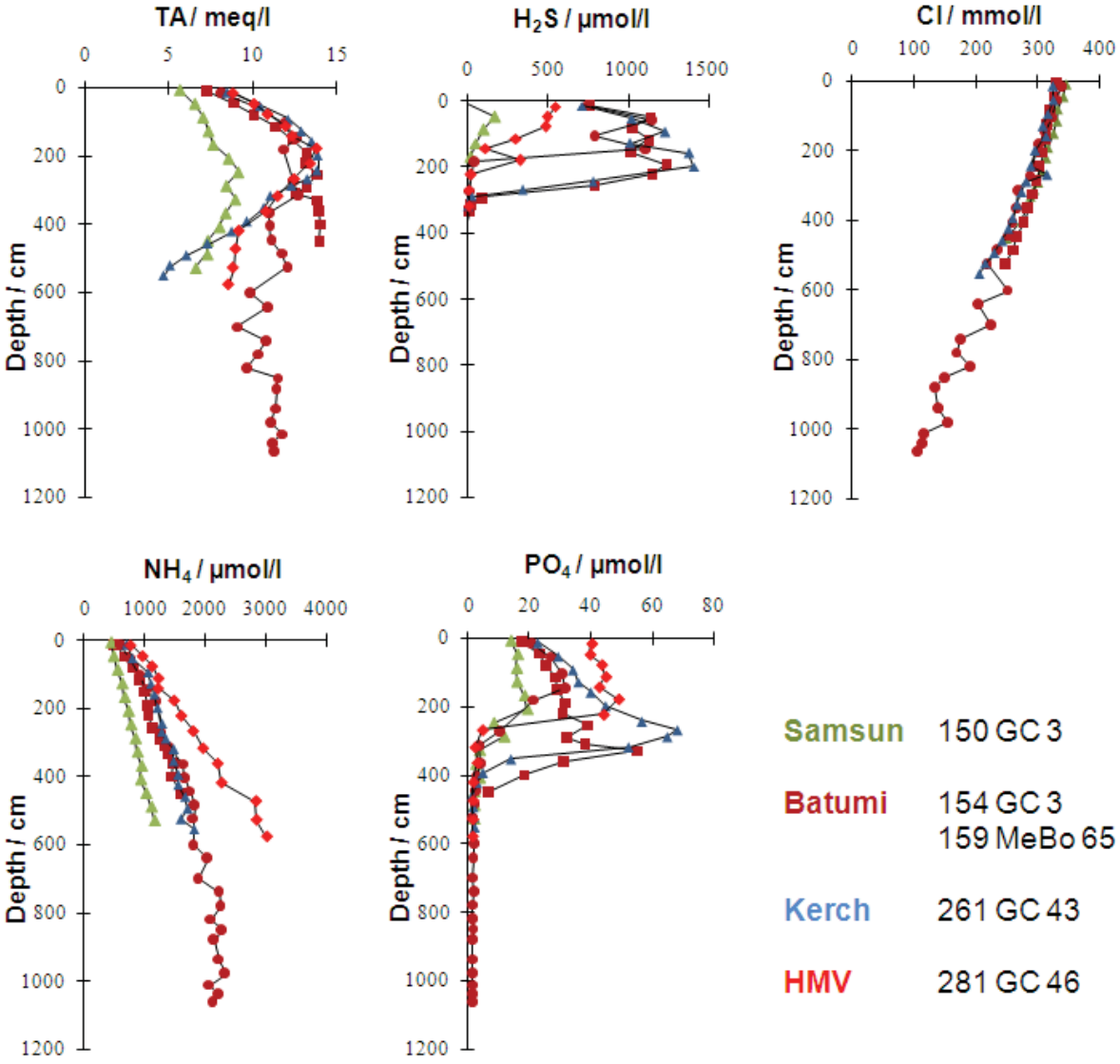

Fig. 91: Reference cores at the different research areas. Depths are given with respect to the top of the recovered core and are not corrected for any sediment loss that has occurred.

These well-known basic biogeochemical reactions and their manifestations are also nicely documented in the porewater profiles of all reference cores (Fig. 91). Despite the fact that the investigated areas are located in different water depths (400-2000 m) and geographically in different regions of the Black Sea, differences in porewater profile shapes and concentrations are strikingly similar. This is most likely due to the strong stratification and laterally homogeneous chemistry of the water column in the entire Black Sea. Obvious deviations in phosphate and

hydrogen sulphide depletion depths are due to differences in surface sediment losses during MeBo drilling and GC coring and recovery. Depth corrections will be attempted based on a combination of porewater and sediment variables as well as geological information, such as color scans and core descriptions (Chapter 9.3).

Another peculiarity of Black Sea porewaters that is well documented in the investigated cores, are the linearly decreasing chloride concentrations in the surface sediments (Fig. 91). Chloride and other sea salt ions are still diffusing from the overlying, marine and thus, saline, water body into the salt-depleted lacustrine sediments from before 10,000 years ago. Minimum Cl concentrations of 25-30 mM are reached in 20-25 m sediment depth (Manheim and Schug, 1978; Soulet et al., 2010), which could, unfortunately, not be reached during the MeBo drilling.

Geochemical porewater profiles at the methane seeps and mud volcanoes, presented below, will be discussed with respect to this background situation.

Georgia (Batumi Seep area, Pechori Mound, Poti Seep, Kulevi Ridge, Adjara Ridge)

Offshore Georgia, the prime interests were to finalize the geochemical sampling campaign at the Batumi Seep area that had been started on TTR-15 and M72/3 and getting deep cores from Pechori Mound.

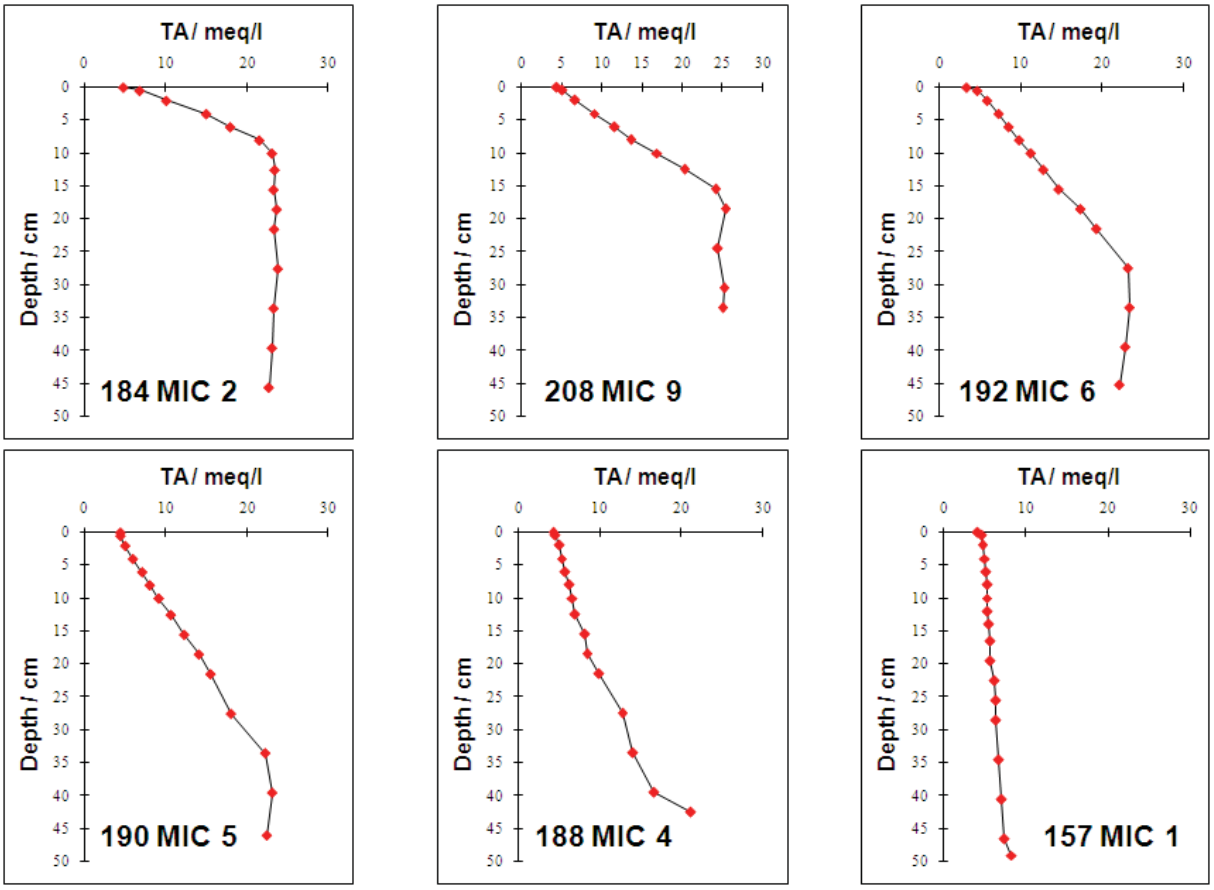

Fig. 92: Total alkalinity profiles of MIC cores taken at sites of different seep activity. High methane fluxes correlate to shallow occurrences of maximum/asymptotic TA values. Consequently, vigorous degassing was observed, particularly in MIC 2 and 9.

The Batumi Seep area has been visited on previous cruises and sediment cores had been collected from different sites with gas bubble emissions. Based on these data it was established

that the area is a pure gas seep, i.e. upward fluid flow does not occur (Haeckel et al., 2008). Consequently, porewater profiles show a mixing of bottom water concentrations into the sediment on a meter-scale. This irrigation-like process is induced by intense and spatially frequent rise of gas bubbles through the surface sediments (Haeckel et al., 2007). Further effort is necessary, however, to achieve a solid and area-wide methane budget for the Batumi Seep area. Therefore, on this cruise several more MIC and GC cores were collected to complete the spatial coverage, particularly with respect to different gas ebullition intensities (Nikolovska et al., 2008) as well as acoustic backscatter intensities (Klaucke et al., 2006). In total, cores from 20 spots exist, covering a large range of porewater-derived methane fluxes. Figure 92 shows a selection of data from this cruise, showing total alkalinity profiles ordered from high to low upward methane fluxes (upper left to lower right plot; a steep TA increase correlates to high CH_4 flux and more intense AOM). Dissolved methane profiles, measured on the same cores (Chapter 12), correlate very well with the other geochemical profiles. In general, high dissolved methane fluxes (and hence high AOM rates) occur along a W-E-striking line that coincides with the occurrence of more intense gas flares and shallow gas hydrate appearances.

The porewater profiles measured at Poti Seep seem to be similar to those of Batumi Seep area, also indicating methane gas seepage.

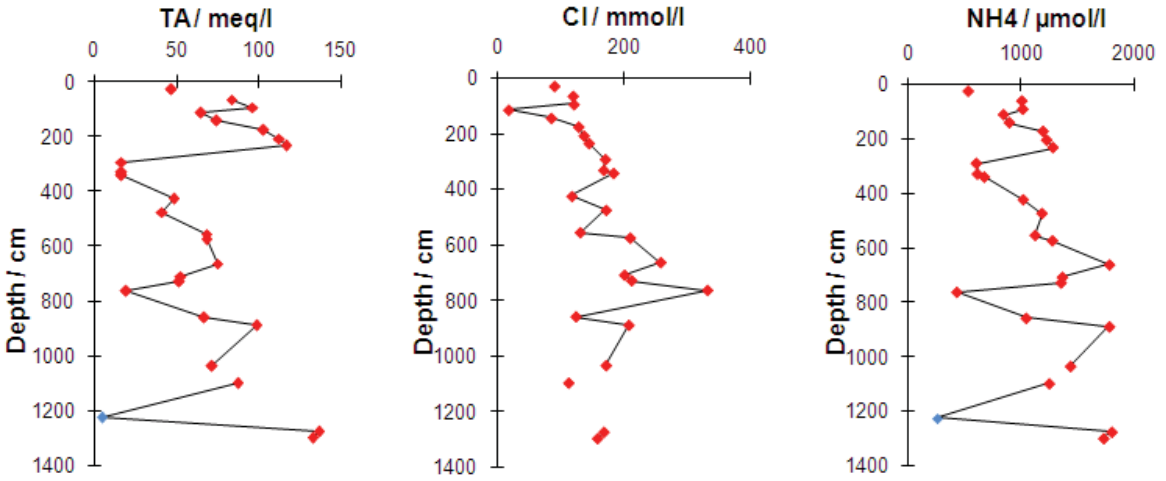

Fig. 93: Porewater TA, Cl, and NH_4 profiles of a MeBo drilling (168 MeBo 67) at Pechori Mound.

In contrast, at Pechori Mound not only methane is seeping, but also oil. Here, upward fluid flow is observed, leading to upward concave porewater profiles. The pore fluids carry signatures from diagenetic processes occurring at large sediment depths and elevated temperatures (Reitz et al., 2011): Li and B are enriched, Cl and K are depleted, pointing at clay mineral dewatering (smectite-illite transformation); Sr isotope ratios indicate that fluids originate from late Oligocene strata. Hence, Pechori Mound was chosen as drill site with MeBo to retrieve sediments from deeper strata than is possible by conventional GC coring. MeBo cores retrieved several thick layers of massive gas hydrate leading to freshening of porewater due to hydrate dissociation upon core retrieval. This is very obvious in the many spikes in TA, Cl, and NH_4 (Fig. 93). Nevertheless, the chloride profile shows increasing concentrations down the core. This might be due to in situ active hydrate formation or old (and more saline) sediments which have

been transported up by the diapir beneath Pechori Mound, but is not evident in the data from shallower GC cores.

Sediments from Kulevi and Adjara Ridge were also heavily oil-stained and further geochemical and isotope analyses will show if here also deep fluids are advecting upwards bearing signals from higher temperature processes.

Turkey (Eregli, Samsun, Ordu Ridge)

In the Turkish waters, sediment cores were taken in the area of Eregli and Samsun. In Eregli, some methane seep activity could be observed in the porewater profiles, but gas hydrates were out of reach for gravity coring and MeBo drilling.

In Samsun, an extensive sediment sampling program was conducted, particularly at Ordu Ridge, where new sites of acoustic high backscatter intensities and gas flares had been found during initial surveys (Chapters 5.3 and 6.3). Three of these patches (#2, #3, and #7) were investigated geochemically. Here, methane fluxes appear to be significantly higher than in Eregli, potentially consuming dissolved sulphate within the top 20 cm of the sediment (estimated from the depth where maximum total alkalinity values (~23 meq/l) are achieved). Degassing of sediments was already observed in MIC cores and gas hydrates occurred within the top 100-200 cm of GC cores. Porewater profiles hint at gas seepage rather than upward fluid advection of methane-rich fluids, because bottom water concentrations are mixed down into depth.

Ukraine (Kerch Flare, Helgoland MV, Dvurechenskii MV)

At the Ukrainian shelf the area of the Kerch gas flare field was investigated. This site is one of the few gas seeps at the Kerch fan that is situated within the thermodynamic stability field of gas hydrates. Most of the other seeps are at shallower water depths where gas hydrates cannot form anymore. Porewater profiles exhibit similar characteristics as in the Batumi Seep area, i.e. the Kerch Flare is a pure gas seep and fluid flow is not evident. Upward methane fluxes seem to be of comparable intensity, leading to an increase in total alkalinity up to ~23 meq/l within the upper 10-15 cm of the sediment and hydrate formation close to the sediment surface (i.e., 50-100 cm; see Figs. 80 and 81, Chapter 9.3).

In the Sorokin Trough the Helgoland (HMV) and Dvurechenskii (DMV) mud volcanoes were investigated. While the DMV has been studied on previous cruises in much detail, only limited geochemical data has been collected from the HMV so far. Within the central most active mud pool of HMV GC coring with temperature logging was performed, even lowering the GC down to several tens of meters. Geochemical data from these deployments as well as surface deployments show very high concentrations of ammonium of up to 13-14 mM and a steep increase in total alkalinity up to values of >35 meq/l (Fig. 94). While TA values are almost twice as high as at the adjacent DMV, in the deep GC deployment at DMV >40 mM of NH_4 were found. These tremendously high amounts of ammonium are likely released from thermal degradation of organic material at very large depths. A GC taken SW of the mud pool penetrated about 1 meter into the sediment, where the core was stopped by a layer of porous gas hydrate (see Fig. 82 in Chapter 9.3). Cl concentrations at HMV (~580 mM) and DMV (~835 mM) are elevated and at DMV it is suggested that the saline fluids might be generated by subcritical phase separation (Reitz et al., 2007). Since, the same diapiric structure is feeding both mud volcanoes,

similar processes, though eventually at different rates and fluid/mud expulsion activities also determine the fluid composition at HMV.

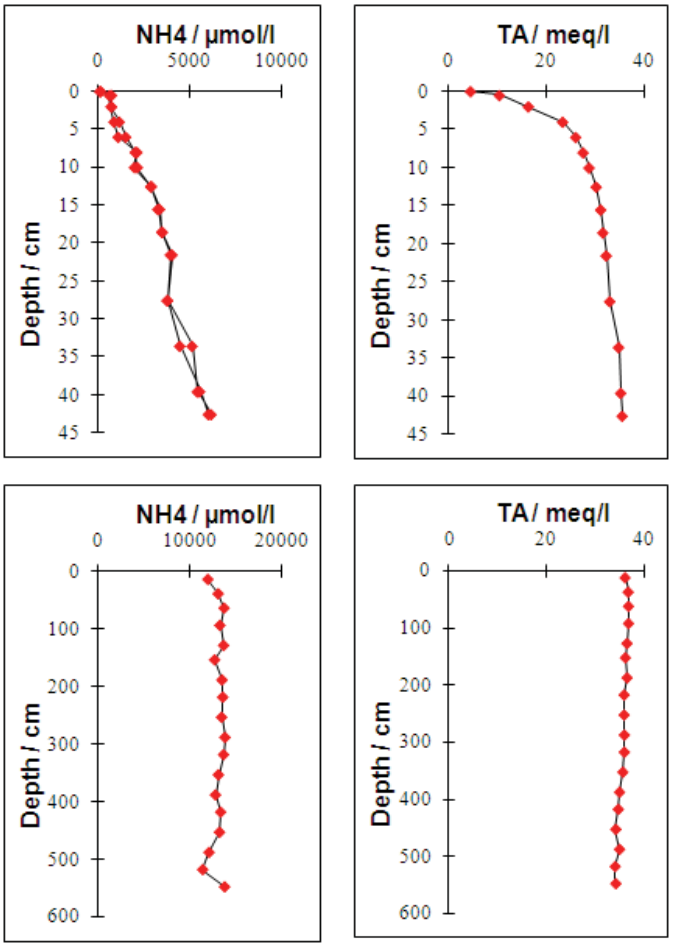

Fig. 94: Porewater TA and NH_4 profiles at Helgoland MV (top row: 277 MIC 20; bottom row: 280 GC 45).

12. In Situ Gas Amounts and Gas Composition

(T. Pape, T. Malakhova, D. Wangner)

During previous cruises to the Eastern Black Sea (POS317/4, TTR-15, M72/3, MSM15/2) shallow gas hydrates associated to numerous hydrocarbon seepage sites (gas seeps, oil seeps, and mud volcanoes) located within the gas hydrate stability zone were discovered. Hydrate-related investigations considered the molecular and isotopic composition of venting gas and hydrate-bound gas, the crystallographic structure of shallow hydrates and their thermodynamic stabilities, and the relevance of geochemical processes controlling hydrate distributions in near-surface sediments.

In addition, for selected cold seeps and mud volcanoes the amounts of shallow hydrate could have been quantified by use of autoclave technique. However, due to the lack of adequate sampling techniques, gas chemical and crystallographic properties of hydrates in the deep subsurface and driving factors affecting their distributions remained unknown, so far.
Therefore, primary works performed during M84/2 aimed at investigating

- quantities of gas and methane in pressured sediment cores collected with the Dynamic Autoclave Piston Corer (DAPC),
- the chemistry and crystallography of hydrates present in deep sediments of known seepage sites drilled with the Meeresboden-Bohrgerät (MeBo; Chapter 8),
- the physico-chemical properties of near-surface hydrates collected with the gravity corer (GC) in order to broaden the existing data set of Black Sea hydrates in known areas and at newly discovered sites,
- vertical methane concentration profiles in near-surface sediments recovered with the mini corer (MIC) for calculations of fluxes and conversion rates of methane.

12.1 Samples and Methods

12.1.1 Sampling

In order to collect pressurized near-surface sediment cores and to quantify gas in situ amounts (Chapter 12.3.) autoclave technology was used during both legs of M84/2 to prevent gas hydrate dissociation and loss of gas induced by pressure decrease. Functionalities of the Dynamic Autoclave Piston Corer I were described elsewhere (e.g. Abegg et al. 2008, Heeschen et al., 2007; Pape et al. 2011; Chapter 9.2). Briefly, the DAPC consists of a cutting barrel and a pressure chamber which allows preserving sediment cores of up to 2.65 m in length under in situ hydrostatic pressure.

Pieces of gas hydrates were extracted from both MeBo cores and gravity cores. For long-term storage and onshore analysis, hydrates were immediately soaked into liquid nitrogen (– 196° C). For onboard gas chemical analysis, the hydrate pieces were cleaned in ice-cooled water and placed in plastic syringe for immediate dissociation. The liberated gas was transferred with a canule into 20 ml glass vials prefilled with supersaturated sodium chloride solution.

For vertical profiling of methane concentrations, sediment samples were taken from cores recovered with the MIC and the GC. For mini cores, sediments were extracted out of the liner with a plastic piston. 3 ml of sediment were taken from selected depths (typically 1–3 cm resolution for MIC, 10–20 cm resolution for GC) using cut-off syringes and transferred into 20

ml glass vials prefilled with 5 ml of 1 M NaOH. Prior to gas chromatographic analysis, the samples were left for 24 h at 4°C and occasionally shaken.

12.1.2 Analytical Methods

For analysis of the molecular composition of gasses collected, a two-channel gas chromatograph was used (Pape et al., 2010). Separation and quantification of C_1- to C_6-hydrocarbons was achieved by using a capillary column connected to a Flame Ionization Detector. Concentrations of oxygen, argon, nitrogen and carbon dioxide as well as methane and ethane were simultaneously determined with a packed mole sieve column coupled to a Thermal Conductivity Detector.

12.2 Preliminary Results and Discussion

During M84/2, in total 272 samples of hydrate-bound gas from 23 GC stations and four MeBo stations, 81 samples from degassing of seven sediment pressure cores, and 731 samples of headspace gas from 20 MIC and 16 GC stations were collected.

12.2.1 Gas and Gas Hydrate Quantification

Stations with the DAPC were conducted for obtaining information on gas contents in newly explored areas (e.g. Poti seep, Ordu Ridge) or for expanding pressure core data sets for sites investigated already during previous cruises (e.g. Kerch Flare, Dvurechenskii MV, Helgoland MV).

Ten stations with the Dynamic Autoclave Piston Corer were performed during M84/2a+b for quantification of gas and gas hydrates in sediments (Chapter 9.2; Table 18). Seven pressure cores could be recovered under in situ hydrostatic pressure, while for two cores (DAPC-2; DAPC-5) leakages resulted in considerable pressure loss. At one station (DAPC-4) the DAPC was not released at the seabed and, thus, no core could be recovered.

Table 18: Overview of stations performed with the Dynamic Autoclave Piston Corer (DAPC) including accumulated gas volumes and calculated gas-sediment ratios.

GeoB No.	Station no.	Area	Recovery pressure	Core length	Core volume	Gas volume released	Gas volume / volume wet sediment
			[bar]	[cm]	[L]	[L]	[L / L]
Offshore Georgia							
15244-4	DAPC-1	Poti seep	98	243	13.0	256.4	19.8
15244-5	DAPC-2	Poti seep	n.a.	104	5.6	n.a.	n.c.
Offshore Turkey							
15267-4	DAPC-3	Ordu Ridge patch #2	83	145	7.7	1.7	0.2
15268-5	DAPC-5	Ordu Ridge patch #2	n.a.	110	5.9	n.a.	n.c.
Kerch Flares							
15513-2	DAPC-6	Kerch Flare	82	164	8.8	85.7	9.8
15516-2	DAPC-7	Kerch Flare	27	243	13.0	13.0	1.0
15518-2	DAPC-8	Kerch Flare	57	200	10.7	40.9	3.8
Sorokin Trough							
15526-1	DAPC-9	Dvurechenskii MV	118	260	13.9	129.1	9.3
15530	DAPC-10	Helgoland MV	115	257	13.9	297.5	21.6

n.a. = not analyzed; n.c. = not calculated

Two stations (DAPC-9, -10) achieved nearly full recovery, while for other stations either shorter cores were recovered or voids spanning over several decimeters became apparent subsequent to the degassing procedure. Compared to results for gas from pressure cores obtained during former expeditions, a high volumetric gas-sediment ratio (19.8) was determined for core DAPC-1 from the Poti seep. However, the highest gas volume collected with the DAPC so far was obtained during station DAPC-10 at the center of the Helgoland MV. This site appeared to be characterized by the presence of 'fresh hydrates' in high density (see also Chapter 9).

12.2.2 Molecular Composition of Gas Samples

During M84/2, the molecular gas composition was analyzed for samples prepared from gas hydrates (GC, MeBo) and from sedimentary gas (DAPC). Results are illustrated in Figure 95.

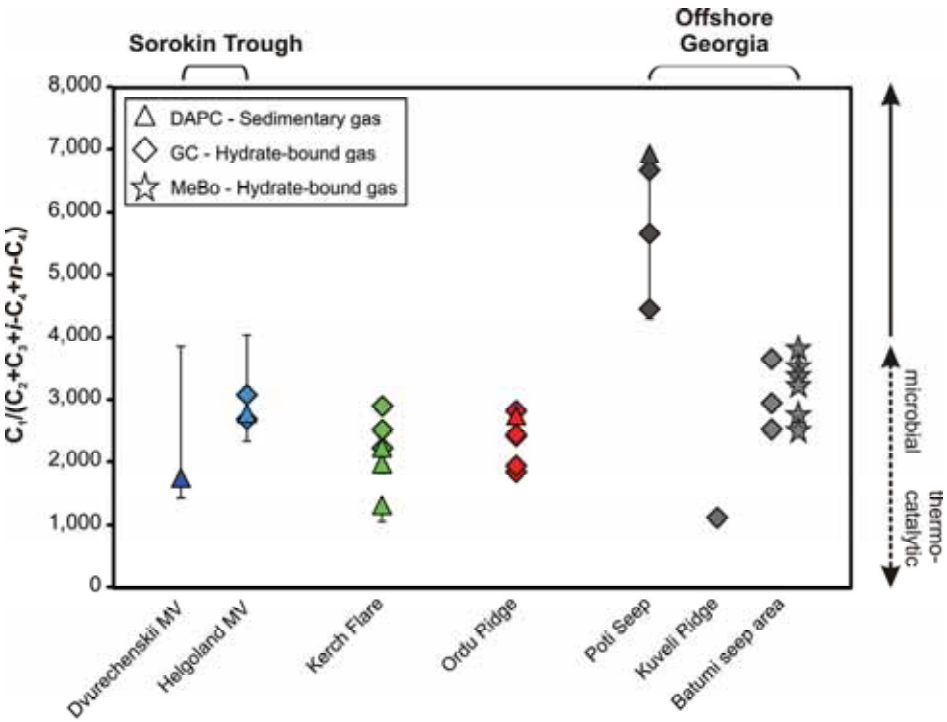

Fig. 95: Overview of hydrocarbon compositions expressed as C_1/C_{2+} ratios in hydrate-bound gas (GC, MeBo), and sedimentary gas (DAPC) sampled at the different working areas during Cruise M84/2. Results for gas hydrates recovered from the Pechori Mound were not included in this overview due to heavy contamination by oil-derived volatiles. Error bars denote the limits of deviation during the DAPC degassing procedure. For the pressure core recovered from Ordu Ridge no error bar is given because only a single gas sample could be collected due to pressure loss during the recovery procedure.

Batumi seep area

The Batumi seep area has been in the focus of intense research during several former expeditions (Pos317/4; TTR-15, M72/3, MSM15/2). It appears that the Batumi seep area is exclusively driven by hydrocarbon migration without recognizable upward fluid flow. Gas and fluid chemistry (Pape et al., 2010; Reitz et al., 2011) as well as abundances of hydrate in shallow sediments (Pape et al., 2011) have already been reported. During M84/2 more than 350 gas samples were recovered from the Batumi seep area (Table 19).

Table 19: List of samples recovered from the Batumi seep area considered for gas chemical analysis during M84/2.

GeoB	Instrument	Hydrate-bound gas	Headspace gas
15236-1	GC-7	6	
15241-2	GC-8		9
15247-2	GC-12	3	12
15249-1	GC-15	8	12
15251-1	GC-16	11	
15252	GC-17	7	
15260-1	GC-24	5	10
15220-5	MeBo-65		6
15236-2	MeBo-68	20	
15220-4	MIC-1 (reference site)		18
15237	MIC-2		28
15239-2	MIC-4		27
15239-2	MIC-5		28
15242	MIC-6		30
15247-1	MIC-7		29
15249-2	MIC-8		26
15251-2	MIC-9		22
15253	MIC-10		30
16260-2	MIC-11		27
	Total	**46**	**314**

The molecular compositions of hydrate-bound gas in hydrate pieces collected with GC from near-surface sediments and that of hydrates drilled at greater depths with MeBo were similar (Fig. 95). Hydrate-bound gas consisted of methane (99.43–99.69 mol-%), carbon dioxide (0.28–0.55%), and ethane (0.02–0.04%). While propane (<0.01%) occurred in all gas samples investigated, *iso*-butane and *n*-butane were only found in two out of six hydrate samples drilled with MeBo. These molecular compositions of hydrate-bound gas are similar to those already published for hydrates collected during M72/3 (Pape et al., 2010).

Pechori Mound

In a previous study gas discharge coupled to fluid flow was proposed for the Pechori Mound (Reitz et al., 2011). In addition, strong impregnations of oil in surface sediments and of hydrates were already observed during earlier sampling campaigns. During M84/2 gas samples were collected during three GC stations and two MeBo stations (Table 20). Such hydrates were impregnated by oil on a mm-scale which hampered manual preparation of pure gas hydrate pieces (see also Chapters 8 and 9).

Table 20: List of samples recovered from the Pechori Mound considered for gas chemical analysis during M84/2.

GeoB	Instrument	Hydrate-bound gas	Oil-stained sediment	Headspace gas
15226	GC-5			26
15255	GC-20	4		
15256	GC-21	5		
15227-1	MeBo-66	2		
15227-3	MeBo-67	26	3	
	Total	**37**	**3**	**26**

Hydrates collected during GC-20 and -21 as well as MeBo-66 and -67 were often found as massive hydrate layers of several decimeters in thickness. Molecular compositions of gas from hydrates recovered with GC-20 and -21 resembled each other with 87.50–89.48 mol-% methane, 10.39–12.01% carbon dioxide, 0.09–0.43% ethane, and about 0.01% propane. In agreement with earlier assumptions, the resulting C_1/C_{2+} ratios < ca. 700 clearly indicated a predominance of thermogenic hydrocarbons at this site. C_2/C_3 ratios were 3.0 and 8.9, respectively.

In contrast to gas compositions of GC-collected hydrates, those of hydrates drilled with the MeBo varied considerably with methane contributing 77.79–90.30 mol-%, carbon dioxide 4.71–14.25%, ethane 0.18–0.64%, and propane 0.27–11.17%. Despite these variances in the gas chemical composition of hydrate-associated volatiles, C_1/C_{2+} ratios were <310 and propane exceeded ethane concentrations for all samples (C_2/C_3 ratios <0.9). A depths correlation for those ratios became not apparent.

The molecular composition of hydrates recovered with MeBo-67 (GeoB15227-3) was investigated in detail with respect to the origin of volatiles associated to hydrates forming at the Pechori Mound. For this, the concentrations of propane, which can be incorporated into the large crystal cages of sII hydrates, was followed with the concentrations of higher hydrocarbons, which due to their molecular sizes do not fit into any of the hydrate crystal cages (Sloan and Koh, 2007). As an example Figure 96 illustrates the positive correlation between propane and an unidentified C_6-hydrocarbon in eleven hydrate pieces.

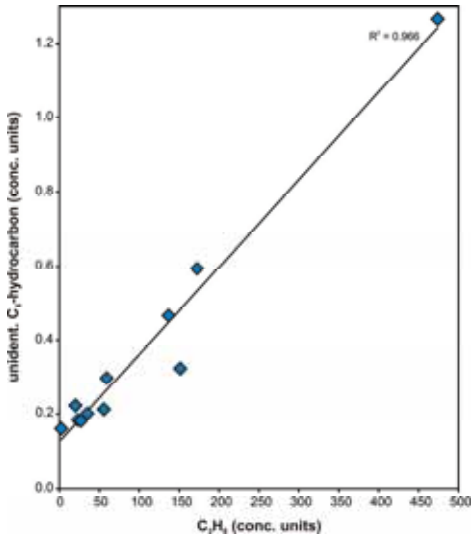

Fig. 96: Positive correlation between concentrations of propane and an unidentified C_6-hydrocarbon in gas released by dissociation of oil-impregnated gas hydrates drilled by MeBo (GeoB 15227-3) at the Pechori Mound.

The correlation between propane and higher hydrocarbon homologues indicates that the chemical composition of gas released during decomposition of such hydrates originated from hydrate-bound volatiles plus components associated to oil impurities. This assumption is supported by results from headspace analysis of warmed, oil-stained sediments that showed volatilization of low-molecular hydrocarbons (propane, butane, etc.) and carbon dioxide during oil degassing. Hence, precise determinations of hydrate-bound volatiles from oil-impregnated hydrate pieces solely by use of techniques available on-board are problematic.

Poti seep

At Poti seep gas hydrates could be sampled at three GC stations, while sedimentary gas was collected at an individual DAPC (DAPC-1) station (Table 21).

Table 21: List of gas samples recovered from the Poti seep.

GeoB	Instrument	Hydrate-bound gas	Headspace gas	Sedimentary gas
15243	GC-9	2		
15244-2	GC-11	7	9	
15244-3	GC-13	14		
15244-4	DAPC-1			20
	Total	**23**	**9**	**20**

The molecular compositions of both, hydrate bound-gas and sedimentary gas from Poti seep were very similar. The gas was strongly dominated by methane (99.51–99.66 mol-%), followed by carbon dioxide (0.27–0.47%), ethane (0.01–0.02%), and propane (<0.01%). *iso*-butane was only found in traces in gas released from DAPC-1. The resulting C_1/C_{2+} ratios >4,400, which were the highest values measured during M84/2 (Fig. 95), indicate a strong dominance of microbial hydrocarbons at this site. The virtual lack of oil-droplets in the sediments, which are present in high density at the oil seep sourced by more thermogenic hydrocarbons (e.g. Pechori Mound) supports this assumption.

Kulevi Ridge

From Kulevi Ridge two oil-stained cores bearing gas hydrates below 110 cmbsf were recovered (Table 22).

Table 22: List of gas samples recovered from the Kulevi during M84/2.

GeoB	Instrument	Hydrate-bound gas	Headspace gas
15258	GC-22	2	6
15259	GC-23		19
	Total	**2**	**25**

Hydrate-bound gas extracted from core GC-22 contained 99.22 mol-% methane, 0.69% carbon dioxide, 0.07% ethane, <0.01% propane, and 0.01% *iso*-butane. The C_1/C_{2+} ratio ≈ 1,080 suggests considerable admixture of thermogenic hydrocarbons at this site. In contrast to oil-stained hydrates from the Pechori Mound oil seep those from the Kulevi Ridge did not show a C_3 over C_2 prevalence. Hence, hydrates at the Kulevi Ridge appear less affected by oil impregnations in comparison to those at Pechori Mound.

Ordu Ridge

Several patches of high backscatter intensity were discovered on the Ordu Ridge off the Turkish coast close to the city of Samsun (Chapter 6). Gas hydrates were collected at four of these patches (#2, #3, #5, #7) by use of GC (Table 23). In addition, a single pressure core was recovered from patch #2.

Table 23: List of samples recovered from the different patches at the Ordu Ridge considered for gas chemical analysis.

GeoB	Instrument	Patch	Hydrate-bound gas	Sedimentary gas	Headspace gas
15268-1	GC-27	#2	23		10
15268-1	DAPC-3	#2		1	
15268-3	MIC-12	#2			28
15503-1	GC-28	#3	9		3
15503-3	MIC-13	#3			29
15504	GC-29	#5	17		
15505	GC-30	#7	28		
15507	GC-31	#7	15		
15505-2	MIC-14	#7			23
Total			**92**	**1**	**93**

All gas samples obtained from the four patches on Ordu Ridge showed relatively uniform molecular compositions. Methane was the predominant hydrocarbon (99.53–99.69 mol-%), followed by carbon dioxide (0.26–0.42%) and ethane (0.03–0.05%). Propane and *iso*-butane were detected in almost all samples with <0.01%. C_1/C_{2+} ratios ranging between about 1,840 and 2,820 suggest that mainly microbial-mediated processes lead to generation of light hydrocarbons present in surface sediments of the Ordu Ridge patches.

Kerch Flare

Although gravity cores and pressure cores at seep sites in the Kerch Flare area were already recovered during M72/3 and MSM15/2, gas hydrates could have been recovered for the first time during MSM15/2. During M84/2, hydrates were collected at three GC stations (Table 24). In addition, three DAPC stations were performed.

Table 24: List of gas samples recovered from the Kerch Flare area during M84/2.

GeoB	Instrument	Hydrate-bound gas	Sedimentary gas	Headspace gas
15513-1	GC-34	5		
15516-1	GC-36	10		3
15518-1	GC-37	9		17
15519-1	GC-38			38
15513-2	DAPC-6		6	
15516-2	DAPC-7		6	
15518-2	DAPC-8		8	
15513-3	MIC-15			30
15516-3	MIC-16			28
15519-2	MIC-17			30
	Total	**24**	**20**	**146**

The gas samples contained 99.64 to 99.69 mol-% of methane, 0.25 to 0.31% of carbon dioxide, and 0.03 to 0.04% of ethane. Propane, *iso*-butane, and *n*-butane occurred only in traces (<0.01%), and *n*-pentane was only present in gas from pressure cores. Similar to observations during MSM15/2, enrichments in methane and depletions in ethane in hydrate-bound gas relative to sedimentary gas from pressure cores indicate preferential incorporation of methane into the hydrate phase, as already proposed for the Batumi seep area (Pape et al., 2010).

Helgoland MV

The Helgoland MV was studied in detail for the first time during MSM15/2, but hydrates could not be sampled during that cruise. Remarkably, during M84/2 massive, near-surface hydrates could be recovered during two GC stations (Table 25) performed close to a site, where a GC could be driven more than 60 m deep into the sediment in the course of deep penetration experiments conducted during MSM15/2 (GeoB14341). Hence, it might be speculated that near-surface hydrate formation in that area of the Helgoland MV preferentially took place in the time period from MSM15/2 (May 2010) to M84/2 (March 2011). With regard to considerable bubble texture of the hydrates with sized inclusions of free gas (see Fig. 82), they appeared to be relatively young in age. A DAPC station was conducted close to site GC-43 in order to determine the hydrate quantity.

Table 25: List of gas samples recovered from the Helgoland MV.

GeoB	Instrument	Hydrate-bound gas	Sedimentary gas	Headspace gas
15524-1	GC-40			30
15525-1	GC-41	31		
15525-3	GC-43	13		
15531	GC-45			30
15532	GC-46			30
15530	DAPC-10		23	
15524-2	MIC-18			31
15525-2	MIC-19			11
15525-4	MIC-20			24
15533-2	MIC-21			22
	Total	**44**	**23**	**178**

Gas from hydrates consisted of methane (99.66–99.67 mol-%), carbon dioxide (0.29–0.31%), ethane (0.03%) and traces of propane, while gas from pressure cores contained a slightly smaller portion of methane (99.31%), and a significantly higher amount of carbon dioxide (0.65%). Portions of ethane, propane, and *iso*-butane in sedimentary gas were similar to those in hydrate bound gas. *n*-butane and *n*-pentane (<0.01% each) were only observed in sedimentary gas. Similar to results for samples obtained during expedition MSM15/2, the resulting C_1/C_{2+} ratios (ca. 2,680–3,050) for all gas types suggest that the major proportion of light hydrocarbons originates from microbial generation.

Dvurechenskii MV

The gas hydrate system at the Dvurechenskii MV was already studied during cruises M52/1 and M72/3. During M84/2 a pressure coring station was performed at a site in the northwestern section of the DMV in order to expand the existing pressure core data set from M72/3 (Table 26).

Table 26: Number of gas samples obtained during degassing of a pressure core collected at Dvurechenskii MV.

GeoB	Instrument	Sedimentary gas
15526-1	DAPC-09	17
	Total	**17**

Similar to results obtained for pressure cores during cruise M72/3 in 2007 at Dvurechenskii MV the gas released from DAPC-9 consisted mainly of methane (99.56 mol-%), amended by carbon dioxide (0.38%) and ethane (0.06%). *iso*- and *n*-butane as well as *n*-pentane were found in traces (<0.01%). The C_1/C_{2+} ratios of gas released from this pressure core and previous cores taken during M72/3 at Dvurechenskii MV were slightly lower (ca. 1.730) than those determined for gas from the near-by Helgoland MV suggesting slightly higher proportions of thermogenic hydrocarbons.

12.2.3 Vertical Methane Concentration Profiles in Surface Sediments of the Batumi Seep Area

For determination of methane concentration profiles by use of the headspace technique sediment samples were extracted from gravity cores and mini cores. In the following results for the Batumi seep area are shown as an example. Backscatter anomalies at the Batumi seep area were previously attributed to the presence of near-surface authigenic carbonates and elevated gas concentrations (Klaucke et al., 2006) diagnostic for active seepage. In order to evaluate the relationship between backscatter intensity and methane concentrations, ten mini cores (MICs) were obtained from sites characterized by moderate to high seafloor backscatter signals. These stations were backed-up by a reference MIC station remote from the Batumi seep area and showing low backscatter intensity.

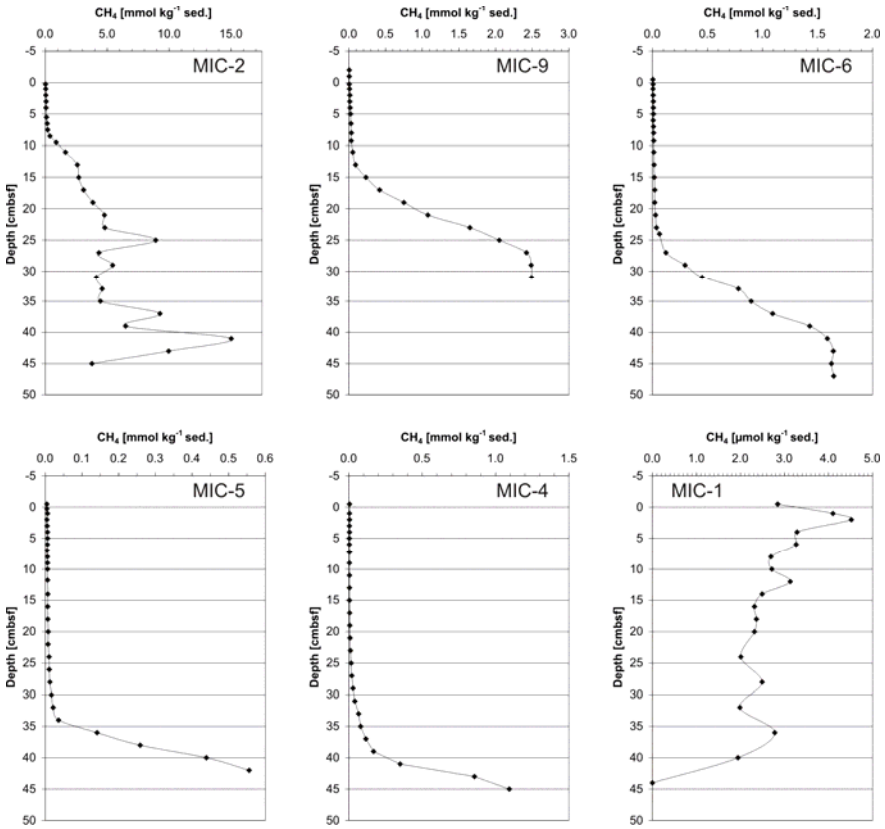

Fig. 97: Methane concentration profiles (in mmol kg^{-1} and µmol kg^{-1} wet sediment, respectively) in six mini cores collected at the Batumi seep area. Sampling sites represent areas of different seafloor backscatter intensity (upper left: high upward CH_4 fluxes, MIC-2; lower right: low upward flux, MIC 1 = background core). Like inorganic geochemical profiles discussed in Chapter 11 for the same mini cores, methane profiles precisely indicate the positioning of the SMTZ.

At the reference site (MIC-1), methane concentrations were comparably low (<5 µmol kg^{-1} wet sediment) and decreased slightly with depth (Fig. 97) indicating methane diffusion into the seabed from the bottom water.

For all other mini cores recovered from sediments characterized by moderate to high backscatter anomalies, a steep gradient with strongly increasing methane concentrations with depths were found. The upper limit of that gradient was located in depths between 8 and 38 cmbsf which points to considerable methane flux from below at those stations. Above the gradient, methane concentrations are reduced due to the anaerobic oxidation of methane. The shallowest gradient was found at station MIC-2 at 8 to 13 cmbsf and highest ex situ methane concentrations were 15 mmol kg^{-1} wet sediment (41 cmbsf). Such gradients could be followed towards depth in longer gravity cores taken at close-by stations.

13. References

Abegg F, Hohnberg HJ, Pape T, Bohrmann G and Freitag J (2008) Development and application of pressure-core-sampling systems for the investigation of gas- and gas-hydrate-bearing sediments. *Deep-Sea Research I: Oceanographic Research Papers* 55(11): 1590-1599.

Akhmetzhanov AM, Ivanov MK, Kenyon NH and Mazzini A (Editors), (2007) Deep-water cold seeps, sedimentary environments and ecosystems of the Black and Tyrrhenian Seas and the Gulf of Cadiz. *IOC Technical Series* No. 72. UNESCO, Paris, 99 pp.

Aloisi G, K Wallmann et al. (2004) Evidence for the submarine weathering of silicate minerals in Black Sea sediments: Possible implications for the marine Li and B cycles. *Geochemistry, Geophysics, Geosystems* 5(4).

Bahr A, Pape T, Abegg F, Bohrmann G, van Weering TCE, Ivanov MK (2010) Authigenic carbonates from the eastern Black Sea as an archive for shallow gas hydrate dynamics – Results from the combination of CT imaging with mineralogical and stable isotope analyses. *Marine and Petroleum Geology*, 27(9), 1819-1829.

Bohrmann G and cruise participants (2011) Report and preliminary results of R/V Maria S. Merian Cruise MSM 15/2, Istanbul (Turkey) - Piraeus (Greece), 10 May - 2 June 2010. Origin and structure of methane, gas hydrates and fluid flows in the Black Sea. Berichte, Fachbereich Geowissenschaften, Universität Bremen, No. 278, 130 pages, Bremen.

Bohrmann G, Pape T, and cruise participants (2007) Report and preliminary results of R/V Meteor cruise M72/3, Istanbul - Trabzon - Istanbul, 17 March - 23 April, 2007. Marine gas hydrates of the Eastern Black Sea. *In Berichte, Fachbereich Geowissenschaften, Universität Bremen,* No. 261, (ed. G. Bohrmann and T. Pape), pp. 176.

Caress DW, Chayes DN (2001) Improved Management of Large Swath Mapping Datasets in MB-System Version 5, Abstract OS11B-0373. *Eos Trans. Fall Meet. Suppl.,* 82(47).

Çifçi G, Dondurur D and Ergün M, (2003) Deep and shallow structures of large pockmarks in the Turkish shelf, Eastern Black Sea. *Geo-Marine Letters*, 23: 311-322.

De Beukelaer SM, MacDonald IR, Guinnasso NL and Murray A (2003) Distinct side-scan sonar, RADARSAT SAR, and acoustic profiler signitures of gas and oil seeps on the Gulf of Mexico slope. *Geo-Marine Letters*, 23: 177-186.

Feseker T, A Dählmann et al. (2009) In-situ sediment temperature measurements and geochemical porewater data suggest highly dynamic fluid flow at Isis mud volcano, eastern Mediterranean Sea. *Marine Geology* 261: 128-137.

Ginzburg AI, Kostianoy AG, Sheremet NA (2004) Seasonal and interannual variability of the Black Sea surface temperature as revealed from satellite data (1982–2000).

Grasshoff K, Ehrhard M, and Kremling K (1999) Methods of Seawater Analysis. Wiley-VCH, Weinheim.

Haeckel M, Reitz A, and Klaucke I, (2008) Methane budget of a large gas hydrate province offshore Georgia, Black Sea, *6th International Conference on Gas Hydrates* (ICGH 2008), Vancouver, Canada.

Haeckel M, Wallmann K, and Boudreau B P (2007) Bubble-induced porewater mixing: A 3-D model for deep porewater irrigation. *Geochimica et Cosmochimica Acta* 71, 5135-5154.

Heeschen KU, Hohnberg HJ, Haeckel M, Abegg F, Drews M, and Bohrmann G (2007) In situ hydrocarbon concentrations from pressurized cores in surface sediments, Northern Gulf of Mexico. *Marine Chemistry* 107(4), 498-515.

Heeschen KU, Haeckel M, Hohnberg HJ, Abegg F, Bohrmann G, (2007) Pressure coring at gas hydrate-bearing sites in the eastern Black Sea off Georgia. *Geophysical Research Abstracts,* 9, 03078.

Jones GA, Gagnon AR (1994) Radiocarbon chronology of Black Sea sediments. *Deep-Sea Research* 41, 531–557.

Klapp SA, Hemes S, Klein H, Bohrmann G, MacDonald I and Kuhs WF (2010) Grain size measurement of natural gas hydrates. *Marine Geology*, 274: 85-94.

Klaucke I, Sahling H, Bürk D, Weinrebe W and Bohrmann G (2005) Mapping deep-water gas emissions with sidescan sonar. *EOS Transactions*, 86(38): 341, 346.

Klaucke I, Sahling H, Weinrebe W, Blinova V, Bürk D, Lursmanashvili N and Bohrmann G (2006) Acoustic investigations of cold seeps offshore Georgia, eastern Black Sea. *Marine Geology*, 231(1-4): 51-67.

Krastel S, V Spiess et al. (2003) Acoustic investigations of mud volcanoes in the Sorokin Trough, Black Sea. *Geo-Marine Letters* 23: 230-238.

Kwiecien O, Arz HW, Lamy F, Wulf S, Bahr A, Röhl U and Haug GH (2008) Estimated reservoir ages of the Black Sea since the last glacial, *Radiocarbon* 50(1), 99–118.

Lamy F, Arz HW, Bond G, Bah, A and Pätzold J (2006) Multicentennial-scale hydrological changes in the Black Sea and northern Red Sea during the Holocene and the Arctic/North Atlantic Oscillation, *Paleoceanography 2*, PA1008.

Limonov AF, Woodside JM, Ivanov MK (1994) Mud volcanism in the Mediterranean and Black seas and shallow structure of the Eratosthenes Seamount. *UNESCO reports in marine science* 64, 173 pp.

Manheim FT and Schug DM (1978) Interstitial waters of Black Sea cores. In: Ross, DA and Neprochnov, YP Eds.), *Initial Report of the Deep Sea Drilling Project*. U.S. Government Printing Office, Washington.

Major CO., Goldstein SL, Ryan WBF, Lericolais G, Piotrowski AM, Hajdas I (2006) The co-evolution of Black Sea level and composition through the last deglaciation and its paleoclimatic significance. *Quaternary Science Reviews* 25, 2031-2047.

Minshull & Keddie (2010) Measuring the geotherm with gas hydrate bottom-simulating reflectors: a novel approach using three-dimensional seismic data from the Black Sea, *Terra Nova* 22, 131-136.

Neretin LN, Böttcher ME, Jørgensen BB, Volkov II, Lüschen H, Hilgenfeld K (2004) Pyritization processes and greigite formation in the advancing sulfidization front in the Upper Pleistocene sediments of the Black Sea. *Geochimica et Cosmochimica Acta* 68(9), 2081-2093.

Nikishin, AM, MV Korotaev et al. (2003) The Black Sea basin: tectonic history and Neogene-Quarternary rapid subsidence modelling. *Sedimentary Geology* 156: 149-168.

Nikolovska A, Sahling H and Bohrmann G (2008) Hydroacoustic methodology for detection, localization, and quantification of gas bubbles rising from the seafloor at gas seeps from the eastern Black Sea. *Geochemistry Geophysics Geosystems* 9 (10), Q10010, doi:10.1029/2008GC002118.

Oguz T, Latun VS, Latif MA, Vladimirov VV, Sur HI, Markov AA, Ozsoy E, Kotovshchikov BB, Eremeev VV, Unluata U (1993) Circulation in the surface and intermediate layers of the Black sea. *Deep-Sea Research* 40 (8), 1597– 1612.

Oguz T, Malanotte-Rizzoli P (1996) Seasonal variability of wind and thermohaline-driven circulation in the Black Sea: modeling studies. *J. Geophys. Res*. 101 (C7), 16551– 16569.

Pape T, Bahr A, Klapp SA, Abegg F, Bohrmann G (2011) High-intensity gas seepage causes rafting of shallow gas hydrates in the southeastern Black Sea. *Earth and Planetary Science Letters* 307, 35-46.

Pape T, Bahr A, Rethemeyer J, Kessler JD, Sahling H, Hinrichs K.U, Klapp SA, Reeburgh WS, Bohrmann G (2010b) Molecular and isotopic partitioning of low-molecular weight hydrocarbons during migration and gas hydrate precipitation in deposits of a high-flux seepage site. *Chemical Geology*, 269(3-4), 350-363.

Pape T, Kasten S, Zabel M, Bahr A, Abegg F, Hohnberg HJ, Bohrmann G (2010a) Gas hydrates in shallow deposits of the Amsterdam mud volcano, Anaximander Mountains, Northeastern Mediterranean Sea. *Geo-Marine Letters*, 30(3-4), 187-206.

Reilinger RE, SC McClusky et al. (1997) Global positioning system measurements of present-day crustal movements in the Arabia-Africa-Eurasia plate collision zone. *Journal of Geophysical Research* 102(B5): 9983- 9999.

Reitz A, Haeckel M, Wallmann K, Hensen C, and Heeschen K (2007) Origin of salt-enriched pore fluids in the northern Gulf of Mexico. *Earth and Planetary Science Letters* 259, 266-282.

Reitz A, Pape T, Haecke, M, Schmidt M, Berner U, Scholz F, Liebetrau V, Aloisi G, Weise SM, Wallmann K (2011) Sources of fluids and gases expelled at cold seeps offshore Georgia, eastern Black Sea. *Geochimica et Cosmochimica Acta,* 75(11), 3250-3268.

Robinson AG, Ed. (1997) Regional and Petroleum geology on the Black Sea and surrounding region, *American Association of Petroleum Geologists*.

Ross DA and ET Degens (1974) Recent sediments of Black Sea. The Black Sea – Geology, Chemistry and Biology. ET Degens and DA Ross. Tusla, USA, *American Association of Petroleum Geologists*: 183-199.

Sahling H, Blinova V, Bürk D, Cifci G, Corpur S, Dondurur D, Klaucke I, Lursmanashvili N, Okay S, Renken J and Schott T (2004) Report and preliminary results of R/V Poseidon cruise P317/4. 235, *Berichte, Fachbereich Geowissenschaften* No 235, Bremen.

Sahling H, Bohrmann G, Artemov YG, Bahr A, Brüning M, Klapp SA, Klaucke I, Kozlova E, Nikolovska A, Pape T, Reitz A and Wallmann K (2009) Vodyanitskii mud volcano, Sorokin Trough, Black Sea: Geological characterization and quantification of gas bubble streams. *Marine and Petroleum Geology,* 26(9): 1799-1811.

Seeberg-Elverfeldt J, Schlüter M, Feseker T and Kölling M (2005) Rhizon sampling of porewaters near the sediment-water interface of aquatic systems. *Limnology and Oceanography:* Methods 3, 361-371.

Sloan ED, Koh CA (2007) Clathrate hydrates of natural gases. *CRC Press*, Boca Raton.

Solomon EA, Kastner M, MacDonald IR and Leifer I (2009) Considerable methane fluxes to the atmosphere from hydrocarbon seeps in the Gulf of Mexico. Nature Geoscience, 2: 561-565.

Soulet G, Delaygue G, Vallet-Coulomb C, Böttcher M E, Sonzogni C, Lericolais G, and Bard E, (2010) Glacial hydrologic conditions in the Black Sea reconstructed using geochemical pore water profiles. *Earth and Planetary Science Letters* 296, 57-66.

Tolmazin D, (1985) Changing Coastal Oceanography of the Black Sea.

Tugolesov DA, AS Gorshkov et al. (1985). Tectonics of the Mesozoic Sediments of the Black Sea Basin. *Nedra, Moscow*.

Ulrick JU (1975) Principles of underwater acoustics. McGraw-Hill Book

Wagner-Friedrichs M (2007) Seafloor seepage in the Black Sea: Mud volcanoes, seeps and diapiric structures imaged by acoustic methods. *PhD Thesis, University of Bremen*, Bremen, 154 pp.

Appendix 1: Station List

					Time (UTC)			Begin / on seafloor			End / off seafloor			Recovery
Date	St.	Instrument	GeoB	Location/	Position	on	off	Latitude	Longitude	Water depth (m)	Latitude	Longitude	Water depth (m)	Remarks
2011	No.		St. No.		(S*, T*, P*)	Begin depth	depth End	N	E		N	E		
26.02.	135	SVP-1	15201	Rim of Eregli area	S	22:58 23:33	23:33 00:04	41°42.493	30°28.745	1837				SVP (-1600 m) for MBES calibration
27.02.	136	MB/PS-1	15202	Eregli area	S	00:58	13:30	41°42.666	30°29.219	1818	41°29.375	30°53.069	1095	Bathymetry and flare detection survey + setup of acoustic systems, duration 12h32m
27.02.	137	GC-1	15203	Eregli patch 1	S	14:36	15:03 15:16	15:42	41°28.536	30°51.649	1026			GC with T-logs (3/5) 34.6kN,strong H2S smell, no GH, 3.1 m core recovery
27.02.	138	GC-2	15204	Eregli patch 1	S	16:14	16:38 16:48	17:15	41°28.470	30°51.633	1022			GC with T-logs (3/4), no GH, 2.5 m core recovery
27.02.	139	MB/PS-2	15205	Eregli area	S	17:40	04:27	41°26.638	30°53.472	1186	41°32.590	30°52.480	1255	Flare & bathymetry survey; several new flares found, duration 10h47m
28.02.	140	SVP-2	15206	Eregli area	S	05:27	05:30 05:30	05:41	41°28.197	30°51.790	1010			SVP (-200 m) for MBES calibration
28.02.	141	MB/PS-3	15207	Eregli area	S	06:05	07:39	41°28.268	30°51.812	1010	41 °25.198	30°51.75	838	New bathymetry, old and some new flares found, duration 1h34m
28.02.	142	MeBo-63	15208	Eregli patch 1	P	08:28	22:17	41°27.365	30°51.142	975				Drill depth 8 m (1p-4P), 5.98 m core recovery
28.02.	143	MB/PS-4	15209	Eregli area	S	22:37	05:20	41°27.366	30°51.173	972	41°27.793	30°52.491	983	New flares on plateau west of Eregli 1 & 2, duration 6h43m
01.03.	144	AUV-39	15210	Eregli patch 1	S	05:30	12:50	41°27.598	30°52.382	982	41°27.599	30°52.382	984	Ground fault
01.03.	145	LDP-1	15211	Eregli area	S	9:40 10:14	10:43	41°28.075	30°52.392	996				Test deployment, no pressure core recovery
01.03.	146	AUV-40	15212	Eregli area	S	11:37	12:50	41°27.813	30°52.479	993	41°27.714	30°53.310	991	
01.03.	147	MB/PS-5	15213	Eregli area	S	13:05	18:37	41°27.910	30°52.793	989	41°44.925	31°27.022	1924	Bathymetry and flare survey during transit, duration 5h32m
02.03.	148	SVP-3	15214	Samsun area	S	14:52 15:06	15:07 15:22	42°04.434	36°28.051	1079				SPV (-400 m) for MBES calibration
02.03.	149	MB/PS-6	15215	Samsun area	S	15:30	16:46	42°04.498	36°28.152	1081	42°03.112	36°40.982	385	duration 1h16m
02.03.	150	GC-3	15216	Samsun area	S	17:00 17:13	17:13 17:28	42°03.000	36°41.192	388				397 m rope, 34.2 kn, reg. core liner, 576 cm recovery, penetrated to deep
02.03.	151	MB/PS-7	15217	Samsun area	S	17:36	07:55	42°02.978	36°41.278	404	42°00.518	37°47.562	1981	Bathymetric mapping & flare detection, duration 14h19m
03.03.	152	SVP-4	15218	Georgia	S	18:58 18:35	18:35 20:12	42°03.211	40°22.153	1804				SVP (-1795) for MBES calibration
03.03.	153	MB/PS-8	15219	Georgia	S	20:36	03:28	42°03.176	40°22.379	1807	41°57.818	41°18.210	874	Bathymetry and flare survey, many flares detected, duration 6h52m
04.03.	154	GC-4	15220-1	Batumi seep reference	S	04:16 04:37	04:38 05:02	41°57.144	41°16.851	879				32.4 kN 540 cm core recovery
04.03.	155	LDP-2	15220-2	Batumi seep reference	S	05:23 05:44	05:44 07:45	41°57.145	41°16.851	878				16.1 kN, 100 % core recovery but no pressure, due to flap failure
04.03.	156	MeBo-64	15220-3	Batumi seep reference	P	06:41	10:23	41°57.174	41°16.850	878				Mission aborded due to failure of pressure sensor
04.03.	157	MIC-1	15220-4	Batumi seep reference	S	10:40 11:04	11:05 10:24	41°57.155	41°16.874	878				4 cores, well preserved, undisturbed surface
04.03.	158	MB/PS-9	15221	Batumi seep	S	11:25	14:00	41°57.178	41°16.868	881	41°57.075	41°18.508	896	Best settings of EM122 & 710 for flares surveys found, duration 2h35m
04.03.	159	MeBo-65	15220-5	Batumi seep reference	P	14:46	08:01	41°57.171	41°16.853	878				drill depth 14.15 m (1P-6P), 10.9 m core recovery
05.03.	160	AUV-41	15222	Batumi seep	S	08:57	10:15	41°57.587	41°17.920	854	41°57.776	41°17.837	860	Mission aborded
05.03.	161	MB/PS-10	15223	Poti seep	S	10:29	12:58	41°57.759	41°17.698	842	41°57.698	41°18.277	847	Flares at and around Poti seep mapped, duration 2h29m
05.03.	162	AUV-42	15224	Batumi seep	S	13:16	13:21	41°57.570	41°17.910	859	41°57.570	41°17.910	859	Mission canceld
05.03.	163	MB/PS-11	15225	Adjara, Pec, Col	S	14:34	04:08	41°56.038	41°21.801	1071	41°58.628	41°07.572	1285	Flares found at known locations and OSO cluster, duration 13h34m
06.03.	164	GC-5	15226	Pechori mound	S	04:48 05:15	05:15 05:44	41°58.780	41°07.591	936				34.1 kN, 5 m core recovery
06.03.	165	MeBo-66	15227-1	Pechori mound	P	06:50	13:18	41°58.963	41°07.595	1025				2 GeoB No. 15227-1 & 15226-2, drill depth, **core recovery**
06.03.	166	MB/PS-12	15228	Georgia	S	13:36	17:48	41°58.939	41°07.589	1024	41°58.589	41°07.541	1130	Bathymetry gaps filled west of Adjara ridge, flares found 10nm SW of Colkheti, duration 4h12m
06.03.	167	SVP-5	15227-2	Pechori mound	S	18:07 18:16	18:16 18:24	41°59.000	41°07.532	1031	41°59.000	41°07.541	1127	
06.03.	168	MeBo-67	15227-3	Pechori mound	P	18:33	08:34	41°58.985	41°07.590	1027				Drill depth 19.1 m (1P+2R-3R), **core recovery**
07.03.	169	LDP-3	15227-4	Pechori mound	S	08:59 09:19	09:26 09:54	41°58.981	41°07.541	1026				
07.03.	170	MB/PS-13	15229	Georgia	S	09:53	15:20	41°58.981	41°07.541	1026	42°06.977	41°23.491	713	Bathymetry gaps filled, duration 5h27m
07.03.	171	SVP-6	15230	Kulevi ridge	S	15:22 15:32	15:32 15:42	42°07.000	41°23.46	713				
07.03.	172	MB/PS-14	15231	Kulevi ridge	S	15:48	02:48	42°07.029	41°23.398	721	42°05.283	41°08.971	1087	Sites of intensive seepage found, gaps in bathymetry filled, duration 11h
08.03.	173	AUV-43	15224-2	Batumi seep	S	04:06	05:29	41°57.361	41°18.018	838	42°57.561	41°17.919	862	
08.03.	174	MB/PS-15	15232	Kobuleti Ridge	S	06:20	08:23	41°55.892	41°16.75	951	41°55.969	41°17.987	1055	Flare and bathymetry survey, duration 2h3m
08.03.	175	AUV-44	15224-3	Batumi seep	S	08:42	09:22	41°57.570	41°17.831	863	41°57.570	41°17.838	841	

Appendix 1: Continuation Station List

						Time (UTC)			Begin / on seafloor			End / off seafloor			Recovery
Date	St.	Instrument	GeoB	Location/	Position	on	off		Latitude	Longitude	Water depth (m)	Latitude	Longitude	Water depth (m)	
2011	No.		St. No.		(S*, T*, P*)	Begin	depth	depth	End	N	E	N	E		Remarks
08.03.	176	MB/PS-16	15233	Kobuleti Ridge	S	09:45			11:25	41°58.561	41°16.122	991	41°57.791	41°18.071	1356	Bathymetry survey to complete backscatter data, duration 1h40m
08.03.	177	AUV-45	15224-4	Batumi seep	S	11:35			12:49	41°57.597	41°17.881	860	41°57.678	41°17.809	862	
08.03.	178	MB/PS-17	15234	Georgia	S	12:55			03:44	41°57.680	41°17.809	862	41°52.290	41°17.321	883	Bathymetry in SE part of research area completed, new flare sites found, duration 14h49m
09.03.	179	GC-6	15235-1	Adjara Ridge	S	04:00	04:23	04:23	04:46	41°52.278	41°17.273	880				34.59 kN, 250 cm recovery, no GH, oil impregnated below sapropel
09.03.	180	LDP-4	15235-2	Adjara Ridge	S	05:02	05:25	05:25	05:54	41°52.278	41°17.273	878				15.64 kN, 100 % recoverey but no pressure core due to flap failure
09.03.	181	MB/PS-18	15238	Adjara Ridge	S	06:05			07:08	41°52.440	41°17.500	880	41°52.341	41°17.173	892	Flare survey, GeoB no. 15238 due to inconsistencies station labeling!, duration 1h2m
09.03.	182	GC-7	15236-1	Batumi seep	T	08:05	08:51	08:52	09:10	41°57.580	41°17.411	838				34 kN, GH at 195 cm, 225 cm core recovery
09.03.	183	AUV-46	15224-5	Batumi seep	S	09:19			11:11	41°57.880	41°17.411	837	41°5.510	41°18.10	842	3 x 53 cm core, 4.3 kN, Posidonia position
09.03.	184	MIC-2	15237	Batumi seep	T	11:42	12:27		12:46	41°57.489	41°17.462	840				
09.03.	185	MeBo-68	15236-2	Batumi seep	P	14:30			11:08	41°57.590	41°17.350	838	41°57.578	41°57.371	839	1-2P & 3-5 R, failure of hydralic pump, Posidonia
10.03.	186	AUV-47	15224-6	Batumi seep	S	11:53			13:04	41°57.541	41°17.112	837	41°57.420	41°17.371	841	ground fault
10.03.	187	MIC-3	15239-1	Batumi seep	S	14:10	14:36	14:37	14:56	41°57.520	41°17.500	840				3 cores have not released, 5.36 kN
10.03.	188	MIC-4	15239-2	Batumi seep	P	15:10	15:49	15:51	16:00	41°57.520	41°17.500	840				3 cores 50 cm, 1 core 30cm, 4.14 kN
10.03.	189	MB/PS-19	15240	Adjara & Kobuleti Rdg.	S	16:05			06:00	41°57.294	41°17.771	841	41°57.530	41°17.320	832	Flare and bathymetry survey, new sites of intensive seepage found, duration 13h54m
11.03.	190	MIC-5	15241-1	Batumi seep	P	06:10	06:32	06:32	06:53	41°57.462	41°17.182	848				
11.03.	191	GC-8	15241-2	Batumi seep	P	07:05	07:33	07:56	07:55	41°57.466	41°17.182	840				Carbonates at top and no GH, plastic bag
11.03.	192	MIC-6	15242	Batumi seep	T	08:25	08:44	08:45	09:04	41°57.550	41°17.230	840				1 liner lost, close to target position
11.03.	193	GC-9	15243	Poti seep	T	09:43	10:02	10:03	10:22	41°57.907	41°18.270	875				GH, plastic bag
11.03.	194	GC-10	15244-1	Poti seep	T	10:45	11:03	11:04	11:20	41°57.879	41°18.346	868				no rcovery
11.03.	195	GC-11	15244-2	Poti seep	T	11:34	11:50	11:51	12:08	41°57.879	41°18.346	868				140 cm core recovery, massive GH at bottom, 1.2 m/s
11.03.	196	SVP-7	15245	Pechori mound	S	12:20	12:25	12:25	12:29	41°57.880	41°18.330	868				100 m
11.03.	197	MB/PS-20	15246	SW Georgia	S	12:33			08:47	41°57.880	41°18.330	868	41°58.050	41°18.060	900	Bathymetry completed, few new flares found, old flares verified, duration 20h14m
12.03.	198	MIC-7	15247-1	Batumi seep	P	09:02	09:26	09:26	09:45	41°57.565	41°17.089	840				4 cores 30-48 cm, 4.69 kN
12.03.	199	GC-12	15247-2	Batumi seep	P	10:02	10:19	10:23	10:45	41°57.570	41°17.102	842				plastic bag, 32.1 kN, GH in cc and lower 10cm, GH flakes dispersed
12.03.	200	AUV-48	15224-7	Batumi	S	11:40			12:30	41°57.498	41°18.052	843	41°57.509	41°18.052	842	Pressure sensor failure
12.03.	201	GC-13	15244-3	Poti seep	T	14:50	15:13	15:13	15:36	41°57.876	41°18.329	876				197 core recovery, liner, 29.74 kN, GH layer at bottom and cc preserved in liquid N
12.03.	202	GC-14	15248	Poti seep background	S	16:00	16:23	16:23	16:48	41°58.049	41°18.451	907				574 cm core recovery, liner, 38.07 kN
12.03.	203	GC-15	15249-1	Batumi seep	P	17:25	17:53	17:53	18:17	41°57.605	41°17.260	842				GH at bottom (sparse), 27.1 kN, Target position: 41°57.605N 41°17.259E
12.03.	204	MB/PS-21	15250	Batumi & Colkheti	S	18:24			03:42	41°57.600	41°17.210	839	41°57.620	41°16.960	844	Flare monitoring at Batumi and Colkheti seep, duration 9h18m
13.03.	205	MIC-8	15249-2	Batumi seep	P	04:02	04:30	04:31	04:50	41°57.608	41°17.264	840				5.12 kN
13.03.	206	DAPC-1	15244-4	Poti seep	S	05:35	05:57	06:07	06:27	41°57.871	41°18.312	870				100 bar pressure
13.03.	207	GC-16	15251-1	Batumi seep	P	07:12	07:35	07:45	08:07	41°57.632	41°17.079	842				2 GH preserved in liquid N (from cc & 110 cm), with T-logs (4/4), 30 kN
13.03.	208	MIC-9	15251-2	Batumi seep	P	08:14	08:39	08:40	09:00	41°57.632	41°17.075	842				
13.03.	209	GC-17	15252	Batumi seep	T	09:25	09:47	09:58	10:15	41°57.538	41°17.433	839				T-logs (4/4), 80 cm core recovery, GH in cc and dispersed chips, 30.3 kN
13.03.	210	MIC-10	15253	Batumi seep	P	10:45	11:08	11:09	11:34	41°57.469	41°17.270	847				3 liners full, 1 empty, 4.3 kN
13.03.	211	GC-18	15227-5	Pechori mound	P	12:23	12:52	13:03	13:27	41°58.985	41°07.588	1015				T-logs (4/4), oily sediments, no GH, ~ 1.7 m penetration (by sediments outside), ~ 1 m recovery, liner, 35.5 kN
13.03.	212	GC-19	15254	Pechori mound reference	T	13:55	14:20	14:31	14:58	41°58.800	41°07.872	1085				T-logs (4/4), liner, over penetration, 43.89
13.03.	213	GC-20	15255	Pechori mound	T	15:33	16:04	16:14	16:38	41°58.893	41°07.607	1010				Plastic bag, GH in core and floating on sea surface, oil rich sediments, 70 cm, 26.2 kN
13.03.	214	GC-21	15256	Pechori mound	T	16:55	17:21	17:28	17:52	41°58.938	41°07.518	1025				
13.03.	215	MB/PS-22	15257	Kobuleti & Kulevi ridge	S	18:14			06:45	41°58.470	41°05.900	1224	42°08.290	41°23.210	890	Bathymetry and flare survey, mapping of temporal variability of seepage at Colkheti, PARASOUND failure, duration 12h31m

Appendix 1: Continuation Station List

						Time (UTC)			Begin / on seafloor			End / off seafloor			Recovery	
Date	St.	Instrument	GeoB	Location/	Position	on	off		Latitude	Longitude	Water	Latitude	Longitude	Water		
2011	No.		St. No.		(S*, T*, P*)	Begin	depth	depth	End	N	E	depth (m)	N	E	depth (m)	Remarks
14.03.	216	GC-22	15258	G2 Kulevi ridge	T	07:07	07:34	07:34	07:53	42°07.104	41°22.753	712				Maybe GH in cc, 130 cm recovery, oil stained sediments, liner, 30.68 kN
14.03.	217	GC-23	15259	G1 Kulevi ridge	T	09:03	09:27	09:28	09:55	42°05.753	41°08.449	1121				Layers and lamination, signs of slumping, no GH, sandy dry material, 31.8 kN
14.03.	218	GC-24	15260-1	Batumi seep	P	11:07	11:29	11:29	12:00	41°57.580	41°17.392	839				T-logs (4/4), plastic foil, dispersed GH, 31.81 kN, 240 cm core recovery
14.03.	219	MIC-11	15260-2	Batumi seep	P	12:05	12:35	12:35	12:54	41°57.583	41°17.398	839				
14.03.	220	GC-25	15261	Colkheti seep	T	13:58	14:23	14:33	15:12	41°58.082	41°06.154	1123				T-logs (3/4), liner, oily sediements, no GH, 39.01 kN
14.03.	221	DAPC-2	15244-5	Poti seep	P	16:20	16:43	16:43	17:00	41°57.874	41°18.331	868				
14.03.	222	MB/PS-23	15262	Transit towards Samsun	S	17:30			04:26	41°57.897	41°18.191	870	42°14.990	39°37.910	1970	Bathymetry survey in western research area on transit towards Samsun (Turkey), break of profile 01:49 to 02:16 to forced course change outside research area (collision course with Battery failed, no successful station.
15.03.	223	SVP-8	15263	Samsun	S	11:23	11:32	11:38	41°50.402	37°57.184	2039					
15.03.	224	MB/PS-24	15264	Samsun	S	12:05		14:26	41°50.403	37°57.184	2040	41°38.723	37°33.042	1662	duration 2h21m	
15.03.	225	SVP-9	15265	Samsun	S	14:28	14:39	14:48	41°38.718	37°33.058	1666					
15.03.	226	MB/PS-25	15266	Ordu ridge	S	14:50		05:40	41°38.718	37°33.058	1655	41°23.316	37°37.069	1286	duration 14h50m	
16.03.	227	GC-26	15267	Ordu ridge patch#18	T	6:16	6:41	6:41	6:08	41°24.221	37°35.270	1254				74 cm core recovery, lower section archived, section 2 dumped, 33.3 kN, no GH but bubbles rising
16.03.	228	GC-27	15268-2	Ordu ridge patch#02	T	9:47	10:19	10:19	11:04	41°32.670	37°37.460	1535				150 bar, no gas, 32.5 kN
16.03.	229	DAPC-3	15268-1	Ordu ridge patch#02	P	8:19	8.51	9:30	9:53	41°32.661	37°37.449	1534				GH in liquid N, liner,
16.03.	230	MB/PS-26	15269	Transit towards Trabzon	S	11:07			22:27	41°32.659	37°37.458	1535	41°18.058	38°19.887	1853	Bathymetry survey, duration 11h20m
19.03.	231	SVP-10	15501	Samsun	T	12:50	12:53	12:53	13:10	41°18.169	38°19.867	1854				
19.03.	232	MB/PS-27	15502	Samsun	S	13:26			06:18	41°18.180	38°19.760	1854	41°33.180	37°37.580	1573	duration 16h52m
20.03.	233	MIC-12	15268-3	Ordu ridge patch#02	P	06:36	07:10	07:13	07:48	41°32.670	37°37.460	1537				Rope tension 7.5 kN, 4 liners full
20.03.	234	DAPC-4	15268-4	Ordu ridge patch#02	T	07:51	08:31	09:11	09:34	41°32.670	37°37.440	1536				150 bar, no core due to technical failure, empty autoclave
20.03.	235	GC-28	15503-1	Ordu ridge patch#03	T	9:37	10:32	10:33	11:02	41°32.443	37°36.888	1522				1.2 m/s into sediment, 38.2 kN = max. rope tension, wrong position initially given, moved 370 m to the correct location, GH in core catcher and lowermost core segment
20.03.	236	LDP-5	15503-2	Ordu ridge patch#03	T	11:19	11:57	11:57	12:40	41°32.440	37°36.890	1521				?
20.03.	237	GC-29	15504	Ordu ridge patch#05	T	12:53	13:22	13:22	13:55	41°31.843	37°36.496	1509				without F. logger, 1.0 m/s into the sediment, 33.1 kN rope tension, Banana
20.03.	238	GC-30	15505-1	Ordu ridge patch#07	T	14:56	15:27	15:27	16:03	41°31.160	37°37.338	1493				1.2 m/s into sediment, without T-logger, 33.5 kN rope tension
20.03.	239	MB/PS-28	15506	Ordu ridge	S	16:10			06:54	41°31.160	37°37.340	1494	41°27.180	37°39.600	1567	duration 14h44m
21.03.	240	MIC-13	15503-3	Ordu ridge patch#03	P	07.45	08:17	08:20	08:52	41°32.416	37°36.867	1518				0.5 m/s into sediment, 7.9 kN rope tension, 3 cores full, 1 empy (lost)
21.03.	241	DAPC-5	15268-5	Ordu ridge patch#02	T	09:13	09:48	10:31	10:51	41°32.670	37°37.460	1536				?
21.03.	242	MIC-14	15505-2	Ordu ridge patch#07	P	11:15	11:43	11:45	12:16	41°31.164	37°37.352	1499				0.5 m/s into sediment, 6.9 kN rope tension, 4 cores
21.03.	243	GC-31	15507	Ordu ridge patch#07	T	12:24	12:59	12:59	13:31	41°31.138	37°37.347	1505				without T-logger, into sediment 1.2 m/s, max. rope tension 18.2 kN, GH
21.03.	244	GC-32	15508	Ordu ridge	T	14:54	15:31	15:31	16:18	41°22.850	37°48.160	1526				1.2 m/s into sediment, rope tension 31.2 kN
21.03.	245	SVP-11	15509	Samsun	T	16:40	16:49	16:58	17:06	41°22.850	37°48.170	1528				
21.03.	246	MB/PS-29	15510	Samsun	S	17:39			07:22	41°22.050	37°45.440	1683	42°29.660	37°14.470	2095	duration 13h43m
22.03.	247	MB/PS-30	15511	Ukraine	S	19:08			11:25	43°24.950	36°25.230	2160	44°37.440	35°42.350	998	duration 16h17m
23.03.	248	GC-33	15512-1	Kerch Flare	P	11:34	11:54	12:05	12:35	44°37.420	35°42.359	906				30 kN rope tension, no hydrates, T-logger
23.03.	249	GC-34	15513-1	Kerch Flare	P	12:52	13:16	13:26	13:49	44°37.386	35°42.164	878				T-logger, 10' in sediment, 1.2 m/s in sediment, 39.9 kN, GH finally disperse
23.03.	250	DAPC-6	15513-2	Kerch Flare	T	?	?	?	?	44°37.386	35°42.164	878				?
23.03.	251	MIC-15	15513-3	Kerch Flare	T	15:26	15:28	15:55	16:16	44°37.386	35°42.164	878				Penetrated in sediment at 882 m rope length, 4.77 kN
23.03.	252	SVP-12	15514	Kerch Flare	T	16:20	16:26	16:37	16:44	44°37.380	35°42.160	880				
23.03.	253	MB/PS-31	15515	Kerch Flare	S	17:08			10:16	44°36.840	35°42.090	929	44°36.810	35°42.020	928	duration 17h8m
24.03.	254	GC-35	15512-2	Kerch Flare	P	10:35	10:55	10:57	11:18	44°37.419	35°42.359	894				3m core barrel, 1.2 m/s in sediment, 29.9 kN rope tension, 1.5m sediment, but not at the base
24.03.	255	LDP-6	15512-3	Kerch Flare	T	11:25	11:46	11:46	12:10	44°37.419	35°42.357	895				?
24.03.	256	GC-36	15516-1	Kerch Flare	T	12:30	12:54	13:04	13:28	44°37.230	35°42.282	889				T-logger, 10' in sediment, 1.2 m/s in sediment, 38 kN rope tension, GH
24.03.	257	DAPC-7	15516-2	Kerch Flare	T	13:39	14:05	14:05	14:34	44°37.230	35°42.282	889				
24.03.	258	MIC-16	15516-3	Kerch Flare	P	14:54	15:10	15:39	15:02	44°37.243	35°42.286	888				5.43 kN rope tension, 4 liners full
24.03.	259	MB/PS-32	15517	Kerch Flare	S	16:05			11:11	44°37.010	35°42.590	910	44°37.340	35°43.130	952	duration 19h7m
25.03.	260	GC-37	15518-1	Kerch Flare	T		11:47	11:57	12:15	44°37.182	35°42.279	887				10' in sediment, 30 kN rope tensionm CC with GH (disperse, very fine)

Appendix 1: Continuation Station List

Date	St.	Instrument	GeoB	Location/	Position	Time (UTC)			Begin / on seafloor			End / off seafloor			Recovery	
						on	off		Latitude	Longitude	Water depth (m)	Latitude	Longitude	Water depth (m)		
2011	No.		St. No.		(S*, T*, P*)	Begin	depth	depth	End	N	E		N	E		Remarks
25.03.	261	GC-38	15519-1	Kerch Flare	T	12:41	12:58	13:01	13:11	44°37.171	35°41.763	896				10' in sediment, slacking into sediment 0.8 m/s, 38 kN rope tension
25.03.	262	GC-39	15520	Kerch Flare	T		14:32	14:34	14:44	44°37.166	35°42.261	890				1.2 into sediment, 10' in sediment, 29 kN rope tension, no GH
25.03.	263	DAPC-8	15518-2	Kerch Flare	T	15:24	15:46	15:47	16:22	44°37.180	35°42.270	885				
25.03.	264	MIC-17	15519-2	Kerch Flare	P	16:52	17:29	17:47	17:55	44°37.105	35°41.759	896				0.5 m/s into sediment, 4.5 kN rope tension
25.03.	265	MB/PS-33	15521	Kerch Flare	S	18:00			11:06	44°37.180	35°41.820	891	44°36.080	34°52.940	1542	duration 17h6m
26.03.	266	SVP-13	15522	Kerch Flare	T	11:10	11:17	11:25	11:33	44°36.100	34°53.200	1522				
26.03.	267	MB/PS-34	15523	Kerch Flare	S	11:53			05:13	44°35.770	34°52.280	1543	44°28.480	34°3.370	1995	duration 17h20m
27.03.	268	GC-40	15524-1	Helgoland MV	T	05:46	06:39	06:49	07:41	44°17.322	35°0.065	2082				0.3 m/s into sediment, 10' T-logging, 50.3 kN (!) rope tension
27.03.	269	MIC-18	15524-2	Helgoland MV	P	07:47	07:52	08:34	09:18	44°17.329	35°0.081	2080				9.4 kN rope tension, 1 core good with bottom water, 3 cores with ~1cm water over sediment
27.03.	270	GC-41	15525-1	Helgoland MV	T	09:38	10:19	10:44	11:56	44°17.311	35°0.037	2088				deep penetration, T-logger, UTC: 10:19 - first down, 10' in sediment, 39.67 kN; 10:31 - heaving to 1980m, moving ship 20m to SW; 10:44 - second down, 10' in sediment, 33.7 kN, out
27.03.	271	DAPC-9	15526-1	Dvurechenskii MV	T	12:29	13:15	13:15	14:18	44°16.970	34°58.670	2054				
27.03.	272	GC-42	15527	Dvurechenskii MV	T	14:25	14:42	15:29	18:16	44°17.041	34°58.891	2051				deep penetration, t-logger, 15:29 - the deepest penetration; 36.6 kN last max. rope tension, slacking into sediment with 1.2 m/s, heaving 0.2 m/s, lowering was done in 35 to 70 mbsf
27.03.	273	MB/PS-35	15528	Kerch Fan	S	18:31			02:40	44°17.054	34°58.898	2060	44°17.110	35°0.280	2081	duration 32h9m
29.03.	274	LDP-7	15529	Dvurechenskii MV	T	03:10	03:54	03:55	04:48	44°16.950	34°58.670	2054				
29.03.	275	MIC-19	15525-2	Helgoland MV	P	05:10	05:17	06:03	07:00	44°17.311	35°0.037	2088				0.4 m/s into sediment, 2075m rope length: rope tension release, 8.9 kN rope tension, 4 liners full without bottom water, sediment very liquid, extr. Gas rich, 1 core completly lost during retrieval, 2 cores 1/2 full lost, 1 core 3/4 fulll lost
29.03.	276	GC-43	15525-3	Helgoland MV	T	07:09	07:49	08:01	08:54	44°17.311	35°0.037	2088				rope tension release at ~2070m, water depth not correct because of very soft sediment, 10' in sediment, 35.6 kN rope tension, no sediment retrieved, gas hydrate in cc
29.03.	277	MIC-20	15525-4	Helgoland MV	P	08:58	09:05	09:46	10:28	44°17.311	35°0.037	2088				same location as MIC-19, 0.4 m/s into sediment, 9 kN rope tension, 4 cores 30-45 cm recovery
29.03.	278	DAPC-10	15530	Helgoland MV	T	10:38	11:21	11:21	12:14	44°17.300	35°0.040	2080				
29.03.	279	GC-44	15531	Helgoland MV	T	12:33	13:18	13:36	15:24	44°17.304	35°0.042	2079				deep penetration, T-logger, 2099 rope length, empty liner, 34.9 kN max. rope tension
29.03.	280	GC-45	15532	Helgoland MV	T	16:02	16:48	16:59	17:50	44°17.295	35°0.044	2079				T-logger, 10' in sediment, 1.2 m/s into sediment, 44.1 kN rope tension, 2115m rope length
29.03.	281	GC-46	15533-1	DMV-HMV Background	T	18:20	19:03	19:14	20:00	44°18.166	34°59.162	2054				background, T-logger, 0.8 m/s into sediment, 10'in sediment, 43.6 kN rope tension
29.03.	282	MIC-21	15533-2	DMV-HMV Background	P	20:04	20:06	20:51	21:34	44°18.166	34°59.162	2054				background, 0.5 m/s into sediment, 8.8 kN rope tension, 4 liners full with ~30cm
29.03.	283	LDP-8	15533-3	MV west of DMV	T	21:58	22:43	22:45	23:30	44°18.166	34°59.162	2054				
29.03.	284	MB/PS-36	15534	DMV + HMV	S	23:43			13:00	44°17.220	34°58.590	2074	43°17.530	33°7.920	2171	duration 13h17m
30.03.	285	SVP-14	15535	Eregli	T	22:52	23:02	23:02	23:10	42°9.560	31°19.500	2147				
30.03.	286	MB/PS-37	15536	Eregli	S	23:28			07:37	42°9.580	31°19.600	2148	41°41.980	30°29.650	1793	duration 32h5m

AUV Autonomous Underwater Vehicle
DAPC Dynamic Autoclave Piston Corer
GC Gravity Corer
LDP Lotvariante des Druckprobennehmers (Pressure Piston Corer)
MB/PS MultiBeam/ PARASOUND survey
MeBo Meeresboden Bohrgerät (Seafloor drill rig)
MIC Mini Corer
SVP Sound Velocity Profile

* P = POSIDONIA S = ship position T = target position

Appendix 2: Gravity Corer and Mini Corer Deployments during M84/2b

Station Number M84/2	Area	Equipped with	T-logger	OBJECTIVES Technical description	Sediment recovery
GC-1 Stat. 137 GeoB 15203	Eregli 1 Turkey	Plastic foil Core catcher –lids 5 T-Logger	Logger 1-5 (SN 1854330, 1854333, 1854335, 1854336, 1854339) Only 1 logger in sediment: ~ 0.068 °C/m	*Sediment reconnaissance* Lowering with 1 m/s, T-Logger SN 1854333 no recording, logger SN 1854339 lost, too much wire out, no sediments at outside of barrel, Without Posidonia	Core length about 3.1 m, strong sulphide smell, gas-rich, only Unit I, no sign for gas hydrates, no sample taken, no porewater taken, sediment described and dumped
GC-2 Stat. 138 GeoB 15204	Eregli 1 Turkey	Plastic foil Core catcher –lids 4 T-Logger	Logger 1-5 (SN 1854330, 1854333, 1854335, 1854336) Only 1 logger in sediment: ~ 0.10 °C/m	*Sediment reconnaissance* Lowering with 1 m/s, T-Logger SN 1854336 nearly lost, too much wire out, no sediments at outside of barrel, without Posidonia	Core length about 2.5 m, strong sulphide smell, gas-rich, only Unit I, no sign for gas hydrates, no sample taken, no porewater taken, sediment described and dumped
GC-3 Stat. 150 GeoB 15216	Archangelsky Ridge, Working Area Sinop, Turkey	Plastic liner core catcher-lamella	Without T-Logger	*Sediment reconnaissance for planned MeBo drilling* Lowered with 1 m/sec. Penetration too deep, sediment on and in weight without Posidonia	5.76 m sediment recovery. Porewater taken, sediments described and archived.
GC-4 Stat. 154 GeoB 15220-1	Reference south of Batumi Seep, Georgia	Plastic liner, core catcher-lamella	Without T-Logger	*Complementary to MeBo GeoB 15220-3* Lowered with 0.5 m/sec, good penetration, without Posidonia	4.83 m sediment recovery. Porewater taken, sediments described and archived.
MIC-1 Stat. 157 GeoB 15220-4	Reference south of Batumi Seep, Georgia	4 cores		*Complementary to MeBo GeoB 15220-5* Lowered with 0.6 m/sec, Good penetration, undisturbed surface with overlaying bottom water	All 4 cores ~50 cm filled, porewater and methane samples taken. Sediments preserved for biomarker studies. Sediments described.
GC-5 Stat. 164 GeoB 15226	Pechori Mound	Plastic liner, core catcher-lamella.	Without T-Logger	*Sediment reconnaissance* Lowered with 1 m/sec, good penetration, without Posidonia	487 cm sediments, no gas hydrates, oil impregnated in lower part, porewater and methane samples taken. Sediments described and archived.
GC-6 Stat. 179 GeoB 15235-1	Adjara Ridge, Flare Cluster 3	Plastic foil, core catcher-lamella	Without T-Logger	*Sediment reconnaissance* Deployed at high backscatter patch in EM 122. Lowered with 1 m/sec, gas emission and oil drops were released when core was close to the sea surface.	~250 cm sediments, no gas hydrates, oil impregnated sediments below sapropel, sediment described and dumped.
MIC-2 Stat. 184 GeoB 15237	Batumi Seep, Georgia	4 cores		*Geochemical flux study* Lowered with 0.6 m/sec, good penetration, undisturbed surface with overlaying bottom water, Posidonia did not work, but close to target position 41°57.498'N, 41°17.462'E	3 cores ~53 cm filled, degassing of lower sediments, porewater and methane samples taken. Sediments preserved for biomarker studies. Sediments described.
GC-7 Stat. 181 GeoB 15236-1	Batumi Seep, Georgia	Plastic foil, core catcher-lamella	Without T-Logger	*Complementary to MeBo GeoB 15236-2* Lowered with 1 m/sec, good penetration	~ 225 cm sediment recovery, gas hydrate pieces, sediment described and dumped.
MIC- 3 Stat. 187 GeoB 15239-1	Batumi Seep, Georgia	3 cores		*Geochemical flux study* Lowered with 0.4 cm/s, not released, maybe too slowly lowered or not enough cable paid out, Posidonia did not work but close to target position 41°57.520'N, 41°17.500'E	Empty.

Station Number M84/2	Area	Equipped with	T-logger	OBJECTIVES Technical description	Sediment recovery
MIC-4 Stat. 188 GeoB 15239-2	Batumi Seep, Georgia	3 cores		*Geochemical flux study* Lowered with 0.5 cm/s, good penetration, undisturbed surface with overlaying bottom water, Posidonia worked	2 cores filled 50 cm, 1 core ~30 cm, sediments not degassing, porewater and methane samples taken. Sediments described.
MIC-5 Stat. 190 GeoB 15241-1	Batumi Seep, Georgia	4 cores		*Geochemical flux study* Lowered with 0.5 cm/s, good penetration, undisturbed surface with overlaying bottom water, With Posidonia.	4 cores filled ~50 cm, sediments not degassing, porewater and methane samples taken. Sediments described.
GC-8 Stat. 191 GeoB 15241-2	Batumi Seep, Georgia	Plastic foil Core catcher –lids	Without T-Logger	*Geochemical flux study* Lowered with 1 m/sec, good penetration. With Posidonia,	~ 208 cm sediment recovery, sediment described and dumped.
MIC-6 Stat. 192 GeoB 15242	Batumi Seep, Georgia	4 cores		*Geochemical flux study* Lowered with 0.5 cm/s, good penetration, undisturbed surface with overlaying bottom water, Posidonia did not work. 1 liner lost	2 cores filled ~50 cm, 1 with 30 cm, sediments not degassing, porewater and methane samples taken. Sediments described.
GC-9 Stat. 193 GeoB 15243	Poti Seep, Georgia	Plastic foil, core catcher-lamella	Without T-Logger	*Sediment reconnaissance* Lowered with 1.2 m/sec, good penetration. Posidonia not working.	~ 146 cm sediment recovery, small hydrates in CC, sediment described and dumped.
GC-10 Stat. 194 GeoB 15244-1	Poti Seep, Georgia	Plastic foil, core catcher-lamella	Without T-Logger	*Sediment reconnaissance* Lowered with 1.2 m/sec, bad penetration, probably not enough rope released during penetration. Without Posidonia.	No sediment recovery
GC-11 Stat. 195 GeoB 15244-2	Poti Seep, Georgia	Plastic foil, core catcher-lamella	Without T-Logger	*Sediment reconnaissance* Lowered with 1.2 m/sec, good penetration. Without Posidonia.	~ 140 cm sediment recovery, massive hydrate at base; geochemical sampling, sediment described and dumped.
MIC-7 Stat. 198 GeoB 15247-1	Batumi Seep	4 cores		*Geochemical flux study* Lowered with 0.5 cm/s, good penetration, undisturbed surface with overlaying bottom water, With Posidonia.	4 cores filled 30 to 48 cm with sediments
GC-12 Stat. 199 GeoB 15247-2	Batumi Seep	Plastic foil, core catcher-lamella	Without T-Logger	*Geochemical flux study* Lowered with 1.2 m/sec, good penetration. With Posidonia.	Gas hydrates in core catcher and lowermost 10 cm of core. Gas hydrate tabular shaped.
GC-13 Stat. 201 GeoB 15244-3	Poti Seep	Plastic liner, core catcher-lamella	Without T-Logger	*Gas hydrate sampling* Lowered with 1.0 m/sec, without Posidonia	197 cm sediments, gas hydrates at lowermost sediments and in core catcher, no geochemical sampling, core described and archived.
GC-14 Stat. 202 GeoB 15248	Reference next to Poti Seep	Plastic liner, core catcher-lamella,	Without T-Logger	*Sedimentological studies* Lowered with 0.5 m/sec, without Posidonia	574 m sediments, core cut in 1 m segments, not opened, archived
GC-15 Stat. 203 GeoB 15249-1	Batumi Seep	Plastic foil, core catcher-lamella	Without T-Logger	*Geochemical flux study* Lowered with 1.2 m/sec, With Posidonia.	Some gas hydrates at base, dispersed, few
MIC-8 Stat. 205 GeoB 15249-2	Batumi Seep	4 cores		*Geochemical flux study* Lowered with 0.5 cm/s, good penetration, undisturbed surface with overlaying bottom water, with Posidonia	4 cores filled with 45 cm sediments
DAPC-1 Stat. 206 GeoB 15244-4	Poti Seep			*Gas quantification*	

Station Number M84/2	Area	Equipped with	T-logger	OBJECTIVES Technical description	Sediment recovery
GC-16 Stat. 207 GeoB 15251-1	Batumi Seep	Plastic foil, core catcher-lamella	T-Logger 1-4 (SN1854330, 1854335, 1854404, 1854407)	*Geochemical flux study* Lowered with 1.2 m/sec, 10 min in sea bottom, with Posidonia.	
MIC-9 Stat. 208 GeoB 15251-2	Batumi Seep	4 cores		*Geochemical flux study* Lowered with 0.5 cm/s, with Posidonia	Good sediment recovery
GC-17 Stat. 209 GeoB 15252	Batumi Seep	Liner, core catcher-lids	T-Logger 1-4 (spacing 60 cm)	*Core catcher test* Lowered with 1.2 m/sec, lids of core catcher bended, not closed, without Posidonia	Strongly degassing at sea surface, ~80 cm of sediments, gas hydrates in core catcher, many hydrate chips in core, no porewater sampling, sediments not described and dumped
MIC-10 Stat. 210 GeoB 15253	Batumi Seep	4 cores		*Geochemical flux study* Lowered with 0.5 cm/s, with Posidonia	3 cores filled
GC-18 Sta. 211 GeoB 15227-5	Pechori Mound	Liner	T-Logger 1-4 (spacing 125 cm)	*Complementary to MeBo GeoB 15227-5* With Posidonia	~1.7 m sediments on outside barrel, 1.3 m sediments in liner, oily sediments, no gas hydrates, cores not opened, no geochemical sampling, not described, archived
GC-19 Stat. 212 GeoB 15254	Pechori Mound-outside rim	Plastic foil	T-Logger 1-4	*Hydrate distribution* Lowered with 1 m/sec, deeply penetrated, without Posidonia	~6 m of sediments with typical Black Sea stratigraphy, difficult to remove sediments from liner, no geochemical sampling, sediments described and dumped
GC-20 Stat. 213 GeoB 15255	Pechori Mound –rim	Plastic foil	T-Logger 1-4	*Hydrate distribution* Lowered with 1.2 m/sec, without Posidonia	Strongly degassing at sea surface, hydrates lost to water, hydrate pieces in core catcher, white (frozen), ~70 cm of oily sediments
GC-21 Stat. 214 GeoB 15256	Pechori Mound-center	Liner	T-Logger 1-4, only 5 min in sediments, tip of logger 1 broken	*Hydrate distribution* Lowered with 1.2 m/sec, without Posidonia	Strongly degassing at sea surface, big hydrate piece at bottom of core, white (frozen). Hydrates “pop-corn”-like, making sounds when bursting, 2.03 m of oily sediments, cores not opened, no geochemical sampling, not described, archived
GC-22 Stat. 216 GeoB 15258	G2, Kulevi Ridge-east	Liner	Without T-Logger	*Sediment reconnaissance* Lowered with 1.2 m/sec, without Posidonia.	Only 1.3 m of sediments recovered. Gas hydrate expansion probably pushed sediments upward into weight. Mud clast in weight. Small pieces of gas hydrates in core catcher (sample for gas analytics taken). Sediments very dry.
GC-23 Stat. 217 GeoB 15259	G1, Kulevi Ridge-west	Liner	Without T-Logger	*Sediment reconnaissance* Lowered with 1.2 m/sec, without Posidonia.	Only weakly degassing at sea surface, no gas hydrates in core, sandy material, dry,
GC-24 Stat. 218 GeoB 15260-1	Batumi Seep	Plastic foil	T-Logger 1-4, placed 60 cm apart	*Geochemical flux study* Lowered with 1.2 m/sec, 10 min in sea bottom, with Posidonia.	240 cm sediment recovery, in lower section abundant layered gas hydrates, white. Some hydrates frozen. Geochemical sampling, sediments described and dumped.
MIC-11 Stat. 219 GeoB 15260-2	Batumi Seep	4 cores		*Geochemical flux study* Lowered with 0.5 cm/s, with Posidonia	Good sediment recovery, 4 cores

Station Number M84/2	Area	Equipped with	T-logger	OBJECTIVES Technical description	Sediment recovery
GC-25 Stat. 220 GeoB 15261	Colkheti Seep	Liner	T-Logger 1-4, placed 125 cm apart	*Sediment reconnaissance* Lowered with 1.2 m/sec, Without Posidonia.	Only ~1.3 m sediments, some oil, not much, not degassing at sea surface, no hydrates, no porewater sampling, described and archived.
DAPC-2 Stat. 221 GeoB 15244-5	Poti Seep			*Gas quantification*	Pore water sampling, sediment documented.
DAPC-3 Stat. 229 GeoB 15268-1	Ordu ridge patch#02			*Gas quantification*	Pore water sampling, sediment documented.
MIC-12 Stat. 233 GeoB 15268-3	Samsun, Ordu Ridge Patch 2, Flare	4 cores		Lowered with 0.5 m/sec, Good penetration, undisturbed surface with overlaying bottom water, with Posidonia	All 4 cores 40-45 cm filled, porewater, methane and pollen/spore study samples taken. Sediments described.
DAPC-4 Stat. 234 GeoB 15268-4	Ordu ridge patch#02			*Gas quantification*	No pressure on core
GC-28 Stat. 235 GeoB 15503	Samsun, Ordu Ridge Patch 3, Flare	PVC Liner Core catcher –lamella	without T-Logger	*Sediment reconnaissance* Lowering with 1.2 m/s, , Without Posidonia	Core length about 3 m, strong sulphide smell, gas-rich, massive hydrates, porewater and hydrate samples taken, sediment described and archived
GC-29 Stat. 237 GeoB 15504	Samsun, Ordu Ridge, high backscatter without flare	PVC Liner Core catcher –lamella	without T-Logger	*Sediment reconnaissance* Lowering with 1.0 m/s, , Without Posidonia	Banana. 2.10 m of sediment recovered, gas-rich, signs of hydrate presence, carbonates, no sampling, sediment described and archived
GC-30 Stat. 238 GeoB 15505-1	Samsun, Ordu Ridge Patch 7, Flare	PVC Liner Core catcher –lamella	without T-Logger	*Sediment reconnaissance* Lowering with 1.2 m/s, , Without Posidonia	Core length about 240 cm, strong sulphide smell, gas-rich, massive hydrates in core catcher, porewater and hydrate samples taken, sediment described and archived
MIC-13 Stat. 240 GeoB 15503-3	Samsun, Ordu Ridge Patch 3, Flare	4 cores		Lowered with 0.5 m/sec, Good penetration, undisturbed surface with overlaying bottom water, with Posidonia	3 cores 45-50 cm filled, porewater, and methane samples taken. Sediments described.
DAPC-5 Stat. 241 GeoB 15268-5	Ordu ridge patch#02			*Gas quantification*	Pore water sampling, sediment documented.
MIC-14 Stat. 242 GeoB 15505-2	Samsun, Ordu Ridge Patch 7, Flare	4 cores		Lowered with 0.5 m/sec, Good penetration, undisturbed surface with overlaying bottom water, with Posidonia	4 cores 40-50 cm filled, porewater, methane and radiocarbon samples taken. Sediments described.
GC-31 Stat. 243 GeoB 15507	Samsun, Ordu Ridge Patch 7, Flare	PVC Liner Core catcher –lamella	without T-Logger	*Gas hydrates* Lowering with 1.2 m/s, , Without Posidonia	Core length about 157 cm, strong sulphide smell, gas-rich, massive hydrates, porewater and hydrate samples taken, sediment described and archived
GC-32 Stat. 244 GeoB 15508	Samsun, New Ridge	PVC Liner Core catcher –lamella	without T-Logger	*Sediment reconnaissance* Lowering with 1.2 m/s, without Posidonia	Core length about 300 cm, sulphide smell, gas-rich, no hydrates, porewater and hydrate samples taken, sediment described, color scanned and archived

Station Number M84/2	Area	Equipped with	T-logger	OBJECTIVES Technical description	Sediment recovery
GC-33 Stat. 248 GeoB 15512-1	Kerch Strait, Flare	PVC Liner Core catcher –lamella	with T-Logger	*Gas hydrates* Lowering with 1.2 m/s, with Posidonia	Core length about 100 cm, sulphide smell, gas-rich, no hydrates, porewater and hydrate samples taken, sediment described and archived
GC-34 Stat. 249 GeoB 15513-1	Kerch Strait, Flare	PVC Liner Core catcher –lamella	with T-Logger	*Gas hydrates* Lowering with 1.2 m/s, with Posidonia	Core length about 570 cm, overpenetrated, sulphide smell, gas-rich, small platy hydrates below 27 cm, porewater, hydrate, pollen/spore samples taken, sediment described and archived
DAPC-6 Stat. 250 GeoB 15513-2	Kerch Strait, Flare			*Gas quantification*	Pore water sampling, sediment documented.
MIC-15 Stat. 251 GeoB 15513-3	Kerch Strait, Flare	4 cores		Lowered with 0.5 m/sec, good penetration, undisturbed surface with overlaying bottom water, with Posidonia	4 cores ~45 cm filled, porewater, methane samples taken. Sediments described.
GC-35 Stat. 254 GeoB 15512-2	Kerch Strait, Flare	PVC Liner Core catcher –lamella	without T-Logger 3 m barrel	*Gas hydrates* Lowering with 1.2 m/s, with Posidonia	Core length about 135 cm, sulphide smell, gas-rich, no hydrates, no sampling, sediment described and archived
GC-36 Stat. 256 GeoB 15516-1	Kerch Strait, Flare	PVC Liner Core catcher –lamella	with T-Logger	*Gas hydrates* Lowering with 1.2 m/s, with Posidonia (not working)	Core length about 475 cm, overpenetrated, sulphide smell, gas-rich, small platy hydrates, porewater, hydrate samples taken, sediment described and archived
DAPC-7 Stat. 257 GeoB 15516-2	Kerch Strait, Flare			*Gas quantification*	Pore water sampling, sediment documented.
MIC-16 Stat. 258 GeoB 15516-3	Kerch Strait, Flare	4 cores		Lowered with 0.5 m/sec, good penetration, undisturbed surface with overlaying bottom water, with Posidonia	4 cores ~45 cm filled, gas-rich, porewater, methane samples taken. Sediments described.
GC-37 Stat. 260 GeoB 15518-1	Kerch Strait, Flare	PVC Liner Core catcher –lamella	with T-Logger	*Gas hydrates* Lowering with 1.2 m/s, without Posidonia	Core length about 357 cm, overpenetrated, sulphide smell, gas-rich, platy hydrates, porewater, hydrate samples taken, sediment described and archived
GC-38 Stat. 261 GeoB 15519-1	Kerch Strait, Background	PVC Liner Core catcher –lamella	with T-Logger	*Background* Lowering with 0.8 m/s, without Posidonia	Core length about 574 cm, slightly overpenetrated, sulphide smell, no hydrates, porewater, methane samples taken, sediment described and archived
GC-39 Stat. 262 GeoB 15520	Kerch Strait, Flare	PVC Liner Core catcher –lamella	with T-Logger	*Gas hydrates* Lowering with 1.2 m/s, without Posidonia	Core length about 163 cm, overpenetrated, sulphide smell, gas-rich, no hydrates, no samples, sediment described and archived
DAPC-8 Stat. 263 GeoB 15518-2	Kerch Strait, Flare			*Gas quantification*	Pore water sampling, sediment documented.
MIC-17 Stat. 264 GeoB 15519-2	Kerch Strait, Background	4 cores		Lowered with 0.5 m/sec, good penetration, undisturbed surface with overlaying bottom water, with Posidonia	1 core with 30 cm, 3 cores with ~45 cm filled, porewater, methane, coccolith samples taken. Sediments described.

Station Number M84/2	Area	Equipped with	T-logger	OBJECTIVES Technical description	Sediment recovery
GC-40 Stat. 268 GeoB 15524-1	Helgoland MV	PVC Liner Core catcher – lamella	with T-Logger	*Sediment, gas hydrates* Lowering with 0.3 m/s, without Posidonia	Core length about 457 cm, overpenetrated, sulphide smell, gas-rich, no hydrates, porewater and methane samples, sediment described and archived
MIC-18 Stat. 269 GeoB 15524-2	Helgoland MV	4 cores		Lowered with 0.5 m/sec, with Posidonia	1 core with 40 cm, 3 cores with completely filled, porewater methane samples taken. Sediments described.
GC-41 Stat. 270 GeoB 15525-1	Helgoland MV	PVC Liner Core catcher – lamella	with T-Logger	*Deep penetration T-logging* Lowering with 1.2 m/s, no deep penetration, without Posidonia	Core length about 100 cm, sulphide smell, gas-rich, abundant and partly massive hydrates, porewater and methane samples, sediment described and archived
DAPC-9 Stat. 271 GeoB 15526-1	Dvurechenskii MV			*Gas quantification*	Pore water sampling, sediment documented.
GC-42 Stat. 272 GeoB 15527	Helgoland MV	PVC Liner Core catcher – lamella	with T-Logger	*Deep penetration T-logging* Lowering with 1.2 m/s until ~70 mbsf, without Posidonia	Core length about 400 cm, sulphide smell, gas-rich, porewater and methane samples, sediment described and archived
MIC-19 Stat. 275 GeoB 15525-2	Helgoland MV	4 cores		Lowered with 0.4 m/sec, with Posidonia	1 core with 40 cm, 3 cores completely filled but sediment lost during retrieval because of liquid sediment, GH in liner. Methane samples taken. Sediments described.
GC-43 Stat. 276 GeoB 15525-3	Helgoland MV	PVC Liner Core catcher – lamella	with T-Logger	*Sediment,T-logging* Lowering with 1.2 m/s, without Posidonia	No sediment in liner, GH in core catcher, floating on sea surface.
MIC-20 Stat. 277 GeoB 15525-4	Helgoland MV	4 cores		Lowered with 0.4 m/sec, with Posidonia	4 Liners with ~30 cm sediment and bottom water, methane, pore water samples taken, described.
DAPC-10 Stat. 278 GeoB 15530	Helgoland MV			*Gas quantification*	Pore water sampling, sediment documented.
GC-44 Stat. 279 GeoB 15531	Helgoland MV	PVC Liner Core catcher – lamella	with T-Logger	*Deep T-logging* Lowering with 1.2 m/s until 2099 m rope length, without Posidonia	No sediment in liner, GH floating on sea surface.
GC-45 Stat. 280 GeoB 15532	Helgoland MV	PVC Liner Core catcher – lamella	with T-Logger	*Sediment, T-logging* Lowering with 1.2 m/s until ~20 mbsf, stopped, lowering with 1.0 m/s until 35 mbsf, without Posidonia	569 cm recovery, warm mud, methane, porewater samples taken. Sediment described, documented, archieved.
GC-46 Stat. 281 GeoB 15533-1	Back-ground	PVC Liner Core catcher – lamella	with T-Logger	*Sediment* Lowering with 0.8 m/s, without Posidonia	590 cm recovery, overpenetration, methane, porewater and pollen/spore samples taken. Sediment described, documented, archieved.
MIC-21 Stat. 282 GeoB 15533-2	Back-ground	4 cores		Lowered with 0.5 m/sec, with Posidonia	4 Liners with ~30 cm sediment and bottom water, methane, pore water samples taken, described.

Appendix 3: Survey List

Station	Survey No.	GeoB No.	Area	Start	End	Echolot System	Purpose	Observations/remarks
136	1	15202	Eregli	27.02.2011 00:58	27.02.2011 13:30	EM122 + PS	Calibration of EM122 and searching for flares and subbottom anomalies	Known flare positions are active and additionally flare locations have been found. Subbottom with numerous blankings.
139	2	15205	Eregli	27.02.2011 17:40	28.02.2011 04:27	EM122 + PS	Additional flare search and filling gaps in bathymetry	Two new flare locations on the plateau but no other flares along the eastern ridge
141	3	15207	Eregli	28.02.2011 06:05	28.02.2011 07:39	EM122 + PS	Due to cancelled AUV dive filling the time gap with short survey over the known flare positions	Several flares observed
143	4	15209	Eregli	28.02.2011 22:37	01.03.2011 05:20	EM122 + PS	Additional flare search and filling gaps in bathymetry	Three strong and one weak flare at the western ridge observed
147	5	15213	Eregli	01.03.2011 13:05	01.03.2011 18:37	EM122 + PS	Leaving the working area and fill gaps on the way	One new flare passed and some small blankings observed
149	6	15215	Samsun	02.03.2011 15:30	02.03.2011 16:46	EM122 + EM710 + PS	Line from the limit of the working area on top of the Archangalsky ridge	No flares observed, but several pockmarks
151	7	15217	Samsun	02.03.2011 17:36	03.03.2011 07:55	EM122 + EM710 + PS	Mapping, flare search and subbottom observation	Pockmarks in shallower regions, slumping and several flares observed
153	8	15219	Colkheti, Pechori, Batumi	03.03.2011 20:36	04.03.2011 03:28	EM122 + PS	Flare search over Pechori, Colheti and Batumi	High activity at all sites
158	9	15221	Batumi	04.03.2011 11:25	04.03.2011 14:00	EM122 + 710	Testing the settings for multibeam WCL over Batumi	Successfully settings set
161	10	15223	Poti Seep	05.03.2011 10:29	04.03.2011 12:	EMs+PS	Detailed flare survey over Poti	Flare area distinguished
163	11	15225	Adjara Ridge Colkheti & Pechori	05.03.2011 13:40 05.03.2011 20:43	05.03.2011 20:43 06.03.2011 04:28	EMs + PS	Flare survey on Adjara Ridge sites A1, A2, and A3 Flare survey at Colkheti and Pechori	Flare cluster mapped in detail. Flares well mapped.
166	12	15228	Kobuleti Ridge	06.03.2011 13:40	06.03.2011 18:36	EMs + PS	Bathymetry at Western Kobuleti Ridge	Additional flares found.
170	13	15231	Kobuleti Ridge	07.03.2011 09:53	07.03.2011 15:20	EMs + PS	Backscatter mapping west of Batumi Seep	Good coverage
172	14	15232	G 2 G 1 Transit to Batumi	07.03.2011 15:50 08.03.2011 01:30 08.03.2011 02:49	08.03.2011 03:50 08.03.2011 02:49 08.03.2011 03:50	EMs + PS	Detailed flare survey at flare G2 Three crossings of G1 Backscatter mapping	Flares rise very high in water column at G2 Flares less intensive at G1 compared to G2 Good coverage
174	15	15233	Kobuleti Ridge	08.03.2011 05:59	08.03.2011 08:35	EMs + PS	Backscatter mapping	Good coverage
176	16	15234	Kobuleti Ridge	08.03.2011 09:18	08.03.2011 11:30	EMs + PS	Backscatter mapping	Good coverage
178	17	15238	South part of working area Georgia	08.03.2011 12:57	09.03.2011 04:00	EMs + PS	Bathmetry and flare survey	Several new flares in EM 122 and Parasound, full bathymetric coverage in southern sector
181	18	15240	Adjara Transit to Batumi	09.03.2011 06:00 09.03.2011 07:10	09.03.2011 07:11 09.03.2011 07:54	EMs + PS	Detailed flare survey at Flare Cluster A4 Enlarging the area mapped by EM 122	Flares in two cluster
189	19	15346	Adjara-Ridge E of Kobuleti Ridge	10.03.2011 15:58 10.03.2011 22:58	10.03.2011 22:58 11.03.2011 05:00	EMs + PS	Flare survey on Adjara Ridge and backscatter survey E of Kobuleti Ridge	Intensive emissions at Adjara Flare Cluster A 3, additional weak flares E of Kobulti Ridge
197	20	15246	Northern part of working area Georgia	11.03.2011 12:35	12.03.2011 08:55	EM122 + PS	Bathymetry	Good coverage, no new flare locations
204	21	15250	Batumi & Colkheti	12.03.2011 18:24	13.03.2011 04:=3	EMs + PS	Temporal variation in flares	Areas crossed several times (Batumi ~14 times, Colkheti ~7 times)
215	22	15257	Colkheti Kobuleti Ridge Batumi Northern part of working area Georgia	13.03.2011 17:53 13.02.2011 20:49 13.02.2011 23:18 14.03.2011 01:10	13.02.2011 20:49 13.02.2011 23:18 14.03.2011 01:10	EMs + PS EMs + PS EMs + PS EMs + PS	Temporal variation in flares Looking for backscatter anomaly near Iberia Temporal variation in flares Bathymetry	Area crossed 7 times Blanking and flares at backscatter anomaly Area crossed 4 times Good coverage, no new flare locations
222	23	15262	Transit to Samsun	14.03.2011 17:30	15.03.2011 04:26	EM122+PS	Bathymetry filled during transit	Additional coverage in deep water
224	24	15264	SE-Samsun	15.03.2011 12:05	15.03.2011 14:26	EM122+PS	Bathymetry and flare survey	5 N-S lines for total coverage and detailed BS-map over the Ordu ridge - several flares found related to high reflectivity patches and updomed structures
226	25	15266	SE-Samsun	15.03.2011 14:50	16.03.2011 05:40	EM122+PS	Additional batymetry and detailed flare survey over the detected BS-patches to prove their activity	Found further BS-patches and crossing of the most pronounced patches in the central part shows that only few of them are recently active degassing
230	26	15269	Transit to trabzon	16.03.2011 11:07	16.03.2011 22:27	EM122+PS	Additional bathymetry survey during transit to trabzon	Found a mud volcanoe structure with a flare in the soust-eastern edge of the working area

Station	Survey No.	GeoB No.	Area	Start	End	Echolot System	Purpose	Observations/remarks
232	27	15502	SE-Samsun	19.03.2011 13:26	17.03.2011 06:18	EM122+PS	Bathymetry and detailed flare survey in the north of Ordu ridge	Good coverage of the SE-part of the working area and new flare locations and BS-anomalies detected
239	28	15506	SE-Samsun	20.3.2011 16:10	21.03.2011 06:54	EM122+PS	Covering gaps in bathymetry and flare survey of the	West of Ordu additional ridge with similar flat platform geometry
246	29	15510	Leaving Samsun	21.03.2011 17:39	22.03.2011 07:22	EM122+PS	Filling last gaps of the bathymetry	Total map now availably for the SE part of the working area Samsun
247	30	15511	Ukraine-Kerch	22.03.2011 19:08	23.03.2011 11:25	EMs+PS	Reaching ukrainian working area - bathymetry and flare survey along the fan to Kerch-flare	Numerous flares documented and known flares confirmed with both systems. Kerch-Flare is active degassing as well
253	31	15515	Kerch	23.03.2011 16:40	24.03.2011 10:16	EMs+PS	Covering the entire margin around Kerch-Flare for a high resolution bathymetry and backscatter map as well as flare documentation for the entire box	Several flares have been observed and the resulting detailed backscatter map shows a high reflectivity patch in almost 700 m water depth
259	32	15517	Kerch	24.03.2011 16:05	25.03.2011 11:11	EMs+PS	Completely covering survey along the margin east of Kerch-Flare	High amount of flares recorded and several sliding structures visible in bathymetry map, especially in EM710
265	33	15521	Kerch	25.03.2011 18:00	26.03.2011 11:06	EMs+PS	Detailed survey over Kerch flare to document recent activity and bathymetry survey to the west of Kerch flare where another margin area should be mapped for bathymentry and also flares	Activity at Kerch flare could be documented in detail and new map west of Kerch-Flare shows totally different erosional characteristics than the areas before and as well less flare activity
267	34	15523	Kerch	26.03.2011 17:52	27.03.2011 11:06	EMs+PS	Completing Survey 33 after SVP	
273	35	15528	Sorokin Trough and Kerch	27.03.2011 18:31	29.03.2011 02:40	EMs+PS	Crossing the mud volcanoes in the Sorokin Trough to observe their actual activity and aditional survey at the estern area covered during St. 259 to fill the gaps of th EM710 grid and complete the flare documentation. Last purpose was to cross the intense BS-patch found during St.253	Several MV show activity, the eastern area is now entirely covered for a highly detailed map and at the BS-patch have been high flare activity and blanking in the SLF signal observed
284	36	15534	DMV and leaving the ukrainian working area	29.03.2011 23:43	30.03.2011 13:00	EM122+PS	Detailed flare survey over DMV and bathymetry during transit in direction to Eregli	Flares of DMV and Helgoland MV crossed several times for exact center detection - bathymetry filled during transit with 8 to 10 kn
286	37	15536	Eregli	30.03.2011 23:28	01.04.2011 06:37	EM122+PS	Bathymetry and flare survey	Filled all gaps of earlier surveys for complete bathymetry and backscatter map - several new flare areas related to high backscatter patches found

Appendix 4: Gas Hydrate Sampling

Gas hydrate inventory M84/2 stored in liquic nitrogen								
Tool	GeoB Number	Area	Barrel	Segment	Depth -(Intervall)	Description	Storage	Storage bag	Comment
MeBo-67	GeoB 15227-3	Pechori Mound	1P	1	23 cm	gas hydrate, brownish	liquid nitrogen	GeoB 15227-3 Bag 2	
MeBo-67	GeoB 15227-3	Pechori Mound	1P	1	80 cm	gas hydrate, brownish	liquid nitrogen	GeoB 15227-3 Bag 2	
MeBo-67	GeoB 15227-3	Pechori Mound	1P	1	87 cm	gas hydrate, brownish	liquid nitrogen	GeoB 15227-3 Bag 2	
MeBo-67	GeoB 15227-3	Pechori Mound	1P	1	112 cm	gas hydrate, brownish	liquid nitrogen	GeoB 15227-3 Bag 2	
MeBo-67	GeoB 15227-3	Pechori Mound	1P	2	18 cm	gas hydrate, brownish	liquid nitrogen	GeoB 15227-3 Bag 2	
MeBo-67	GeoB 15227-3	Pechori Mound	1P	2	65 cm	gas hydrate, brownish	liquid nitrogen	GeoB 15227-3 Bag 2	
MeBo-67	GeoB 15227-3	Pechori Mound	1P	core catcher		gas hydrate, brownish	liquid nitrogen	GeoB 15227-3 Bag 1	
MeBo-67	GeoB 15227-3	Pechori Mound	3R	2	57 cm	gas hydrate, brownish	liquid nitrogen	GeoB 15227-3 Bag 2	
MeBo-67	GeoB 15227-3	Pechori Mound	3R	2	76 cm	gas hydrate, brownish	liquid nitrogen	GeoB 15227-3 Bag 2	
MeBo-67	GeoB 15227-3	Pechori Mound	4R	1	75 cm	gas hydrate, brownish	liquid nitrogen	GeoB 15227-3 Bag 2	Deep frozzen at 09:55 UTC
MeBo-67	GeoB 15227-3	Pechori Mound	4R	1	110 cm	gas hydrate, brownish	liquid nitrogen	GeoB 15227-3 Bag 2	
MeBo-67	GeoB 15227-3	Pechori Mound	4R	2	108 - 114 cm	gas hydrate, brownish	liquid nitrogen	GeoB 15227-3 Bag 2	Deep frozen at 10:09 UTC, images by Vlad and VD
MeBo-67	GeoB 15227-3	Pechori Mound	4R	2	116 -120 cm	gas hydrate, brownish	liquid nitrogen	GeoB 15227-3 Bag 2	
MeBo-67	GeoB 15227-3	Pechori Mound	4R	core catcher		gas hydrate, brownish	liquid nitrogen	GeoB 15227-3 Bag 1	
MeBo-67	GeoB 15227-3	Pechori Mound	5R	core catcher		gas hydrate, brownish	liquid nitrogen	GeoB 15227-3 Bag 1	
MeBo-67	GeoB 15227-3	Pechori Mound	7R	1	30-35 cm	gas hydrate, brownish	liquid nitrogen	GeoB 15227-3 Bag 2	Images by VD of gas hydrates in core and of hand specimens
MeBo-67	GeoB 15227-3	Pechori Mound	7R	core catcher		gas hydrate, brownish	liquid nitrogen	GeoB 15227-3 Bag 1	
MeBo-67	GeoB 15227-3	Pechori Mound	8R	2	44 - 62 cm	gas hydrates, massive			Images by VD in core
MeBo-67	GeoB 15227-3	Pechori Mound	8R	2	75 - 120 cm	gas hydrates, massive			Images of hand specimen (96-106 cm) by VD
MeBo-67	GeoB 15227-3	Pechori Mound	8R	core catcher		gas hydrate, brownish	liquid nitrogen	GeoB 15227-3 Bag 1	
MeBo-67	GeoB 15227-3	Pechori Mound	9R	1	52 - 125 cm	gas hydates, massive, oil-rich			Images of hand specimen (78 - 86 cm) by VD
MeBo-67	GeoB 15227-3	Pechori Mound	9R	core catcher		gas hydrate, brownish	liquid nitrogen	GeoB 15227-3 Bag 1	
MeBo-68	GeoB 15236-2	Batumi Seep	2P		very top (0-10 cm)	gas hydrate, white, 2 cm thick	liquid nitrogen	GeoB 15236-2 Bag	
MeBo-68	GeoB 15236-2	Batumi Seep	2P		very top (0-10 cm)	gas hydrate, white, 7 cm thick	liquid nitrogen	GeoB 15236-2 Bag	
MeBo-68	GeoB 15236-2	Batumi Seep	2P	1	top (10-20 cm)	gas hydrate, white, 5 cm thick	liquid nitrogen	GeoB 15236-2 Bag	
MeBo-68	GeoB 15236-2	Batumi Seep	2P	1	very bottom	gas hydrate, white	liquid nitrogen	GeoB 15236-2 Bag	sampled outside at same time as GH from core catcher
MeBo-68	GeoB 15236-2	Batumi Seep	2P	core catcher		gas hydrate, white	liquid nitrogen	GeoB 15236-2 Bag	
MeBo-68	GeoB 15236-2	Batumi Seep	3P	core catcher		gas hydrate, white	liquid nitrogen	GeoB 15236-2 Bag	
GC-7	GeoB 15236-1	Batumi Seep			195 cm	gas hydrate, white	liquid nitrogen	Bag 3	
GC-24	GeoB 15260	Batumi Seep			210 cm	gas hydrate, white, in layers, with sediments	liquid nitrogen	Bag 3	
GC-24	GeoB 15260	Batumi Seep			240-245 cm	gas hydrate, white, in layers, with sediments	liquid nitrogen	Bag 3	
GC-12	GeoB 15244-2	Poti Seep			130 - 140 cm	gas hydrate, white, massive, 10 cm thick	liquid nitrogen		
GC-13	GeoB 15244-3	Poti Seep		core catcher		gas hydrates, white, tabular shaped, within	liquid nitrogen		
GC-27	GeoB15268-1	Ordu Ridge, patch #02		core catcher		gas hydrate, white, in layers, with sediments	liquid nitrogen		first samole immediately after recovery
GC-27	GeoB15268-1	Ordu Ridge, patch #02		core catcher		gas hydrate, white, in layers, with sediments	liquid nitrogen		sampled by Thomas 5 min after first sample
GC-27	GeoB15268-1	Ordu Ridge, patch #02		core catcher	168-170 cm	gas hydrate, white, massive layer	liquid nitrogen		sampled by Gerhard 15 min after recovery from opened core,
GC-28	GeoB15503-1	Ordu Ridge, patch #03			45-65 cm	gas hydrate, massive	liquid nitrogen		
GC-28	GeoB15503-1	Ordu Ridge, patch #03				gas hydrate, massive	liquid nitrogen		
GC-28	GeoB15503-1	Ordu Ridge, patch #03				gas hydrate, massive	liquid nitrogen		
GC-29	GeoB15505-3	Ordu Ridge, patch #05				knoll of gas hydrate	liquid nitrogen		
GC-31	GeoB15507	Ordu Ridge, patch #07			156cm (biggest one)	knoll of gas hydrate	liquid nitrogen		
GC-31	GeoB15507	Ordu Ridge, patch #07				knoll of gas hydrate	liquid nitrogen		
GC-31	GeoB15507	Ordu Ridge, patch #07				knoll of gas hydrate	liquid nitrogen		
GC-34	GeoB15513-1	Kerch flare			418cm	two small pieces of gas hydrate	liquid nitrogen	no lable	
GC-34	GeoB15513-1	Kerch flare			320cm	one small piece of gas hydrate	liquid nitrogen	bag 2	
GC-34	GeoB15513-1	Kerch flare			101cm	two small pieces of gas hydrate	liquid nitrogen	bag 3	
GC-36	GeoB15516-1	Kerch flare			100-105cm	gas hydrate, white, in layers, with black	liquid nitrogen	bag 1	
GC-36	GeoB15516-1	Kerch flare			162cm	3 pieces of gas hydrate, white, in layers, with black	liquid nitrogen	bag 2	
GC-37	GeoB15518	Kerch flare			bottom	two pieces of gas hydrate,with black sediments	liquid nitrogen	bag 1	
GC-37	GeoB15518	Kerch flare			325cm	one big piece piece ,black sediment	liquid nitrogen	bag 2	
GC-41	GeoB15525	Helgoland MV			bottom	massive GH with sediment(several big	liquid nitrogen	bag1 and 2(one bag is not	sample immediately after recovery
GC-43	GeoB15525-3	Helgoland MV			bottom	one small piece and one big piece(2*2*3cm)	liquid nitrogen	bag1 and 2(one bag is not	sample fom bottom immediately after recovery

Appendix 5: MeBo Drillings

GeoB15208-1 MeBo	METEOR EXPEDITION M84/2		
Location: Eregli 1	Lat.: 41°27.412'N	Lon.: 30°51.138'N	Date: 28.02.2011
Water depth: 975 m	Drill depth: 8 mbsf	Recovery: 5.98 m	

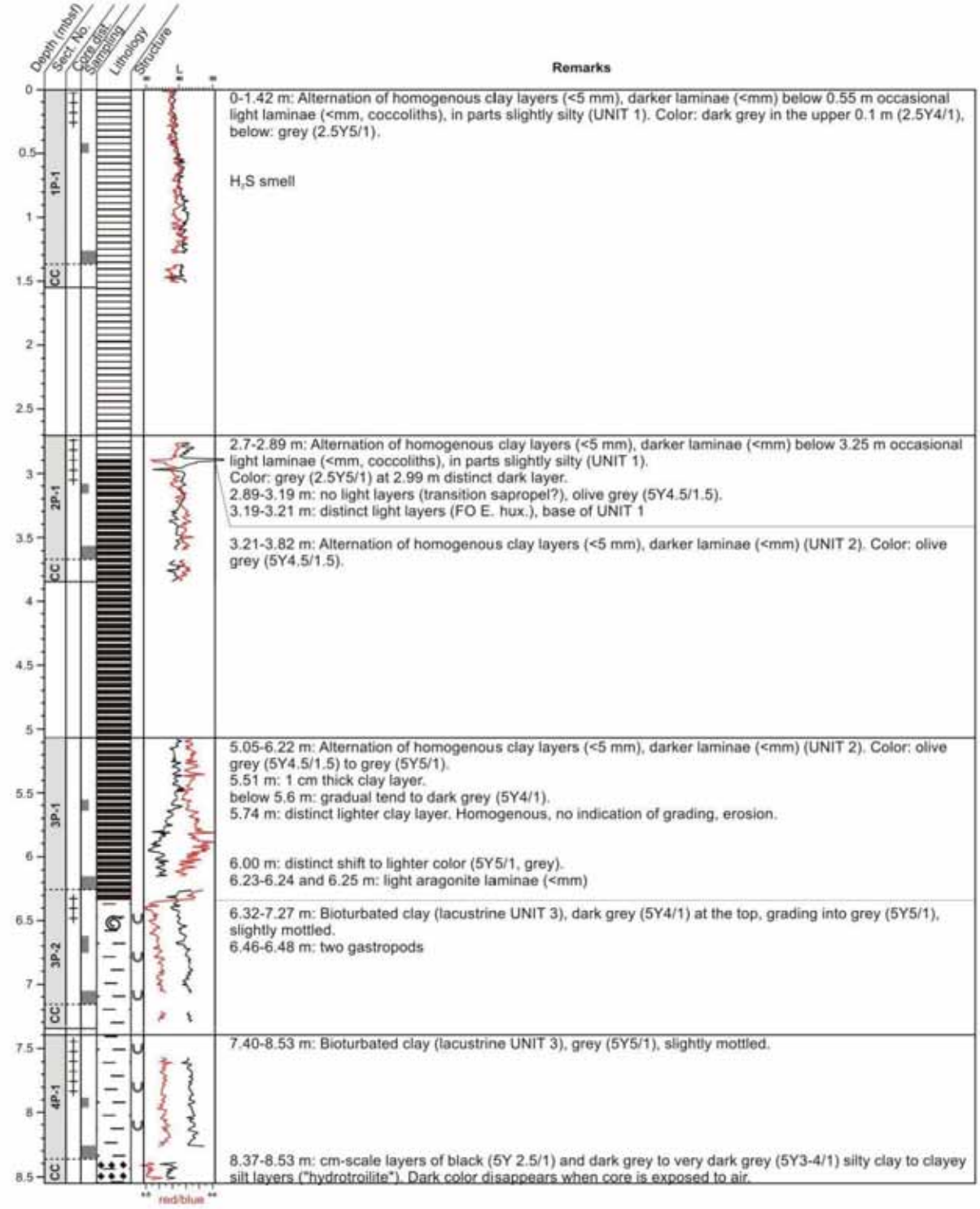

Continuation: Appendix 5: MeBo Drillings

GeoB15220-5 MeBo	METEOR EXPEDITION M84/2	(Part 1 of 2)
Location: Batumi Reference	Lat.: 41°57.156'N Lon.: 41°16.842'E	Date: 05.03.2011
Water depth: 878 m	Drill depth: 14.15 mbsf Recovery: 10.90 m	

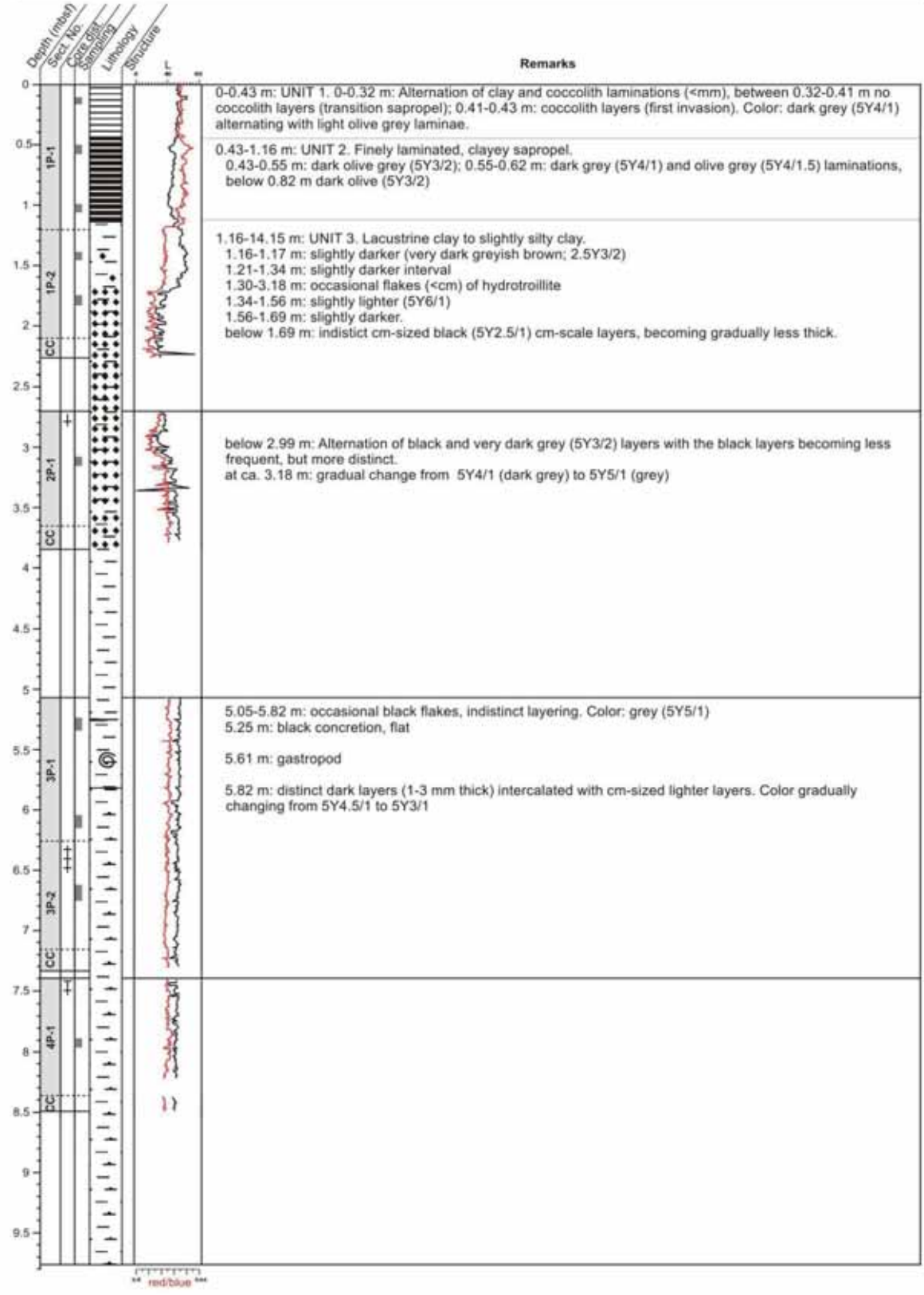

Continuation: Appendix 5: MeBo Drillings

GeoB15220-5 MeBo	METEOR EXPEDITION M84/2	(Part 2 of 2)
Location: Batumi Reference	Lat.: 41°57.156'N Lon.: 41°16.842'E	Date: 05.03.2011
Water depth: 878 m	Drill depth: 14.15 mbsf Recovery: 10.90 m	

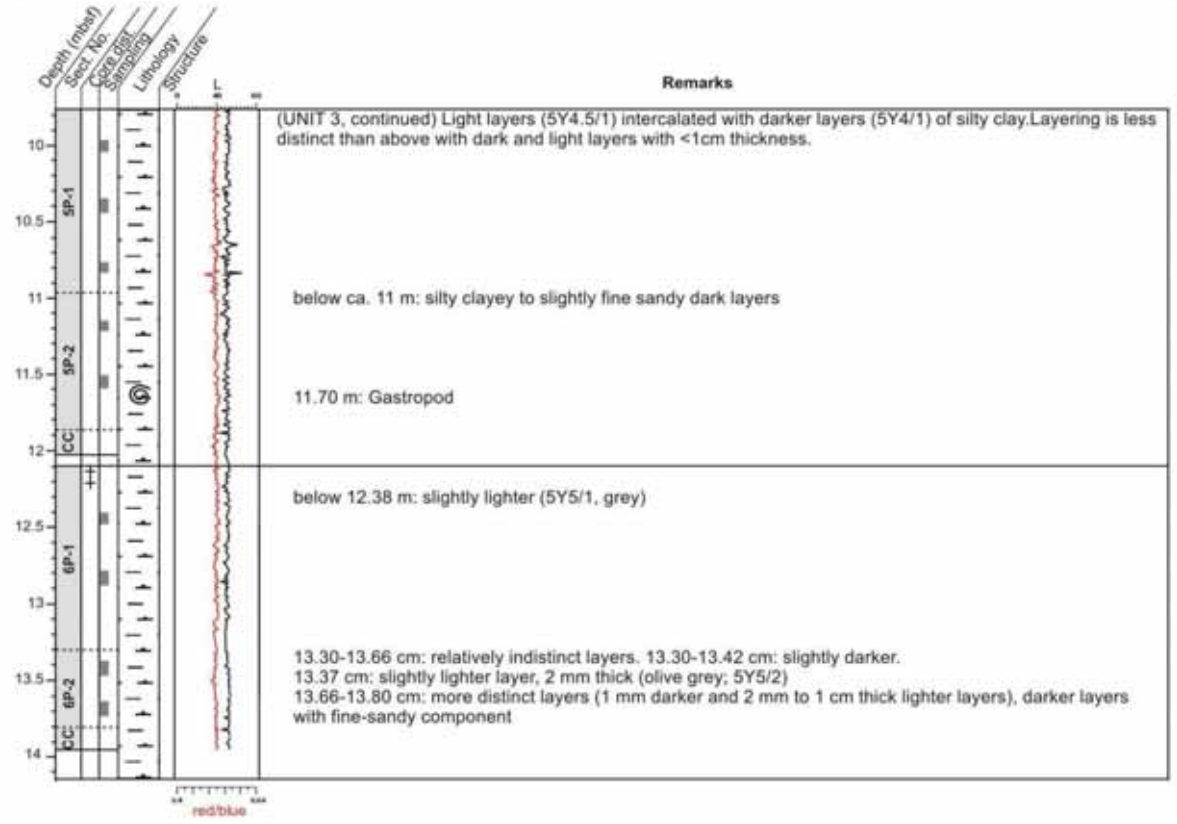

Continuation: Appendix 5: MeBo Drillings

GeoB15227-1 MeBo	METEOR EXPEDITION M84/2
Location: Pechori Mound	Lat.: 41°58.938'N Lon.: 41°07.587'E Date: 05.03.2011
Water depth: 1025 m	Drill depth: 5.05 mbsf Recovery: 3.76 m

Remarks

0-0.08 m: void
0.08-0.11 m: moussy fine-sandy clay, dark brown (10YR4/3), oil-stained
0.11-0.28 m: heavily distorted layers of coccolith laminae (5Y4.5/1, grey to dark grey) intercaleted by dark (5Y3/1, very dark grey), finely laminated intervals. Light and dark intervals of ca. 1 cm thickness. Moderately oil stained. (Unit 1). Relatively stiff.
0.28-0.42 m: as above but with regular bedding. Relatively stiff. Few oil drops. No Gashydrates.
0.42-1.36 m: clay to slightly silty clay, grey to dark grey (5Y4.5/1) oil-stained with abundant finely dispersed to cm-thick platy gas hydrates. Occasional coccolith-bearing light layers in the otherwise completely homogenized sediment (smear slides at 10, 23, 76, 94 cm section depth). Sediment is generally soupy to moussy.
0.42-1.36 m: soupy to moussy sediment
0.83-0.96 m: stiffer interval with some light laminations, dark brown (10YR3/3)

2.70-2-79 m: fine sand
2.79-5.10 m: oil-stained clay with occasional sand-sized particles and abundant finely dispersed and platy massive fabric.
2.70-3.23 m: moussy
3.23-3.74 m: soupy

3.74-4.66 m: moussy, party soupy sediment
3.86-3.94 m: silty to fine sandy clay
4.00-4.03 m: silty to slightly fine sandy clay

4.63-4.64 m: fine sandy clay
4.66-5.10 m: soupy

Continuation: Appendix 5: MeBo Drillings

GeoB15227-3 MeBo	METEOR EXPEDITION M84/2	(PART 1 of 2)
Location: Pechori Mound	Lat.: 41°59.000'N Lon.: 41°07.540'E	Date: 05.03.2011
Water depth: 1027 m	Drill depth: 19.10 mbsf Recovery: 13.17 m	

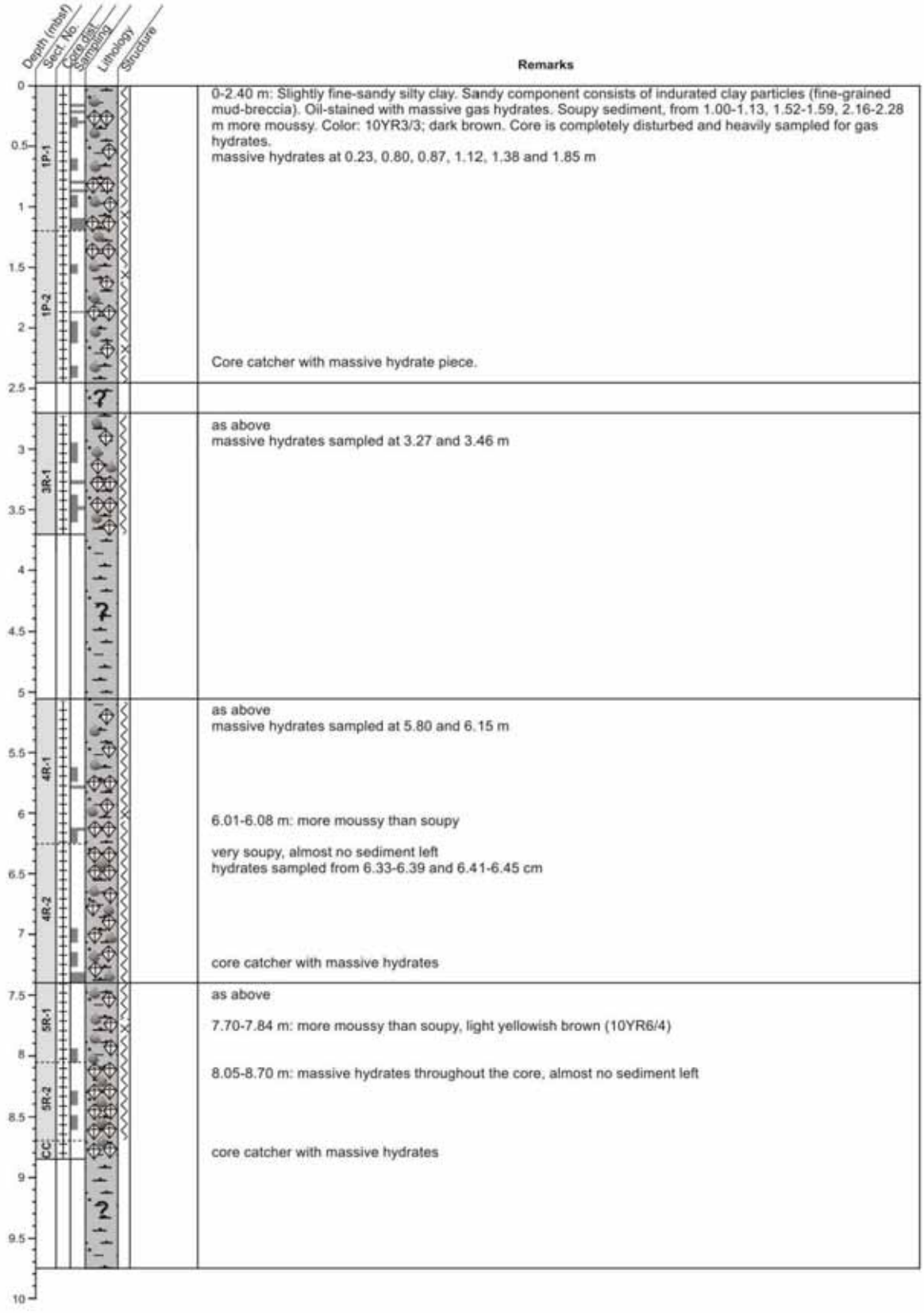

Continuation: Appendix 5: MeBo Drillings

GeoB15227-3 MeBo	METEOR EXPEDITION M84/2	(PART 2 of 2)
Location: Pechori Mound	Lat.: 41°59.000'N Lon.: 41°07.540'E	Date: 05.03.2011
Water depth: 1027 m	Drill depth: 19.10 mbsf Recovery: 13.17 m	

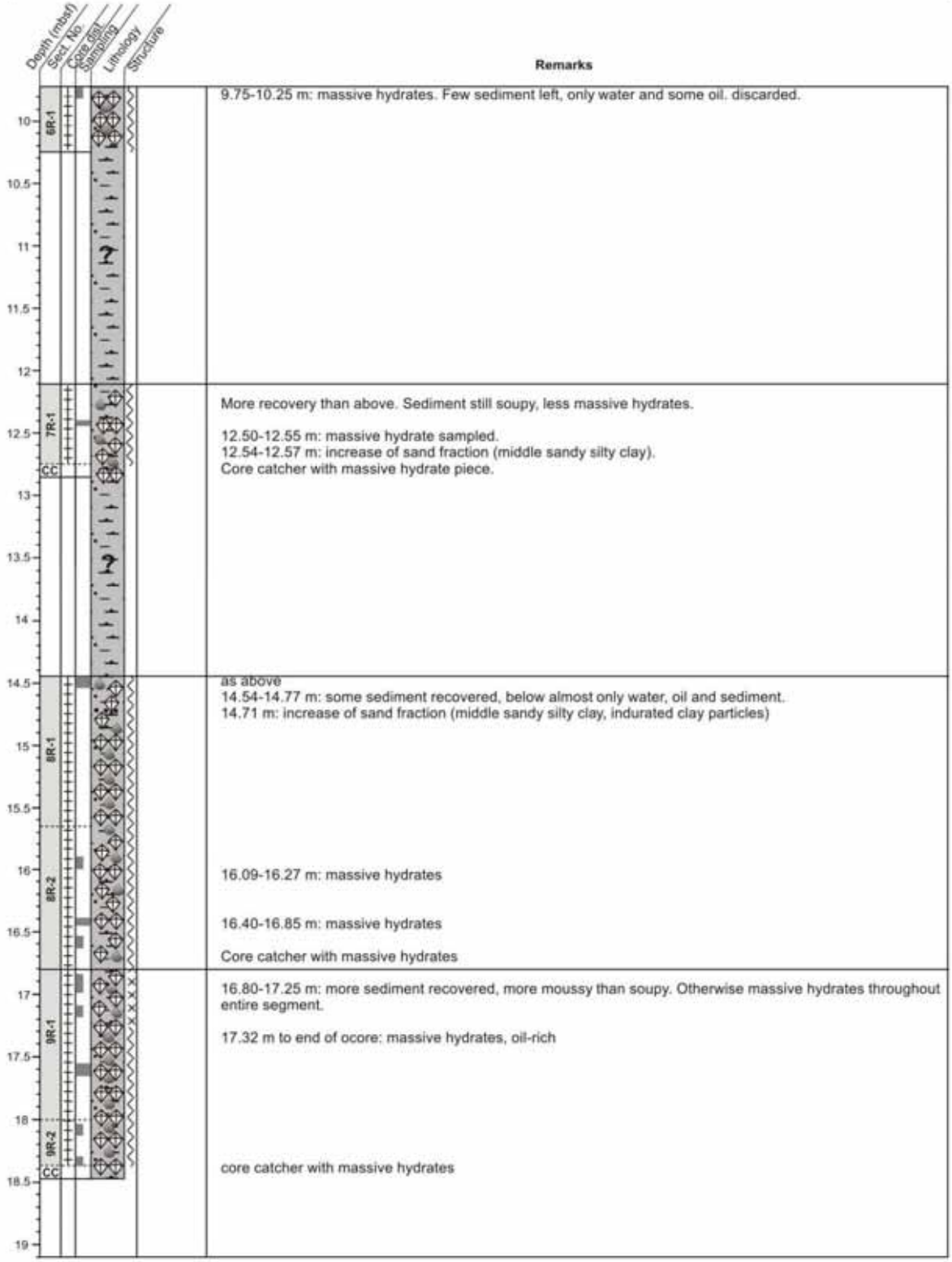

Continuation: Appendix 5: MeBo Drillings

GeoB15236-2 MeBo	METEOR EXPEDITION M84/2		
Location: Batumi Seep	Lat.: 41°57.590'N	Lon.: 41°17.350'E	Date: 10.03.2011
Water depth: 838 m	Drill depth: 838 mbsf	Recovery: 596 m	

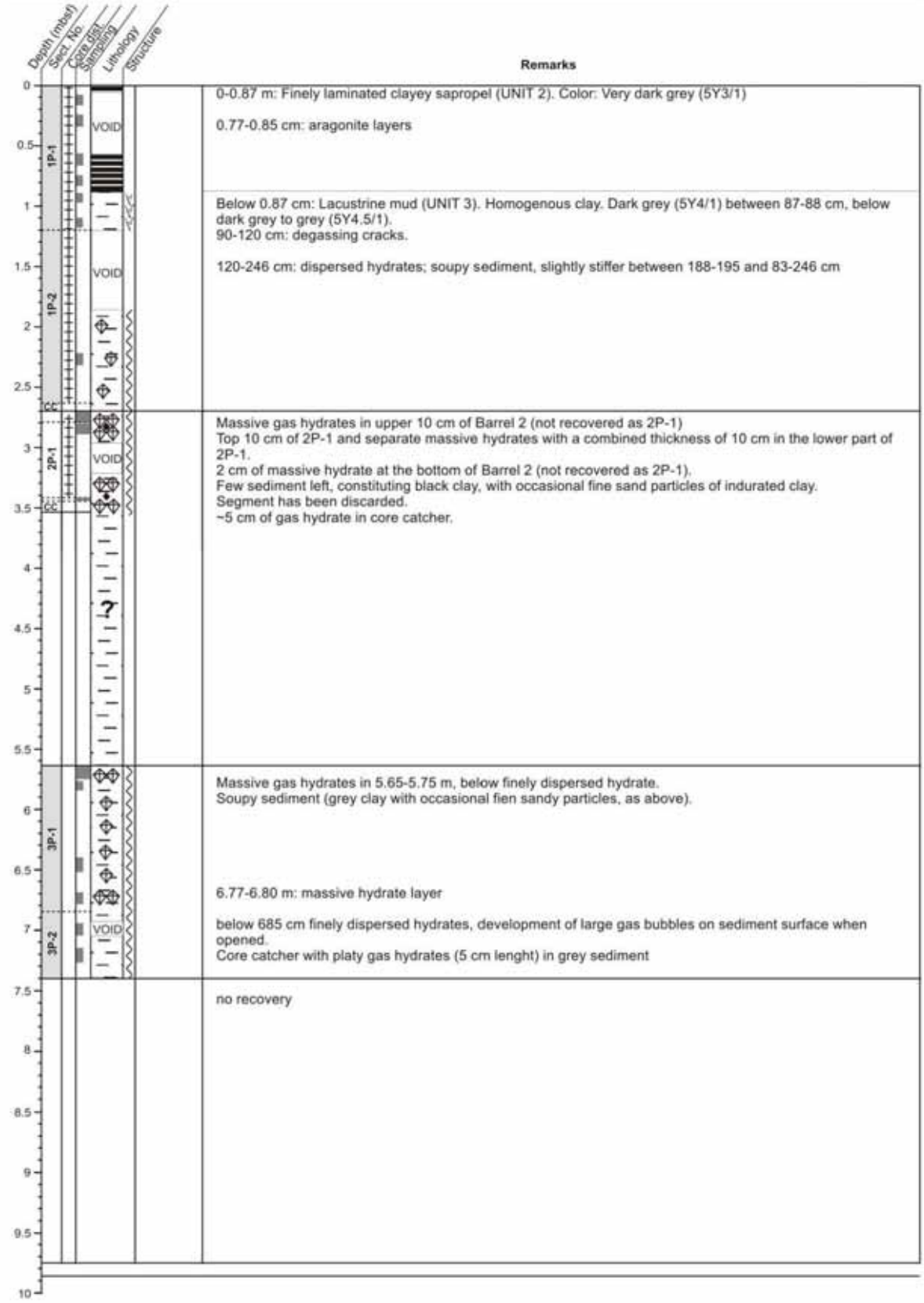

Appendix 6: Core Descriptions

Lithological descriptions of gravity cores retrieved during M84/2

GeoB 15203 GC-1	METEOR EXPEDITION M84/2
Location: Eregli 1	
Lat.: 41°28.536'N	Date: 27.02.2011
Lon.: 30°51.658'E	Recovery: 310 cm
Water depth: 1028 m	Liner: plastic hose

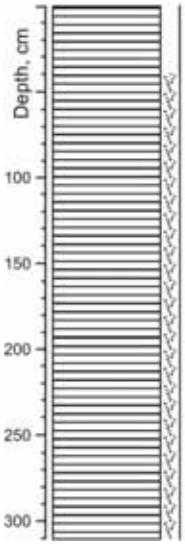

0-310 cm. UNIT 1: Clay to slightly silty clay, with fine (<mm) light laminations (coccolith layers). Color: dark grey (10YR 4/1).

below 20 cm: degassing structures

strong H_2S smell

GeoB 15204 GC-2	METEOR EXPEDITION M84/2
Location: Eregli 1	
Lat.: 41°28.470'N	Date: 27.02.2011
Lon.: 30°51.632'E	Recovery: 255 cm
Water depth: 1022 m	Liner: plastic hose

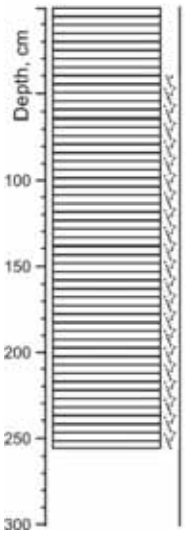

0-255 cm. UNIT 1: Clay to slightly silty clay, with fine (<mm) light laminations (coccolith layers). Color: dark grey (10YR 4/1).

below 40 cm: degassing structures

strong H_2S smell

255-300 cm: Indication of double penetration (new surface)

GeoB 15216 GC-3 **METEOR EXPEDITION M84/2**

Location: Archangelsky Ridge

Lat.: 41°03.00'N Date: 02.03.2011

Lon.: 30°41.19'E Recovery: 600 cm

Water depth: 384.9 m Liner: PVC

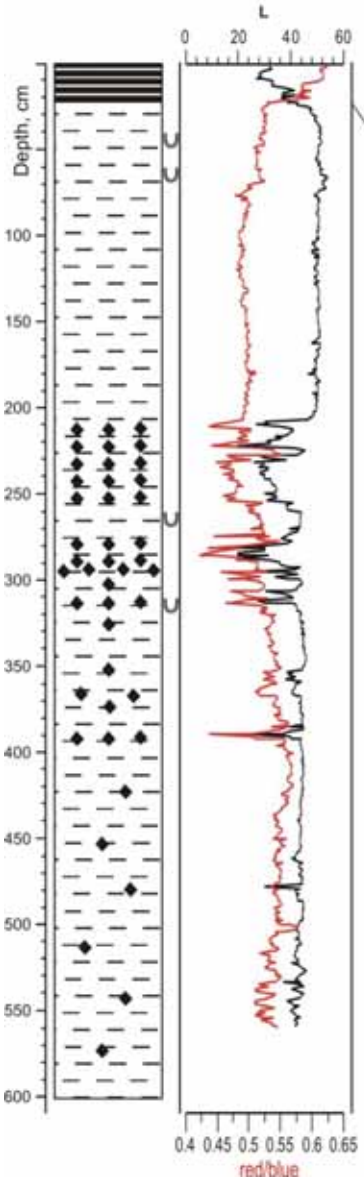

0-21 cm. UNIT 2: Finely (<mm) laminated, clayey to slightly silty clayey sapropel, dark olive grey (5Y3/2) to very dark grey (5Y5/1), lighter towards the base of the sapropel (olive grey, 5Y4/2).
14-18.5 cm: Light aragonite layers.

0-21 cm. UNIT 3: Clay, 21-24 cm below sapropel dark to very dark grey (5Y4.5/1), from 24-257 cm grey (2.5Y5/0 to 2.5Y6/0).
41-70 cm: mottled.
55-75 cm: weak H_2S smell.

212-257 cm: dark interval (very dark grey, 2.5Y3/0) with indistinct layers, lighter and more patchy at the base. Dark parts: silty clay to clayey silt.

257-483 cm: slightly reddish grey (10Y5/1) ("red layers").
267-275 cm: dark layers, mottled
275-296 cm: dark layers, 2 cm of black layer at base.

312-314 cm: black interval
314-320 cm: dark mottles

351-372 cm: indistinct dark layers and patches.
352-355 cm: flakes of hydrotroillite.

390 cm: black flakes

422-600 cm: dark grey mottles, patchy, indistinct

450-600 cm: dispersed sulfidic minerals
460-600 cm: mottles, indistinct

503 cm: brownish layer, indistinct

510-536 cm: rough-shaped structures with slightly changing color
536-600 cm: mottled, aprtly indistinct layers
Remark: dark color ("hydrotroillite") disappears when exposed to air.

GeoB 15220-1 GC-4 **METEOR EXPEDITION M84/2**

Location: Batumi Reference Station

Lat.: 41°57.127'N Date: 04.03.2011

Lon.: 41°16.855'E Recovery: 483 cm

Water depth: 878 m Liner: PVC

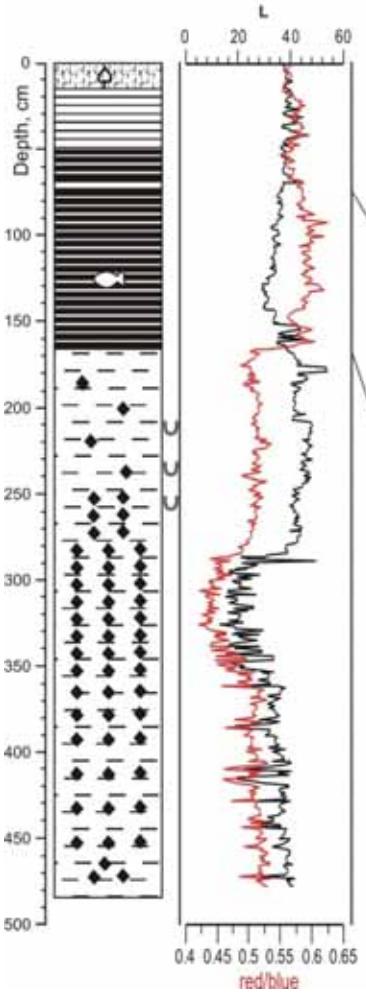

0-72 cm. UNIT 1: Upper part (0-14 cm) dark grey (5Y4/1) finely (<mm) laminated clay, fluffy without distinct light layers. Below finely (<mm) laminated dark grey (5Y4/1) clay with light (5Y6/2, light olive grey) bands of coccolith-layers. Slight H_2S smell.
- 11 cm: piece of wood (4 cm long)
- 37-42 cm: darker interval
- 44 cm: distinct group of coccolith layers
- 51-69 cm: transition sapropel. 64.5 cm = light layer
- 69-72 cm: basal coccolith layers

72-166 cm. UNIT 2: Finely (<mm) laminated clay (sapropel). Very dark grey (5Y3/1) grading into very dark greyish brown (2.5Y3/2) below ~140 cm.
- 106 cm: isolated light <1 mm lamination (smear slide: coccoliths)
- 124 cm: flat, cm-scale phosphatic concretion (fish remains), very dark brown (10YR2/2)
- 127 cm: flat, 5 cm long phosphatic concretion (fish remains)
- 129 cm: nodular concretion (wood?)
- 139.5 cm: light layer (smear slide: relatively abundant aragonite needles)
- 150 cm: aragonite layers
- 155-164 cm: aragonite layers (5Y7/3, pale yellow)

166-483 cm: UNIT 3: lacustrine mud (slightly silty clay to silty clay)
- 166-171 cm: dark grey to grey (5Y4.5/1)
- 170-286 cm: finely dispersed hydrotroillite flakes
- 171-190 cm: grey (5Y5/1)
- 190-203 cm: 5Y4.5/1 (dark grey to grey)
- 203-207 cm: 5Y5/1 (grey)
- 207-209 cm: 5Y4.5/1 (dark grey to grey)
- 211-251 cm: mottled, bioturbated
- 250-284 cm: rel. distinct dark layers (~2 mm thick) in cm-intervals
- 284-463 cm: cm-scale black layers (5Y2.5/1) in cm-scale alternation with lighter intervals. Becoming gradually less frequent and disctinct

463-483 cm: indistinct dark grey to black layers and dark grey mottles

GeoB 15226 GC-5	**METEOR EXPEDITION M84/2**
Location: Pechori Mound	
Lat.: 41°58.794'N	Date: 06.03.2011
Lon.: 41°07.569'E	Recovery: 487 cm
Water depth: 1045 m	Liner: PVC

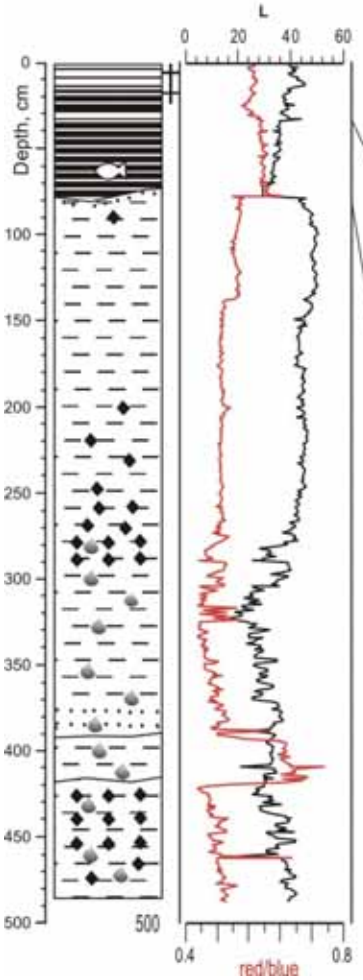

0-33 cm. UNIT 1: Finely (<mm) laminated clay with light bands of coccolith-layers (5Y5/1).
16-29 cm: transition sapropel (5Y4.5/1, dark grey)
29-33 cm: basal group of coccolith layers
upper 25 cm: core disturbed while core retrieval.
sediment layers are inclined

33-77 cm. UNIT 2: Finely (<mm) laminated clay (sapropel). Inclined sediment layers.
33-66 cm: olive grey (5Y4/2)
55 cm: isolated light <1 mm lamination
63 cm: fish remains
66-78 cm: dark olive grey
76 cm: cm thick very slightly oil stained yellowish brown layer (10YR5/6)
Note: No aragonite layers. deformed sediment between 70-77 cm (slumping). Erosional truncation at the base of Unit 2. 5 mm thick fine-sandy layer at base (2.5Y3/0, very dark grey)

77-487 cm: UNIT 3: lacustrine mud (clay to slightly silty clay)
H_2S smell from 77 to ca. 200 cm
78-96 cm: grey (2.5Y5/0) with few indistinct dark flakes
96-108 cm: (light) grey (5Y6/1)
108-118 cm: grey (5Y5/1)
118-136 cm: (light) grey (5Y6/1)
136-200 cm: indistict layering of lighter (5Y5.5/1, grey) and darker layers (2.5Y4/0, dark grey)
176-487 cm: gas bubbles occur at smoothed sediment surface
200-289 cm: slightly dark/light mottled, getting more pronounced further downcore.
273-289 cm: dark interval (5Y2.5/1, black), darker parts sulity clay
279-392 cm: oil-stained cracks
289-303 cm: lighter interval (5Y5/1, grey)
303-379 cm: dark interval, getting lighter downcore, disturbed bedding, relative indistinct layers
333-359 cm: less oil stained
344-364 cm: large mottels
364-379 cm: relatively distinct disturbed layers, oil-stained faults
377 and 383 cm: 5 mm thick slightly clayey, silty fine sand layers, oil-stained
390-417 cm: dark yellowish brown (10YR4/4) clay, slightly oil stained down to 429 cm. clay above this layer is stiff, below softer. Upper and lower conctact discordant
417-487 cm: distinct layers with undulating base, several cm thick, occasionally truncated by fault, upper part black (5Y2.5/19, gradually getting lighter.
426-465 cm: very fine, oil-stained cracks,
463-487 cm: indistinct layers with mottles
465-487 cm: very fine cracks with oil staining and very fine oil drops

GeoB 15235-1 GC-6	**METEOR EXPEDITION M84/2**
Location: Adjara Ridge	
Lat.: 41°57.277'N	Date: 09.03.2011
Lon.: 41°17.270'E	Recovery: 150 cm
Water depth: 887 m	Liner: Plastic hose

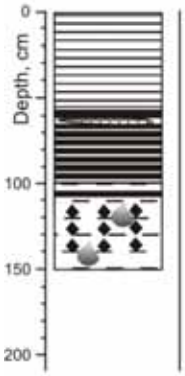

0-65 cm. UNIT 1: Finely laminated coccolith ooze. Color from 5Y5/1 (grey) in lighter parts to 5Y6/3 (pale olive) in darker intervals.
54 cm: final invasion coccoliths:
54-62 cm: transition sapropel
62-65 cm: basal coccolith layers (first occurrence), carbonate cemented

65-107 cm. UNIT 2: Finely (<mm) laminated clay (sapropel). Very dark grey (5Y3.5/1) to dark grey (5Y4/1) alternations with some distinct dark layers. Lower part lighter (5Y5.5/1, grey).
73 cm: two thin (2-3 mm) light layers resembling Unit 3 material ("Degens layers"?)
80-83 cm: two 3 mm thick light layers; 80 cm: top aragonite layer
100-103 cm: thick interval of Unit 3-like mud

107-150 cm: UNIT 3: lacustrine mud.
below 111 cm: oil-stained cracks; below 175 cm: oil in entire sediment
113-115 cm: black interval (5Y2.5/1)
128-140 cm: black interval (indistinct layer)

GeoB 15236-1 GC-7	**METEOR EXPEDITION M84/2**
Location: Batumi Seep Area	
Lat.: 41°57.581'N	Date: 09.03.2011
Lon.: 41°17.422'E	Recovery: 220 cm
Water depth: 840 m	Liner: Plastic hose

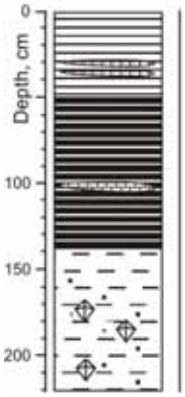

0-49 cm. UNIT 1: Finely laminated coccolith ooze. Color: 5Y5/2 (olive grey).
31-32, 35-37 cm: carbonate-cemented coccolith ooze layers

49-139 cm. UNIT 2: Finely (<mm) laminated clay (sapropel), dark olive grey (5Y3/2), dark grey (5Y4/1) towards the base.
100-103 cm: carbonate-cemented sapropel layers

139-220 cm: UNIT 3: Clay, slightly fine-sandy because of indurated clay particles. Sand content increases slightly towards base of core. Color: grey, below 200 cm light grey to grey (5Y6/1).
below 170 cm: finely dispersed, cm-sized gas hydrates

GeoB 15241-2 GC-8	**METEOR EXPEDITION M84/2**
Location: Batumi Seep Area	
Lat.: 41°57.469'N	Date: 11.03.2011
Lon.: 41°17.177'E	Recovery: 208 cm
Water depth: 849 m	Liner: Plastic hose

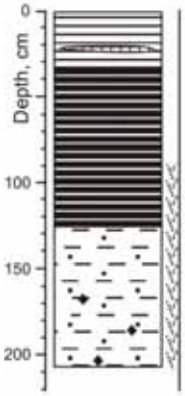

0-33 cm. UNIT 1: Finely laminated coccolith ooze. Color: 5Y5/2 (olive grey). First occurrence of E. hux. at 33 cm, transition sapropel from 30-32 cm.
20-22 cm: carbonate-cemented coccolith ooze layers. Above this interval slightly sandy components,

33-126 cm. UNIT 2: Finely (<mm) laminated clay (sapropel), dark olive grey (5Y3/2), dark grey (5Y4/1) towards the base.
below 90 cm: degassing structures
99 cm: single light lamination
108 cm: uppermost aragonite layer, 124 cm: base of aragonite layers

126-208 cm: UNIT 3: Clay, slightly fine-sandy because of indurated clay particles. Color: light grey to grey (5Y6/1). Abundant degassing cracks.

164 cm: some dark flakes
Generally strong H_2S smell

GeoB 15243 GC-9	**METEOR EXPEDITION M84/2**
Location: Poti Seep	
Lat.: 41°57.907'N	Date: 11.03.2011
Lon.: 41°18.270'E	Recovery: 146 cm
Water depth: 875 m	Liner: Plastic hose

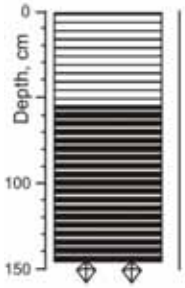

0-53 cm. UNIT 1: Finely laminated coccolith ooze. Color: 5Y5/2 (olive grey). First occurrence of E. hux. at 53 cm, transition sapropel from 36-50 cm.

53-146 cm. UNIT 2: Finely (<mm) laminated clay (sapropel), dark olive grey (5Y3/2) to dark grey (5Y4/1)
below 90 cm: degassing structures

127 cm: single light lamination

Small gas hydrates in core catcher

GeoB 15244-2 GC-11	**METEOR EXPEDITION M84/2**
Location: Poti Seep	
Lat.: 41°57.876'N	Date: 11.03.2011
Lon.: 41°18.329'E	Recovery: 140 cm
Water depth: 867 m	Liner: Plastic hose

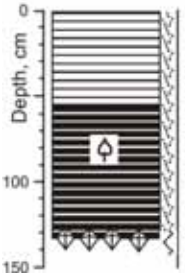

0-53 cm. UNIT 1: Finely laminated coccolith ooze. Color: 5Y5/2 (olive grey). First occurrence of E. hux. at 53 cm, final invasion at ca. 40 cm (heavy core disturbance due to sampling)
Degassing structures throughout core

53-140 cm. UNIT 2: Finely (<mm) laminated clay (sapropel), dark olive grey (5Y3/2) to dark grey (5Y4/1)

74 and 88 cm: wood remains
118-128 cm: aragonite layers
130-140 cm: massive hydrate layer, unclear if in Unit 2 and 3
lowest 10 cm soupy sediment

GeoB 15247-2 GC-12	**METEOR EXPEDITION M84/2**
Location: Batumi Seep Area	
Lat.: 41°57.565'N	Date: 12.03.2011
Lon.: 41°17.089'E	Recovery: 140 cm
Water depth: 840 m	Liner: Plastic hose

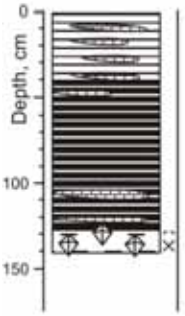

0-40 cm. UNIT 1: Finely laminated coccolith ooze. Color: 5Y5/2 (olive grey).
0-50 cm: carbonate-cemented layers

40-128 cm. UNIT 2: Finely (<mm) laminated clay (sapropel), dark olive grey (5Y3/2), dark grey (5Y4/1) towards the base.
104-108 cm: carbonate-cemented sapropel layers

128-140 cm: UNIT 3: Lacustrine mud, grey to light grey (5Y6/1).
128 cm: hydrate layer, 3mm thick, bubble fabric, below finely dispersed hydrates. Sediment gets moussy.

GeoB 15249-1 GC-15	**METEOR EXPEDITION M84/2**
Location: Batumi Seep Area	
Lat.: 41°57.605'N	Date: 12.03.2011
Lon.: 41°17.260'E	Recovery: 153 cm
Water depth: 842 m	Liner: Plastic hose

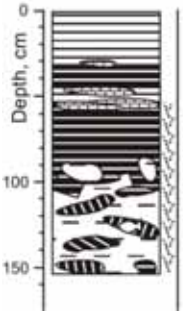

0-32 cm. Finely laminated coccolith ooze, gassy, soft. Color: 5Y5/2 (olive grey).
32-48 cm: no disinguishable lamination, sediment is moussy, relatively dark.
32-36 cm: sapropel-like clast with ca. 1 cm big concretion.
46-61 cm: carbonate-cemented layers, particularly between 48-52 cm. The latter interval is characterised by distiguishable laminations, as pale yellow cemented intervals, presumably base of Unit 1 (coccolith layers).
52-76 cm: gas-rich sediment almost moussy
76-104 cm: dark olive grey sapropel, indurated with low water content, partly as clasts with random orientation. Some degassing cracks
80 cm: grey lacustrine mud intruded into sapropel layers.
104-153 cm: dominant grey lacustrine clay but with abundant clasts of indurated sapropel. Some aragonite layers are visible.
128 cm: fishbones in sapropel-like sediments

GeoB 15251-1 GC-16	**METEOR EXPEDITION M84/2**
Location: Batumi Seep Area	
Lat.: 41°57.632'N	Date: 13.03.2011
Lon.: 41°17.079'E	Recovery: 180 cm
Water depth: 842 m	Liner: Plastic hose

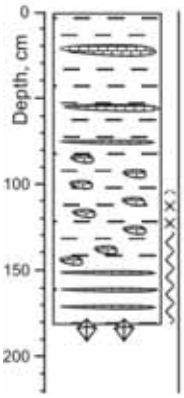

Highly disturbed clay to silty clay with abundant carbonate-cementation throughout the core. Most prominent intervals at 20-25, 54-56, 75-77, 150-165 cm. Lighter (5Y5/1) interval in the upper 23 cm, slightly darker bewtween 23 and 96 cm. Occasional light layers in the darker interval are rich in coccoliths (smearslides). Unit 1?
96-180 cm: grey clay
Hydrates in core catcher.

GeoB 15254 GC-19	**METEOR EXPEDITION M84/2**
Location: Pechori Reference Station	
Lat.: 41°58.800'N	Date: 13.03.2011
Lon.: 41°07.872'E	Recovery: 600 cm
Water depth: 1085 m	Liner: Plastic hose

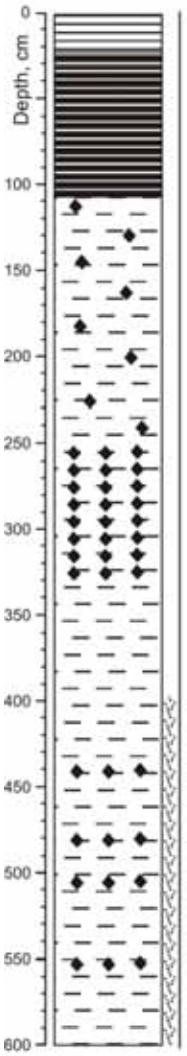

0-30 cm. UNIT 1: Upper part (0-14 cm) dark grey (5Y4/1) finely (<mm) laminated clay, fluffy without distinct light layers. Below finely (<mm) laminated dark grey (5Y4/1) clay with light (5Y6/2, light olive grey) bands of coccolith-layers. Slight H_2S smell.
22-28 cm: transition sapropel. 64.5 cm = light layer
28-30 cm: basal coccolith layers

30-107 cm. UNIT 2: Finely (<mm) laminated clay (sapropel). Very dark grey (5Y3/1) grading into very dark greyish brown (2.5Y3/2) in the lower part.
93-103 cm: aragonite layers (5Y7/3, pale yellow)

107-600 cm: UNIT 3: lacustrine mud (clay to silty clay) ith occasional black flakes of sulfidic minerals.
250-323 cm: black interval, 2-3 mm thick layering, getting gradally lighter until 365, below no layering distinguishable.

Below 393 degassing cracks.

Hardened bacl layers (2-3 mm) at 441, 482, 506 and 551 cm.

GeoB 15255 GC-20	**METEOR EXPEDITION M84/2**
Location: Pechori Rim	
Lat.: 41°58.893'N	Date: 13.03.2011
Lon.: 41°07.607'E	Recovery: 70 cm
Water depth: 1011 m	Liner: Plastic hose

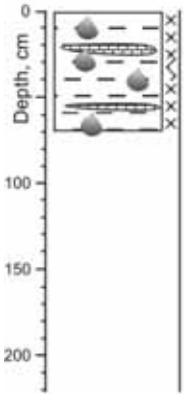

Highly disturbed clay to silty clay with abundant carbonate-cementation throughout the upper 25 cm of the core. Gashydrate are present in the entire core. Massive layer at 25-38 cm, smaler pieces below Carbonates: irregular shaped, pebbles as well as cemented coccolith layers.
28-40 cm: soupy layer, otherwise moussy.

GeoB 15258 GC-22	**METEOR EXPEDITION M84/2**
Location: Kulevi Ridge G2	
Lat.: 41°7.104'N	Date: 14.03.2011
Lon.: 41°22.753'E	Recovery: 142 cm
Water depth: 712 m	Liner: PVC

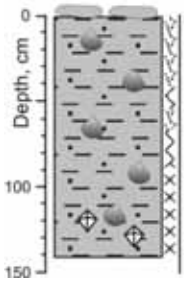

0-142 cm: Dark brown (5Y4/1) clay with sand-sized mud clasts. On top of liner 2 mudclasts have been found, 2 cm thick and 5-8 cm in diameter.
Oil-stained throughout core.
Degassing cracks,
soupy texture between 40-54, 64-86 cm,
moussy between 102-142 cm.

Below 110 cm: fine (<mm to 5 mm) gas hydrates. Sediment becomes also quite stiff and slightly darker (very dark brown, 5Y3/1)

GeoB 15259 GC-23	**METEOR EXPEDITION M84/2**
Location: Kulevi Ridge G1	
Lat.: 41°5.753'N	Date: 14.03.2011
Lon.: 41°8.449'E	Recovery: 270 cm
Water depth: 1121 m	Liner: PVC

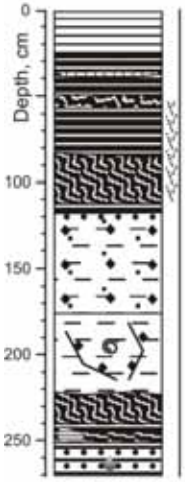

0-24 cm (?). UNIT 1: Finely laminated coccolith ooze with clear laminations in the upper 15 cm. Color: 5Y5/1 (grey).
17-17.5 and 23-24 cm: series of light coccolotih layers
24-37 cm: no light laminations (transition sapropel?), dark grey (5Y4/1)

24 (?)-115 cm. UNIT 2: Dark grey (5Y4/1) clay (sapropel) with faint laminations.
48-88 cm: occasional intercalation of 0.5 cm thick, slightly lighter clay layers.
50-54 cm: irregular bedding, bending of cm-thick lighter and darker layers
50-115 cm: degassing cracks, sediment is getting stiffer
56-58 cm: slightly lighter interval
60-73 cm: slightly darker
88 cm: unconformity, from 88 to 111 cm folded layers (slumping)
102-112 cm: aragonite laminae, folded
112-114 cm: aragonite laminae, not deformed

115 cm: 1 cm-thick, dark grey interval of fine sandy clayey silt
116-222 cm: UNIT 3: grey (5Y6/1) clay, slightly fine-sandy because of indurated clay particles and occasional calcareous microfossils.
123-173 cm: regular intercalation of sulfidic dark (very dark grey to black) layers in cm-intervals.
Hiatus at 173 cm?
173-222 cm: structureless clay, distincly stiffer than before, black-stained fault planes and cracks.
196 and 198 cm: small gastropods (~2 mm)

222-223 cm: erosive unconformity, irregular surface, above a ca. 2 mm thick darker layer.
222-240: distorted sediment (slumped). Very stiff dark grey sapropelic clay with <mm light laminations of coccolith ooze (smear slides at 224 and 243 cm). One distinct black layer in between. Eemian Sapropel?
240 cm: unconformity. 240-246 cm: same material as above, regular bedding, but with cm-sized clast of white, finely laminated material

252 cm: sharp contact. 252-270 cm: pale yellow layers of relatively well-cemented silty sand (carbonaceous particles, coccolith-bearing (smear-slide at 254 cm), intercalated with very dark grey, mm-thick clay layers. Clay layers have bituminous smell. Slightly oil-stained material in core catcher.

GeoB 15260-1 GC-24	**METEOR EXPEDITION M84/2**
Location: Batumi Seep Area	
Lat.: 41°75.580'N	Date: 14.03.2011
Lon.: 41°17.392'E	Recovery: 270 cm
Water depth:839 m	Liner: Plastic hose

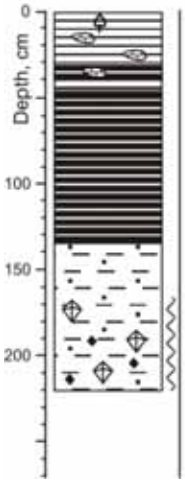

0-45 cm. UNIT 1: Finely laminated coccolith ooze. Color: 5Y5/2 (olive grey).
Two wood branches (8 cm length) at 5 cm
15-35 cm: carbonates
30-42 cm: transition sapropel
42-45 cm: basal coccolith layer

45-132 cm. UNIT 2: Finely (<mm) laminated clay (sapropel), dark olive grey (5Y3/2)
121-128 cm: aragonite laminae

132-270 cm: UNIT 3: Clay, slightly fine-sandy because of indurated clay particles. Color: grey (5Y4/1).
below 165 cm: moussy-soupy sediment.
below 168 cm: finely dispersed, cm-sized gas hydrates
below 186 cm: some flakes of sulfidic minerals.

GeoB 15261 GC-25	**METEOR EXPEDITION M84/2**
Location: Colkheti Seep	
Lat.: 41°58.082'N	Date: 14.03.2011
Lon.: 41°06.154'E	Recovery: 170 cm
Water depth: 1123 m	Liner: PVC

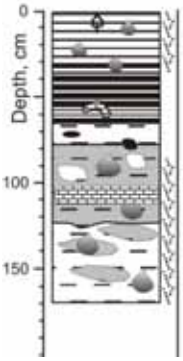

0-37 cm. Finely laminated coccolith ooze (UNIT 1), slightly oil-stained at bedding planes, degassing cracks until 38 cm. Color: 5Y5/2 (olive grey).
Wood branch (5 cm length) at 8 cm.
30-32 cm: series of light layers
32-35 cm: dark interval sapropel
35-37 cm: basal coccolith layers

37-65 cm. Finely (<mm) laminated clay (sapropel, UNIT 2?), dark olive grey (5Y3/2)
56 cm: carbonate-cemented fragment of Unit 1, flat, irregular shaped, subrounded
57-58 cm: light layers (smear slide: coccoliths) (displaced or base of Unit 1?)
65-67 cm: indistinct contact to dominantely grey sediments (UNIT 3).
67-78 cm: dominantely grey sediment with cm-sized parts of sapropel.
78-113 cm: dominated by brownish-grey sediment
below 83 cm: disturbed, gas-rich. Oil-stained along cracks.
92, 95, 100 cm: small (<cm) patches of pale yellow ooze
110-113 cm: laminated, cemented pale yellow layers (ca. 2 mm thick)
113-170 cm: increasing amount of grey, Unit 3-like material with abundant brownish-grey patches.

GeoB 15268-2 GC-27	**METEOR EXPEDITION M84/2**
Location: Samsun, Ordu Ridge Patch 2	
Lat.: 41°32.670'N	Date: 16.03.2011
Lon.: 37°37.460'E	Recovery: 294 cm
Water depth: 1535 m	Liner: PVC

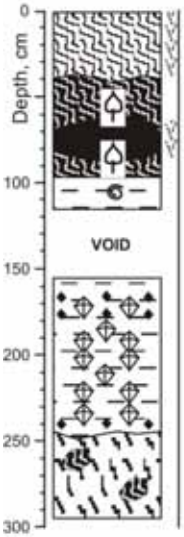

0-22 cm Finely laminated, olive grey (5Y5/1) coccolith ooze with distinct but deformed laminations, relatively soft with few degassing cracks (UNIT 1)
22-24 cm: discontinuity, wavy

24-64 cm: slighty stiffer, few cracks, dominant olive (5Y3/2) clay with some light olive grey (5Y6/2) layers, deformed.
54 cm: wood fragment (~3 mm)

64-80 cm: dark (very dark greyish brown, 2.5Y3/2) clayey clast, with subparallel degassing crakcs, stiffer than above.

80-98 cm: heavily folded laminae of light material (smearslide @ 85 cm: aragonite) in layers of olive (5Y3/2) dark olive grey (5Y6/2) color as above, but with lighter layers dominating.
88 cm: wood.
96-98 cm: at base darker layer (5Y5/2, olive grey) and olive (5Y5/3) layer. Base of UNIT 2.

98-260 cm: grey to light grey (5Y6/1) clay, lacustrine mud, Unit 3.
104 cm: gastropod (3 mm)
114-155 cm: void
166-177 cm:black (5Y2.5/1) layer
168-242 cm: gas hydrates massive and fine dispersed. Sediment relatively stiff with exception of direct contact to massive hydrates.
168-171 cm: massive hydrates
192-195, 199-202, 222-229, 234-238 cm: massive hydrates
242-244 cm: black layer

Stiff, heavily deformed clayey material. 244-253: some light laminae (smearslides @ 248 and 251 cm: coccoliths). Contains subangular clasts of very dark greyish brown sapopel-like material, similar to the clast at 64-80 cm; in some cases with spots of pale yellow material (smearslide: big flakes of mica, rare coccoliths). Rest of the matrixwith olive (5Y5/4) and olive grey (5Y5/2) layers (cm-scale). Occasional indistinct, elongated patches of black (5Y2.5/1) sediment. Light layers at base (smearsliede 287 cm: aragonite). Older (Eemian?) sapropel, reworked, extruded by diapiric activity?

GeoB 15503-1 GC-28	**METEOR EXPEDITION M84/2**
Location: Ordu Ridge Patch 3 Flare	
Lat.: 41°32.443'N	Date: 20.03.2011
Lon.: 37°36.888'E	Recovery: 298 cm
Water depth: 1523 m	Liner: PVC Liner

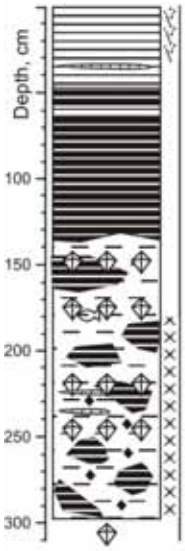

0-64 cm: UNIT 1, finely laminated coccolith ooze, grey (5Y5/2, olive grey). Upper 31 cm heavily affected by degassing, sedimentary structures mostly disurbed. Below 20 cm more distinct light laminations visible.
- 36-37 cm: slightly carbonate cemented interval
- 47-62 cm: transition sapropel
- 62-64 cm: coccolith layers (smear slide)

64-136 cm: relatively stiff sapropel, without distinguishable laminations. Degassing cracks abundant.
- 110-116 cm: slightly less stiff interval, dark olive grey (5Y3/2)

136-298 cm: grey (5Y5/1) clay (UNIT 3) with clasts of relatively stiff, sapropel-like material in sizes of up to 10 cm.
- 138 cm: patch with light layers (smear slide: aragonite). Clasts show signs of heavy deformation.
- 145-164 cm: massive hydrates
- 163 cm: light layers in sapropel-like patch (aragonite)
- 168 cm: fish
- 172-178 cm: massiv hydrates
- 178-298 cm: moussy sediment
- 190-298 cm: flakes of black sulfidic minerals
- 202 cm: olive (5Y5/4) clast with carbonate, platy
- 220-225 cm: gas hydrates
- 222 cm: black flakes
- 233 cm: carbonate, platy
- 243 cm: small, elongated carbonate
- 249-253: massive hydrate
- below 282 cm: more abundant black flakes

core catcher contains small hydrates

GeoB 15504 GC-29	**METEOR EXPEDITION M84/2**
Location: Ordu Ridge Patch 5	
Lat.: 41°31.843'N	Date: 20.03.2011
Lon.: 37°36.496'E	Recovery: 210 cm
Water depth: 1589 m	Liner: PVC

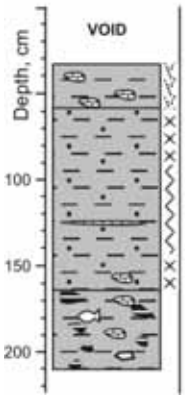

32-90 cm: grey clay, stiff, degassing
32-58 cm: abundant carbonate pebbles, rounded
58-90 cm: clay with fine sandy particles, softer, moussy

90-166 cm: clay with small, sand-sized black particles
90-142 cm: soupy
122 cm: carbonate

142-166 cm: moussy

166-210 cm: stiff mud-breccia with some small carbonate clasts, degassing cracks, <cm-scale dark, sapropelic material and small flakes of lighter material in grey clay matrix.

GeoB 15505-1 GC-30	**METEOR EXPEDITION M84/2**
Location: Ordu Ridge Patch 7, Flare	
Lat.: 41°31.843'N	Date: 20.03.2011
Lon.: 37°36.496'E	Recovery: 210 cm
Water depth: 1589 m	Liner: PVC

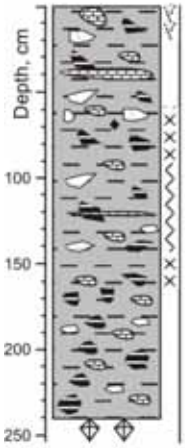

2 cm carbonate (irregular-shaped) at top. Otherwise grey (5Y5/1) clay with abundant pebbles of carbonate, not fully cemented. Soft and gas-rich in upper 17 cm.
28 cm relatively stiff, dark, laminated clast at 28 cm
31 cm: very small flake of black material
38-40 cm: massive carbonate layer
41-66 cm: dominant brownish (5Y5/3) matrix, interval with light sandy layers (pale yellow, 5Y5/3)and dark sapropel-sized fragments in cm-size. Carbonate pebbles and plates throughout the core.
66-78 cm: lighter interval (5Y6/1, light grey) with sapropel clasts but few light layers.
78-145 cm: darker than above, but with indistinct changes between lighter and slightly darker matrix.
120 cm: 1 cm layered carbonate
148-156 cm: light interval with few clasts

156-178 cm: slightly darker matrix with few of the sandy light material
175-179 cm: lighter interval, almost barren of clasts
179-190 cm: darker matrix, abundant light sandy material
190-240 cm: lighter than above, only few of the light sandy patches

Core catcher with massive hydrates

GeoB 15507 GC-31	**METEOR EXPEDITION M84/2**
Location: Ordu Ridge Patch 7, Flare	
Lat.: 41°31.138'N	Date: 21.03.2011
Lon.: 37°37.347'E	Recovery: 157 cm
Water depth: 1505 m	Liner: PVC

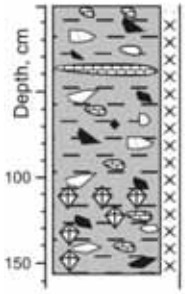

0-4 cm: Highly water saturated clay with white, indurated particles, up to 1 mm in size
4-157 cm: Clay, stiffer than at top, with occasional small clasts
18-22 cm: clayey inclusions, semi-lithified, up to 1 cm in size
37-44 cm: light olive grey, carbonate-cemented interval

109-114 cm: massive hydrate
122 cm: carbonate-cemented clasts with fine layering.
122 cm: gas hydrate
134 and 138 cm: gas hydrate pieces
139-152 cm: vain of hydrate

GeoB 15508 GC-32 **METEOR EXPEDITION M84/2**

Location: Samsun, New Ridge

Lat.: 41°22.848'N

Lon.: 37°48.156'E

Water depth: 1527 m

Date: 21.03.2011

Recovery: 300 cm

Liner: PVC

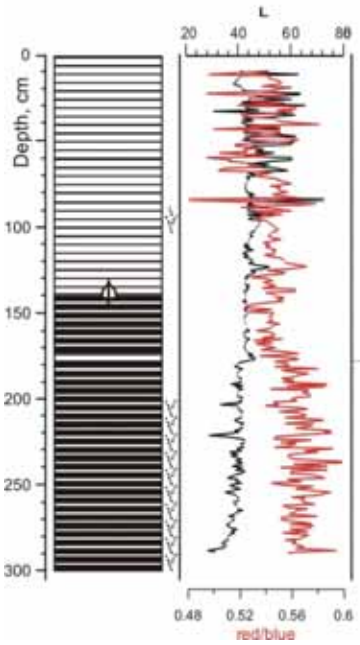

0-179 cm. UNIT 1: Finely (<mm) laminated coccolith ooze comprising dark grey (5Y4/1) clay with light (5Y6/2, light olive grey) of coccolith-layers. Intercalated are homogeneous grey clay layers of up to 1 cm thickness getting more frequently downcore. Core disturbance in upper 80 cm.
Strong H_2S smell troughout core.
54 cm: black stripe

85-103 cm: degassing structures

140 cm: part of a leaf
140-175 cm: transition sapropel

179-300 cm. UNIT 2: Finely (<mm) laminated clay (sapropel), very dark grey (5Y3/1). Aragonite layers not reached. Homogeneous clay layers are more abundant than before, cm-scale alternation of clay layer and sapropel.

200-300 cm: degassing

GeoB 15512-1 GC-33 **METEOR EXPEDITION M84/2**

Location: Kerch Flare

Lat.: 41°37.420'N

Lon.: 35°42.359'E

Water depth: 906 m

Date: 23.03.2011

Recovery: 101 cm

Liner: PVC

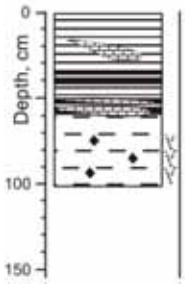

0-58 (?) cm. UNIT 1: Finely laminated coccolith ooze, very water-rich. Color: 5Y5/2 (olive grey).
9 cm: spot, covered with greenish film (bacteria?)
17-27 cm: tilted, partly cemented coccolith ooze, irregular, not as a layer, olive grey (5Y5/2)
31 cm: final occurrence of *E. huxleyi*
32-44 cm: transition sapropel (dark grey, 5Y4/1)
44-47 cm: lighter interval (first occurrence of *E. huxleyi*? Smear slide at 44 cm with some coccoliths but a lot of calcareous (?) debris), 5Y5/2, olive grey
47-50 cm: dark grey (5Y4/1, dark grey) clay (sapropel?)
52 cm: weakly cemented carbonate layer
57-60 cm: carbonate-cemented layer (5Y6/1 light grey), abundant coccoiths in smear slide at 56 cm.

58-101 cm: grey (5Y5/1) clay with sparse black flakes (UNIT 3)
below 71 cm: affected by heavy degassing

GeoB 15513-1 GC-34	**METEOR EXPEDITION M84/2**
Location: Kerch Flare	
Lat.: 41°37.386'N	Date: 23.03.2011
Lon.: 35°42.164'E	Recovery: 557 cm
Water depth: 878 m	Liner: PVC

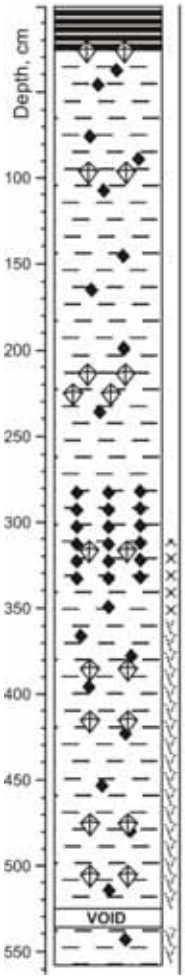

0-27 cm. UNIT 2: Finely (<mm) laminated, clayey tsapropel, dark olive grey (5Y3/2) to very dark grey (5Y5/1). shows some degassing structures. Platy gas hydrates at the base of the sapropel (27-32 cm). No aragonite layers discernable.

27-557 cm. UNIT 3: Grey clay,
34-48, 75-108 cm: black flakes

94-104 cm: hydrates

146-149 cm: larger black patches
160-165, 196-210 cm: black flakes

213-216, 223-228 cm: gas hydrates
237-240 cm: black flakes

282-334 cm: black interval with light layers intercalated
307-353 cm: moussy
318 cm: platy hydrates
334-557 cm: clay is more olive grey (5Y5/2) than grey.
318 cm: platy hydrates
334-384 cm: black flake, occasional flakes until 557 cm
353 cm an below: stiff with some degassing cracks

383-389, 418-423, 473-474, 509-514 cm: gas hydrates, dispersed, platy

525-537 cm: void

GeoB 15512-2 GC-35	**METEOR EXPEDITION M84/2**
Location: Kerch Flare	
Lat.: 44°37.419'N	Date: 24.03.2011
Lon.: 35°42.359'E	Recovery: 137 cm
Water depth: 894 m	Liner: PVC

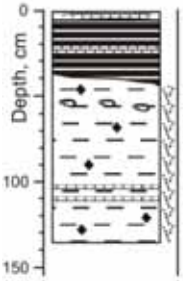

0-7 cm: pale olive (5Y6/3), slightly carbonate cemented clay with light laminations (coccolith ooze).
7-21 cm: olive grey (5Y5/2), finely laminated clay (sapropel) with mm-scale homogenous clay layers
21-25 cm: pale olive (5Y6/3), slightly carbonate cemented interval

38-43 cm: diffuse boundary between sapropel-like sediment and grey clay of Unit 3, with some black flakes
49-54 cm: carbonate particles (<cm in size), light olive grey (5Y6/2), below light grey to grey (5Y6/1)
103 and 111 cm: carbonate layers

GeoB 15516-1 GC-36	**METEOR EXPEDITION M84/2**
Location: Kerch Flare	
Lat.: 41°37.230'N	Date: 24.03.2011
Lon.: 35°42.282'E	Recovery: 476 cm
Water depth: 888 m	Liner: PVC

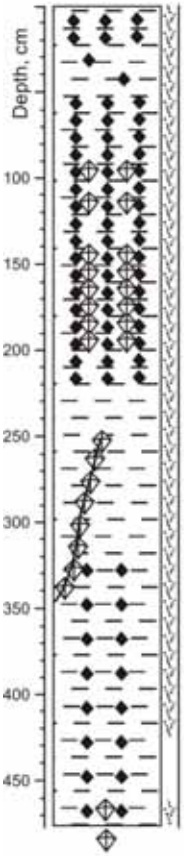

0-476 cm. UNIT 3: Grey clay
0-425 cm: degassing structures
2-23 cm: black layers
23-52 cm: black flakes
52-220 cm: black layers, 168-220 cm: completely black
220-328 cm: no black flakes
328-476 cm: indistinct dark layers, cm-scale
462-475 cm: degassing cracks

platy gas hydrates between 94-95, 100-102, 114-115, 144-145, 151-159, 166-170, 173-175, 178-189, 195-203 cm
vain-filling hydrate from 255-350 cm (3-4 mm thick)
466-477 cm: very fine hydrate
CC: very fine hydrate

GeoB 15518-1 GC-37	**METEOR EXPEDITION M84/2**
Location: Kerch Flare	
Lat.: 41°37.182'N	Date: 25.03.2011
Lon.: 35°42.279'E	Recovery: 375 cm
Water depth: 887 m	Liner: PVC

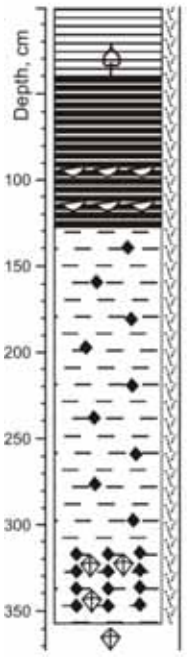

0-40 cm: UNIT 1: finely laminated coccolith ooze, olive grey (5Y5/2)
47 cm: wood branch

40-128 cm: UNIT 2: dark grey (5Y4/1) sapropel
96 and 116 cm: light layer with shell hash
42; 58-60, 95, 105, 115 cm: homogenous clay layers, ~1 cm thick
no aragonite layers, but also no sign of hiatus

128-257 cm: UNIT 3: laxustrine mud, grey (5Y5/1), at the top 1 cm of homogeneous olive grey (5Y5/2) clay
128-357 cm: black flakes
318-357 cm: gas hydrates, partly in massive layers (118-124 cm)

generally degassing cracks, from 318-357 almost moussy.

Gas hydrate in core catcher

GeoB 15519-1 GC-38 **METEOR EXPEDITION M84/2**

Location: Kerch, Background

Lat.: 41°37.171'N Date: 25.03.2011

Lon.: 35°41.763'E Recovery: 574 cm

Water depth: 896 m Liner: PVC

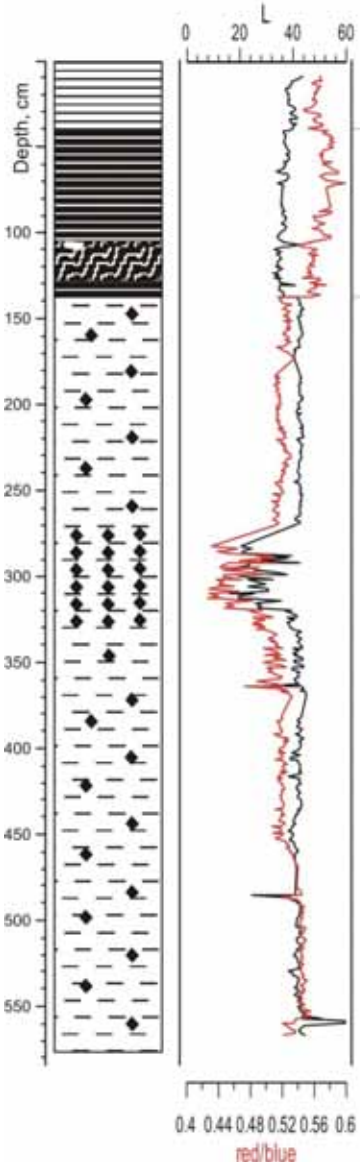

0-41 cm: UNIT 1. Finely laminated, olive grey (5Y5/2) coccolith ooze.
27, 28, 38 cm: homogenous, grey (5Y5/1) clay layers (~0.5 cm thick)

41-139 cm: UNIT 2. Dark olive grey sapropel.

105-129 cm: disturbed bedding (slumping?) including a patch of grey (5Y5/1) clay at 107-109 cm, presumably with Unit 3 material
129-139 cm: undisturbed aragonite layers

139-574 cm: UNIT 3. Dark grey clay with isolated black patches

272-330 cm: black interval, dominated by "hydrotroillite"

330-574 cm: rare black patches

GeoB 15520 GC-39	**METEOR EXPEDITION M84/2**
Location: Kerch, Flare	
Lat.: 41°37.166'N	Date: 25.03.2011
Lon.: 35°42.261'E	Recovery: 163 cm
Water depth: 887 m	Liner: PVC

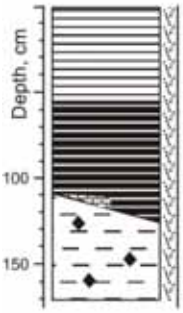

0-54 cm: UNIT 1. Finely laminated coccolith ooze, dark grey (5Y4/1) in the upper 3 cm, below olive grey olive grey (5Y4.5/2).
- 2-12 cm: carbonate cemented interval
- 28-29 cm: band of light (Olive grey, 5Y5/2) layers
- 38, 44-45 cm: homogeneous clay layers
- 47-49 cm: band of coccolith layes (smear slide)
- 53-54 cm: basal coccolith layers

54-110 cm: UNIT 2. Finely laminated sapropel (dark grey, 5Y4/1), at the top 2 cm of homogeneous clay layer (grey to dark grey, 5Y4.5/1)
- 95 cm: 1 cm thick homogeneous clay layer

110-126 cm: oblique, erosive boundary between Unit 2 and Unit 3.
110-116 cm: carbonate cementation along the boundary
110-163 cm: UNIT 3. Grey (5Y5/1) clay with few drk patches

entire core strongly affected by degassing.

GeoB 15524-1 GC-40	**METEOR EXPEDITION M84/2**
Location: Helgoland MV	
Lat.: 41°17.322'N	Date: 27.03.2011
Lon.: 35°0.065'E	Recovery: 457 cm
Water depth: 2082 m	Liner: PVC

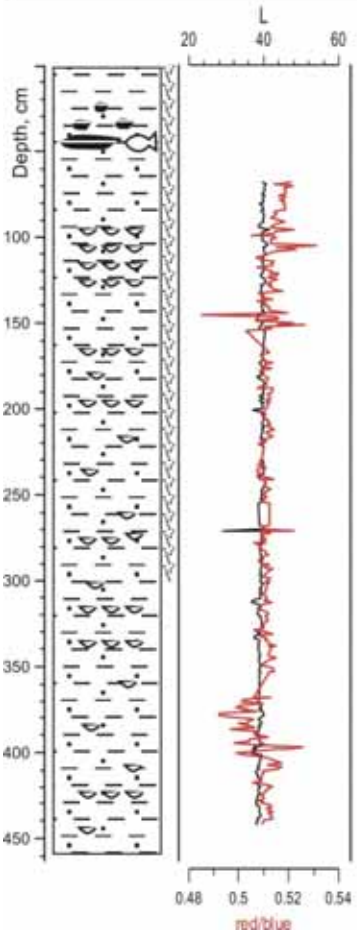

0-59 cm: extremely water saturated grey (5Y5/1) clay, degassing
- 25-29 cm: small (few mm) clasts of dark material (sapropel)
- below 30 cm: increasing content of sand particles (clay pebbles and dark minerals)
- 34-38 cm: bigger (~2 mm) clasts of sapropel
- 42-46 cm: big clast of sapropel with light laminations (smear slide: coccoliths)
- 46 cm: fish remains (2 cm patch)
- 50-59 cm: bubbles from degassing

degassing structures down to 300 cm, becoming less distinct below 160 cm

below 59 cm: grey clay with varying amounts of sand particles, stiffer than before
- 93 cm: homogenous clay layer
- 95-96 cm: homogenous clay layer, <mm sized shell debris at bottom
- 104.5-105.5 cm: three shell hash layers, intercalated with homogenous clay layers, lowermost layers is the thickest (2-3 mm)
- until 109 cm: sequence of ~0.5 cm thick clay layers with coarser material at base
- 109-110 cm: fine sandy clay layer
- 110-111.5 cm: clay layer
- 112 cm: coarse layer with shell hash. Below continued alternation of fine-sand and clay layers
- 126, 126.5 cm: coarse layers with some shell debris, intercalated with clay layers
- 130-146 cm: fine sandy clay
- 145-152 cm: mm-thick pale yellow layer (smear slide: coccoliths), below mm of light olive grey clay, below sandy clay until 152 cm, fining downward, with cm-sized clast of lithified, black shale; base: shell hash
- 152-457 cm: sandy clay, occasional shell fragments (mm-sized), below 180 cm increasing amount of mm-sized shell fragments
- 165 cm: shell hash
- 182 cm: clay layer
- 197.5 cm: clay layer with shell hash at base
- 210 cm: clay layer
- 225-230 cm: void

below 240 cm: shell fragments getting bigger (up to 2-3 mm in size)
occasional fragments (~5 mm in size) of dark, lithified clasts, rounded
- 273-273.5 cm: 2 discontinous shell hash layers, coccolith-bearing (smear slides)
- 305, 312 cm: shell hash (< mm sized)
- 314 cm: coarser shell hash with 5 mm sized shell fragments
- 333-335 cm: sandy mud, shell fragments
- 424 cm: shell hash

GeoB 15525-1 GC-41	**METEOR EXPEDITION M84/2**
Location: Helgoland MV, deep T-logging	
Lat.: 41°17.311'N	Date: 25.03.2011
Lon.: 35°00.037'E	Recovery: 100 cm
Water depth: 2088 m	Liner: PVC

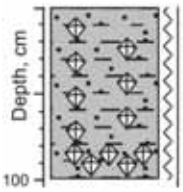

0-100 cm: fine-grained mud breccia without clasts bigger than 1 mm.
Very soupy sediment, gas hydrates occur thorughout the core, particularly massive below 82 cm.
Hydrates are typically preserved with bubble fabric.
Rare shell fragments are present (mm-sized).

GeoB 15527 GC-42	**METEOR EXPEDITION M84/2**
Location: Dvurechenskii MV, deep T-logging	
Lat.: 44°17.041'N	Date: 27.03.2011
Lon.: 34°58.891'E	Recovery: 400 cm
Water depth: 2051 m	Liner: PVC

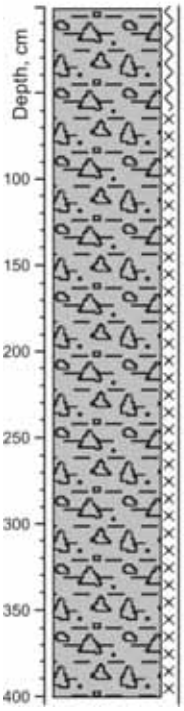

0-400 cm: dark grey (5Y4/1) mudbreccia with clasts of up to 4 cm in size. Upper 60 cm is very water-rich (soupy), below with signs of heavy degassing to moussy texture.
Mudclasts have been found in the following depths: 20, 27, 32, 80, 98-100, 102, 121, 123, 134, 138, 194, 216, 243, 244, 290, 296, 325, 327, 334, 339, 343, 360, 390 cm

GeoB 15525-3 GC-43	**METEOR EXPEDITION M84/2**
Location: Helgoland MV, deep T-Logging	
Lat. 44°17.303'N	Date: 29.03.2011
Lon.: 35°00.039'E	Recovery: -
Water depth: 2080 m	Liner: PVC

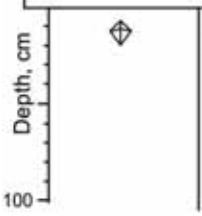

Liquid clay, gas hydrates in core catcher. Outside of core barrel stained with mud and shell hash (2-3 mm in size). No sediment left in liner.

GeoB 15532 GC-45	**METEOR EXPEDITION M84/2**
Location: Background	
Lat.: 41°17.295'N	Date: 29.03.2011
Lon.: 35°00.044'E	Recovery: 569 cm
Water depth: 2078 m	Liner: PVC

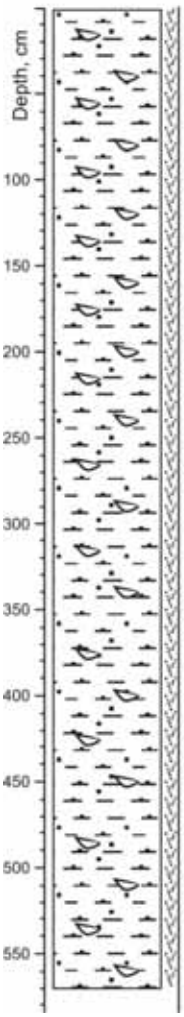

0-569 cm: Structureless grey clay with shell debris (up to 4 mm in size), rock-clasts (dominantely blsand-sized ack in color). Affected by degassing, especially in upper 20 cm. Mud was warm (21.6 at core catcher) when taken out of liner.

GeoB 15533-1 GC-46	**METEOR EXPEDITION M84/2**
Location: Background	
Lat.: 41°18.166'N	Date: 29.03.2011
Lon.: 34°59.162'E	Recovery: 590 cm
Water depth: 2054 m	Liner: PVC

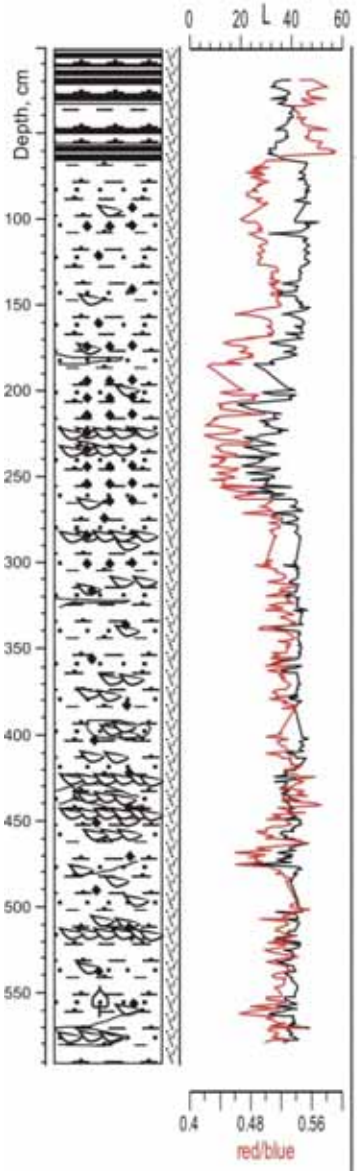

0-64 cm: Finely lamianted clayey, silty sapropel (UNIT 2), intercalated with silty clayey turbidites.
- 18-20, 24-28.5, 29.5-30, 31-31.5 cm: turbidites
- 30-31 cm: aragonite layers
- 32.5-47 cm: massive silty clayey turbidite, with irregular lower boundary
- 49-54 cm: turbidite

64-590 cm: Grey (5Y5/1) lacustrine mud (UNIT 3) intercalated with abundant turbidites, ranging from mm to dm in thickness. Slight brownish hue until 149 cm.
- 64-92 cm: some layers of sandy black material (thickness up to 1.5 mm). Black patches of hydrotroillite around 90-92 cm
- 102 cm: black interval, sandy
- 108-110 cm: sandy layers with dark patches
- 137-139 cm: sandy layer
- 143-145 cm: sandy layer, darker
- 153-156 cm: diffuse dark grey (5Y4/0) interval, below more greenish hue
- 166-169 cm: mm-sized sandy layer, flaser bedding
- 170-185 cm: cm-sized black layers in grey (2.5Y5/0) clay
- 179-181 cm: sand layer, wedge-shaped
- 190-208 cm: diffuse, cm-thick black layers
- 207-211 cm: silty clay
- 208-265 cm: dominantely black with few light layers
- 214-216 cm: sand
- 225 cm: mm thick layer with shell debris
- 230-231.5 cm: lenticular bed with shell debris
- 231.5-251 cm: cm-thick layering of clayey to silty clay
- 251.5 cm: silty sand
- 265 cm and below: dominantely slight greenish hue
- 274 cm: silty black flakes, 0.5 cm in length
- 276-277 cm: sand with few shell debris
- 287-289 cm: shell debris with sand layer at base
- 299 cm: black sandy layer
- below 299 cm: less abundant black flakes, alternation of lighter and darker layers, from mm-scale to ~3 cm in thickness
- 311 cm: discontinous shell debris layer
- 319-320 cm: sand layer with shell debris
- 322-324 cm: wedge-shaped sandy layer
- 327.5 and 332 cm: mm thick sandy layers
- 337-339 cm: black layer, below flaser-bedded, mm-thick sand layers
- 357-360 cm: brownish sand layer with some shell debris, wedge-shaped
- 362-364 cm: dark, coarse sand layer with shell debris at base
- 379 cm: discontinuous sand layer
- 389-391 cm: grey clay
- 393 cm: pocket with sand and shell debris in silty clay
- 411-412 cm: 2 darker layers with shell debris. Upper layer continuous, lower discontinuous
- 422-423 cm: shell-debris
- 423-424 cm: clay
- 424-430 cm: massive horizon of shell debris
- 430-432 cm: sand layer
- 432-440 cm: slumped (?) package of clay and silty clay with large pockets of shell debris
- 440-442 cm: brownish sand,
- 445-450 cm: shell layer
- 450-459 cm: indistinct darker intervals with faults
- 459-461 cm: mm-thick sand layers with shell horizon at base
- 467 cm: discontinous sand layer
- 470-480 cm: fault-intersected indistinct dark/light layers. Black pocket with shell fragments at 478 cm.
- 480 cm: black clayey flakes
- 488-489 cm: two sand layers
- 492-493 cm: fault-intersected sandy-silty layers
- 497-499 cm: mm-scale sandy layers
- 502 cm: light grey clay
- 508-509 cm: darker interval, below shell debris
- 515-518 cm: mm-scale sand layers
- 517-523 cm: shell debris, irregular base
- 528 and 530 cm: sand layers
- 533-535 cm: sand wedge
- 535-536.5 cm: mm-thick sand layers
- 539-543 cm: mm-scale sandy layers in silt, flaser-bedding
- 545 cm: discontinuous shell layer
- 552-555 cm: indistinct darker interval
- 556-558 cm: flaser-bedded sand layers, mm-thick
- 559 cm: shell debris
- 561-569 cm: fault-intersected indistinct lighter and darker intervals. Wood branch at 563 cm.
- 571-572 cm: wedge with shell debris
- 574 cm: mm-thick sand layer

Lithological descriptions of DAPCs retrieved during M84/2

GeoB 15244-4 DAPC-1 METEOR EXPEDITION M84/2	
Location: Poti Seep	
Lat.: 41°57.871'N	Date: 13.03.2011
Lon.: 41°18.312'E	Recovery: 262 cm
Water depth: 870 m	Liner: PVC

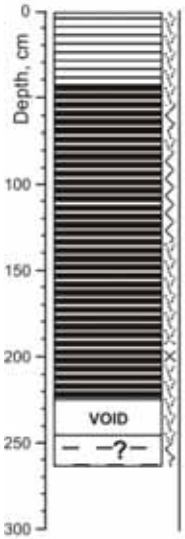

0-42 cm. UNIT 1 (?): Finely laminated coccolith ooze. Color: 5Y5/2 (olive grey). 39-42 cm: few light layers (First occurrence E. hux.?). Upper 23 cm are dominated by light layers. Interval 23-39 cm might be transition sapropel.

42-262 cm. UNIT 2 (?): Finely (<mm) clay (sapropel), dark grey (5Y4/1). Laminations are not distinguishable, subparallel degassing cracks in < cm-scale might indicate former laminations. When not soupy or moussy, the sediment is stiff and low in water content.
52-65, 80-136 cm: soupy

190-204 cm: moussy
210 cm: single light lighter
224-243 cm: void
240 cm: some relict light layers (aragonite?)
246-262 cm: some sand-sized clay pebbles. UNIT 3?
250-263 cm: soupy

GeoB 15244-5 DAPC-2 METEOR EXPEDITION M84/2	
Location: Poti Seep	
Lat.: 41°57.878'N	Date: 14.03.2011
Lon.: 41°18.320'E	Recovery: 244 cm
Water depth: 870 m	Liner: PVC

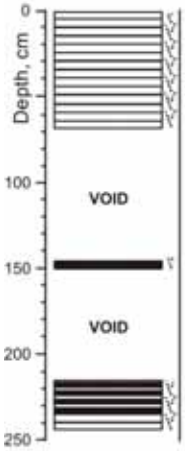

Finely laminated, olive grey (5Y5/2) coccolith ooze (Unit 1) with clearly visible laminations until 69 cm. Degassing cracks belwo 10 cm.

69-144 cm: void

144-150 cm: sapropel-like, grey to dark grey (5Y4.5/1) sediment without distinguishable laminations

150-215: void

215-244 cm: continued sapropel-like sediment but with white layers (smearsliedes: coccoliths) at 233-234 cm. Presuably base of Unit 1.

GeoB 15268-1 DAPC-3 METEOR EXPEDITION M84/2

Location: Samsun, high backscatter

Lat.: 41°32.661'N Date: 16.03.2011

Lon.: 37°37.449'E Recovery: 145 cm

Water depth: 1534 m Liner: PVC

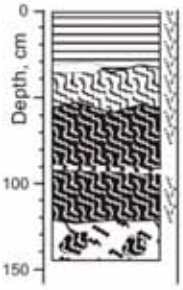

0-33 cm: finely laminated, olive grey (5Y5/1) coccolith ooze, very water-rich in upper 10 cm (UNIT 1). Intercalated with mm-scale homogeneous grey clay layers (like "Degens layers").
- 0-77 cm: degassing cracks
- 22-23 cm: 1 cm thick grey clay layer, discontinuous, fading out
- 33-35 cm: 2 cm thick clay layer, ending abruptly,

33-64 cm: deformed, tilted coccolith layers
- 37-41 cm: grey layer
- 49 and 61 cm: prominent grey layer
- 62-64 cm: light coccolith layers, base of coccolith-bearing interval

64-122 cm: indistinct layering of sapropel-like, finely laminated layers and homogenous grey clay layers
- 79-85 cm: darker sapropel, few clay layers
- 90-92 cm: coccolith layers, with 1 cm thick grey clay layer above and below (Base of Unit 1?)
- 92-122 cm: sapropel (finely laminated, Unit 2?), irregular interbedding of homogenous clay layers, quite stiff
- 97-125 cm: degassing cracks

122-145 cm: stiff clay, indistinct alternation of more sapropel-like material and homogenous clay layers with subangular clasts several cm in size. Clasts consist of very dark greyish brown sapopel-like material. Older (Eemian?) sapropel, reworked, extruded by diapiric activity?

GeoB 15268-5 DAPC-5 METEOR EXPEDITION M84/2

Location: Ordu Ridge Patch 2

Lat.: 41°32.670'N Date: 21.03.2011

Lon.: 37°37.440'E Recovery: 110 cm

Water depth: 1536 m Liner: PVC

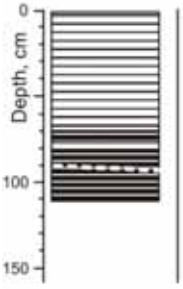

0-39 cm: UNIT 1. Finely laminated grey (5Y5/1) coccolith ooze interbedded with homogeneous clay layers of up to 2 cm in thickness.
- 34-35, 52-53,59-60 cm: grey clay layers
- 68-78 cm: transition sapropel.
- 78-80 cm: basal coccolith layers

80-110 cm: UNIT 2. Sapropel with intercalation of homogenous clay layers, more frequent than in Unit 1. Slightly deformed.

GeoB 15513-2 DAPC-6 METEOR EXPEDITION M84/2

Location: Kerch Flare

Lat.: 44°37.386'N Date: 23.03.2011

Lon.: 35°42.164'E Recovery: 199 cm

Water depth: 878 m Liner: PVC

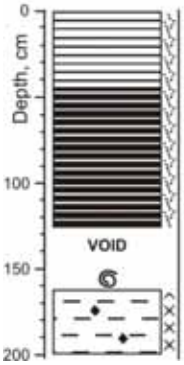

0-44 cm: Finely laminated, olive grey (5Y5/2) coccolith ooze (UNIT1).
Degassing cracks until 126 cm

44- max. 157 cm: finely laminated sapropel, grey to dark grey (5Y4.5/1) (UNIT 2)

126-161 cm: void (water). Former gas hydrate layer?
157 cm: gastropod (*Turricaspia* sp.), ~4 mm in size

ca. 157-199 cm: grey lacustrine mud (UNIT 3), moussy

GeoB 15516-2 DAPC-7 METEOR EXPEDITION M84/2

Location: Kerch Flare

Lat.: 44°37.23'N Date: 24.03.2011

Lon.: 35°42.28'E Recovery: 247 cm

Water depth: 889 m Liner: PVC

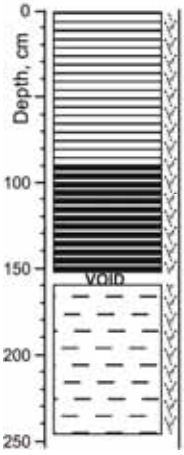

0-89 cm: Finely laminated, dark grey (5Y4/1) coccolith ooze (UNIT 1).
Degassing cracks until 247 cm

89-152 cm: finely laminated sapropel, olive grey (5Y4/2) (UNIT 2)

152-156 cm: void

156-247 cm: grey (5Y5/1) lacustrine mud (UNIT 3)

GeoB 15518-2 DAPC-8 METEOR EXPEDITION M84/2

Location: Kerch Flare

Lat.: 44°37.180'N Date: 25.03.2011

Lon.: 35°42.270'E Recovery: 200 cm

Water depth: 890 m Liner: PVC

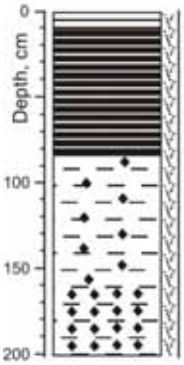

0-10 cm: Finely laminated, grey (5Y5/1) coccolith ooze (UNIT 1). Very water-rich.
Some degassing cracks

10-83 cm: Finely laminated, dark grey (5Y4/1) sapropel (UNIT 2). 10-26 cm water-rich, soft. Degassing cracks.
Intercalation of homogeneous grey clay layers (~0.5 cm thick) at 36, 58 and 75 cm.

83-200 cm: Grey (5Y6/1) clay (UNIT 3) with more degassing structures than in Units 1 and 2.

136-167 cm: black flakes
167-183 cm: black interval, heavily affected by degassing.

GeoB 15526-1 DAPC-9 METEOR EXPEDITION M84/2

Location: Dvurechenskii MV

Lat.: 44°16.970'N Date: 27.03.2011

Lon.: 34°58.670'E Recovery: 260 cm

Water depth: 2054 m Liner: PVC

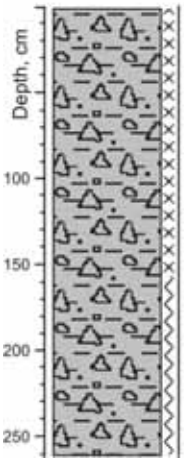

0-200 cm: dark grey (5Y4/1) mudbreccia with clasts of up to 2 cm in size.
0-155 cm: moussy
155-260 cm: soupy

GeoB 15530 DAPC-10	METEOR EXPEDITION M84/2
Location: Helgoland MV	
Lat.: 41°17.300'N	Date: 29.03.2011
Lon.: 35°00.040'E	Recovery: 257 cm
Water depth: 2080 m	Liner: PVC

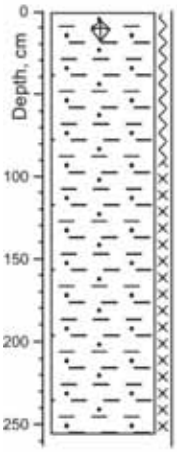

Grey (5Y5/1) clay with few sand-sized particles. In some parts more sandy but exact location of sandy layers is difficult to discern due to the heavy degassing and soupy characteristics of the sediment.
−10 cm: remnant gas hydrate pieces
0-90 cm: soupy
90-257 cm: very water-rich, heavily degassing, moussy

Lithological descriptions of Mini Corers retrieved during M84/2

GeoB 15220-4 MIC-1	METEOR EXPEDITION M84/2
Location: Batumi Seep Area	
Lat. 41°57.155'N	Date: 04.03.2011
Lon.: 41°16.874'E	Recovery: 51 cm
Water depth: 878 m	Liner: PVC

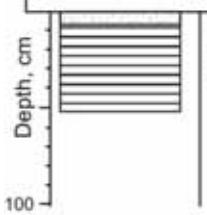

0-51 cm: UNIT 1. Uppermost 5 cm: fluff, very dark grey (5Y3/1), below alternation of grey (5Y5/1) to dark grey (5Y4/1) clay with light grey (5Y7/1) coccolith layers. Becomes slightly lighter (5Y5/1) below 28 cm.

GeoB 15237 MIC-2	METEOR EXPEDITION M84/2
Location: Batumi Seep Area	
Lat. 41°57.490'N	Date: 09.03.2011
Lon.: 41°17.452'E	Recovery: 52 cm
Water depth: 840 m	Liner: PVC

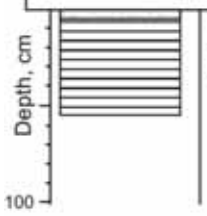

0-52 cm: UNIT 1. Uppermost 4 cm: fluff, very dark grey (5Y3/1), below alternation of grey (5Y5/1) to olive grey (5Y2/2) clay with light grey (5Y7/1) coccolith layers.

GeoB 15239-2 MIC-4 **METEOR EXPEDITION M84/2**

Location: Batumi Seep Area

Lat. 41°57.520'N Date: 10.03.2011

Lon.: 41°17.500'E Recovery: 32 cm

Water depth: 840 m Liner: PVC

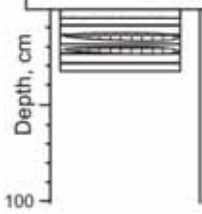

0-32 cm: UNIT 1. Uppermost 3 cm: fluff, very dark grey (5Y3/1), getting lighter below 7 cm with alternation of grey (5Y5/1) to olive grey (5Y2/2) clay with light grey (5Y7/1) coccolith layers.
Carbonate-cemented intervals at 16 and 20-22 cm.

GeoB 15241-1 MIC-5 **METEOR EXPEDITION M84/2**

Location: Batumi Seep Area

Lat. 41°57.469'N Date: 11.03.2011

Lon.: 41°17.177'E Recovery: 52 cm

Water depth: 848 m Liner: PVC

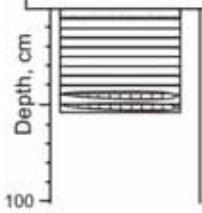

0-52 cm: UNIT 1. Uppermost 3 cm: fluff, very dark grey (5Y3/1), getting lighter below 7 cm with alternation of grey (5Y5/1) to olive grey (5Y2/2) clay with light grey (5Y7/1) coccolith layers.
Carbonate-cemented intervals at 45 and 48-50 cm.

GeoB 15242 MIC-6 **METEOR EXPEDITION M84/2**

Location: Batumi Seep Area

Lat. 41°57.550'N Date: 11.03.2011

Lon.: 41°17.230'E Recovery: 32 cm

Water depth: 840 m Liner: PVC

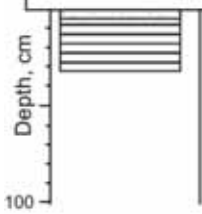

0-32 cm: UNIT 1. Uppermost 4 cm: fluff, very dark grey (5Y3/1), getting lighter with alternation of grey (5Y5/1) to olive grey (5Y2/2) clay with light grey (5Y7/1) coccolith layers.

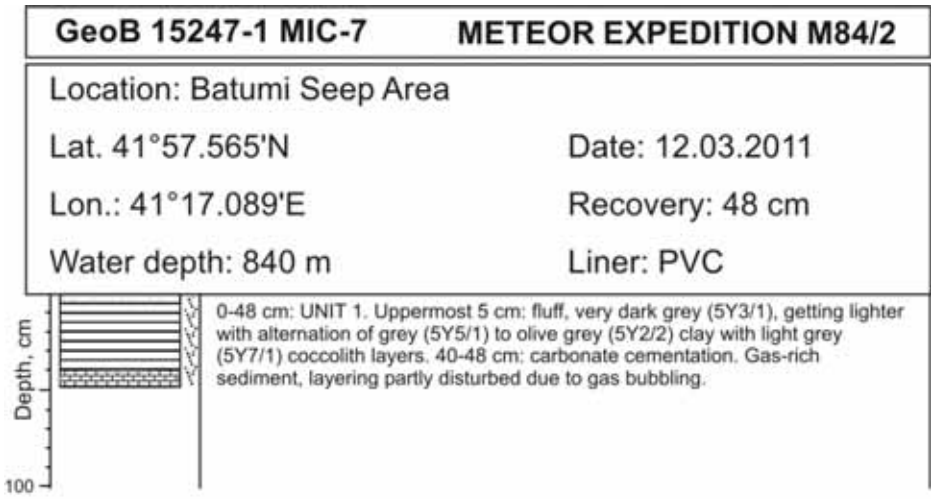
GeoB 15247-1 MIC-7 METEOR EXPEDITION M84/2
Location: Batumi Seep Area
Lat. 41°57.565'N
Lon.: 41°17.089'E
Water depth: 840 m
Date: 12.03.2011
Recovery: 48 cm
Liner: PVC
Depth, cm
100
0-48 cm: UNIT 1. Uppermost 5 cm: fluff, very dark grey (5Y3/1), getting lighter with alternation of grey (5Y5/1) to olive grey (5Y2/2) clay with light grey (5Y7/1) coccolith layers. 40-48 cm: carbonate cementation. Gas-rich sediment, layering partly disturbed due to gas bubbling.

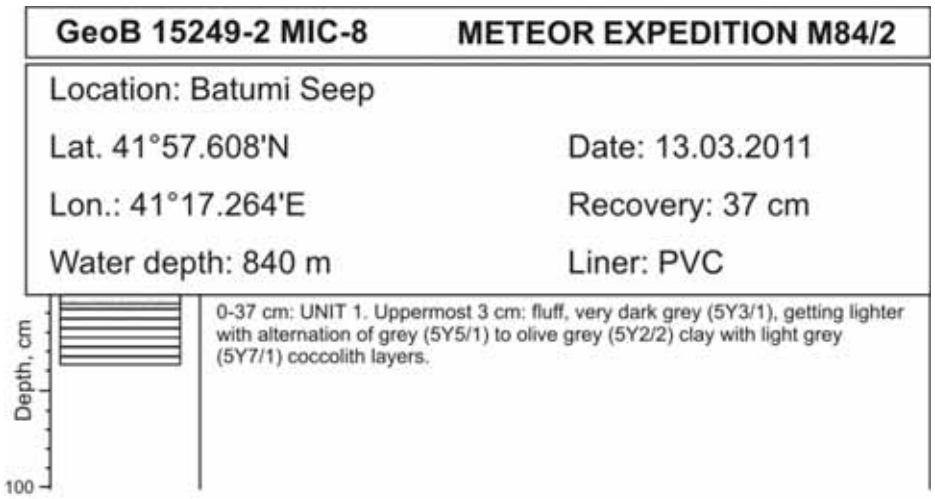
GeoB 15249-2 MIC-8 METEOR EXPEDITION M84/2
Location: Batumi Seep
Lat. 41°57.608'N
Lon.: 41°17.264'E
Water depth: 840 m
Date: 13.03.2011
Recovery: 37 cm
Liner: PVC
Depth, cm
100
0-37 cm: UNIT 1. Uppermost 3 cm: fluff, very dark grey (5Y3/1), getting lighter with alternation of grey (5Y5/1) to olive grey (5Y2/2) clay with light grey (5Y7/1) coccolith layers.

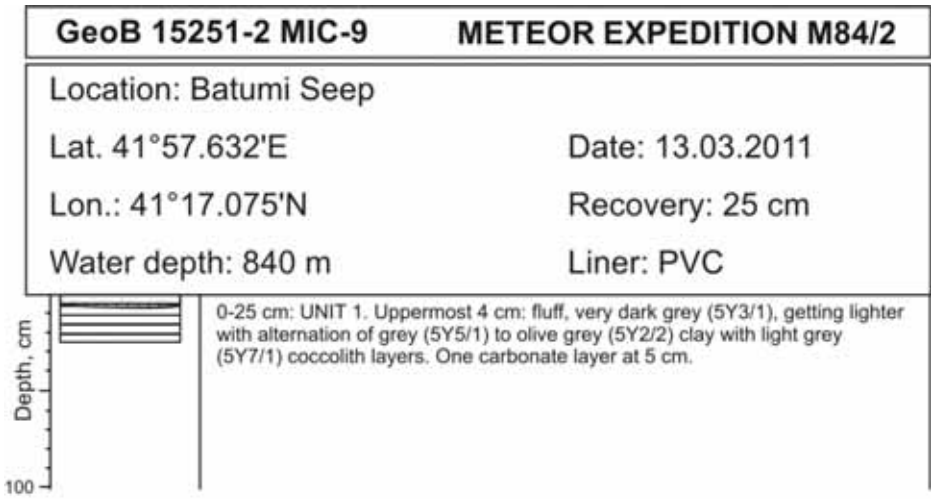
GeoB 15251-2 MIC-9 METEOR EXPEDITION M84/2
Location: Batumi Seep
Lat. 41°57.632'E
Lon.: 41°17.075'N
Water depth: 840 m
Date: 13.03.2011
Recovery: 25 cm
Liner: PVC
Depth, cm
100
0-25 cm: UNIT 1. Uppermost 4 cm: fluff, very dark grey (5Y3/1), getting lighter with alternation of grey (5Y5/1) to olive grey (5Y2/2) clay with light grey (5Y7/1) coccolith layers. One carbonate layer at 5 cm.

GeoB 15253 MIC-10 **METEOR EXPEDITION M84/2**

Location: Batumi Seep Area

Lat. 41°57.469'N Date: 11.03.2011

Lon.: 41°17.270'E Recovery: 48 cm

Water depth: 847 m Liner: PVC

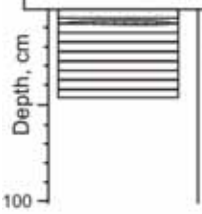

0-48 cm: UNIT 1. Uppermost 6 cm: fluff, very dark grey (5Y3/1), getting lighter with alternation of grey (5Y5/1) to olive grey (5Y2/2) clay with light grey (5Y7/1) coccolith layers. One carbonate layer at 8 cm.

GeoB 15260-2 MIC-11 **METEOR EXPEDITION M84/2**

Location: Batumi Seep Area

Lat. 41°57.583'N Date: 14.03.2011

Lon.: 41°17.398'E Recovery: 31 cm

Water depth: 839 m Liner: PVC

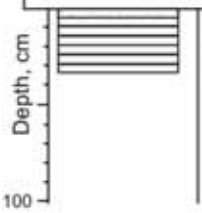

0-31 cm: UNIT 1. Uppermost 2 cm: fluff, very dark grey (5Y3/1), getting lighter with alternation of grey (5Y5/1) to olive grey (5Y2/2) clay with light grey (5Y7/1) coccolith layers.

GeoB 15268-3 MIC-12 **METEOR EXPEDITION M84/2**

Location: Ordu Ridge Patch 02

Lat. 41°32.670'N Date: 20.03.2011

Lon.: 37°37.460'E Recovery: 47 cm

Water depth: 1537 m Liner: PVC

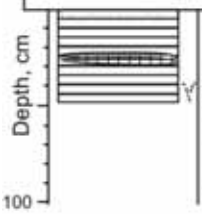

0-52 cm: UNIT 1. Uppermost 4 cm: fluff, below dark grey (5Y4/1) coccolith ooze, fine laminated (<mm scale), getting gradually lighter towards the base (5Y5/1, grey).
23 cm: 4 mm thick carbonate cemented interval
28 cm: more massive carbonate
below 39 cm: degassing cracks.

Strong H_2S smell

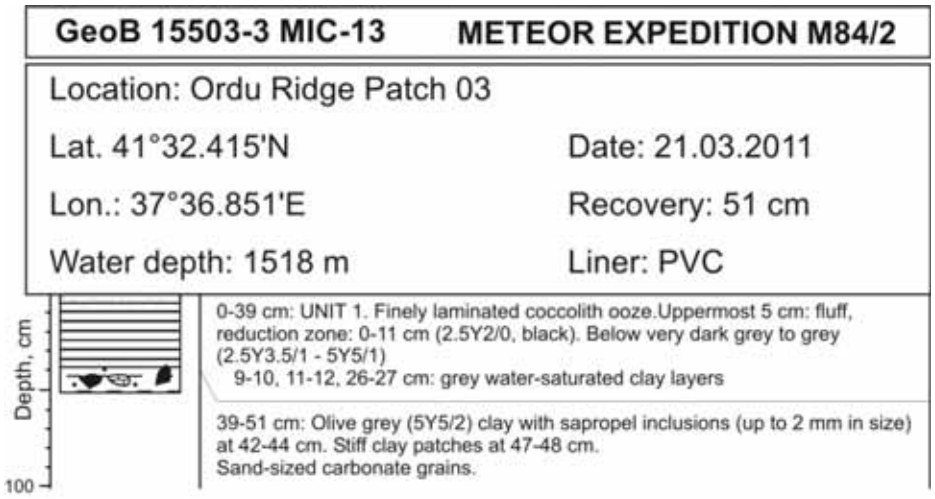
GeoB 15503-3 MIC-13 METEOR EXPEDITION M84/2
Location: Ordu Ridge Patch 03
Lat. 41°32.415'N
Date: 21.03.2011
Lon.: 37°36.851'E
Recovery: 51 cm
Water depth: 1518 m
Liner: PVC
Depth, cm
100
0-39 cm: UNIT 1. Finely laminated coccolith ooze.Uppermost 5 cm: fluff, reduction zone: 0-11 cm (2.5Y2/0, black). Below very dark grey to grey (2.5Y3.5/1 - 5Y5/1)
9-10, 11-12, 26-27 cm: grey water-saturated clay layers
39-51 cm: Olive grey (5Y5/2) clay with sapropel inclusions (up to 2 mm in size) at 42-44 cm. Stiff clay patches at 47-48 cm.
Sand-sized carbonate grains.

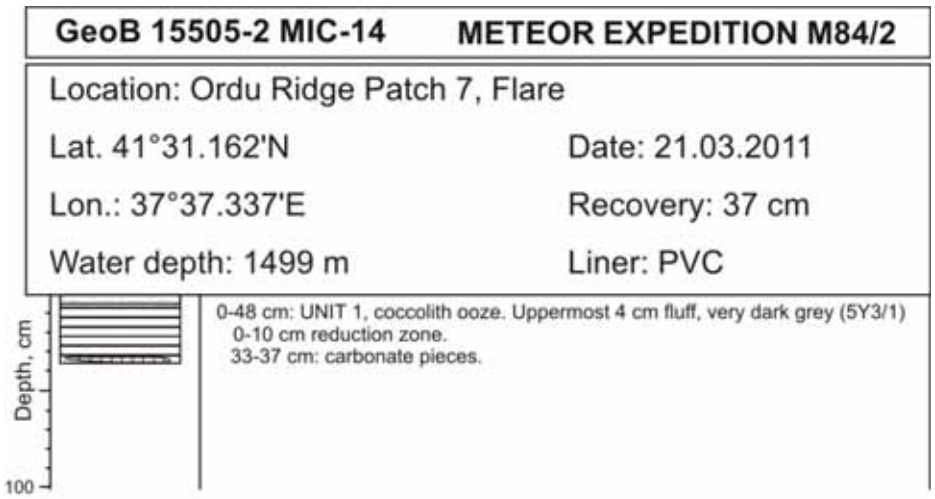
GeoB 15505-2 MIC-14 METEOR EXPEDITION M84/2
Location: Ordu Ridge Patch 7, Flare
Lat. 41°31.162'N
Date: 21.03.2011
Lon.: 37°37.337'E
Recovery: 37 cm
Water depth: 1499 m
Liner: PVC
Depth, cm
100
0-48 cm: UNIT 1, coccolith ooze. Uppermost 4 cm fluff, very dark grey (5Y3/1)
0-10 cm reduction zone.
33-37 cm: carbonate pieces.

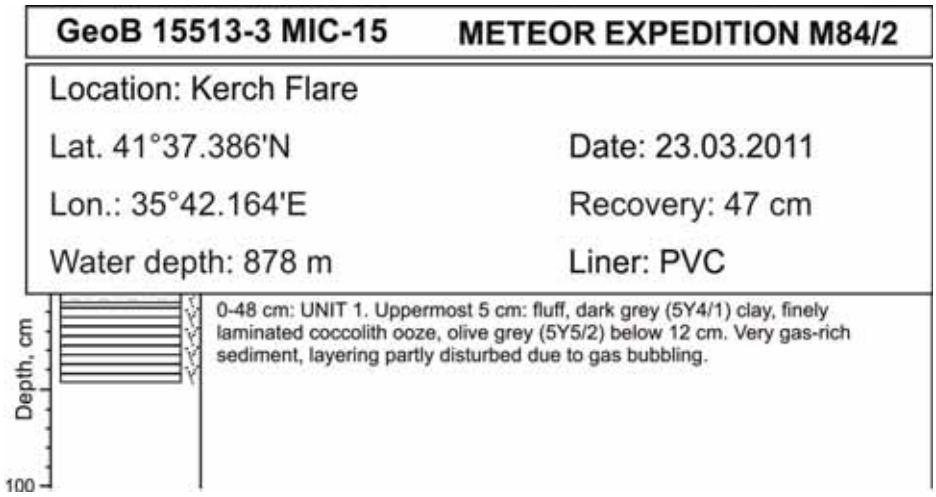
GeoB 15513-3 MIC-15 METEOR EXPEDITION M84/2
Location: Kerch Flare
Lat. 41°37.386'N
Date: 23.03.2011
Lon.: 35°42.164'E
Recovery: 47 cm
Water depth: 878 m
Liner: PVC
Depth, cm
100
0-48 cm: UNIT 1. Uppermost 5 cm: fluff, dark grey (5Y4/1) clay, finely laminated coccolith ooze, olive grey (5Y5/2) below 12 cm. Very gas-rich sediment, layering partly disturbed due to gas bubbling.

GeoB 15516-3 MIC-16 METEOR EXPEDITION M84/2

Location: Kerch Flare

Lat. 44°37.243'N Date: 24.03.2011

Lon.: 35°42.286'E Recovery: 47 cm

Water depth: 888 m Liner: PVC

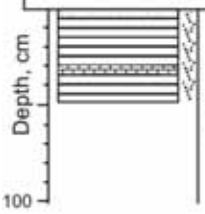

0-48 cm: UNIT 1. Uppermost 5 cm: fluff, very dark grey (5Y3/1), getting lighter with alternation of grey (5Y5/1) to olive grey (5Y2/2) clay with light grey (5Y7/1) coccolith layers.
27.5-30.5 cm: homogenous grey clay layer
30.5-31.5 and 32 cm: carbonate cementation
Very gas-rich sediment, layering partly disturbed due to gas bubbling.

GeoB 15519-2 MIC-17 METEOR EXPEDITION M84/2

Location: Kerch Background

Lat. 44°37.105'N Date: 25.03.2011

Lon.: 35°41.759'E Recovery: 29 cm

Water depth: 896 m Liner: PVC

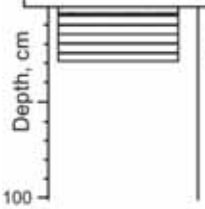

0-51 cm: UNIT 1. Uppermost 2 cm: fluff, dark grey (5Y4/1), finely laminated coccolith ooze.
7-8, 24-26 cm: homogeneous clay layers, grey to dark grey (5Y4.5/1)

GeoB 15524-2 MIC-18 METEOR EXPEDITION M84/2

Location: Helgoland MV

Lat. 44°17.329'N Date: 27.03.2011

Lon.: 35°00.081'E Recovery: 59 cm

Water depth: 2080 m Liner: PVC

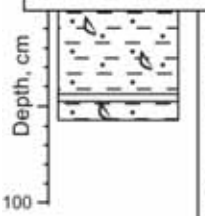

Alternation of more or less sand-bearing clay layers, up to several cm in thickness. mm-sized shell fragments are observed in the sand bearing intervals.
0-9 cm: very soft clay layer with very few sand particles
9-10 cm: Clay layer
10-18 cm: slightly sandy clay
18, 19-22 cm cm: more sandy intervals
22-28 cm: clay
24.5 cm: mm-thick layer of sapropel-like material
31 cm: 2-3 mm thick sandy layer
33-34 cm: sandy layer
36 cm: 2 mm thick sandy layer
45-48 cm: sapropel (very dark grey) with light coccolith layers (Unit 1 fragment), no indication for reworking
48-51 cm: clay
51 cm: 3 mm thick Unit 1- like sediment
Distinct H_2S smell

GeoB 15525-2 MIC-19 **METEOR EXPEDITION M84/2**

Location: Helgoland MV

Lat. 44°17.311'N Date: 29.03.2011

Lon.:35°0.037'E Recovery: ~25 cm

Water depth: 2088 m Liner: PVC

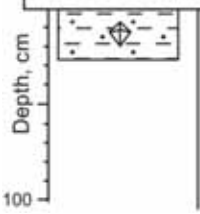

Liquid, extremely gaseous clay with some sand-sized particles (dark minerals, clay pebbles).
Gas hydrates with bubble fabric, ca. 3 cm in diameter

GeoB 15525-4 MIC-20 **METEOR EXPEDITION M84/2**

Location: Helgoland MV

Lat. 44°17.311'N Date: 29.03.2011

Lon.: 35°0.037'E Recovery: 34 cm

Water depth: 2088 m Liner: PVC

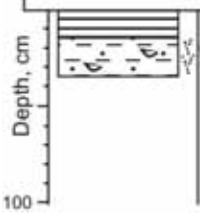

0-15 cm: UNIT 1. Finely laminated coccolith ooze. Laminations faintly visible despite heavy degassing of core; very water-rich. Uppermost 1 cm: fluff.
~ 5 cm: intercalation of clay layer with mm-sized shells fragments.

15-34 cm: Grey (5Y5/1) clay with sandy particles (dark minerals, rounded indurated clay particles and some shell debris of up to 2-3 mm in size.
Degassing bubbles in sediment.
20-22 cm: void due to degassing

GeoB 15533-2 MIC-21 **METEOR EXPEDITION M84/2**

Location: Background

Lat. 44°17.300'N Date: 29.03.2011

Lon.: 35°00.040'E Recovery: 28 cm

Water depth: 2080 m Liner: PVC

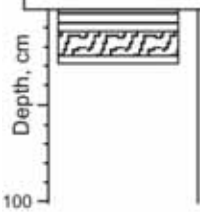

0-4 cm: Fluff
4-5 cm: light grey layer with light lamiantions
5-8 cm: grey interval, faintly laminated, no distinct coccolith layers
8-12 cm: slightly darker as above, laminations, no distinct coccolith layers
12-26 cm: distorted light laminations (coccolith-bearing, smear slide) interbedded with lenses of homogeneous grey clay
26-28 cm: non-distorted light laminations

Appendix 7: List of sampled cores and collected sub-samples

Station Device	GeoB No.	Area	Latitude (N)	Longitude (E)	Water depth / m	PW	Poros / CNS	IC	ICP-AES /MS	DIC	$\delta^{13}C_{DIC}$	Iso	Length of core / cm	No. of samples
142 MeBo 63	15208-1	Eregli I	41°27.365'	30°51.142'	975	X	X	X	X	X	X	X	580	10
150 GC 3	15216-1	Samsun	42°03.000'	36°14.492'	388	X	X	X	X	X	X	X	576	14
154 GC 4	15220-1	Batumi Reference	41°57.144'	41°16.851'	878	X	X	X	X	X	X	X	484	14
157 MIC 1	15220-4	Batumi Reference	41°57.155'	41°16.874'	878	X	X	X	X	X	X	X	52	18
159 MeBo 65	15220-5	Batumi Reference	41°57.171'	41°16.853'	878	X	X	X	X	X	X	X	1090	25
164 GC 5	15226-1	Pechori Mound	41°58.780'	41°07.591'	1045	X	X	X	X	X	X	X	502	24
165 MeBo 66	15227-1	Pechori Mound	41°58.963'	41°07.595'	936	X	X	X	X	X	X	X	376	10
168 MeBo 67	15227-3	Pechori Mound	41°58.985'	41°07.590'	1027	X	X	X	X	X	X	X	1317	25
179 GC 6	15234-1	Adjara Ridge	41°52.278'	41°17.273'	887	X	X	X	X	X	X	X	249	9
182 GC 7	15236-1	Batumi Seep area	41°57.580'	41°17.411'	838	X	X	X	X	X	X	X	215	14
184 MIC 2	15237-1	Batumi Seep area	41°57.489'	41°17.462'	844	X	X	X	X	X	X	X	56	15
185 MeBo 68	15236-2	Batumi Seep area	41°57.590'	41°17.350'	838	X	X	X	X	X	X	X	596	14
188 MIC 4	15238-1	Batumi Seep area	41°57.520'	41°17.500'	840	X	X	X	X	X	X	X	46	15
190 MIC 5	15241-1	Batumi Seep area	41°57.462'	41°17.182'	848	X	X	X	X	–	–	X	49	15
191 GC 8	15241-2	Batumi Seep area	41°57.466'	41°17.182'	840	X	X	X	X	–	–	X	208	11
192 MIC 6	15242	Batumi Seep area	41°57.550'	41°17.230'	840	X	X	X	X	–	–	X	47	15
195 GC 11	15244-2	Poti Seep	41°05.879'	41°18.346'	868	X	X	X	X	–	–	X	135	10
198 MIC 7	15247-1	Batumi Seep area	41°57.565'	41°17.089'	840	X	X	X	X	–	–	X	47	15
199 GC 12	15247-2	Batumi Seep area	41°57.570'	41°17.102'	842	X	X	X	X	–	–	X	140	11
203 GC 15	15249-1	Batumi Seep area	41°57.605'	41°17.260'	842	X	X	X	X	–	–	X	150	10
205 MIC 8	15249-2	Batumi Seep area	41°57.608'	41°17.264'	843	X	X	X	X	–	–	X	50	15
206 DAPC 1	15244-4	Poti Seep	41°57.87'	41°18.310'	870	X *)	–	X	X	–	–	–	260	20
207 GC 16	15251-1	Batumi Seep area	41°57.632'	41°17.079'	845	X	X	X	X	–	–	X	175	11
208 MIC 9	15251-2	Batumi Seep area	41°57.632'	41°17.075'	842	X	X	X	X	–	–	X	35	13
210 MIC 10	15253	Batumi Seep area	41°57.469'	41°17.270'	847	X	X	X	X	–	–	X	48	15
216 GC 22	15258	Kulevi Ridge G2	42°07.099'	41°22.743'	713	X	X	X	X	X	X	X	140	8
217 GC 23	15259	Kulevi Ridge G1	42°05.751'	41°08.436'	1121	X	X	X	X	X	X	X	270	12
218 GC 24	15260-1	Batumi Seep area	41°57.580'	41°17.390'	837	X	X	X	X	–	–	X	270	15
219 MIC 11	15260-2	Batumi Seep area	41°57.580'	41°17.390'	839	X	X	X	X	–	–	X	839	15
228 GC 27	15268-1	Ordu Ridge (Patch #18)	41°32.661'	37°37.449'	1534	X	X	X	X	X	X	X	308	15

Station Device	GeoB No.	Area	Latitude (N)	Longitude (E)	Water depth / m	PW	Poros / CNS	IC	ICP-AES	DIC	$\delta^{13}C_{DIC}$	Iso	Length of core / cm	No. of samples
233 MIC 12	15268-3	Ordu Ridge (Patch #02)	41°32.670'	37°37.460'	1537	X	X	X	X	X	X	X	44	15
235 GC 28	15503-1	Ordu Ridge (Patch #03)	41°32.443'	37°36.888'	1522	X	X	X	X	X	X	X	287	14
238 GC 30	15505-1	Ordu Ridge (Patch #07)	41°31.160'	37°37.338'	1493	X	X	X	X	X	X	X	231	11
240 MIC 13	15503-3	Ordu Ridge (Patch #03)	41°32.415'	37°36.851'	1518	X	X	X	X	X	X	X	47	15
242 MIC 14	15505-2	Ordu Ridge (Patch #07)	41°31.162'	37°37.337'	1499	X	X	X	X	X	X	X	36	15
243 GC 31	15507	Ordu Ridge (Patch #07)	41°31.138'	37°37.347'	1505	X	X	X	X	X	X	X	157	9
244 GC 32	15508	Samsun (New Ridge)	41°22.850'	37°48.160'	1526	X	X	X	X	X	X	X	301	12
249 GC 34	15513-1	Kerch Flare	44°37.386'	35°42.164'	878	X	X	X	X	X	X	X	558	24
250 DAPC 6	15513-2	Kerch Flare	44°37.386'	35°42.164'	878	X *)	–	X	X	–	–	–	199	6
251 MIC 15	15513-3	Kerch Flare	44°37.386'	35°42.164'	878	X	X	X	X	X	X	X	45	13
256 GC 36	15516-1	Kerch Flare (Patch #2)	44°37.230'	35°42.282'	889	X	X	X	X	–	–	X	504	20
257 DAPC 7	15516-2	Kerch Flare (Patch #2)	44°37.230'	35°42.282'	889	X *)	–	X	X	–	–	–	235	6
258 MIC 16	15516-3	Kerch Flare (Patch #2)	44°37.243'	35°42.286'	888	X	X	X	X	–	–	X	42	14
260 GC 37	15518-1	Kerch Flare	44°37.182'	35°42.279'	887	X	X	X	X	–	X	X	357	10
261 GC 38	15519-1	Kerch Flare Reference	44°37.171'	35°41.763'	896	X	X	X	X	–	–	X	574	17
263 DAPC 8	15518-2	Kerch Flare	44°37.180'	35°42.270'	885	X *)	–	X	X	–	–	–	205	9
264 MIC 17	15519-2	Kerch Flare Reference	44°37.105'	35°41.759'	896	X	X	X	X	–	–	X	45	14
268 GC 40	15524-1	Helgoland MV	44°17.322'	35°00.065'	2082	X	X	X	X	–	X	X	443	16
269 MIC 18	15524-2	Helgoland MV	44°17.329'	35°00.081'	2080	X	X	X	X	–	X	X	47	15
270 GC 41	15525-1	Helgoland MV	44°17.311'	35°00.037'	2088	X	X	X	X	–	–	X	100	3
271 DAPC 9	15526-1	Dvurechenskii MV	44°16.970'	34°58.670'	2054	X *)	–	X	X	–	–	–	250	11
272 GC 42	15526-2	Dvurechenskii MV	44°17.041'	34°58.891'	2051	X	X	X	X	–	–	X	380	12
277 MIC 20	15525-4	Helgoland MV	44°17.304'	35°00.042'	2079	X	X	X	X	–	X	X	46	15
278 DAPC 10	15530	Helgoland MV	44°17.300'	35°00.040'	2080	X *)	X	X	X	–	–	X	255	10
280 GC 45	15532	Helgoland MV	44°17.295'	35°00.044'	2079	X	X	X	X	–	X	X	570	18
281 GC 46	15533-1	Helgoland MV Reference	44°18.166'	34°59.162'	2054	X	X	X	X	–	–	X	590	14
282 MIC 21	15533-2	Helgoland MV Reference	44°18.166'	34°59.162'	2054	X	X	X	X	–	–	X	26	11

GC = gravity corer; MIC = mini-corer; MeBo = seafloor drilling device; PW = porewater analyses of TA, H_2S, NH_4, PO_4, SiO_4, Cl;
IC = ion chromatography (SO_4, Br, Cl, I); ICP-AES = inductively-coupled atomic emission spectroscopy (for various dissolved cations); Iso = Isotope ratios of porewater O, H, Cl, Sr, Li; *) Onboard DAPC samples were only analyzed for TA (and occasionally also for Cl and NH_4).

Publications of this series:

No. 1 **Wefer, G., E. Suess and cruise participants**
Bericht über die POLARSTERN-Fahrt ANT IV/2, Rio de Janeiro - Punta Arenas, 6.11. - 1.12.1985.
60 pages, Bremen, 1986.

No. 2 **Hoffmann, G.**
Holozänstratigraphie und Küstenlinienverlagerung an der andalusischen Mittelmeerküste.
173 pages, Bremen, 1988. (out of print)

No. 3 **Wefer, G. and cruise participants**
Bericht über die METEOR-Fahrt M 6/6, Libreville - Las Palmas, 18.2. - 23.3.1988.
97 pages, Bremen, 1988.

No. 4 **Wefer, G., G.F. Lutze, T.J. Müller, O. Pfannkuche, W. Schenke, G. Siedler, W. Zenk**
Kurzbericht über die METEOR-Expedition No. 6, Hamburg - Hamburg, 28.10.1987 - 19.5.1988.
29 pages, Bremen, 1988. (out of print)

No. 5 **Fischer, G.**
Stabile Kohlenstoff-Isotope in partikulärer organischer Substanz aus dem Südpolarmeer (Atlantischer Sektor). 161 pages, Bremen, 1989.

No. 6 **Berger, W.H. and G. Wefer**
Partikelfluß und Kohlenstoffkreislauf im Ozean.
Bericht und Kurzfassungen über den Workshop vom 3.-4. Juli 1989 in Bremen.
57 pages, Bremen, 1989.

No. 7 **Wefer, G. and cruise participants**
Bericht über die METEOR - Fahrt M 9/4, Dakar - Santa Cruz, 19.2. - 16.3.1989.
103 pages, Bremen, 1989.

No. 8 **Kölling, M.**
Modellierung geochemischer Prozesse im Sickerwasser und Grundwasser.
135 pages, Bremen, 1990.

No. 9 **Heinze, P.-M.**
Das Auftriebsgeschehen vor Peru im Spätquartär. 204 pages, Bremen, 1990. (out of print)

No. 10 **Willems, H., G. Wefer, M. Rinski, B. Donner, H.-J. Bellmann, L. Eißmann, A. Müller, B.W. Flemming, H.-C. Höfle, J. Merkt, H. Streif, G. Hertweck, H. Kuntze, J. Schwaar, W. Schäfer, M.-G. Schulz, F. Grube, B. Menke**
Beiträge zur Geologie und Paläontologie Norddeutschlands: Exkursionsführer.
202 pages, Bremen, 1990.

No. 11 **Wefer, G. and cruise participants**
Bericht über die METEOR-Fahrt M 12/1, Kapstadt - Funchal, 13.3.1990 - 14.4.1990.
66 pages, Bremen, 1990.

No. 12 **Dahmke, A., H.D. Schulz, A. Kölling, F. Kracht, A. Lücke**
Schwermetallspuren und geochemische Gleichgewichte zwischen Porenlösung und Sediment im Wesermündungsgebiet. BMFT-Projekt MFU 0562, Abschlußbericht. 121 pages, Bremen, 1991.

No. 13 **Rostek, F.**
Physikalische Strukturen von Tiefseesedimenten des Südatlantiks und ihre Erfassung in Echolotregistrierungen. 209 pages, Bremen, 1991.

No. 14 **Baumann, M.**
Die Ablagerung von Tschernobyl-Radiocäsium in der Norwegischen See und in der Nordsee.
133 pages, Bremen, 1991. (out of print)

No. 15 **Kölling, A.**
Frühdiagenetische Prozesse und Stoff-Flüsse in marinen und ästuarinen Sedimenten.
140 pages, Bremen, 1991.

No. 16 **SFB 261 (ed.)**
1. Kolloquium des Sonderforschungsbereichs 261 der Universität Bremen (14.Juni 1991):
Der Südatlantik im Spätquartär: Rekonstruktion von Stoffhaushalt und Stromsystemen.
Kurzfassungen der Vorträge und Poster. 66 pages, Bremen, 1991.

No. 17 **Pätzold, J. and cruise participants**
Bericht und erste Ergebnisse über die METEOR-Fahrt M 15/2, Rio de Janeiro - Vitoria,
18.1. - 7.2.1991. 46 pages, Bremen, 1993.

No. 18 **Wefer, G. and cruise participants**
Bericht und erste Ergebnisse über die METEOR-Fahrt M 16/1, Pointe Noire - Recife,
27.3. - 25.4.1991. 120 pages, Bremen, 1991.

No. 19 **Schulz, H.D. and cruise participants**
Bericht und erste Ergebnisse über die METEOR-Fahrt M 16/2, Recife - Belem, 28.4. - 20.5.1991.
149 pages, Bremen, 1991.

No. 20 **Berner, H.**
Mechanismen der Sedimentbildung in der Fram-Straße, im Arktischen Ozean und in der Norwegischen See. 167 pages, Bremen, 1991.

No. 21 **Schneider, R.**
Spätquartäre Produktivitätsänderungen im östlichen Angola-Becken: Reaktion auf Variationen im Passat-Monsun-Windsystem und in der Advektion des Benguela-Küstenstroms.
198 pages, Bremen, 1991. (out of print)

No. 22 **Hebbeln, D.**
Spätquartäre Stratigraphie und Paläozeanographie in der Fram-Straße. 174 pages, Bremen, 1991.

No. 23 **Lücke, A.**
Umsetzungsprozesse organischer Substanz während der Frühdiagenese in ästuarinen Sedimenten.
137 pages, Bremen, 1991.

No. 24 **Wefer, G. and cruise participants**
Bericht und erste Ergebnisse der METEOR-Fahrt M 20/1, Bremen - Abidjan, 18.11.- 22.12.1991.
74 pages, Bremen, 1992.

No. 25 **Schulz, H.D. and cruise participants**
Bericht und erste Ergebnisse der METEOR-Fahrt M 20/2, Abidjan - Dakar, 27.12.1991 - 3.2.1992.
173 pages, Bremen, 1992.

No. 26 **Gingele, F.**
Zur klimaabhängigen Bildung biogener und terrigener Sedimente und ihrer Veränderung durch die Frühdiagenese im zentralen und östlichen Südatlantik. 202 pages, Bremen, 1992.

No. 27 **Bickert, T.**
Rekonstruktion der spätquartären Bodenwasserzirkulation im östlichen Südatlantik über stabile Isotope benthischer Foraminiferen. 205 pages, Bremen, 1992. (out of print)

No. 28 **Schmidt, H.**
Der Benguela-Strom im Bereich des Walfisch-Rückens im Spätquartär. 172 pages, Bremen, 1992.

No. 29 **Meinecke, G.**
Spätquartäre Oberflächenwassertemperaturen im östlichen äquatorialen Atlantik.
181 pages, Bremen, 1992.

No. 30 **Bathmann, U., U. Bleil, A. Dahmke, P. Müller, A. Nehrkorn, E.-M. Nöthig, M. Olesch, J. Pätzold, H.D. Schulz, V. Smetacek, V. Spieß, G. Wefer, H. Willems**
Bericht des Graduierten Kollegs. Stoff-Flüsse in marinen Geosystemen.
Berichtszeitraum Oktober 1990 - Dezember 1992. 396 pages, Bremen, 1992.

No. 31 **Damm, E.**
Frühdiagenetische Verteilung von Schwermetallen in Schlicksedimenten der westlichen Ostsee.
115 pages, Bremen, 1992.

No. 32 **Antia, E.E.**
Sedimentology, Morphodynamics and Facies Association of a mesotidal Barrier Island Shoreface (Spiekeroog, Southern North Sea). 370 pages, Bremen, 1993.

No. 33 **Duinker, J. and G. Wefer (ed.)**
Bericht über den 1. JGOFS-Workshop. 1./2. Dezember 1992 in Bremen. 83 pages, Bremen, 1993.

No. 34 **Kasten, S.**
Die Verteilung von Schwermetallen in den Sedimenten eines stadtbremischen Hafenbeckens.
103 pages, Bremen, 1993.

No. 35 **Spieß, V.**
Digitale Sedimentographie. Neue Wege zu einer hochauflösenden Akustostratigraphie.
199 pages, Bremen, 1993.

No. 36 **Schinzel, U.**
Laborversuche zu frühdiagenetischen Reaktionen von Eisen (III) - Oxidhydraten in marinen Sedimenten.189 pages, Bremen, 1993.

No. 37 **Sieger, R.**
CoTAM - ein Modell zur Modellierung des Schwermetalltransports in Grundwasserleitern.
56 pages, Bremen, 1993. (out of print)

No. 38 **Willems, H. (ed.)**
Geoscientific Investigations in the Tethyan Himalayas. 183 pages, Bremen, 1993.

No. 39 **Hamer, K.**
Entwicklung von Laborversuchen als Grundlage für die Modellierung des Transportverhaltens von Arsenat, Blei, Cadmium und Kupfer in wassergesättigten Säulen. 147 pages, Bremen, 1993.

No. 40 **Sieger, R.**
Modellierung des Stofftransports in porösen Medien unter Ankopplung kinetisch gesteuerter Sorptions- und Redoxprozesse sowie thermischer Gleichgewichte. 158 pages, Bremen, 1993.

No. 41 **Thießen, W.**
Magnetische Eigenschaften von Sedimenten des östlichen Südatlantiks und ihre paläozeanographische Relevanz. 170 pages, Bremen, 1993.

No. 42 **Spieß, V. and cruise participants**
Report and preliminary results of METEOR-Cruise M 23/1, Kapstadt - Rio de Janeiro, 4.-25.2.1993. 139 pages, Bremen, 1994.

No. 43 **Bleil, U. and cruise participants**
Report and preliminary results of METEOR-Cruise M 23/2, Rio de Janeiro - Recife, 27.2.-19.3.1993 133 pages, Bremen, 1994.

No. 44 **Wefer, G. and cruise participants**
Report and preliminary results of METEOR-Cruise M 23/3, Recife - Las Palmas, 21.3. - 12.4.1993 71 pages, Bremen, 1994.

No. 45 **Giese, M. and G. Wefer (ed.)**
Bericht über den 2. JGOFS-Workshop. 18../19. November 1993 in Bremen. 93 pages, Bremen, 1994.

No. 46 **Balzer, W. and cruise participants**
Report and preliminary results of METEOR-Cruise M 22/1, Hamburg - Recife, 22.9. - 21.10.1992. 24 pages, Bremen, 1994.

No. 47 **Stax, R.**
Zyklische Sedimentation von organischem Kohlenstoff in der Japan See: Anzeiger für Änderungen von Paläoozeanographie und Paläoklima im Spätkänozoikum. 150 pages, Bremen, 1994.

No. 48 **Skowronek, F.**
Frühdiagenetische Stoff-Flüsse gelöster Schwermetalle an der Oberfläche von Sedimenten des Weser Ästuares. 107 pages, Bremen, 1994.

No. 49 **Dersch-Hansmann, M.**
Zur Klimaentwicklung in Ostasien während der letzten 5 Millionen Jahre: Terrigener Sedimenteintrag in die Japan See (ODP Ausfahrt 128). 149 pages, Bremen, 1994.

No. 50 **Zabel, M.**
Frühdiagenetische Stoff-Flüsse in Oberflächen-Sedimenten des äquatorialen und östlichen Südatlantik. 129 pages, Bremen, 1994.

No. 51 **Bleil, U. and cruise participants**
Report and preliminary results of SONNE-Cruise SO 86, Buenos Aires - Capetown, 22.4. - 31.5.93 116 pages, Bremen, 1994.

No. 52 **Symposium: The South Atlantic: Present and Past Circulation.**
Bremen, Germany, 15 - 19 August 1994. Abstracts. 167 pages, Bremen, 1994.

No. 53 **Kretzmann, U.B.**
57Fe-Mössbauer-Spektroskopie an Sedimenten - Möglichkeiten und Grenzen. 183 pages, Bremen, 1994.

No. 54 **Bachmann, M.**
Die Karbonatrampe von Organyà im oberen Oberapt und unteren Unteralb (NE-Spanien, Prov. Lerida): Fazies, Zyklo- und Sequenzstratigraphie. 147 pages, Bremen, 1994. (out of print)

No. 55 **Kemle-von Mücke, S.**
Oberflächenwasserstruktur und -zirkulation des Südostatlantiks im Spätquartär. 151 pages, Bremen, 1994.

No. 56 **Petermann, H.**
Magnetotaktische Bakterien und ihre Magnetosome in Oberflächensedimenten des Südatlantiks. 134 pages, Bremen, 1994.

No. 57 **Mulitza, S.**
Spätquartäre Variationen der oberflächennahen Hydrographie im westlichen äquatorialen Atlantik. 97 pages, Bremen, 1994.

No. 58 **Segl, M. and cruise participants**
Report and preliminary results of METEOR-Cruise M 29/1, Buenos-Aires - Montevideo, 17.6. - 13.7.1994
94 pages, Bremen, 1994.

No. 59 **Bleil, U. and cruise participants**
Report and preliminary results of METEOR-Cruise M 29/2, Montevideo - Rio de Janiero 15.7. - 8.8.1994. 153 pages, Bremen, 1994.

No. 60 **Henrich, R. and cruise participants**
Report and preliminary results of METEOR-Cruise M 29/3, Rio de Janeiro - Las Palmas 11.8. - 5.9.1994. Bremen, 1994. (out of print)

No. 61 **Sagemann, J.**
Saisonale Variationen von Porenwasserprofilen, Nährstoff-Flüssen und Reaktionen in intertidalen Sedimenten des Weser-Ästuars. 110 pages, Bremen, 1994. (out of print)

No. 62 **Giese, M. and G. Wefer**
Bericht über den 3. JGOFS-Workshop. 5./6. Dezember 1994 in Bremen.
84 pages, Bremen, 1995.

No. 63 **Mann, U.**
Genese kretazischer Schwarzschiefer in Kolumbien: Globale vs. regionale/lokale Prozesse.
153 pages, Bremen, 1995. (out of print)

No. 64 **Willems, H., Wan X., Yin J., Dongdui L., Liu G., S. Dürr, K.-U. Gräfe**
The Mesozoic development of the N-Indian passive margin and of the Xigaze Forearc Basin in southern Tibet, China. – Excursion Guide to IGCP 362 Working-Group Meeting "Integrated Stratigraphy". 113 pages, Bremen, 1995. (out of print)

No. 65 **Hünken, U.**
Liefergebiets - Charakterisierung proterozoischer Goldseifen in Ghana anhand von Fluideinschluß - Untersuchungen. 270 pages, Bremen, 1995.

No. 66 **Nyandwi, N.**
The Nature of the Sediment Distribution Patterns in ther Spiekeroog Backbarrier Area, the East Frisian Islands. 162 pages, Bremen, 1995.

No. 67 **Isenbeck-Schröter, M.**
Transportverhalten von Schwermetallkationen und Oxoanionen in wassergesättigten Sanden. - Laborversuche in Säulen und ihre Modellierung -. 182 pages, Bremen, 1995.

No. 68 **Hebbeln, D. and cruise participants**
Report and preliminary results of SONNE-Cruise SO 102, Valparaiso - Valparaiso, 95.
134 pages, Bremen, 1995.

No. 69 **Willems, H. (Sprecher), U.Bathmann, U. Bleil, T. v. Dobeneck, K. Herterich, B.B. Jorgensen, E.-M. Nöthig, M. Olesch, J. Pätzold, H.D. Schulz, V. Smetacek, V. Speiß. G. Wefer**
Bericht des Graduierten-Kollegs Stoff-Flüsse in marine Geosystemen.
Berichtszeitraum Januar 1993 - Dezember 1995. 45 & 468 pages, Bremen, 1995.

No. 70 **Giese, M. and G. Wefer**
Bericht über den 4. JGOFS-Workshop. 20./21. November 1995 in Bremen. 60 pages, Bremen, 1996. (out of print)

No. 71 **Meggers, H.**
Pliozän-quartäre Karbonatsedimentation und Paläozeanographie des Nordatlantiks und des Europäischen Nordmeeres - Hinweise aus planktischen Foraminiferengemeinschaften.
143 pages, Bremen, 1996. (out of print)

No. 72 **Teske, A.**
Phylogenetische und ökologische Untersuchungen an Bakterien des oxidativen und reduktiven marinen Schwefelkreislaufs mittels ribosomaler RNA. 220 pages, Bremen, 1996. (out of print)

No. 73 **Andersen, N.**
Biogeochemische Charakterisierung von Sinkstoffen und Sedimenten aus ostatlantischen Produktions-Systemen mit Hilfe von Biomarkern. 215 pages, Bremen, 1996.

No. 74 **Treppke, U.**
Saisonalität im Diatomeen- und Silikoflagellatenfluß im östlichen tropischen und subtropischen Atlantik. 200 pages, Bremen, 1996.

No. 75 **Schüring, J.**
Die Verwendung von Steinkohlebergematerialien im Deponiebau im Hinblick auf die Pyritverwitterung und die Eignung als geochemische Barriere. 110 pages, Bremen, 1996.

No. 76 **Pätzold, J. and cruise participants**
Report and preliminary results of VICTOR HENSEN cruise JOPS II, Leg 6, Fortaleza - Recife, 10.3. - 26.3. 1995 and Leg 8, Vítoria - Vítoria, 10.4. - 23.4.1995.
87 pages, Bremen, 1996.

No. 77 **Bleil, U. and cruise participants**
Report and preliminary results of METEOR-Cruise M 34/1, Cape Town - Walvis Bay, 3.-26.1.1996.
129 pages, Bremen, 1996.

No. 78 **Schulz, H.D. and cruise participants**
Report and preliminary results of METEOR-Cruise M 34/2, Walvis Bay - Walvis Bay, 29.1.-18.2.96
133 pages, Bremen, 1996.

No. 79 **Wefer, G. and cruise participants**
Report and preliminary results of METEOR-Cruise M 34/3, Walvis Bay - Recife, 21.2.-17.3.1996.
168 pages, Bremen, 1996.

No. 80 **Fischer, G. and cruise participants**
Report and preliminary results of METEOR-Cruise M 34/4, Recife - Bridgetown, 19.3.-15.4.1996. 105 pages, Bremen, 1996.

No. 81 **Kulbrok, F.**
Biostratigraphie, Fazies und Sequenzstratigraphie einer Karbonatrampe in den Schichten der Oberkreide und des Alttertiärs Nordost-Ägyptens (Eastern Desert, N'Golf von Suez, Sinai). 153 pages, Bremen, 1996.

No. 82 **Kasten, S.**
Early Diagenetic Metal Enrichments in Marine Sediments as Documents of Nonsteady-State Depositional Conditions. Bremen, 1996.

No. 83 **Holmes, M.E.**
Reconstruction of Surface Ocean Nitrate Utilization in the Southeast Atlantic Ocean Based on Stable Nitrogen Isotopes. 113 pages, Bremen, 1996.

No. 84 **Rühlemann, C.**
Akkumulation von Carbonat und organischem Kohlenstoff im tropischen Atlantik: Spätquartäre Produktivitäts-Variationen und ihre Steuerungsmechanismen. 139 pages, Bremen, 1996.

No. 85 **Ratmeyer, V.**
Untersuchungen zum Eintrag und Transport lithogener und organischer partikulärer Substanz im östlichen subtropischen Nordatlantik. 154 pages, Bremen, 1996.

No. 86 **Cepek, M.**
Zeitliche und räumliche Variationen von Coccolithophoriden-Gemeinschaften im subtropischen Ost-Atlantik: Untersuchungen an Plankton, Sinkstoffen und Sedimenten. 156 pages, Bremen, 1996.

No. 87 **Otto, S.**
Die Bedeutung von gelöstem organischen Kohlenstoff (DOC) für den Kohlenstoffffluß im Ozean. 150 pages, Bremen, 1996.

No. 88 **Hensen, C.**
Frühdiagenetische Prozesse und Quantifizierung benthischer Stoff-Flüsse in Oberflächensedimenten des Südatlantiks. 132 pages, Bremen, 1996.

No. 89 **Giese, M. and G. Wefer**
Bericht über den 5. JGOFS-Workshop. 27./28. November 1996 in Bremen. 73 pages, Bremen, 1997.

No. 90 **Wefer, G. and cruise participants**
Report and preliminary results of METEOR-Cruise M 37/1, Lisbon - Las Palmas, 4.-23.12.1996. 79 pages, Bremen, 1997.

No. 91 **Isenbeck-Schröter, M., E. Bedbur, M. Kofod, B. König, T. Schramm & G. Mattheß**
Occurrence of Pesticide Residues in Water - Assessment of the Current Situation in Selected EU Countries. 65 pages, Bremen 1997.

No. 92 **Kühn, M.**
Geochemische Folgereaktionen bei der hydrogeothermalen Energiegewinnung. 129 pages, Bremen 1997.

No. 93 **Determann, S. & K. Herterich**
JGOFS-A6 "Daten und Modelle": Sammlung JGOFS-relevanter Modelle in Deutschland. 26 pages, Bremen, 1997.

No. 94 **Fischer, G. and cruise participants**
Report and preliminary results of METEOR-Cruise M 38/1, Las Palmas - Recife, 25.1.-1.3.1997, with Appendix: Core Descriptions from METEOR Cruise M 37/1. Bremen, 1997.

No. 95 **Bleil, U. and cruise participants**
Report and preliminary results of METEOR-Cruise M 38/2, Recife - Las Palmas, 4.3.-14.4.1997. 126 pages, Bremen, 1997.

No. 96 **Neuer, S. and cruise participants**
Report and preliminary results of VICTOR HENSEN-Cruise 96/1. Bremen, 1997.

No. 97 **Villinger, H. and cruise participants**
Fahrtbericht SO 111, 20.8. - 16.9.1996. 115 pages, Bremen, 1997.

No. 98 **Lüning, S.**
Late Cretaceous - Early Tertiary sequence stratigraphy, paleoecology and geodynamics of Eastern Sinai, Egypt. 218 pages, Bremen, 1997.

No. 99 **Haese, R.R.**
Beschreibung und Quantifizierung frühdiagenetischer Reaktionen des Eisens in Sedimenten des Südatlantiks. 118 pages, Bremen, 1997.

No. 100 **Lührte, R. von**
Verwertung von Bremer Baggergut als Material zur Oberflächenabdichtung von Deponien - Geochemisches Langzeitverhalten und Schwermetall-Mobilität (Cd, Cu, Ni, Pb, Zn). Bremen, 1997.

No. 101 **Ebert, M.**
Der Einfluß des Redoxmilieus auf die Mobilität von Chrom im durchströmten Aquifer. 135 pages, Bremen, 1997.

No. 102 **Krögel, F.**
Einfluß von Viskosität und Dichte des Seewassers auf Transport und Ablagerung von Wattsedimenten (Langeooger Rückseitenwatt, südliche Nordsee). 168 pages, Bremen, 1997.

No. 103 **Kerntopf, B.**
Dinoflagellate Distribution Patterns and Preservation in the Equatorial Atlantic and Offshore North-West Africa. 137 pages, Bremen, 1997.

No. 104 **Breitzke, M.**
Elastische Wellenausbreitung in marinen Sedimenten - Neue Entwicklungen der Ultraschall Sedimentphysik und Sedimentechographie. 298 pages, Bremen, 1997.

No. 105 **Marchant, M.**
Rezente und spätquartäre Sedimentation planktischer Foraminiferen im Peru-Chile Strom. 115 pages, Bremen, 1997.

No. 106 **Habicht, K.S.**
Sulfur isotope fractionation in marine sediments and bacterial cultures. 125 pages, Bremen, 1997.

No. 107 **Hamer, K., R.v. Lührte, G. Becker, T. Felis, S. Keffel, B. Strotmann, C. Waschkowitz, M. Kölling, M. Isenbeck-Schröter, H.D. Schulz**
Endbericht zum Forschungsvorhaben 060 des Landes Bremen: Baggergut der Hafengruppe Bremen-Stadt: Modelluntersuchungen zur Schwermetallmobilität und Möglichkeiten der Verwertung von Hafenschlick aus Bremischen Häfen. 98 pages, Bremen, 1997.

No. 108 **Greeff, O.W.**
Entwicklung und Erprobung eines benthischen Landersystemes zur in situ-Bestimmung von Sulfatreduktionsraten mariner Sedimente. 121 pages, Bremen, 1997.

No. 109 **Pätzold, M. und G. Wefer**
Bericht über den 6. JGOFS-Workshop am 4./5.12.1997 in Bremen. Im Anhang: Publikationen zum deutschen Beitrag zur Joint Global Ocean Flux Study (JGOFS), Stand 1/1998. 122 pages, Bremen, 1998.

No. 110 **Landenberger, H.**
CoTReM, ein Multi-Komponenten Transport- und Reaktions-Modell. 142 pages, Bremen, 1998.

No. 111 **Villinger, H. und Fahrtteilnehmer**
Fahrtbericht SO 124, 4.10. - 16.10.199. 90 pages, Bremen, 1997.

No. 112 **Gietl, R.**
Biostratigraphie und Sedimentationsmuster einer nordostägyptischen Karbonatrampe unter Berücksichtigung der Alveolinen-Faunen. 142 pages, Bremen, 1998.

No. 113 **Ziebis, W.**
The Impact of the Thalassinidean Shrimp Callianassa truncata on the Geochemistry of permeable, coastal Sediments. 158 pages, Bremen 1998.

No. 114 **Schulz, H.D. and cruise participants**
Report and preliminary results of METEOR-Cruise M 41/1, Málaga - Libreville, 13.2.-15.3.1998. Bremen, 1998.

No. 115 **Völker, D.J.**
Untersuchungen an strömungsbeeinflußten Sedimentationsmustern im Südozean. Interpretation sedimentechographischer Daten und numerische Modellierung. 152 pages, Bremen, 1998.

No. 116 **Schlünz, B.**
Riverine Organic Carbon Input into the Ocean in Relation to Late Quaternary Climate Change. 136 pages, Bremen, 1998.

No. 117 **Kuhnert, H.**
Aufzeichnug des Klimas vor Westaustralien in stabilen Isotopen in Korallenskeletten. 109 pages, Bremen, 1998.

No. 118 **Kirst, G.**
Rekonstruktion von Oberflächenwassertemperaturen im östlichen Südatlantik anhand von Alkenonen. 130 pages, Bremen, 1998.

No. 119 **Dürkoop, A.**
Der Brasil-Strom im Spätquartär: Rekonstruktion der oberflächennahen Hydrographie während der letzten 400 000 Jahre. 121 pages, Bremen, 1998.

No. 120 **Lamy, F.**
Spätquartäre Variationen des terrigenen Sedimenteintrags entlang des chilenischen Kontinentalhangs als Abbild von Klimavariabilität im Milanković- und Sub-Milanković-Zeitbereich. 141 pages, Bremen, 1998.

No. 121 **Neuer, S. and cruise participants**
Report and preliminary results of POSEIDON-Cruise Pos 237/2, Vigo – Las Palmas, 18.3.-31.3.1998. 39 pages, Bremen, 1998

No. 122 **Romero, O.E.**
Marine planktonic diatoms from the tropical and equatorial Atlantic: temporal flux patterns and the sediment record. 205 pages, Bremen, 1998.

No. 123 **Spiess, V. und Fahrtteilnehmer**
Report and preliminary results of RV SONNE Cruise 125, Cochin – Chittagong, 17.10.-17.11.1997. 128 pages, Bremen, 1998.

No. 124 **Arz, H.W.**
Dokumentation von kurzfristigen Klimaschwankungen des Spätquartärs in Sedimenten des westlichen äquatorialen Atlantiks. 96 pages, Bremen, 1998.

No. 125 **Wolff, T.**
Mixed layer characteristics in the equatorial Atlantic during the late Quaternary as deduced from planktonic foraminifera. 132 pages, Bremen, 1998.

No. 126 **Dittert, N.**
Late Quaternary Planktic Foraminifera Assemblages in the South Atlantic Ocean: Quantitative Determination and Preservational Aspects. 165 pages, Bremen, 1998.

No. 127 **Höll, C.**
Kalkige und organisch-wandige Dinoflagellaten-Zysten in Spätquartären Sedimenten des tropischen Atlantiks und ihre palökologische Auswertbarkeit. 121 pages, Bremen, 1998.

No. 128 **Hencke, J.**
Redoxreaktionen im Grundwasser: Etablierung und Verlagerung von Reaktionsfronten und ihre Bedeutung für die Spurenelement-Mobilität. 122 pages, Bremen 1998.

No. 129 **Pätzold, J. and cruise participants**
Report and preliminary results of METEOR-Cruise M 41/3, Vítoria, Brasil – Salvador de Bahia, Brasil, 18.4. - 15.5.1998. Bremen, 1999.

No. 130 **Fischer, G. and cruise participants**
Report and preliminary results of METEOR-Cruise M 41/4, Salvador de Bahia, Brasil – Las Palmas, Spain, 18.5. – 13.6.1998. Bremen, 1999.

No. 131 **Schlünz, B. und G. Wefer**
Bericht über den 7. JGOFS-Workshop am 3. und 4.12.1998 in Bremen. Im Anhang: Publikationen zum deutschen Beitrag zur Joint Global Ocean Flux Study (JGOFS), Stand 1/ 1999. 100 pages, Bremen, 1999.

No. 132 **Wefer, G. and cruise participants**
Report and preliminary results of METEOR-Cruise M 42/4, Las Palmas - Las Palmas - Viena do Castelo; 26.09.1998 - 26.10.1998. 104 pages, Bremen, 1999.

No. 133 **Felis, T.**
Climate and ocean variability reconstructed from stable isotope records of modern subtropical corals (Northern Red Sea). 111 pages, Bremen, 1999.

No. 134 **Draschba , S.**
North Atlantic climate variability recorded in reef corals from Bermuda. 108 pages, Bremen, 1999.

No. 135 **Schmieder, F.**
Magnetic Cyclostratigraphy of South Atlantic Sediments. 82 pages, Bremen, 1999.

No. 136 **Rieß, W.**
In situ measurements of respiration and mineralisation processes – Interaction between fauna and geochemical fluxes at active interfaces. 68 pages, Bremen, 1999.

No. 137 **Devey, C.W. and cruise participants**
Report and shipboard results from METEOR-cruise M 41/2, Libreville – Vitoria, 18.3. – 15.4.98. 59 pages, Bremen, 1999.

No. 138 **Wenzhöfer, F.**
Biogeochemical processes at the sediment water interface and quantification of metabolically driven calcite dissolution in deep sea sediments. 103 pages, Bremen, 1999.

No. 139 **Klump, J.**
Biogenic barite as a proxy of paleoproductivity variations in the Southern Peru-Chile Current. 107 pages, Bremen, 1999.

No. 140 **Huber, R.**
Carbonate sedimentation in the northern Northatlantic since the late pliocene. 103 pages, Bremen, 1999.

No. 141 **Schulz, H.**
Nitrate-storing sulfur bacteria in sediments of coastal upwelling. 94 pages, Bremen, 1999.

No. 142 **Mai, S.**
Die Sedimentverteilung im Wattenmeer: ein Simulationsmodell. 114 pages, Bremen, 1999.

No. 143 **Neuer, S. and cruise participants**
Report and preliminary results of Poseidon Cruise 248, Las Palmas - Las Palmas, 15.2.-26.2.1999. 45 pages, Bremen, 1999.

No. 144 **Weber, A.**
Schwefelkreislauf in marinen Sedimenten und Messung von in situ Sulfatreduktionsraten. 122 pages, Bremen, 1999.

No. 145 **Hadeler, A.**
Sorptionsreaktionen im Grundwasser: Unterschiedliche Aspekte bei der Modellierung des Transportverhaltens von Zink. 122 pages, 1999.

No. 146 **Dierßen, H.**
Zum Kreislauf ausgewählter Spurenmetalle im Südatlantik: Vertikaltransport und Wechselwirkung zwischen Partikeln und Lösung. 167 pages, Bremen, 1999.

No. 147 **Zühlsdorff, L.**
High resolution multi-frequency seismic surveys at the Eastern Juan de Fuca Ridge Flank and the Cascadia Margin – Evidence for thermally and tectonically driven fluid upflow in marine sediments. 118 pages, Bremen 1999.

No. 148 **Kinkel, H.**
Living and late Quaternary Coccolithophores in the equatorial Atlantic Ocean: response of distribution and productivity patterns to changing surface water circulation. 183 pages, Bremen, 2000.

No. 149 **Pätzold, J. and cruise participants**
Report and preliminary results of METEOR Cruise M 44/3, Aqaba (Jordan) - Safaga (Egypt) – Dubá (Saudi Arabia) – Suez (Egypt) - Haifa (Israel), 12.3.-26.3.-2.4.-4.4.1999. 135 pages, Bremen, 2000.

No. 150 **Schlünz, B. and G. Wefer**
Bericht über den 8. JGOFS-Workshop am 2. und 3.12.1999 in Bremen. Im Anhang: Publikationen zum deutschen Beitrag zur Joint Global Ocean Flux Study (JGOFS), Stand 1/ 2000. 95 pages, Bremen, 2000.

No. 151 **Schnack, K.**
Biostratigraphie und fazielle Entwicklung in der Oberkreide und im Alttertiär im Bereich der Kharga Schwelle, Westliche Wüste, SW-Ägypten. 142 pages, Bremen, 2000.

No. 152 **Karwath, B.**
Ecological studies on living and fossil calcareous dinoflagellates of the equatorial and tropical Atlantic Ocean. 175 pages, Bremen, 2000.

No. 153 **Moustafa, Y.**
Paleoclimatic reconstructions of the Northern Red Sea during the Holocene inferred from stable isotope records of modern and fossil corals and molluscs. 102 pages, Bremen, 2000.

No. 154 **Villinger, H. and cruise participants**
Report and preliminary results of SONNE-cruise 145-1 Balboa – Talcahuana, 21.12.1999 – 28.01.2000. 147 pages, Bremen, 2000.

No. 155 **Rusch, A.**
Dynamik der Feinfraktion im Oberflächenhorizont permeabler Schelfsedimente. 102 pages, Bremen, 2000.

No. 156 **Moos, C.**
Reconstruction of upwelling intensity and paleo-nutrient gradients in the northwest Arabian Sea derived from stable carbon and oxygen isotopes of planktic foraminifera. 103 pages, Bremen, 2000.

No. 157 **Xu, W.**
Mass physical sediment properties and trends in a Wadden Sea tidal basin. 127 pages, Bremen, 2000.

No. 158 **Meinecke, G. and cruise participants**
Report and preliminary results of METEOR Cruise M 45/1, Malaga (Spain) - Lissabon (Portugal), 19.05. - 08.06.1999. 39 pages, Bremen, 2000.

No. 159 **Vink, A.**
Reconstruction of recent and late Quaternary surface water masses of the western subtropical Atlantic Ocean based on calcareous and organic-walled dinoflagellate cysts. 160 pages, Bremen, 2000.

No. 160 **Willems, H. (Sprecher), U. Bleil, R. Henrich, K. Herterich, B.B. Jørgensen, H.-J. Kuß, M. Olesch, H.D. Schulz,V. Spieß, G. Wefer**
Abschlußbericht des Graduierten-Kollegs Stoff-Flüsse in marine Geosystemen. Zusammenfassung und Berichtszeitraum Januar 1996 - Dezember 2000. 340 pages, Bremen, 2000.

No. 161 **Sprengel, C.**
Untersuchungen zur Sedimentation und Ökologie von Coccolithophoriden im Bereich der Kanarischen Inseln: Saisonale Flussmuster und Karbonatexport. 165 pages, Bremen, 2000.

No. 162 **Donner, B. and G. Wefer**
Bericht über den JGOFS-Workshop am 18.-21.9.2000 in Bremen: Biogeochemical Cycles: German Contributions to the International Joint Global Ocean Flux Study. 87 pages, Bremen, 2000.

No. 163 **Neuer, S. and cruise participants**
Report and preliminary results of Meteor Cruise M 45/5, Bremen – Las Palmas, October 1 – November 3, 1999. 93 pages, Bremen, 2000.

No. 164 **Devey, C. and cruise participants**
Report and preliminary results of Sonne Cruise SO 145/2, Talcahuano (Chile) - Arica (Chile), February 4 – February 29, 2000. 63 pages, Bremen, 2000.

No. 165 **Freudenthal, T.**
Reconstruction of productivity gradients in the Canary Islands region off Morocco by means of sinking particles and sediments. 147 pages, Bremen, 2000.

No. 166 **Adler, M.**
Modeling of one-dimensional transport in porous media with respect to simultaneous geochemical reactions in CoTReM. 147 pages, Bremen, 2000.

No. 167 **Santamarina Cuneo, P.**
Fluxes of suspended particulate matter through a tidal inlet of the East Frisian Wadden Sea (southern North Sea). 91 pages, Bremen, 2000.

No. 168 **Benthien, A.**
Effects of CO2 and nutrient concentration on the stable carbon isotope composition of C37:2 alkenones in sediments of the South Atlantic Ocean. 104 pages, Bremen, 2001.

No. 169 **Lavik, G.**
Nitrogen isotopes of sinking matter and sediments in the South Atlantic. 140 pages, Bremen, 2001.

No. 170 **Budziak, D.**
Late Quaternary monsoonal climate and related variations in paleoproductivity and alkenone-derived sea-surface temperatures in the western Arabian Sea. 114 pages, Bremen, 2001.

No. 171 **Gerhardt, S.**
Late Quaternary water mass variability derived from the pteropod preservation state in sediments of the western South Atlantic Ocean and the Caribbean Sea. 109 pages, Bremen, 2001.

No. 172 **Bleil, U. and cruise participants**
Report and preliminary results of Meteor Cruise M 46/3, Montevideo (Uruguay) – Mar del Plata (Argentina), January 4 – February 7, 2000. Bremen, 2001.

No. 173 **Wefer, G. and cruise participants**
Report and preliminary results of Meteor Cruise M 46/4, Mar del Plata (Argentina) – Salvador da Bahia (Brazil), February 10 – March 13, 2000. With partial results of METEOR cruise M 46/2. 136 pages, Bremen, 2001.

No. 174 **Schulz, H.D. and cruise participants**
Report and preliminary results of Meteor Cruise M 46/2, Recife (Brazil) – Montevideo (Uruguay), December 2 – December 29, 1999. 107 pages, Bremen, 2001.

No. 175 **Schmidt, A.**
Magnetic mineral fluxes in the Quaternary South Atlantic: Implications for the paleoenvironment. 97 pages, Bremen, 2001.

No. 176 **Bruhns, P.**
Crystal chemical characterization of heavy metal incorporation in brick burning processes. 93 pages, Bremen, 2001.

No. 177 **Karius, V.**
Baggergut der Hafengruppe Bremen-Stadt in der Ziegelherstellung. 131 pages, Bremen, 2001.

No. 178 **Adegbie, A. T.**
Reconstruction of paleoenvironmental conditions in Equatorial Atlantic and the Gulf of Guinea Basins for the last 245,000 years. 113 pages, Bremen, 2001.

No. 179 **Spieß, V. and cruise participants**
Report and preliminary results of R/V Sonne Cruise SO 149, Victoria - Victoria, 16.8. - 16.9.2000. 100 pages, Bremen, 2001.

No. 180 **Kim, J.-H.**
Reconstruction of past sea-surface temperatures in the eastern South Atlantic and the eastern South Pacific across Termination I based on the Alkenone Method. 114 pages, Bremen, 2001.

No. 181 **von Lom-Keil, H.**
Sedimentary waves on the Namibian continental margin and in the Argentine Basin – Bottom flow reconstructions based on high resolution echosounder data. 126 pages, Bremen, 2001.

No. 182 **Hebbeln, D. and cruise participants**
PUCK: Report and preliminary results of R/V Sonne Cruise SO 156, Valparaiso (Chile) - Talcahuano (Chile), March 29 - May 14, 2001. 195 pages, Bremen, 2001.

No. 183 **Wendler, J.**
Reconstruction of astronomically-forced cyclic and abrupt paleoecological changes in the Upper Cretaceous Boreal Realm based on calcareous dinoflagellate cysts. 149 pages, Bremen, 2001.

No. 184 **Volbers, A.**
Planktic foraminifera as paleoceanographic indicators: production, preservation, and reconstruction of upwelling intensity. Implications from late Quaternary South Atlantic sediments. 122 pages, Bremen, 2001.

No. 185 **Bleil, U. and cruise participants**
Report and preliminary results of R/V METEOR Cruise M 49/3, Montevideo (Uruguay) - Salvador (Brasil), March 9 - April 1, 2001. 99 pages, Bremen, 2001.

No. 186 **Scheibner, C.**
Architecture of a carbonate platform-to-basin transition on a structural high (Campanian-early Eocene, Eastern Desert, Egypt) – classical and modelling approaches combined. 173 pages, Bremen, 2001.

No. 187 **Schneider, S.**
Quartäre Schwankungen in Strömungsintensität und Produktivität als Abbild der Wassermassen-Variabilität im äquatorialen Atlantik (ODP Sites 959 und 663): Ergebnisse aus Siltkorn-Analysen. 134 pages, Bremen, 2001.

No. 188 **Uliana, E.**
Late Quaternary biogenic opal sedimentation in diatom assemblages in Kongo Fan sediments. 96 pages, Bremen, 2002.

No. 189 **Esper, O.**
Reconstruction of Recent and Late Quaternary oceanographic conditions in the eastern South Atlantic Ocean based on calcareous- and organic-walled dinoflagellate cysts. 130 pages, Bremen, 2001.

No. 190 **Wendler, I.**
Production and preservation of calcareous dinoflagellate cysts in the modern Arabian Sea. 117 pages, Bremen, 2002.

No. 191 **Bauer, J.**
Late Cenomanian – Santonian carbonate platform evolution of Sinai (Egypt): stratigraphy, facies, and sequence architecture. 178 pages, Bremen, 2002.

No. 192 **Hildebrand-Habel, T.**
Die Entwicklung kalkiger Dinoflagellaten im Südatlantik seit der höheren Oberkreide. 152 pages, Bremen, 2002.

No. 193 **Hecht, H.**
Sauerstoff-Optopoden zur Quantifizierung von Pyritverwitterungsprozessen im Labor- und Langzeit-in-situ-Einsatz. Entwicklung - Anwendung – Modellierung. 130 pages, Bremen, 2002.

No. 194 **Fischer, G. and cruise participants**
Report and Preliminary Results of RV METEOR-Cruise M49/4, Salvador da Bahia – Halifax, 4.4.-5.5.2001. 84 pages, Bremen, 2002.

No. 195 **Gröger, M.**
Deep-water circulation in the western equatorial Atlantic: inferences from carbonate preservation studies and silt grain-size analysis. 95 pages, Bremen, 2002.

No. 196 **Meinecke,G. and cruise participants**
Report of RV POSEIDON Cruise POS 271, Las Palmas - Las Palmas, 19.3.-29.3.2001. 19 pages, Bremen, 2002.

No. 197 **Meggers, H. and cruise participants**
Report of RV POSEIDON Cruise POS 272, Las Palmas - Las Palmas, 1.4.-14.4.2001. 19 pages, Bremen, 2002.

No. 198 **Gräfe, K.-U.**
Stratigraphische Korrelation und Steuerungsfaktoren Sedimentärer Zyklen in ausgewählten Borealen und Tethyalen Becken des Cenoman/Turon (Oberkreide) Europas und Nordwestafrikas. 197 pages, Bremen, 2002.

No. 199 **Jahn, B.**
Mid to Late Pleistocene Variations of Marine Productivity in and Terrigenous Input to the Southeast Atlantic. 97 pages, Bremen, 2002.

No. 200 **Al-Rousan, S.**
Ocean and climate history recorded in stable isotopes of coral and foraminifers from the northern Gulf of Aqaba. 116 pages, Bremen, 2002.

No. 201 **Azouzi, B.**
Regionalisierung hydraulischer und hydrogeochemischer Daten mit geostatistischen Methoden. 108 pages, Bremen, 2002.

No. 202 **Spieß, V. and cruise participants**
Report and preliminary results of METEOR Cruise M 47/3, Libreville (Gabun) - Walvis Bay (Namibia), 01.06 - 03.07.2000. 70 pages, Bremen 2002.

No. 203 **Spieß, V. and cruise participants**
Report and preliminary results of METEOR Cruise M 49/2, Montevideo (Uruguay) - Montevideo, 13.02 - 07.03.2001. 84 pages, Bremen 2002.

No. 204 **Mollenhauer, G.**
Organic carbon accumulation in the South Atlantic Ocean: Sedimentary processes and glacial/interglacial Budgets. 139 pages, Bremen 2002.

No. 205 **Spieß, V. and cruise participants**
Report and preliminary results of METEOR Cruise M49/1, Cape Town (South Africa) - Montevideo (Uruguay), 04.01.2001 - 10.02.2001. 57 pages, Bremen, 2003.

No. 206 **Meier, K.J.S.**
Calcareous dinoflagellates from the Mediterranean Sea: taxonomy, ecology and palaeoenvironmental application. 126 pages, Bremen, 2003.

No. 207 **Rakic, S.**
Untersuchungen zur Polymorphie und Kristallchemie von Silikaten der Zusammensetzung Me2Si2O5 (Me:Na, K). 139 pages, Bremen, 2003.

No. 208 **Pfeifer, K.**
Auswirkungen frühdiagenetischer Prozesse auf Calcit- und Barytgehalte in marinen Oberflächen-sedimenten. 110 pages, Bremen, 2003.

No. 209 **Heuer, V.**
Spurenelemente in Sedimenten des Südatlantik. Primärer Eintrag und frühdiagenetische Überprägung. 136 pages, Bremen, 2003.

No. 210 **Streng, M.**
Phylogenetic Aspects and Taxonomy of Calcareous Dinoflagellates. 157 pages, Bremen 2003.

No. 211 **Boeckel, B.**
Present and past coccolith assemblages in the South Atlantic: implications for species ecology, carbonate contribution and palaeoceanographic applicability. 157 pages, Bremen, 2003.

No. 212 **Precht, E.**
Advective interfacial exchange in permeable sediments driven by surface gravity waves and its ecological consequences. 131 pages, Bremen, 2003.

No. 213 **Frenz, M.**
Grain-size composition of Quaternary South Atlantic sediments and its paleoceanographic significance. 123 pages, Bremen, 2003.

No. 214 **Meggers, H. and cruise participants**
Report and preliminary results of METEOR Cruise M 53/1, Limassol - Las Palmas – Mindelo, 30.03.2002 - 03.05.2002. 81 pages, Bremen, 2003.

No. 215 **Schulz, H.D. and cruise participants**
Report and preliminary results of METEOR Cruise M 58/1, Dakar – Las Palmas, 15.04..2003 – 12.05.2003. Bremen, 2003.

No. 216 **Schneider, R. and cruise participants**
Report and preliminary results of METEOR Cruise M 57/1, Cape Town – Walvis Bay, 20.01. – 08.02.2003. 123 pages, Bremen, 2003.

No. 217 **Kallmeyer, J.**
Sulfate reduction in the deep Biosphere. 157 pages, Bremen, 2003.

No. 218 **Røy, H.**
Dynamic Structure and Function of the Diffusive Boundary Layer at the Seafloor. 149 pages, Bremen, 2003.

No. 219 **Pätzold, J., C. Hübscher and cruise participants**
Report and preliminary results of METEOR Cruise M 52/2&3, Istanbul – Limassol – Limassol, 04.02. – 27.03.2002. Bremen, 2003.

No. 220 **Zabel, M. and cruise participants**
Report and preliminary results of METEOR Cruise M 57/2, Walvis Bay – Walvis Bay, 11.02. – 12.03.2003. 136 pages, Bremen 2003.

No. 221 **Salem, M.**
Geophysical investigations of submarine prolongations of alluvial fans on the western side of the Gulf of Aqaba-Red Sea. 100 pages, Bremen, 2003.

No. 222 **Tilch, E.**
Oszillation von Wattflächen und deren fossiles Erhaltungspotential (Spiekerooger Rückseitenwatt, südliche Nordsee). 137 pages, Bremen, 2003.

No. 223 **Frisch, U. and F. Kockel**
Der Bremen-Knoten im Strukturnetz Nordwest-Deutschlands. Stratigraphie, Paläogeographie, Strukturgeologie. 379 pages, Bremen, 2004.

No. 224 **Kolonic, S.**
Mechanisms and biogeochemical implications of Cenomanian/Turonian black shale formation in North Africa: An integrated geochemical, millennial-scale study from the Tarfaya-LaAyoune Basin in SW Morocco. 174 pages, Bremen, 2004. Report online available only.

No. 225 **Panteleit, B.**
Geochemische Prozesse in der Salz- Süßwasser Übergangszone. 106 pages, Bremen, 2004.

No. 226 **Seiter, K.**
Regionalisierung und Quantifizierung benthischer Mineralisationsprozesse. 135 pages, Bremen, 2004.

No. 227 **Bleil, U. and cruise participants**
Report and preliminary results of METEOR Cruise M 58/2, Las Palmas – Las Palmas (Canary Islands, Spain), 15.05. – 08.06.2003. 123 pages, Bremen, 2004.

No. 228 **Kopf, A. and cruise participants**
Report and preliminary results of SONNE Cruise SO175, Miami - Bremerhaven, 12.11 - 30.12.2003. 218 pages, Bremen, 2004.

No. 229 **Fabian, M.**
Near Surface Tilt and Pore Pressure Changes Induced by Pumping in Multi-Layered Poroelastic Half-Spaces. 121 pages, Bremen, 2004.

No. 230 **Segl, M. , and cruise participants**
Report and preliminary results of POSEIDON cruise 304 Galway – Lisbon, 5. – 22. Oct. 2004.
27 pages, Bremen 2004

No. 231 **Meinecke, G. and cruise participants**
Report and preliminary results of POSEIDON Cruise 296, Las Palmas – Las Palmas, 04.04 – 14.04.2003. 42 pages, Bremen 2005.

No. 232 **Meinecke, G. and cruise participants**
Report and preliminary results of POSEIDON Cruise 310, Las Palmas – Las Palmas, 12.04 – 26.04.2004. 49 pages, Bremen 2005.

No. 233 **Meinecke, G. and cruise participants**
Report and preliminary results of METEOR Cruise 58/3, Las Palmas - Ponta Delgada, 11.06 - 24.06.2003. 50 pages, Bremen 2005.

No. 234 **Feseker, T.**
Numerical Studies on Groundwater Flow in Coastal Aquifers. 219 pages. Bremen 2004.

No. 235 **Sahling, H. and cruise participants**
Report and preliminary results of R/V POSEIDON Cruise P317/4, Istanbul-Istanbul ,
16 October - 4 November
2004. 92 pages, Bremen 2004.

No. 236 **Meinecke, G. und Fahrtteilnehmer**
Report and preliminary results of POSEIDON Cruise 305, Las Palmas (Spain) - Lisbon (Portugal), October 28th – November 6th, 2004. 43 pages, Bremen 2005.

No. 237 **Ruhland, G. and cruise participants**
Report and preliminary results of POSEIDON Cruise 319, Las Palmas (Spain) - Las Palmas (Spain), December 6th – December 17th, 2004. 50 pages, Bremen 2005.

No. 238 **Chang, T.S.**
Dynamics of fine-grained sediments and stratigraphic evolution of a back-barrier tidal basin of the German Wadden Sea (southern North Sea). 102 pages, Bremen 2005.

No. 239 **Lager, T.**
Predicting the source strength of recycling materials within the scope of a seepage water prognosis by means of standardized laboratory methods. 141 pages, Bremen 2005.

No. 240 **Meinecke, G.**
DOLAN - Operationelle Datenübertragung im Ozean und Laterales Akustisches Netzwerk in der Tiefsee. Abschlußbericht. 42 pages, Bremen 2005.

No. 241 **Guasti, E.**
Early Paleogene environmental turnover in the southern Tethys as recorded by foraminiferal and organic-walled dinoflagellate cysts assemblages. 203 pages, Bremen 2005.

No. 242 **Riedinger, N.**
Preservation and diagenetic overprint of geochemical and geophysical signals in ocean margin sediments related to depositional dynamics. 91 pages, Bremen 2005.

No. 243 **Ruhland, G. and cruise participants**
Report and preliminary results of POSEIDON cruise 320, Las Palmas (Spain) - Las Palmas (Spain), March 08th - March 18th, 2005. 57 pages, Bremen 2005.

No. 244 **Inthorn, M.**
Lateral particle transport in nepheloid layers – a key factor for organic matter distribution and quality in the Benguela high-productivity area. 127 pages, Bremen, 2006.

No. 245 **Aspetsberger, F.**
Benthic carbon turnover in continental slope and deep sea sediments: importance of organic matter quality at different time scales. 136 pages, Bremen, 2006.

No. 246 **Hebbeln, D. and cruise participants**
Report and preliminary results of RV SONNE Cruise SO-184, PABESIA, Durban (South Africa) – Cilacap (Indonesia) – Darwin (Australia), July 08th - September 13th, 2005. 142 pages, Bremen 2006.

No. 247 **Ratmeyer, V. and cruise participants**
Report and preliminary results of RV METEOR Cruise M61/3. Development of Carbonate Mounds on the Celtic Continental Margin, Northeast Atlantic. Cork (Ireland) – Ponta Delgada (Portugal), 04.06. – 21.06.2004. 64 pages, Bremen 2006.

No. 248 **Wien, K.**
Element Stratigraphy and Age Models for Pelagites and Gravity Mass Flow Deposits based on Shipboard XRF Analysis. 100 pages, Bremen 2006.

No. 249 **Krastel, S. and cruise participants**
Report and preliminary results of RV METEOR Cruise M65/2, Dakar - Las Palmas, 04.07. – 26.07.2005. 185 pages, Bremen 2006.

No. 250 **Heil, G.M.N.**
Abrupt Climate Shifts in the Western Tropical to Subtropical Atlantic Region during the Last Glacial. 121 pages, Bremen 2006.

No. 251 **Ruhland, G. and cruise participants**
Report and preliminary results of POSEIDON Cruise 330, Las Palmas – Las Palmas, November 21th – December 03rd, 2005. 48 pages, Bremen 2006.

No. 252 **Mulitza , S. and cruise participants**
Report and preliminary results of METEOR Cruise M65/1, Dakar – Dakar, 11.06.- 1.07.2005. 149 pages, Bremen 2006.

No. 253 **Kopf, A. and cruise participants**
Report and preliminary results of POSEIDON Cruise P336, Heraklion - Heraklion, 28.04. – 17.05.2006. 127 pages, Bremen, 2006.

No. 254 **Wefer, G. and cruise participants**
Report and preliminary results of R/V METEOR Cruise M65/3, Las Palmas - Las Palmas (Spain), July 31st - August 10th, 2005. 24 pages, Bremen 2006.

No. 255 **Hanebuth, T.J.J. and cruise participants**
Report and first results of the POSEIDON Cruise P342 GALIOMAR, Vigo – Lisboa (Portugal), August 19th – September 06th, 2006. Distribution Pattern, Residence Times and Export of Sediments on the Pleistocene/Holocene Galician Shelf (NW Iberian Peninsula). 203 pages, Bremen, 2007.

No. 256 **Ahke, A.**
Composition of molecular organic matter pools, pigments and proteins, in Benguela upwelling and Arctic Sediments. 192 pages, Bremen 2007.

No. 257 **Becker, V.**
Seeper - Ein Modell für die Praxis der Sickerwasserprognose. 170 pages, Bremen 2007.

No. 258 **Ruhland, G. and cruise participants**
Report and preliminary results of Poseidon cruise 333, Las Palmas (Spain) – Las Palmas (Spain), March 1st – March 10th, 2006. 32 pages, Bremen 2007.

No. 259 **Fischer, G., G. Ruhland and cruise participants**
Report and preliminary results of Poseidon cruise 344, leg 1 and leg 2, Las Palmas (Spain) – Las Palmas (Spain),
Oct. 20th –Nov 2nd & Nov. 4th – Nov 13th, 2006. 46 pages, Bremen 2007.

No. 260 **Westphal, H. and cruise participants**
Report and preliminary results of Poseidon cruise 346, MACUMA. Las Palmas (Spain) – Las Palmas (Spain), 28.12.2006 – 15.1.2007. 49 pages, Bremen 2007.

No. 261 **Bohrmann, G., T. Pape, and cruise participants**
Report and preliminary results of R/V METEOR Cruise M72/3, Istanbul – Trabzon – Istanbul, March 17th – April 23rd, 2007. Marine gas hydrates of the Eastern Black Sea. 130 pages, Bremen 2007.

No. 262 **Bohrmann, G., and cruise participants**
Report and preliminary results of R/V METEOR Cruise M70/3, Iraklion – Iraklion, 21 November – 8 December 2006. Cold Seeps of the Anaximander Mountains / Eastern Mediterranean. 75 pages, Bremen 2008.

No. 263 **Bohrmann, G., Spiess, V., and cruise participants**
Report and preliminary results of R/V Meteor Cruise M67/2a and 2b, Balboa -- Tampico -- Bridgetown, 15 March -- 24 April, 2006. Fluid seepage in the Gulf of Mexico. Bremen 2008.

No. 264 **Kopf, A., and cruise participants**
Report and preliminary results of Meteor Cruise M73/1: LIMA-LAMO (Ligurian Margin Landslide Measurements & Observatory), Cadiz, 22.07.2007 – Genoa, 11.08.2007. 170 pages, Bremen 2008.

No. 265 **Hebbeln, D., and cruise participants**
Report and preliminary results of RV Pelagia Cruise 64PE284. Cold-water Corals in the Gulf of Cádiz and on Coral Patch Seamount (NE Atlantic). Portimão - Portimão, 18.02. - 09.03.2008. 90 pages, Bremen 2008.

No. 266 **Bohrmann, G. and cruise participants**
Report and preliminary results of R/V Meteor Cruise M74/3, Fujairah – Male, 30 October - 28 November, 2007. Cold Seeps of the Makran subduction zone (Continental margin of Pakistan). 161 pages, Bremen 2008.

No. 267 **Sachs, O.**
Benthic organic carbon fluxes in the Southern Ocean: Regional differences and links to surface primary production and carbon export. 143 pages, Bremen, 2008.

No. 268 **Zonneveld, K. and cruise participants**
Report and preliminary results of R/V POSEIDON Cruise P339, Piräus - Messina, 16 June - 2 July 2006. CAPPUCCINO - Calabrian and Adriatic palaeoproductivity and climatic variability in the last two millenia. 61 pages, Bremen, 2008.

No. 269 **Ruhland, G. and cruise participants**
Report and preliminary results of R/V POSEIDON Cruise P360, Las Palmas (Spain) - Las Palmas (Spain), Oct. 29th - Nov. 6th, 2007. 27 pages, Bremen, 2008.

No. 270 **Ruhland, G., G. Fischer and cruise participants**
Report and preliminary results of R/V POSEIDON Cruise 365 (Leg 1+2). Leg 1: Las Palmas - Las Palmas, 13.4. - 16.4.2008. Leg 2: Las Palmas - Las Palmas, 18.4. - 29.4.2008. 40 pages, Bremen, 2009.

No. 271 **Kopf, A. and cruise participants**
Report and preliminary results of R/V POSEIDON Cruise P386: NAIL (Nice Airport Landslide), La Seyne sur Mer, 20.06.2009 – La Seyne sur Mer, 06.07.2009. 161 pages, Bremen, 2009.

No. 272 **Freudenthal, T., G. Fischer and cruise participants**
Report and preliminary results of Maria S. Merian Cruise MSM04/4 a & b, Las Palmas (Spain) – Las Palmas (Spain), Feb 27th – Mar 16th & Mar 19th – Apr 1st, 2007. 117 pages, Bremen 2009.

No. 273 **Hebbeln, D., C. Wienberg, L. Beuck, A. Freiwald, P. Wintersteller and cruise participants**
Report and preliminary results of R/V POSEIDON Cruise POS 385 "Cold-Water Corals of the Alboran Sea (western Mediterranean Sea)", Faro - Toulon, May 29 - June 16, 2009. 79 pages, Bremen 2009.

No. 274 **Zonneveld, K. and cruise participants**
Report and preliminary results of R/V Poseidon Cruises P 366-1 and P 366-2, Las Palmas - Las Palmas - Vigo, 03 -19 May 2008 and 22 -30 May 2008. PERGAMOM Proxy Education and Research cruise off Galicai, Morocco and Mauretania. 47 pages, Bremen 2010.

No. 275 **Wienberg, C. and cruise participants**
Report and preliminary results of RV POSEIDON cruise POS400 "CORICON - Cold-water corals along the Irish continental margin", Vigo - Cork, June 29 - July 15 2010. 46 pages, Bremen 2010.

No. 276 **Villinger, H. and cruise participants**
Report and preliminary results of R/V Sonne Cruise SO 207, Caldera-Caldera, 21 June -13 July, 2010. SeamountFlux: Efficient cooling in young oceanic crust caused by circulation of seawater through seamounts (Guatemala Basin, East Pacific Ocean). 161 pages, Bremen 2010.

No. 277 **Fischer, G. and cruise participants**
Report and preliminary results of RV POSEIDON Cruise POS 396, Las Palmas - Las Palmas (Spain), 24 February - 8 March 2010. 22 pages, Bremen 2011.

No. 278 **Bohrmann, G. and cruise participants**
Report and preliminary results of RV MARIA S. MERIAN Cruise MSM 15/2, Istanbul (Turkey) – Piraeus (Greece), 10 May - 2 June 2010. Origin and structure of methane, gas hydrates and fluid flows in the Black Sea. 130 pages, Bremen 2011.

No. 279 **Hebbeln, D. and cruise participants**
Report and preliminary results of RV SONNE Cruise SO-211, Valparaíso - Valparaíso, 2 November – 29 November 2010. ChiMeBo. Bremen 2011.

No. 280 **Bach, W. and cruise participants**
Report and preliminary results of RV SONNE Cruise SO 216, Townsville (Australia) - Makassar (Indonesia), June 14 – July 23, 2011. BAMBUS, Back-Arc Manus Basin Underwater Solfataras. 87 pages, Bremen 2011.

No. 281 **Bohrmann, G. and cruise participants**
Report and preliminary results of RV METEOR Cruise M84/2, Istanbul – Istanbul, 26 February – 02 April, 2011. Origin and Distribution of Methane and Methane Hydrates in the Black Sea.
164 pages, Bremen 2011.